

**REPUBLIC OF TURKEY
YILDIZ TECHNICAL UNIVERSITY
GRADUATE SCHOOL OF NATURAL AND APPLIED SCIENCES**

**DYNAMIC STABILITY ANALYSIS OF FUNCTIONALLY GRADED
SANDWICH MICRO-BEAMS**

MOHAMMED ALI SAIHOOD AL-SHUIRI

**Ph.D. THESIS
DEPARTMENT OF CIVIL ENGINEERING
PROGRAM OF MECHANICS ENGINEERING**

**ADVISER
ASSIST. PROF. DR. ÇAĞRI MOLLAMAHMUTOĞLU**

İSTANBUL, 2018

REPUBLIC OF TURKEY
YILDIZ TECHNICAL UNIVERSITY
GRADUATE SCHOOL OF NATURAL AND APPLIED SCIENCES

**DYNAMIC STABILITY ANALYSIS OF FUNCTIONALLY GRADED
SANDWICH MICRO BEAMS**

A thesis submitted by MOHAMMED ALI SAIHOOD AL-SHUIAIRI in partial fulfillment of the requirements for the degree of **DOCTOR OF PHILOSOPHY** is approved by the committee on 03.07.2018 in Department of Civil Engineering, Mechanics Engineering Program.

Thesis Adviser

Assist. Prof. Dr. ÇAĞRI MOLLAMAHMUTOĞLU
Yildiz Technical University

Approved By the Examining Committee

Assist. Prof. Dr. ÇAĞRI MOLLAMAHMUTOĞLU
Yildiz Technical University

Assist. Prof. Dr. SERHAT ERDOĞAN
Yildiz Technical University

Prof. Dr. SEMİH KÜÇÜKARSLAN
Istanbul Technical University

Assist. Prof. Dr. AYFER TEKİN ATACAN
Yildiz Technical University

Prof. Dr. REHA ARTAN
Istanbul Technical University

ACKNOWLEDGEMENTS

I would like to articulate my profound gratitude and indebtedness to my supervisor **ASSIST. PROF. Dr. ÇAĞRI MOLLAMAHMUTOĞLU**, he has always been a motivating and a supporting person throughout the study period and in my life stations. It has been a great honor for me to work under his guidance and conduct my studies.

I would then like to express my gratitude for my country, republic of Iraq. It has always been a source of inspiration for me, may Allah give it peace and prosperity again.

I want to thank my family for their continuous encouragement. I am especially thankful to my wife for her help, support, patience and encouragement to complete this study.

Finally, I would like to thank my fellow post graduate students and the people who have been involved directly or indirectly in my endeavor.

July, 2018

Mohammed AL-SHUIAIRI

TABLE OF CONTENTS

	Page
TABLE OF CONTENTS.....	i
LIST OF SYMBOLS.....	iii
LIST OF ABBREVIATIONS.....	v
LIST OF FIGURES.....	vi
LIST OF TABLES.....	xi
ABSTRACT.....	xiv
ÖZET.....	xv
CHAPTER 1	
INTRODUCTION.....	1
1.1 Literature Review.....	1
1.2 Objective of the Thesis.....	4
1.3 Hypothesis.....	5
1.4 Structure of the thesis	5
CHAPTER 2	
LITERATURE REVIEW.....	6
2.1 Sandwich FG beam structures.....	6
2.2 The nonlocal elasticity theory.....	9
2.3 The Strain gradient elasticity theory.....	14
2.4 Nonlocal strain gradient theory.....	17
2.5 Dynamic stability.....	21
CHAPTER 3	
THEORY AND FORMULATION OF FG SANDWICH MICRO-BEAM.....	24
3.1 Introduction.....	24
3.2 Non-local sandwich FG micro-beam strain gradient Model (NLSGT).....	30
3.3 The governing equations for sandwich FG micro-beams.....	32
3.3.1 Higher-order beam theories(HOBTS).....	32
3.3.2 Timoshenko beam theory (TBT).....	43
3.3.3 Euler- Bernoulli beam theory (EBBT).....	48
3.4 Analytical Solution of sandwich FG micro-beam.....	54
3.4.1 Bending of the sandwich FG micro-beam.....	54
3.4.1.1 Euler Bernoulli Beam Theory (EBBT).....	55
3.4.1.2 Timoshenko beam theory (TBT).....	55
3.4.1.3 Higher-order beam theories(HOBTS).....	56

3.4.2 Buckling Problem.....	57
3.4.1.1 Euler Bernoulli Beam Theory (EBBT).....	57
3.4.1.2 Timoshenko beam theory (TBT).....	58
3.4.1.3 Higher-order beam theories(HOBTS).....	58
3.4.3 Free vibration Analysis.....	59
3.5 Generalized differential quadrature method (GDQM).....	59
3.6 Dynamic Stability.....	68
 CHAPTER 4	
RESULTS AND DISCUSSION.....	71
4.1 Verification of the present results.....	71
4.1.1 Static and Buckling analysis.....	71
4.1.2 Elastic foundation and cross section shapes.....	74
4.1.3 Free vibration analysis.....	77
4.2 Dynamic stability of Sandwich FG micro-beam.....	80
4.3 Static, Buckling and Free vibration analysis of Sandwich FG micro-beam.....	100
 CHAPTER 5	
CONCLUSION AND FUTURE WORK.....	153
5.1 Conclusion.....	153
5.2 Future Work.....	155
REFERENCES.....	157
 APPENDIX-A	
VIRTUAL STRAIN AND KINETIC ENERGY.....	165
A.1 First order shear deformation beam theory (FSDBT).....	165
A.2 Euler- Bernoulli beam theory (EBBT).....	165
 APPENDIX-B	
FREE VIBRATION WITH ANALYTICAL SOLUTION.....	166
B. Free vibration with analytical solution.....	167
B.1 First order shear deformation beam theory (FSDBT).....	167
B.2 Euler- Bernoulli beam theory (EBBT).....	167

LIST OF SYMBOLS

$V_c(z)$	Ceramic constituent
ea	Nolocal parameter
l_m	Material length scale parameter
L/h	Aspect (slenderness) ratio
k	Gradient index (power law index)
E	Young's modulus
α	Thermal expansion coefficient
ν	Poisson's ratio
ρ	Material mass density
G	Shear modulus
K_e	Effective Bulk Modulus
G_e	Effective Shear Modulus
$P(t)$	Axial compressive excitation force
L	Length
b	Width
h	Thickness
k_w	Spring constant of Winkler elastic medium
k_s	Spring constant of Pasternak elastic medium
$\nabla^2 = \frac{\partial^2}{\partial x^2}$	Laplacian operator
t_{xx}	Total stress
t_{xz}	Total shear stress
∇	One-dimensional differential operator
σ_{xx}	Classical stress
σ_{xz}	Shear stress
$\sigma_{xx}^{(1)}$	Higher-order stress
$\sigma_{xz}^{(1)}$	Higher-order shear stress
α_0	Principal attenuation kernel function
α_1	Additional kernel function
ϕ	Total bending rotation of the cross-sections

$\Phi(z)$	A function of z that characterizes the transverse shear and stress distribution along the thickness of the beam.
ΔT	Temperature change
U_k	Kinetic energy
U_s	Strain energy
U_{ad}	Additional strain energy due to elastic medium
U_{th}	Strain energy with effect of temperature change
W	Work done by the external applied forces.



LIST OF ABBREVIATIONS

ASDBT	Aydogdu shear deformation beam theory
CCM	Chebyshev collocation method
dof	Degrees of freedom
DQM	Differential quadrature method
EBBT	Euler–Bernoulli beam theory
ESDBT	Exponential shear deformation beam theory
FGM	Functionally graded material
FSDBT	First order shear deformation beam theory
GDQM	Generalized differential quadrature method
GPLRC	Graphene nanoplatelet-reinforced composite
HOSDBT	Higher order shear deformation beam theory
HSDBT	Hyperbolic shear deformation beam theory
MSGT	Modified strain gradient theory
NLSGT	Nonlocal strain gradient theory
PSDBT	Parabolic shear deformation beam theory
SWCNTs	Single-walled carbon nanotubes
TSDBT	Trigonometric shear deformation beam theory

LIST OF FIGURES

		Page
Figure 3.1	A sandwich FG micro-beam subjected to an axial compressive excitation load $\bar{P}(t)$	24
Figure 3.2	Sandwich FG micro-beam a. Model I, b. Model II, c. Model III.....	26
Figure 3.3	Variation of (V_c) cross the thickness of a FG micro-beam with different of gradient index (k) with cross-section types of (1,1,1) and (1,2,1) for Models II, III.....	29
Figure 4.1	First three natural frequencies (MHz) as a function of different small length-scaled parameters. Comparison with [49] (left) and present results (right).....	79
Figure 4.2	Effect of aspect ratio on the instability region for sandwich FG micro beam (Modal III) for cross section shapes (1-1-1) and (1-8-1) with $\eta_s = 0.5$, $l_m = h$, $k = 2$, $\Delta T = 0$, $K_p = K_w = 0$, $ea = 0.5h$, and for S-S boundary conditions....	81
Figure 4.3	Effect of aspect ratio on the instability region for sandwich FG micro beam (Modal II) for cross section shapes (1-1-1) and (1-8-1) with $\eta_s = 0.5$, $k = 2$, $\Delta T = 0$, $ea = 0.5h$, $K_p = K_w = 0$, and $l_m = h$ for S-S boundary conditions.....	82
Figure 4.4	Effect of aspect ratio on the instability region for sandwich FG micro beam (Modal II) with $\eta_s = 0.5$, $k = 2$, $\Delta T = 0$, $ea = 0.5h$, $K_p = K_w = 0$, and $l_m = h$ for (C-S), (C-C) B.Cs.....	83
Figure 4.5	Effect of aspect ratio on the instability region for sandwich FG micro beam (Modal III) with $\eta_s = 0.5$, $k = 2$, $\Delta T = 0$, $ea = 0.5h$, $K_p = K_w = 0$, and $l_m = h$ for (C-S), (C-C) B.Cs.....	83
Figure 4.6	Effect of gradient index (k) on the instability region for sandwich FG micro beam Modal III with $\eta_s = 0.5$, $L/h = 10$, $\Delta T = 0$, $ea = 0.5h$, $K_p = K_w = 0$, and $l_m = h$ for S-S B.Cs.....	84

Figure 4.7	Effect of gradient index (k) on the instability region for sandwich FG micro beam Modal III with $\eta_s = 0.5$, $L/h = 10$, $\Delta T = 0$, $K_p = K_w = 0$, $ea = 0.5h$, and $l_m = h$, for C-S and C-C B.Cs.....	85
Figure 4.8	Effect of static load factor (η_s) on the instability region for sandwich FG micro beam Modal III, II with $\eta_s = 0.5$, $L/h = 10$, $\Delta T = 0$, $ea = 0.5h$, $K_p = K_w = 0$, and $l_m = h$ for S-S B.Cs.....	86
Figure 4.9	Effect of static load factor (η_s) on the instability region for sandwich FG micro beam Modal III with $\eta_s = 0.5$, $L/h = 10$, $\Delta T = 0$, $ea = 0.5h$, $K_p = K_w = 0$, and $l_m = h$ for C-S and C-C boundary conditions.....	86
Figure 4.10	Effect of Temperature change (ΔT) on the instability region for sandwich FG micro beam Modal III with $k = 2$, $L/h = 10$, $l_m = h$, $\eta_s = 0.5$, $K_p = K_w = 0$, & $ea = 0.5h$ for S-S B.Cs.....	87
Figure 4.11	Effect of Temperature change (ΔT) on the instability region for sandwich FG micro beam (Modal III) with $k = 2$, $L/h = 10$, $l_m = h$, $\eta_s = 0.5$, $K_p = K_w = 0$, & $ea = 0.5h$ for C-S and C-C B.Cs.....	88
Figure 4.12	Effect of Temperature change (ΔT) on the instability region for sandwich FG micro beam Modal II with $k = 2$, $L/h = 10$, $l_m = h$, $\eta_s = 0.5$, $K_p = K_w = 0$, & $ea = 0.5h$ for S-S B.Cs.....	89
Figure 4.13	Effect of Dimensionless material length scale parameter (β) on the instability region for sandwich FG micro beam (Modal III) with $\Delta T = 0$, $k = 2$, $L/h = 10$, $\eta_s = 0.5$, $K_p = K_w = 0$, & $\alpha = 0.1$ for S-S boundary conditions.....	90
Figure 4.14	Effect of Dimensionless material length scale parameter (β) on the instability region for sandwich FG micro beam (Modal III) with $\Delta T = 0$, $k = 2$, $L/h = 10$, $\eta_s = 0.5$, $K_p = K_w = 0$, & $\alpha = 0.1$, for various boundary conditions.....	90
Figure 4.15	Effect of Dimensionless material length scale parameter (β) on the instability region for sandwich FG micro beam (Modal II) with $\Delta T = 0$, $k = 2$, $L/h = 10$, $\eta_s = 0.5$, $K_p = K_w = 0$, & $\alpha = 0.1$ for various boundary conditions.....	91

Figure 4.16	Effect of Dimensionless nonlocal parameter (α) on the instability region for sandwich FG micro beam (Modal III) with $\Delta T = 0$, $k = 2$, $L/h = 10$, $\eta_s = 0.5$, $K_p = K_w = 0$, & $\beta = 0.1$ for S-S boundary conditions.....	92
Figure 4.17	Effect of Dimensionless nonlocal parameter (α) on the instability region for sandwich FG micro beam (Modal III) with $\Delta T = 0$, $L/h = 10$, $\eta_s = 0.5$, $K_p = K_w = 0$, and $\beta = 0.1$, for various boundary conditions.....	92
Figure 4.18	Effect of Dimensionless nonlocal parameter (α) on the instability region for sandwich FG micro beam (Modal II) with $k = 2$, $\eta_s = 0.5$, $L/h = 10$, $\Delta T = 0$, $K_p = K_w = 0$, and $\beta = 0.1$	93
Figure 4.19	Effect of cross sectional types on the instability region for sandwich FG micro beam (Modal II,III) with $k = 2$, $\eta_s = 0.5$, $L/h = 10$, $l_m = h$, $\Delta T = 0$, $K_p = K_w = 0$, and $ea = 0.5h$ for various boundary conditions.....	95
Figure 4.20	Effect of boundary conditions various on the instability region for sandwich FG micro beam (Modals I, II, III) for cross section shapes (1-1-1) and (1-8-1) with $k = 2$, $\Delta T = 0$, $L/h = 10$, $\eta_s = 0.5$, $K_p = K_w = 0$, and $\beta = 0.1$	96
Figure 4.21	Effect of dimensionless Pasternak shear parameter (K_p) on the instability region for sandwich FG micro beam (Modal II, III) for cross section shapes (1-1-1) with $k = 2$, $\Delta T = 0$, $L/h = 10$, $l_m = h$, $\eta_s = 0.5$, $K_w = 0$ and $ea = 0.5h$ for various boundary conditions.....	98
Figure 4.22	Effect of dimensionless Winkler shear parameter (K_w) on the instability region for sandwich FG micro beam (Modal II, III) for cross section shapes (1-1-1) with $k = 2$, $\Delta T = 0$, $L/h = 10$, $l_m = h$, $\eta_s = 0.5$, $K_p = 0$ and $ea = 0.5h$ for various boundary conditions.....	99
Figure 4.23	Variation of the dimensionless transverse deflection \bar{w} with the power-law exponent k for different cross-section shape sandwich FG microbeam, $L/h = 10$, $\alpha = 0.1$, $\beta = 0.2$, and for different boundary conditions.....	106
Figure 4.24	Effect of the nonlocal parameter (α) on the dimensionless transverse deflection \bar{w} of sandwich FG microbeam with a various boundary conditions (S-S, C-S, C-C) for different power law index (k) with $L/h = 10$, $K_p = K_w = 0$, $\Delta T = 0$, $\beta = 0.2$ and cross section shape (1-2-1).....	112
Figure 4.25	Effect of the material length scale parameter (β) on the dimensionless transverse deflection \bar{w} of sandwich FG microbeam with a various boundary conditions (S-S, C-S, C-C) for different power law index (k) with $L/h = 10$, $K_p = K_w = 0$, $\Delta T = 0$, $\alpha = 0.2$ and cross section shape (1-2-1).....	113

Figure 4.26	Effect of the nonlocal parameter (α) and the dimensionless material length scale parameter on the dimensionless transverse deflection \bar{w} of sandwich FG microbeam with a cross section shape (1-1-1) and S-S boundary conditions for $k = 2$, $L/h = 10$, $K_p = K_w = 0$, and $\Delta T = 0$	114
Figure 4.27	Thermal effect on the dimensionless transverse deflection, (\bar{w}) with $\alpha = 0.1$, $L/h = 10$, $K_p = K_w = 0$, $\beta = 0.2$ and cross section shape (1-2-1) sandwich FG micro-beam Model III.....	116
Figure 4.28	Effect of the Winkler and Pasternak shear parameter on the dimensionless transverse deflection, \bar{w} for $L/h = 10$, and $\alpha = 1, \beta = 2$. of SS sandwich microbeam for Model III (1-1-1) .(a) $K_w = 0$ (b) $K_p = 0$ with various boundary conditions.....	119
Figure 4.29	Variation of the dimensionless fundamental frequency $\bar{\omega}$ with the power-law exponent k for different cross-section shape sandwich FG microbeam, $L/h = 10$, $\alpha = 0.1$, $\beta = 0.2$, and for different boundary conditions.....	124
Figure 4.30	Variation of the dimensionless buckling load \bar{P} with the power-law exponent k for different cross-section shape sandwich FG microbeam, $L/h = 10$, $\alpha = 0.1$, $\beta = 0.2$, and for different boundary conditions.....	125
Figure 4.31	Effect of the nonlocal parameter (α) on the dimensionless buckling load \bar{P} of sandwich FG microbeam with a various boundary conditions (S-S, C-S, C-C) for different power law index (k) with $L/h = 10$, $K_p = K_w = 0$, $\Delta T = 0$, $\beta = 0.2$ and cross section shape (1-2-1).....	133
Figure 4.32	Effect of the nonlocal parameter (α) on the dimensionless fundamental frequency $\bar{\omega}$ of sandwich FG microbeam with a various boundary conditions (S-S, C-S, C-C) for different power law index (k) with $L/h = 10$, $K_p = K_w = 0$, $\Delta T = 0$, $\beta = 0.2$, and cross section shape (1-2-1).....	134
Figure 4.33	Effect of the material length scale parameter (β) on the dimensionless buckling load \bar{P} of sandwich FG microbeam with a various boundary conditions (S-S, C-S, C-C) for different power law index (k) with $L/h = 10$, $K_p = K_w = 0$, $\Delta T = 0$, $\alpha = 0.2$ and cross section shape (1-2-1).....	135
Figure 4.34	Effect of the material length scale parameter (β) on the dimensionless fundamental frequency $\bar{\omega}$ of sandwich FG microbeam with a various boundary conditions (S-S, C-S, C-C) for different power law index (k) with $L/h = 10$, $K_p = K_w = 0$, $\Delta T = 0$, $\alpha = 0.2$ and cross section shape (1-2-1).....	136
Figure 4.35	The nonlocal parameter (α) and the dimensionless material length scale parameter on the dimensionless buckling load (\bar{P}) of sandwich FG microbeam	

with a cross section shape (1-1-1) and S-S boundary conditions for $k = 2$, $L/h = 10$, $K_p = K_w = 0$, and $\Delta T = 0$137

- Figure 4.36 Effect of the material length scale parameter (β) on the dimensionless buckling load \bar{P} of sandwich FG microbeam with a various boundary conditions (S-S, C-S, C-C) for different power law index (k) with $L/h = 10$, $K_p = K_w = 0$, $\Delta T = 0$, $\alpha = 0.2$ and cross section shape (1-2-1).....138
- Figure 4.37 Effect of the Winkler and Pasternak shear parameter on the dimensionless fundamental frequency, ($\bar{\omega}$) for $L/h = 10$, and $\alpha = 1$, $\beta = 2$ of SS sandwich microbeam for Model III (1-1-1) .(a) $K_w = 0$ (b) $K_p = 0$ with various boundary conditions.....145
- Figure 4.38 Effect of the Winkler and Pasternak shear parameter on the dimensionless buckling load, (\bar{P}) for $L/h = 10$, and $\alpha = 0.1$, $\beta = 0.2$ of SS sandwich microbeam for Model III (1-1-1). (a) $K_w = 0$ (b) $K_p = 0$ with various boundary conditions.....146
- Figure 4.39 Thermal effect on the dimensionless fundamental frequency, $\bar{\omega} = \omega L \sqrt{\rho_m / E_m}$ with $k = 2$, $K_p = K_w = 0$, $\alpha = 0.1$, $\beta = 0.2$ and cross section shape (1-2-1) sandwich FG micro-beam.....150
- Figure 4.40 Thermal effect on the dimensionless critical buckling load $\bar{P} = P / E_m b h$ with $k = 2$, $K_p = K_w = 0$, $\alpha = 0.1$, $\beta = 0.2$, and cross section shape (1-2-1) sandwich FG micro-beam.....151
- Figure 4.41 Variation of the dimensionless fundamental frequency ($\bar{\omega}$) and buckling load (\bar{P}) with the power-law exponent k for cross-section shape (1-1-1) sandwich FG microbeam, $L / h = 10$, $\alpha = 0.1$, $\beta = 0.2$, and for different boundary conditions.....152

LIST OF TABLES

		Page
Table 4.1	Non-Dimensional transverse deflection, $(\bar{w} = 100 E_m I / q L^4 w)$ of the functionally graded nano-beam Model I with the distributed load.....	72
Table 4.2	Dimensionless critical buckling load $(\bar{P} = PL^2 / E_m I)$ of the FG nanobeam Model I.....	73
Table 4.3	Dimensionless critical buckling load $(\bar{P} = P / E_m b h)$ of sandwich FG beams Model III resting on elastic foundation with $K_w, K_p, L/h = 10, k = 0.5, \beta = 0, \alpha = 0$ and $\Delta T = 0$	75
Table 4.4	Dimensionless natural frequency $(\bar{\omega} = \omega L \sqrt{\rho_m / E_m})$ of sandwich FG beams Model III resting on elastic foundation with $K_w, K_p, L/h = 10, k = 0.5, \beta = 0, \alpha = 0$ and $\Delta T = 0$	76
Table 4.5	First three natural frequency of FG microbeams with various boundary conditions under the effect of gradient index, k with $ea = 0.1h$ and $l_m = h$	78
Table 4.6	Material properties of the FGM microbeam constituent.....	100
Table 4.7	Dimensionless transverse deflection $\bar{w} = 100 E_m I / q L^4 w$ of sandwich beams under distributed load for $L / h = 10, \Delta T = 0, K_p = K_w = 0$, and Model II, III (1-1-1)	102
Table 4.8	Dimensionless transverse deflection $\bar{w} = 100 w E_m I / q_0 L^4$ of sandwich microbeams with B.Cs with a cross-section shape (1-1-1) for $\alpha = 0.1, \Delta T = 0, k = 1, K_p = K_w = 0$,	104
Table 4.9	Dimensionless transverse deflection $(\bar{w} = 100 w E_m I / q_0 L^4)$ of sandwich FG microbeams (PSDBT) for various power law index $L / h = 10 \beta = 0.2, \alpha = 0.1$, and $K_p = K_w = 0$,	108
Table 4.10	Dimensionless transverse deflection $\bar{w} = 100 w E_m I / q_0 L^4$ of sandwich FG microbeams Model II,III with various B.Cs with a cross-section shape (1-1-1) for $L/h = 10, \Delta T = 0, k = 1 K_p = K_w = 0$,	110

Table 4.11	Dimensionless transverse deflection ($\bar{w} = 100 w E_m I / q_0 L^4$) of sandwich FG microbeams (PSDBT) with $k = 1$, $L / h = 10$, $\beta = 0.2$, $\alpha = 0.1$, and $K_p = K_w = 0$,	115
Table 4.12	Dimensionless transverse deflection $\bar{w} = 100 w E_m I / q_0 L^4$ of sandwich FG microbeams for $\Delta T = 0$, $\beta = 0.2$, $\alpha = 0.1$ and $k = 2$ with different cross section, aspect ratio, various boundary conditions and elastic foundations.....	118
Table 4.13	Dimensionless natural frequency $\bar{\omega} = \omega L^2 / h \sqrt{\rho_m / E_m}$ of sandwich microbeams with C-S B.C with a cross-section shape (1-1-1) for $\Delta T = 0$, $k = 1$, $K_p = K_w = 0$,	121
Table 4.14	Dimensionless critical buckling load $P_{cr} = \bar{P}_{cr} L^2 / E_m I$ of sandwich microbeams with various B.Cs with a cross-section shape (1-1-1) for $\Delta T = 0$, $k = 1$, $K_p = K_w = 0$,	122
Table 4.15	Dimensionless natural frequency $\bar{\omega} = \omega L^2 / h \sqrt{\rho_m / E_m}$ of sandwich FG microbeams (PSDBT) for various gradient index $L/h = 10$, $\beta = 0.2$, $\alpha = 0.1$, $\Delta T = 0$ and $K_p = K_w = 0$,	127
Table 4.16	Dimensionless critical buckling load $\bar{P} = P L^2 / E_m I$ of sandwich FG microbeams (PSDBT) for various power law index $L/h = 10$, $\Delta T = 0$, $\beta = 0.2$, $\alpha = 0.1$, and $K_p = K_w = 0$,	128
Table 4.17	Dimensionless critical buckling load $P_{cr} = \bar{P}_{cr} L^2 / E_m I$ of sandwich microbeams with various B.Cs with a cross-section shape (1-1-1) for $\Delta T = 0$, $k = 1$ $K_p = K_w = 0$,	130
Table 4.18	Dimensionless natural frequency $\bar{\omega} = \omega L^2 / h \sqrt{\rho_m / E_m}$ of sandwich microbeams with various B.Cs with a cross-section shape (1-1-1) for $\Delta T = 0$, $k = 1$ $K_p = K_w = 0$,	131
Table 4.19	The three dimensionless natural frequency $\bar{\omega} = \omega L^2 / h \sqrt{\rho_m / E_m}$ of sandwich FG microbeams Model II (PSDBT) with C-C B.C for $L/h = 10$, $\beta = 0.2$, $\alpha = 0.1$ and $K_p = K_w = 0$	139
Table 4.20	The three dimensionless natural frequency $\bar{\omega} = \omega L^2 / h \sqrt{\rho_m / E_m}$ of sandwich FG microbeams Model III (PSDBT) for $L/h = 10$, $\beta = 0.2$, $\alpha = 0.1$, and $K_p = K_w = 0$,	140

Table 4.21	Dimensionless natural frequency $\bar{\omega} = \omega L \sqrt{\rho_m / E_m}$ of sandwich FG microbeams for $\Delta T = 0$, $\beta = 0.2$, $\alpha = 0.1$, and $k = 2$, with different cross section, aspect ratio, various boundary conditions and elastic foundations.....	142
Table 4.22	Dimensionless critical buckling load $\bar{P} = P / E_m b h$ of sandwich FG microbeams for $\Delta T = 0$, $\beta = 0.2$, $\alpha = 0.1$, and $k = 2$, with different cross section, aspect ratio, various boundary conditions and elastic foundations.....	143
Table 4.23	Dimensionless natural frequency $\bar{\omega} = \omega L^2 / h \sqrt{\rho_m / E_m}$ of sandwich FG microbeams (PSDBT) with $k = 1$, $L/h = 10$, $\beta = 0.2$, $\alpha = 0.1$, and $K_p = K_w = 0$,.....	147
Table 4.24	Dimensionless critical buckling load $\bar{P} = P L^2 / E_m I$ of sandwich FG microbeams (PSDBT) with $k = 1$, $L/h = 10$, $\beta = 0.2$, $\alpha = 0.1$, and $K_p = K_w = 0$,.....	148

ABSTRACT

DYNAMIC STABILITY ANALYSIS OF FUNCTIONALLY GRADED SANDWICH MICRO-BEAMS

Mohammed Al-SHUJAIRI

Department of Civil Engineering

Ph.D Thesis

Adviser: Assist. Prof. Dr. ÇAĞRI MOLLAMAHMUTOĞLU

In this thesis, the static, buckling analysis, free vibration and dynamic stability of size-dependent sandwich functionally graded micro-beam under the action of parametric excitation loads resting on elastic Winkler and Pasternak foundations with temperature change is investigated. Based on the nonlocal strain gradient theory (NLSGT) in conjunction with the various higher-order deformation beam theories (HOBTs), Timoshenko beam theory (TBT) and Euler beam theory (EBT) with Hamilton's principle, the governing equations of motion and corresponding various boundary conditions were obtained. The material properties of the FG part of sandwich micro-beam are varied gradually through the thickness of the micro-beam are calculated by using the Mori-Tanaka homogenization scheme and classical rule of mixture. The dynamic stability, transverse deflection, critical buckling and fundamental frequency can be determined with various boundary conditions (i.e. C-C, C-S, and S-S) by using the generalized differential quadrature method (GDQM). The sandwich FG micro-beam is considered with three different models and various cross section shapes. The Models are functionally graded material (FGM) homogeneous microbeam (Model I), a sandwich beam with FGM core and two homogeneous ceramic and metal skins (Model II) and a sandwich beam with homogeneous core with ceramic and FGM top and bottom skins (Model III). The influence of the dimensionless nonlocal parameter (α), the dimensionless length scale parameter (β), slenderness ratio (L/h), material property gradient index (k), static load factor (η_s), temperature change (ΔT) and various cross section shapes on the dynamic stability, static bending, buckling and free vibration of the sandwich micro-beam are

discussed. To verify the present formulation and the present results (dynamic stability, static, buckling and free vibration), some of the current results are compared with the previously published results. Good agreement is observed.

Keywords: Generalized differential quadrature (GDQ) method; functionally graded material; size dependent sandwich micro-beam; nonlocal strain gradient theory, higher-order shear deformation beam theory ; Dynamic stability.



YILDIZ TECHNICAL UNIVERSITY
GRADUATE SCHOOL OF NATURAL AND APPLIED SCIENCES

**FONKSİYONEL DERECELENDİRİLMİŞ SANDVIÇ MİKRO
KİRİŞLERİN DİNAMİK STABİLİTE ANALİZİ**

Mohammed Al-SHJUAIRI

İNŞAAT MÜHENDSİLİĞİ BÖLÜMÜ

Doktora Tezi

Tez Danışmanı: Dr. Öğr. Ü. ÇAĞRI MOLLAMAHMUTOĞLU

Bu çalışmada Winkler ve Pasternak tipi elastik zemin üzerine mesnetlenmiş mikro sandviç kirişlerin statik, serbest titreşim burkulma ve dinamik stabilite analizleri termal etkiler altında incelenmiştir. Yerel olmayan birim şekil değiştirme gradyeni teorisi bağlamında değişik kiriş teorileri kullanılarak (Euler- Bernoulli, Timoshenko ve diğer yüksek mertebeden teoriler) Hamilton prensibinin uyarlanması sonucunda hareket denklemleri ve sınır koşulları elde edilmiştir. Mikro sandviç kirişin malzeme özellikleri yükseklik boyunca sürekli değiştiği varsayılmış ve eşdeğer özellikler Mori Tanaka ve klasik karışım kurallarına göre hesaplanmıştır. Elde edilen denklemlerin genelleştirilmiş diferansiyel quadratür metodu ile çözümü neticesinde değişik sınır koşulları altında (ankestre, serbest, basit) mikro kirişin statik eğilme, serbest titreşim frekansı ve kırık burkulma yükleri bulunmuştur. Sandviç yapısı olarak üç değişik form model kabul edilmiştir. Bunlar sandviç yapıya sahip olmayan her yeri fonksiyonel derecelendirilmiş baz Model I, orta kısmı fonksiyonel derecelendirilmiş alt ve üst kısmı homojen metal veya seramik Model II ile orta kısmı homojen seramik olup alt ve üst kısmı fonksiyonel derecelendirilmiş Model III' tür. Yerel olmayan teoriye ait parametre (α), karakteristik malzeme parametresi (β), boy/yükseklik oranı (L/h), malzeme karışım oranı (k), statik yük katsayısı (η_s), ve sıcaklık değişimi (ΔT) gibi parametrelerin statik eğilme,

serbest titreşim frekansı, kritik burkulma yükü ve dinamik stabilite üzerine etkileri irdelenmiştir. Formülasyonun bu sonuçlar için mükemmel çözümler ürettiği görülmüştür.

Anahtar Kelimeler: Genelleştirilmiş diferansiyel quadratür metodu; Fonksiyonel derecelendirilmiş malzeme; Boyut etkisi olan sandviç mikro kiriş; Yerel onamayan şekil değiştirme gradyeni teorisi; Yüksek mertebe kayma kirişi teorisi; Dinamik stabilite.



INTRODUCTION

1.1 Literature Review

A new category of composite material name functionally graded material, have been broadly explored in the past few years due to their distinct features. FGMs are materials consisting of a combination of two different separate components with continuous gradient characteristics; both mechanical and physical. FGMs have numerous benefits compared to other material structures due to their continuous gradient characteristics. Normally these features change along particular directions for example along the thickness or axial directions. Generally FGMs are composed of metal and ceramic; metal prevents material from breaking when subjected to heat stress while ceramic which high thermal resistance-low strength and offers resistance at extreme temperatures. Together these materials are characterized by toughness, high strength and resistance to high temperature and corrosion. The idea of FGM was suggested at the first in 1984 during the space plane project in Japan by an association of material scientists. In conventional composite materials the distinct property differences of constituent materials stress may sometimes occur at the interfaces between two different constituent materials due to mismatches in the material properties. FGMs overcome this problem make composites applicable in airplanes, vehicles, military and defense projects, space crafts, biomedical field, electronics, energy and engineering constructions. Due to the numerous benefits of FGMs, in recent years there has been research and scientific publications on the dynamic stability, dynamic, and buckling properties of FGM. Additionally there have also been efforts to better understand the mechanical performance of FGM.

Among various configurations, one of the important specific forms of composite structures is so called sandwich form. Because of their high strength-weight ratio, sandwich structures have extensively been employed in may engineering applications like airplanes, space crafts,

marine and many other fields. Normal sandwich structures consist of a soft core bonded to two skins usually made from tough material. These structures usually exhibit delamination failures at the bond interfaces where the integration of different constituent materials causes abrupt changes in material properties. To overcome this problem, the sandwich FG structure are used. In sandwich FG structures, either the core or skins are formed from FGMs. In this case the characteristics of the composite materials change smoothly from one surface to the another, hence avoiding concentrated stress levels usually developed in layered materials. Sandwich structures made of FGMs exhibit improved characteristics for example higher stiffness, long fatigue life, and thermal resistances, etc. For this reason FG sandwich materials are vastly used in aerospace, civil and automotive industries. To realize more durable and economically friendly structures it is necessary to consider the properties of FG sandwich structures. This is due to the sandwich functionally graded micro-beam have been of great interest in the past few years. Despite this fact, minimal research has been undertaken on the properties of sandwich functionally graded micro-beam.

In kinematical aspect there are many beam theories which have been widely used to examine the behavior of FG beam structures. First of all the Euler-Bernoulli beam theory (EBBT) is based on the assumption that the plane cross sections of beam remain plane and normal to the deformed axis of the beam after bending. This theory is very useful for a thin beam (slender beam). On the other hand as the beam becomes thicker, then EBBT should be modified to include the ever increasing effect of the transverse shear. For moderately deep FG beam structure, CBT overestimates fundamental frequencies and buckling loads and underestimates deflection due to neglecting the effect of transverse shear deformation. In order to include this effect, Timoshenko beam theory (TBT) or the first order shear deformation beam theory (FSBDT) was suggested. Due to FSBDT cross-sections remain plane but no longer remain normal to the mid-plane after deformation. FSBDT assumed shear deformation with relaxing the kinematics with an additional rotation of the cross-section due to shear deformation. This corresponds to constant shear deformation through the depth of the beam hence a shear correction factor is required in order to take into account the shear stress variation on the cross section. An additional improvement can be introduced by assuming the variation of shear stress distribution. Higher-order shear deformation beam theories consider this effect as they take into account the warping of the cross-section and they satisfy the zero transverse shear stress boundary conditions of the beam's top and bottom free surfaces. There are various higher order theories depending on the assumption they made for the nature of the shear stress distribution. The well-known higher order beam theories are the parabolic shear deformation

beam theory (PSDBT) [74], trigonometric shear deformation beam theory (TSDBT) [75], hyperbolic shear deformation beam theory (HSDBT) [76], exponential shear deformation beam theory (ESDBT) [77], and a recently published shear deformation beam theory (ASDBT) [78].

Micro-beams are most prevalent structures in Micro-Electromechanical Systems (MEMS) and Nano-Electromechanical Systems (NEMS). They make up the elements structured as thin film Shape Memory Alloys of micro and nano scale [86], electrically excited MEMS devices [87] and Atomic Force Microscopes [88]. Size effect is very important in these applications and therefore studies should be conducted to understand the characteristics of these small scale configurations. The classical continuum theory is not able to take into account the size effect seen in microstructures since it does not have any additional micro scale considerations to define structures of this scale. It is therefore necessary to revise the traditional elasticity theory to deal with the size dependent behavior. A number of higher order continuum theories have been initiated in the past few years to developed size dependent elastic models. In order to take into consideration the size effect, Eringen[79] suggested the nonlocal theory of elasticity which is among the size dependent theories of continuum. According to Eringen's theory stress field at a reference point does not depend on the strain at this point but also depends on the strains at the neighbor points in the continuum. For the last decade the theory of Eringen have been particularly utilized to examine the behavior of size dependent beams to investigate the static, buckling and also free vibration analysis of micro structures [11-29]. Although the theory of nonlocal elasticity by Eringen's has been extensively applied in the design of microstructures this theory only represents the softening behavior of structures and is not able to show the effect of stiffness enhancement. As another approach to the problem Aifantis[84] came up with the strain gradient theory. This theory consists of a single microscale parameter making it better than the strain gradient theory by Mindlin[81] that has five additional parameters. Aifantis theory has been utilized for various microstructural analysis problems. For example, K. G. Tsepoura et al [113] have solved the problem of a bar under static loading, wave propagation analysis and forced longitudinal vibrations based on the Aifantis's strain gradient theory. S. Papargyri-Beskou et al [114] studied the bending and buckling of Bernoulli–Euler beams based on the Aifantis Strain gradient theory. The governing equations of equilibrium for both bending and buckling problems were derived both by combining the corresponding basic equations and by using a variational statement. At the end Aifantis's theory has the ability of reflecting micro-structural stiffness enhancement unlike the Eringen's nonlocal theory.

Recently Lim, Zhang, and Reddy [47] published a paper in which the theory of Eringen is used together with strain gradient theory by Aifantis to come up with a hypothesized hybrid theory known as nonlocal strain gradient theory. This suggested theory depends on the structure of thermodynamics on wave propagation in TBT and EBBT. The NLSGT asserts that stress accounts for both non-gradient nonlocal stress field [79] and higher order pure gradient stress field [80]. The model for nonlocal strain gradient consists of two separate small length-scale specifications; the nonlocal parameter (ea) and the material length scale parameter (l_m) for the material. The (l_m) takes into account the impact of strain gradient field while (ea) accounts for nonlocal elastic stress field.

Another important class of problems for MEMS development is concerning the dynamical stability of micro structures. One of the most common type of dynamic stability arises when the beam is under axially pulsating normal force which can be assumed harmonic in nature. The interaction between the frequency of the axial load and the beam's lateral vibration frequency may result in parametric instabilities and usually failure which can occur at much lower load levels than the static buckling load. Thus determining the regions of safe operation conditions so that beam is operating outside of the instability regions is utmost importance in the design of micro-beam structures under the effect of a variable axial load.

1.2 Objective of the Thesis

The objectives of thesis will be:

- 1- Investigation of the dynamic stability of sandwich micro-beam in the frame work of HOBTs.
- 2- Study of the static bending, free and buckling analysis of sandwich FG micro-beam by using different HOBTs based on NLSGT.
- 3- Examination the effect of the dimensionless nonlocal parameter(α), the dimensionless material length scale parameter(β), aspect ratio(L/h), power law index(k), dimensionless elastic foundation with Winkler and Pasternak springs(K_p, K_w), temperature change(ΔT), static load factor (η_s) and various the cross section shapes on the dynamic stability, static, free and buckling analysis of a sandwich FG micro-beam.

4- Using the GDQ method, different boundary conditions (i.e. Simply-Simply, Clamped-Simply, Clamped-Clamped) and several types of Model with different cross section shapes will be considered to illustrate the effects on the dynamic stability, buckling analysis, free vibration and static bending, of sandwich FG micro-beam in detail.

1.3 Hypothesis

This study investigates the static, buckling analysis, dynamic stability and free vibration of size dependent sandwich FG microbeam based on the various higher order beam theories (HOBTs) in conjunction with nonlocal strain gradient theory (NLSGT) resting on two elastic foundation including Winkler and Pasternak shear layer springs and thermal effect.

Studies of the dynamic instability problem, static bending, buckling and free vibration of the sandwich FG micro-beams are very limited when compared these with the ordinary (homogeneous) FG micro-beams. In addition, to the best of authors' knowledge, there is not any reported study related with the dynamic stability of FG sandwich microbeam which is based on the NLSGT formulation in conjunction with the HOBTs with different boundary conditions.

1.4 Structure of the thesis

The thesis is arranged in five chapters. **Chapter one** presents a general introduction to the functionally graded material, sandwich FG and micro-structures and enlists the main objectives of the thesis. **Chapter two** provides a literature review of the former research in compliance with the investigated categories of the thesis. Previous researches about the sandwich FG beam, the nonlocal elasticity, the Strain gradient, nonlocal strain gradient theories and dynamic stability were explained in this chapter. **Chapter three** includes details of the governing equations and associated B.Cs of sandwich FG micro-beam and solved with numerical and analytical solutions. **Chapter four** presents and discusses the results which were obtained from the numerical solutions. **Chapter five** provides the summary and the conclusions of the work, and a number of recommendations for future work.

CHAPTER 2

LITERATURE REVIEW

The subject of the present thesis investigates the static, buckling, free analysis and dynamic stability of the size-dependent sandwich FG micro-beam subjected to parametric excitation with the NLSGT in conjunction with different HOBTs with resting on two elastic foundations including Winkler and Pasternak shear layer springs and thermal effect, the literature review contain the five main parts.

2.1 Sandwich FG beam structures

Nguyen T.K. et al [1] have investigated free vibration and buckling analysis of sandwich FG beam based on the HOBTs. The equations of motion and also the corresponding B.Cs can be derived by using the Lagrange's equations and solved these equations analytical to give the buckling loads and natural frequency for sandwich FG beam structure in conjunction with various boundary conditions. There are many parameter influences on the fundamental frequency (ω) and buckling loads (P) of the sandwich FG beam are investigated such as different boundary conditions, aspect ratio, material property gradient index and different cross-section shape (the ratio of core to the skins). The properties of material for sandwich FG beam changing smoothly through the thickness direction [1].

Nguyen T.K. et al [2] have illustrated free vibration and buckling analysis of sandwich FG beams structures based on the Quasi-3D shear deformation beam theory with various boundary conditions. The governing equation and the relate B.Cs can be derived via the Lagrange's equations. These equations can be solved by a Ritz-type analytical solution in order to obtain the buckling loads and natural frequency. There are two kinds of the sandwich FG beam, firstly Model A with FG two skins and ceramic core and the second one is FG core and homogenous skins. The influence parameters with different boundary conditions and

various cross-section shapes on the buckling loads and the fundamental frequency of sandwich FG beam are investigated [2].

Vo T.P. et al [3] have investigated the static of sandwich FG beam structure based on the Quasi-3D shear deformation beam theory with finite element model. There are many types of different cross-section shapes with symmetric and non-symmetrically FG sandwich beam under the action of the point and uniform load. Three kinds of sandwich FG beam (I.) full FG beam, (II.) FG skins and ceramic core and (III.) FG core with homogenous skins. Using the principle of total potential energy to derive the equations of motion and the corresponding boundary conditions and solve analytically by Navier solutions to obtain the deflection and stresses of sandwich FG beam with different gradient index and various core section shape [3].

Vo T.P. et al [4] have presented buckling analysis and free vibration of sandwich FG beam conjunction with HOBTs conjunction with finite element model. The skins of the FG sandwich beam structure is the functionally graded material and the core is ceramic or metal. According to the Hamilton's principle, the governing equations and the corresponding B.Cs are derived. The effect of aspect ratio, power-law index, different boundary conditions and various cross-section shapes on the buckling load and the fundamental frequency of sandwich FG beams, are illustrated [4].

Yang Y. et al [5] have studied free vibration of the sandwich FG beams based on meshfree boundary-domain integral equation method with finite element method. There are two types of sandwich FG beam, I. homogeneous skin sheets with FG core, II. FG skin sheets and homogeneous core are developed. The material properties such as the stiffness modulus and the density of the material are changing smoothly in the transverse direction by using the exponential function. The equations of motion and the corresponding B.Cs are derived based on the two-dimensional elasticity theory. The influence of power-law index, different boundary conditions, slenderness ratio and cross-section types on the free vibration of sandwich FG beams are discussed [5].

Tossapanon P. et al [6] have illustrated the buckling and free analysis of the sandwich FG beams structure with the FSDBT with Winkler and Pasternak elastic foundations. The structure of sandwich FG beam consists of top and bottom faces made of functionally graded material and core with the ceramic material. The governing equations and the related B.Cs can be derived by using the Chebyshev collocation (CC) method and then used to obtain the fundamental frequency and critical buckling loads with several boundary conditions of FG

sandwich beams. The material properties like Young's modulus is changed gradually across the thickness direction by using the Mori–Tanaka scheme [6].

Şimşek M. et al [7] investigated the static, forced and free analysis of sandwich FG beams with TBT subjected to two successive moving harmonic loads with constant velocity. There are three types of sandwich FG beam I. FGM isotropic beam, II. FGM core with the homogeneous skins and III. FGM skins with the homogeneous core (ceramic). According to the rule of mixture method the material properties of FG part of sandwich FG beam will vary gradually across the thickness. The governing equations and the related different B.Cs are derived by Lagrange's equations, and solved these equations to find the dimensionless transverse deflection and the fundamental frequency via implicit time integration method of Newmark- β . The influences of several parameters such as power-law index, different models, various cross-section shapes, different boundary conditions and the distance between the two double harmonic forces on the static, free and forced of FG sandwich beam is discussed [7].

Luan T. et al [8] investigated the free vibration of FG sandwich beam in conjunction with EBBT, TBT and HOBTs. According to Hamilton's principle the governing equations and different classical and non-classical B.Cs are derived and using the analytical solution to solve these equations and find the natural frequency of FG sandwich beam. The effect of the power-law index, slenderness ratio, various boundary conditions and core to the skins ratio on the fundamental frequency are investigated [8].

Thuc V. et al [9] have examined the buckling and free vibration of the functionally graded sandwich beam with finite element model based on a quasi-3D shear deformation beam theory. The governing equations and relate B.Cs are derived by using Hamilton's principle. The sandwich FG beam is considered with two types, firstly with ceramic core and functionally graded faces and the other one the FG core with the ceramic and metal material for the top and bottom faces, respectively. The influence of power-law index, different boundary conditions, mode shape and cross-section shape on the fundamental frequency and buckling load of sandwich FG beam are examined [9].

Huu-Tai T. et al [10] have examined buckling analysis, free vibration and static of small size FG sandwich microbeam based on the modified couple stress theory (MCST) with TBT theory. According to the Mori–Tanaka homogenization the material properties vary gradually through the thickness direction for FG part of sandwich FG microbeam. FG core with homogenous faces and FG faces with ceramic core are considered for sandwich FG micro-

beam. The analytical solution is utilized to find the deflection, critical buckling and natural frequency for sandwich FG micro-beam with S-S boundary conditions [10].

2.2 The nonlocal elasticity theory

Reddy J. [11] presented buckling, free vibration and static analysis of simply supported beam with various beam theories, EBBT, TBT and Reddy beam theory in conjunction with the nonlocal elasticity theory. The Hamilton principle is used to drive the governing equations and associated B.Cs of nonlocal beam theories. The bending deflection, critical buckling load, and the natural frequency are solved analytically. When the nonlocal parameter decreasing of nonlocal beam structure, the bending deflecting decrease and the buckling load and fundamental frequency increase [11].

Adali S. [12] have utilized the semi-inverse method to drive the variational principles for multi-walled carbon nanotubes subject to buckling loads based on the nonlocal theory of elasticity on an elastic foundation conjunction with the Euler–Bernoulli beams. As well as the natural and geometric various B.Cs are derived by using semi-inverse method [12].

Murmu T. et al [13] illustrated the dynamic stability of a single-walled carbon nanotube (SWCNTs) with Timoshenko beam theory subjected to elastic foundations with Winkler and Pasternak foundation based on nonlocal elasticity theory. A differential quadrature (DG) method is used to solve the equations of motion and associated B.Cs and obtain the numerical solution of buckling load. The effect of the nonlocal parameter, Winkler and Pasternak shear modulus and slenderness ratio on the buckling load for SWCNT are discussed. It can be observed that the buckling load increase with an increase of the Winkler and Pasternak parameters [13].

Buckling analysis for the single-walled carbon nanotube is studied by Pradhan S.C. et al [14] based on the nonlocal elasticity theory conjunction with differential transformation method (DTM) with different B.Cs embedded in the elastic foundation (Winkler foundation). The influence of many parameters on critical buckling force are discussed like nonlocal parameter and Winkler elastic modulus. It can be noticed the critical load ratio's decrease when the Winkler modulus decrease for three boundary conditions (C-C, S-S, C-H) because the more stiffness-hardening for the beam can be obtained with increase the Winkler modulus, but the load ratio increases with Winkler modulus decrease for C-F boundary condition [14].

R Ansari. et al [15] presented axial buckling behavior of small scale nonlocal elastic shell structure with single-walled carbon nanotubes (SWCNTs) subjected to the effect of temperature change. The Rayleigh-Ritz technique is used with the nonlocal elasticity theory

to solve the equation of motion and associated the various B.Cs. The effect of temperature change on SWCNTs by making softer and harder depending on low or high-temperature conditions. The effect of aspect ratio, thermal effect, various boundary conditions and nonlocal parameter on the axial buckling are discussed [15].

The static and buckling analysis of a small-scale FG nano-beam with EBBT and TBT are presented by Şimşek M. et al [16] based on a nonlocal elasticity theory. The minimum total potential energy principle is used to drive the governing equations and the relate B.Cs. Analytical solution of the FG nanobeam is obtained by using the Navier-type solution with simply-supported boundary condition. The power-law form is used to show the changing of the properties of small-scale FG nano-beam across the thickness direction. There are many parameters are influence on the static and buckling behavior of size-dependent FG nano-beam like slenderness ratio and nonlocal parameter are investigated [16].

Aydogdu M. [17] investigated static, buckling analysis and free vibration of small scale nanobeam with various beam theories, EBBT, TBT and HOBTs including Reddy, Levinson and Aydogdu beam theories based on the local elasticity and nonlocal elasticity Eringen theory. The influence of length of the beam and nonlocality on the static, buckling and free vibration size dependent nanobeam are investigated for each case [17].

Murmu T. et al [18] illustrated free vibration of small scale single-elastic walled carbon nanotubes (SWCNT) with thermal effect based on the nonlocal elasticity Eringen theory with EBBT. The SWCNT are embedded in the elastic foundation with Winkler foundation. Differential quadrature (DQ) method is utilized to solve the equation of motion and the corresponding boundary condition with simply supported ends for small scale carbon nanotubes. The effect of temperature variation, nonlocal parameter, shape modes and Winkler elastic constant on the free vibration of SWCNT is investigated [18].

Şimşek M. [19] studied forced vibration of size dependent an elastic single-walled carbon nanotube (SWCNT) subjected to a moving load based on the nonlocal Eringen theory conjunction with classical beam theory with a simply supported boundary condition. Using the modal superposition method and the Newmark's direct method to obtain the time-domain responses. Influence of nonlocal size-dependent effects, aspect ratio, velocity of the moving load on the fundamental frequency and static deflection of the elastic single-walled carbon nanotube, is presented. It can be observed that when the nonlocal parameter increases the static deflections of the SWCNT increase. In the other hand for free vibration, the influence of nonlocal parameter increases at the higher mode [19].

Şimşek M. [20] studied the forced vibration of two identical carbon nanotubes system engagement together by elastic spring subjected to a moving nanoparticle in conjunction with the nonlocal elasticity theory based on EBBT. The analytical solution of the equations of motion and the B.Cs can be solved by using the Galerkin method and the direct integration method of Newmark- β . The effect of slenderness ratio, nonlocal small scale, elastic spring constant and the moving nanoparticle on the force vibration are investigated. The deflections with the classical theory are always less than the deflection obtained by the nonlocal elasticity theory because of the nonlocal parameter. Here unlike a single carbon nanotubes system, there are two values of critical velocity for double carbon nanotubes system subject to a moving nanoparticle [20].

Eltaher M. et al [21] examined free vibration of small scale FG nano-beam with EBBT based on the nonlocal elasticity Eringen's theory. According to the rule of mixture method the material properties of small scale FG nano-beam change smoothly across the thickness. Hamilton's principle is used to drive the equations and relate B.Cs. The finite element method has solved the equation of motion and to discretize the model [21].

Thai H. [22] illustrated the static, buckling and free vibration of size dependent nano-beam based on the nonlocal elasticity Eringen's theory conjunction with the classical beam theory, the TBT and the HOBTs (Reddy's beam theory). Hamilton's principle is used to drive the equations of motion and the corresponding B.Cs. The transverse deflection, buckling load and the fundamental frequency are proposed with S-S boundary condition. It can be seen when increasing of nonlocal parameter, the buckling load and natural vibration decreasing, while as the deflection increase of particularly with the higher value of small nonlocal parameter [22].

Şimşek M. [23] Investigated the free vibration of small scale FG axial nanorod with the variable cross-section with the Eringen's elasticity theory. The fundamental frequency of axial FG tapered nanorod can be obtained by using the Galerkin method with different B.Cs. Using the rule of mixture, the material properties like modulus of elasticity and density of material are changing continues along the length direction of the size dependent FG tapered nanorod. The effect of many parameters on the free longitudinal vibration of AFG nanorod is illustrated such as taper ratio, different change of the cross-sectional area and small nonlocal parameter. For clamped-clamped boundary condition the influence of nonlocal parameter is more clear for size dependent AFG nanorod than the clamped- free boundary condition [23].

Rahmani O. et al [24] have presented the free vibration of FG nano-beam with TBT based on nonlocal Eringen's elasticity theory. The equations of motion and the relate B.Cs are derived via Hamilton's principle. According to the rule of mixture method, the material properties of

small scale FG nanobeam varies smoothly across the thickness but the Poisson ratio is constant across the thickness. Using the principle of minimum potential energy to solve the equation of motion and corresponding the boundary condition of small scale FG nano-beam. The influence the effect the parameters (aspect ratio, nonlocal parameter, and gradient index) on the fundamental frequency of FG nano-beam with S-S B.C are investigated [24].

Buckling analysis and free vibration of small scale FG micro-beam with thermal effect is investigated by Ebrahimi F. et al [25] based on the nonlocal elasticity theory with TBT. The analytical solution with Navier approach are used to solve the governing equations and the corresponding S-S B.Cs. The material properties with temperature change are changed gradually across the thickness of the small size FG micro-beam according to the rule of mixture. Hamilton's principle are used to drive the equations of motion and the relate B.Cs for the thermal buckling and free vibration of FG micro-beam. The influence of many parameters like nonlocal parameter, slenderness ratio, gradient index and temperature change on the on the buckling load and the fundamental frequency of size dependent FG micro-beam with thermal effect are investigated [25].

Also, Ebrahimi F. et al [26] studied free vibration of small scale FG microbeam with the EBBT based on nonlocal Eringen's elasticity theory. The governing equations and the corresponding B.Cs are derived by Hamilton's principle. The Navier approach are used to solve the governing equations and the relate B.Cs for size dependent FG microbeam. The material properties vary smoothly through the thickness by using the Mori-Tanaka homogenization. There are many parameters will be the influence on the natural frequency of size dependent FG microbeam such as length to the thickness ratio, small nonlocal parameter, the number of modes and different boundary conditions are presented [26].

Again Ebrahimi F. et al[27] illustrated the free vibration analysis of small scale FG nano-beam with temperature change based on the nonlocal Eringen's elasticity theory with the EBBT. The equations of motion and relate B.Cs are derived by Hamilton's principle. Differential transformation method (DTM) with a Navier approach is used to solve the equations of motion and the related various B.Cs (C-C) and (S-S). The effect of the temperature change, various boundary conditions, gradient index and mode number on the small scale FG microbeam are presented [27].

Mohammad N. et al [28] illustrated the buckling analysis of FG nano-beam with classical beam theory (CBT) based on the Eringen's elasticity theory. Here the properties of material of small scale FG nanobeam vary continuously through two directions with axial (length) and the thickness. The principle of minimum potential energy is used to drive the equations of

motion and the relate B.Cs. According to the Generalized differential quadrature method (GDQM), the governing equation can be solved and obtained the critical buckling load for size dependent FG nanobeam. In the end, there are many parameter effects on the buckling load like nonlocal parameter and gradient index [28].

Ansari R. et al [29] investigated the free vibration of size dependent FG nano-beam in the postbuckling domain with FSDBT based on the nonlocal elasticity theory. Hamilton principle is used to drive the equations and the relate different B.Cs (C-C), (C-S) and (S-S) for small size FG nanobeam. According to the generalized differential quadrature (GDQ) method, the nonlinear governing equation von Karman geometric nonlinearity and associated B.Cs are solved and then using the Newton Raphson technique to obtain the value of fundamental frequency [29].

2.3 The Strain gradient elasticity theory

Shengli K. [30] studied static and dynamic analysis of small scale beam with EBBT based on the strain gradient elasticity theory. According to the variational principle the governing equations and the related B.Cs are solved. There are three material length scale parameters and two classical material constant for this model [30].

Akgöz B. et al [31] illustrated static and the free vibration of micro-beam in conjunction with the HOBTs based on the modified strain gradient theory (MSGT). According to Hamilton's principle the governing equations and boundary condition with simply supported are derived. Analytical solutions with Navier approach are used to obtain the value of static deflection under the action of point load and distributed load and the fundamental frequency of the size dependent micro-beam. There are several parameters effects such as aspect ratio and material length scale parameter on the static deflection and natural frequency of microbeam are presented [31].

The static and the free vibration of size dependent microbeam with TBT is investigated by Binglei W. et al [32] based on strain gradient elasticity theory. Hamilton's principle is used to drive the equations of motion and relate boundary condition [32].

Akgöz B. et al [33] have investigated static analysis of small size micro-beam with the EBBT based on the modified strain gradient elasticity and modified couple stress elasticity theories. According to the variational principles the static deflection and rotation of small scale microbeam are used to drive the governing equations and corresponding with four B.Cs. These equations and the boundary conditions can be solved analytically to obtain the value of static deflection and rotation of microbeam. The effect of many parameters on the static

bending of the size dependent microbeam are illustrated like material length scale parameter and aspect ratio [33].

Yuming H. et al [34] illustrated the free vibration of the small size of FG cylindrical micro-shells based on the strain gradient elasticity theory with TBT. According to Mori–Tanaka scheme the properties of size dependent FG cylindrical micro-shells change continuously across the thickness direction. The governing equation and the related B.Cs are derived by Hamilton’s principle. Using double trigonometric series method is used to solve these equations and related B.Cs with S-S and C-C to predict the fundamental frequency of cylindrical FG micro-shells. Moreover, there are several parameters effect on the free vibration analysis of small scale micro-shells such as power law index, different boundary conditions, material length scale parameter and slenderness ratio with length and radius with thickness are investigated [34].

Wu J. [35] have illustrated the flexural waves propagating of multi-walled carbon nanotubes with FSDBT based on the gradient elasticity beam theory embedded in an elastic foundation with Pasternak foundation. The influences of the many parameters like Pasternak foundation constant and material length scale parameters on the transverse waves propagating of size dependent multi-walled carbon nanotubes are investigated [35].

Thai S. et al [36] studied the static, buckling and free analysis of small scale FG microplates based on the modified strain gradient elasticity theory in conjunction with the HOSDT with Reddy. The properties of material of FG microplate are assumed to change smoothly through the thickness direction according to the rule of mixture method. The equations of motion and related B.Cs are derived by Hamilton’s principle. There are many parameters influence on the static, buckling load and fundametal frequency of small size FG microplates such as power law index, various boundary conditions and shear deformation effect [36].

Akgöz B. [37] have investigated buckling analysis of size dependent nanobeam with the EBBT based on the modified couple stress (MCST) and modified strain gradient elasticity theory. The governing equations and the corresponding boundary condition with S-S and C-F of nano-beam are derived by the variational principle [37].

Kahrobaiyan M. et al [38] have studied small size non-classical beam elements with EBBT and the non-classical finite element method to capture the small scale dependent of nano or micro-beam based on the strain gradient theory. The mass matrices and stiffness matrices of a size-dependent beam with EBBT are derived by using the Galerkin’s method [38].

Bo Z. et al [39] have illustrated static bending, buckling analysis and free vibration of small scale micro-beam with Timoshenko beam theory based on the strain gradient elasticity theory.

the non-classical theory such as the strain gradient theory with three material length scale parameters to capture the size effect of the Timoshenko beam element [39].

The elastic bending of the bilayered size dependent microbeam with Clamped-Free boundary condition under the action of a moment at the free end in conjunction with the Euler-Bernoulli is investigated by Anqing L. et al [40] based on the strain gradient elasticity theory. According to the variational principle, the governing equations and the related B.Cs are derived [40].

Ansari R. et al [41] have illustrated the free vibration of small scale FG micro-beam with Timoshenko beam theory based on the strain gradient theory. By using the Mori-Tanaka homogenously scheme, the properties of material of small scale FG microbeam are change smoothly across the thickness direction. The equations of motion and the related B.Cs are derived by using Hamilton's principle of size dependent FG microbeam. The effect of several parameters on the natural frequency of FG micro-beam are investigated like aspect ratio, gradient index and material length scale parameter [41].

Ansari R. et al [42] have investigated the nonlinear free vibration analysis of small scale FG microbeam with EBBT and TBT based on the strain gradient elasticity theory with von Karman geometric nonlinearity. According to the rule of the mixture, the material properties of FG microbeam is change continuously across the thickness direction. The equations of motion and the corresponding B.Cs are derived according to Hamilton's principle. On the other hand, these equations and the related B.Cs can be solved by the (GDQ) method. There are many parameters are influence on the nonlinear free vibration of size dependent microbeam such as aspect ratio, gradient index and the material length scale parameters [42].

Ansari R. et al [43] have presented free vibration analysis of small size FG micro-beam based on the strain gradient theory in conjunction with HOBTs. The governing equations and the related B.Cs are employed on the basis of Hamilton's principle and solved these equations analytical by using the Navier approach. The influence of material length scale parameter, power law index and aspect ratio on the fundamental frequency of small size FG micro-beam are presented [43].

Amin S. et al [44] have illustrated the free vibration of small scale of FG microbeam with variable section carrying microparticles subjected to thermal effect based on the FSDBT in conjunction with modified strain gradient theory. The Chebyshev-Ritz method is used to derive the equations of motion and the related B.Cs to obtained the natural frequency of small scale FG microbeam. There are many parameters are used to show the influence of these parameters on the fundamental frequency of small scale FG microbeams such as material

length scale parameter, width taper ratio, gradient index and thermal effect. The material properties of size dependent FG microbeam with thermal effect are varied continuously through the thickness direction [44].

Hamid Z. et al [45] have presented free vibration of axial small scale FG nano-beam with EBBT based on the strain gradient elasticity theory with the elastic foundation as the visco-Pasternak foundation. The governing equations and the related S-S and C-C B.Cs are derived by using Hamilton's principle, and these equations are solved with the differential quadrature (DQ) method. The influence of the radius of the beam, material length scale parameter and the stiffness of the visco-Pasternak foundation on the fundamental frequency are studied [45].

Bo Z. et al [46] have illustrated static, buckling analysis and free vibration of the small size of FG microplates with the elastic foundation with Winkler–Pasternak foundation based on the strain gradient elasticity theory and HOBTs. According to the classical rule of the mixture, the properties of material for small scale FG microplate are changed smoothly across the thickness direction. According to Hamilton's principle, the equations of motion and the associated B.Cs with simply supported are derived. Many parameters are investigated on the static, buckling load and fundamental frequency of small scale FG microplate with material length scale parameter, power law index, slenderness ratio and elastic foundation constant [46].

2.4 Nonlocal strain gradient theory (NLSGT)

Lim C. & Reddy J. [47] combined the Eringen's elasticity theory and strain gradient theory (Aifantis's model) to present a new hybrid theory is called nonlocal strain gradient theory. Also developed the wave propagation with EBBT and TBT for carbon nanotubes (CNTs). For nonlocal strain gradient theory, the increase or decrease the stiffness model depending on the nonlocal parameter (ea) and material length scale parameter (l_m) [47].

Lu L. et al [48] investigated the free vibration of nano-beam structure with sinusoidal shear deformation beam theory based on the NLSGT with two parameters to capture the size dependent, a nonlocal parameter (ea) and a material length scale parameter (l_m). Hamilton's principle is used to derived the equations of motion and the related B.Cs. The fundamental frequency with analytical solutions can be obtained by using the Navier's method. The fundamental frequencies portended with the NLSGT are higher than those obtained by nonlocal theory and lower than those predicted by strain gradient theory. The size dependent

nano-beam exerts a stiffness-softening or a stiffness-hardening effect dependent on the nonlocal parameter and length scale material parameter [48].

Li L. et al [49] proposed the free vibration of small scale FG microbeam with EBBT and TBT based on the NLSGT. The Hamilton principle is employed to drive the equation of motions and related B.Cs. The analytical solutions of free vibration problem for S-S boundary condition will be solved with the Navier's solution. There are two parameters which the FG microbeam model contains, the first is material length scale parameter (l_m) and the other one is nonlocal parameter (ea). The fundamental frequency of FG microbeam decrease with decrease in the (l_m) or increase the (ea). The size dependent model exerts a stiffness-hardening effect when the (ea) is less than the (l_m), and the FG microbeam exerts stiffness-softening effect when the (ea) is larger than the (l_m) [49].

Li L. et al [50] presented static, buckling and free vibration analysis for small scale FG micro-beam conjunction with EBBT based on NLGRT. The properties of material of axial FG micro-beam change smoothly according to the rule of mixture along the length of the FG micro-beam. Using the (GDQ) method to obtain the critical buckling force and fundamental frequency with various B.Cs for FG micro-beam. The equations of motion and the corresponding B.Cs are derived via Hamilton principle. Two parameters are considered material length scale parameter and the nonlocal parameter for small scale FG axial microbeam structure to investigate designation of nonlocal elastic and strain gradient stress field respectively. Depending on the value of the (ea) and (l_m) the critical buckling force and fundamental frequency of axial size dependent FG micro-beam exert a stiffness-hardening and stiffness-softening [50].

Li L. et al [51] studied longitudinal vibration analysis of small scale rod based on the NLSGT. The analytical solutions are used to predict the fundamental frequency and mode shapes of small scale rod with various B.Cs. The Hamilton's principle is employed to drive the governing equation and the related B.Cs for size dependent rods. The longitudinal vibration analysis can be obtained by using the finite element method with classical and non-classical B.Cs [51].

Again Li L. et al [52] have investigated analytical solutions for the nonlinear post-buckling deflection and critical buckling loads of simply supported small scale axially FG nonlinear with EBBT based on NLSGT. The equations and the corresponding B.Cs can be derived by using Hamilton's principle. The critical buckling load increased with two way first via the

(ea) decreasing when the (l_m) is less than the (ea) and in other words by increasing the (ea) when the (l_m) is larger than the (ea) [52].

Li L. et al [53] developed the flexural wave propagation analysis for small scale FG beam in conjunction with EBBT based on the NLSGT. The relations between phase velocity and wave number are derived via the analytical solution. When the nonlocal parameter (ea) decreasing or the material length scale parameter (l_m) increasing the acoustical phase velocity increase. The material properties of small scale FG micro-beam grade continue through the thickness [53].

Farzad E. et al [54] illustrated damping vibration of size dependent FG viscoelastic nano-beam embedded in the viscoelastic foundation with HOBTs based on NLSGT subjected to hygro-thermal effects. The material properties with thermal effect various smoothly across the thickness of small scale FG nanobeam with Winkler-Pasternak and a viscous layer of infinite parallel dashpots. The equations and different B.Cs (S–S, C–S, and C–C) of size dependent FG nano-beam are solved by using Hamilton's principle with an analytical solution [54].

The nonlinear free vibration of a FG nano-beam with simple supports boundary condition was investigated by Şimşek M. [55] based on the NLSGT with the von-Kármán's geometric nonlinearity in conjunction with classical beam theory. Using Hamilton's principle to drive the governing equations and associated boundary condition. The material properties such as modulus of elasticity and density will change smoothly in the deep direction according to the simple rule of mixture. The Galerkin's method is utilized to reduce the nonlinear partial differential equations to the ordinary nonlinear differential equation with assuming the negligible of axial inertia. It can be observed that the nonlinear frequency ratio increase with the decrease of the dimensionless nonlocal parameter (α) and the increase with increase of the dimensionless material length scale parameter (β) [55].

Farzad E. et al [56] illustrated the wave propagation analysis for small scale FG nano-beam based on NSGT with thermal effect and assumed the properties of material change smoothly across the thickness of the FG nanobeam according to Mori-Tanaka homogenization. The wave frequencies and phase velocities of the size dependent FG nano-beam are found by applying an analytical solution. Also, it can be seen that the phase velocities decreasing and stiffened-softening with increase the nonlocal parameter (ea) and the phase velocities increasing and stiffened-hardening with increase the material length scale parameter (l_m) [56].

As well as Farzad E. et al [57] investigated buckling analysis of size dependent curve FG nano-beam conjunction with a HOBTs based on the NLSGT. Using Hamilton's principle to drive the equations of motion and corresponding boundary condition and solved analytically for S-S and C-C B.Cs. The rule of the mixture is used to graduate the material properties through the radial direction for size dependent curve FG microbeam. The critical buckling load decreasing with increasing opening angle. With increasing the nonlocal parameter (ea) leads to decreasing critical buckling load of curved FG nano-beam. Moreover, increasing the material length scale parameter (l_m) enhances the buckling loads. As well as, it can be observed that the effect of the two parameters on the small scale FG nanobeam conjunction with the lower opening angles is more significant than size dependent FG curved nanobeam with higher opening angles [57].

Farzad E. et al [58] have illustrated free vibration of FG curved nano-beam based on the NLSGT in conjunction with EBBT theory. The FG curved nanobeam resting on Winkler–Pasternak elastic foundation with different boundaries (C-C, C-S, and S-S) are illustrated. According to the Mori-Tanaka homogenization, the material properties of curved FG nanobeam vary gradually in the thickness direction. The equation of motion and the related B.Cs are derived by Hamilton's principle and solved analytically to find the natural frequency of curved FG nano-beams. There are several parameter effects on the fundamental frequency such as material length scale parameter (l_m), nonlocal parameter (ea), Winkler–Pasternak elastic medium, different B.Cs, aspect ratio and power law index are examined [58].

Li L. et al [59] have examined nonlinear bending and free vibration of FG micro-beam with EBBT and TBT based on the NLSGT. The Hamilton's principle is used to derive the governing equations and the related boundary condition. The analytical solution is used to solve these equations to obtain the bending deflection and natural frequency of size dependent nonlinear FG microbeam by using Navier solution and He's variational method. The material properties of FG microbeam are varied smoothly through the thickness via the rule of mixture method. The effect of gradient index, nonlocal parameter (ea), material length scale parameter (l_m) on nonlinear FG microbeam are examined [59].

The free vibration of viscoelastic FG nano-beam resting on a Winkler–Pasternak layer with the viscous layer is investigated by Farzad E. et al [60] based on the NLSGT conjunction with EBBT subjected to thermal and surface effect. The material properties vary gradually through the thickness direction according to the rule of mixture method. Hamilton's principle is used to solved the governing equation and the related B.Cs and solved analytically to obtain the

fundamental frequency of viscoelastic FG nano-beam with (C-C, S-S) B.Cs. The influence of Winkler– Pasternak elastic, viscous layers foundation, nonlocal parameter (ea), material length scale parameter (l_m), surface effect, thermal effect, power law index and aspect ratio on the viscoelastic size dependent FG nanobeams are discussed [60].

2.5 Dynamic stability

Liang L. et al. [61] presented the dynamic stability, free vibration and buckling analysis of a FG micro-beam with FSDBT with modified couple stress theory. They utilized the Mori–Tanaka homogenization scheme to show the material properties of FG micro-beam change continuously through the thickness direction. The governing equations and related B.Cs are derived by using Hamilton's principle and solved these equations via differential quadrature (DQ) method. There are many effective parameters to show the influences on the critical buckling, fundamental frequency and dynamic stability of FG microbeams, such as gradient index, slenderness ratio, material length scale parameter and various boundary conditions [61].

Saffari S. et al. [62] illustrated the dynamic stability of FG nano-beam under the action of dynamic axial and thermal effect loading based on nonlocal elasticity theory conjunction with TBT and embedded in Pasternak elastic foundation. They utilized Gurtin-Murdoch theory to investigate the effect of surface stress on the dynamic instability region of FG nano-beam. The equations of motion and related B.Cs are derived by Hamilton's principle. According to the rule of mixture method, the material properties change smoothly across the thickness direction. They have investigated the effect of power law index, nonlocal parameter, aspect ratio, Pasternak elastic constant, and surface effect on the dynamic stability of S-S size dependent FG nanobeam [62].

Helong W. [63] presented the thermal buckling, free vibration and dynamic instability of FG multilayer graphene nanoplatelet-reinforced composite (GPLRC) beam subjected to thermal effect and a periodic axial loading based on the TBT. According to the rule of mixture, the effective material properties of FG (GPLRC) beams are assumed to vary gradually across the thickness direction. The differential quadrature (DQ) method with Bolotin's method is examined to find the dynamic instability region of FG (GPLRC) beams [63].

Sahmani S. et al [64] have investigated the dynamic stability of FG micro-shells based on the modified couple stress theory with higher-order shear deformation shell theory. According to the Mori-Tanaka homogenization the effective material properties of the size dependent FG

micro-shells vary smoothly through the thickness direction. The dynamic governing equations and corresponding B.Cs are derived via Hamilton's principle. In order to estimate the dynamic instability region, the equation of motion is written with the Mathieu–Hill equations in conjunction with Bolotin's method. The influences of material length scale parameter, static load factor and gradient index on the dynamic stability analysis are examined for FG micro-shells are studied [64].

Ansari R. et al. [65] have investigated the dynamic stability behavior of embedded multi-walled carbon nano-tubes based on the nonlocal elasticity theory with FSDBT under the action of thermal effect with (S-S) B.Cs. The effect of aspect ratio, nonlocal parameter, static load factor, various of temperature and spring constants of the Pasternak elastic medium on the dynamic stability analysis of embedded multi-walled carbon nanotubes are presented [65].

Ansari R. et al [66] have illustrated the dynamic stability, buckling and free vibration of single-walled carbon nanotubes (SWCNTs) based on the nonlocal elasticity theory with EBBT and TBT subjected to axial compression load with thermal effect. It is assumed that the single-walled carbon nanotubes (SWCNTs) are resting on a Winkler type elastic foundation with S-S B.Cs. The effect of static load factor, thermal effect, nonlocal elastic parameter, aspect ratio and spring constant of the Winkler type elastic medium on the dynamic stability behavior of the single-walled carbon nanotubes are investigated [66].

Raheb G. et al [67] have investigated the dynamic stability and the buckling analysis of FG micro-shell based on the modified couple stress theory with Timoshenko shell theory. According to Hamilton's principle, the governing equations and related B.Cs can be derived. Navier solution is used to predict the critical buckling load of FG micro-shell with S-S B.C. In order to obtain the dynamic instability region, the equations of motion are written in the form of Mathieu–Hill equations and solved these equations by Bolotin's method. The effect of material length scale parameter, gradient index, aspect ratio, length to radius ratio and static load factor on the dynamic stability and critical buckling load are illustrated for FG micro-shell are studied [67].

Liao L. et al [68] have presented the buckling, free vibration and dynamic stability behavior of size dependent FG nano-composite beams reinforced by single-walled carbon nano-tubes based on the first order shear beam theory. The effective material properties are assumed change smoothly across the thickness direction for FG carbon nano-tube-reinforced composites by using the rule of mixture method. They utilized the DQ method to solve the dynamic equation of motion and written these equations in the form of Mathieu–Hill

equations to obtain the dynamic instability region and solved these equations by Bolotin's method [68].



THEORY AND FORMULATION OF FG SANDWICH MICRO-BEAM

3.1 Introduction

The sandwich functionally graded micro-beam are present with one core between two skins for two different Model with the length of the sandwich FG micro-beam (L) in axial x-direction, the width (b) in the y-direction, and thickness (h) in the z-direction. The sandwich FG micro-beam structure with the (Winkler and Pasternak) elastic foundation with spring constants K_w and K_p are subject to thermal effect as observed in Fig.(3.1). The sandwich FG micro-beam under the action of the axial excitation load $\bar{P}(t)$. There are three different kinds of the FG sandwich microbeams are considered in this thesis

1. Model I, homogeneous FG micro-beam.
2. Model II, sandwich FG micro-beam with the core made of FG material and the top skin with metal and the bottom skin with ceramic.
3. Model III, sandwich FG micro-beam with the core is made from the ceramic and the two skins are FG material.

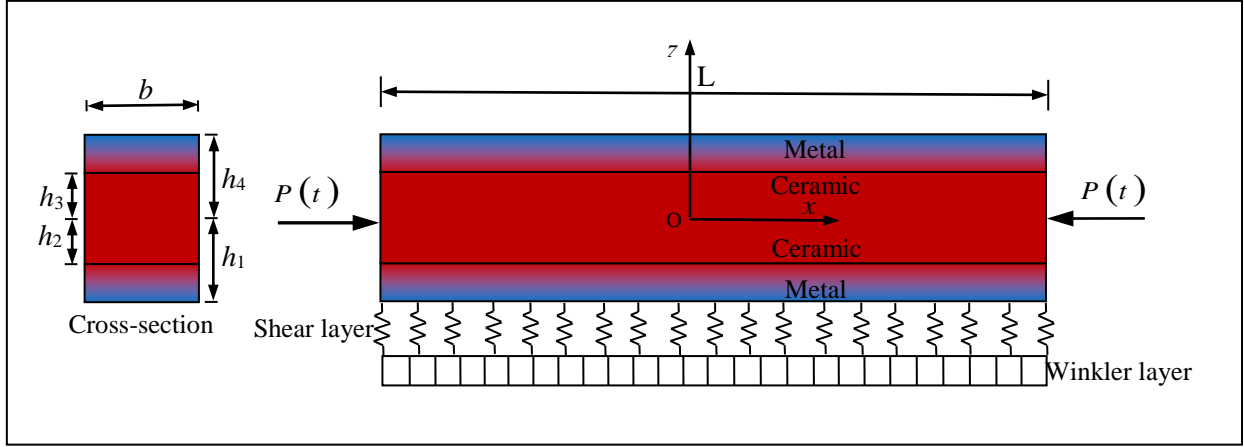


Figure 3.1 A sandwich FG micro-beam subjected to an axial compressive excitation load $\bar{P}(t)$.

For Model I FG homogeneous micro-beam which is made of the metal (m) and the ceramic (c). The metal and ceramic are varying from one surface at the bottom to the other surfaces at the top respectively, it can be noticed in Fig.(3.2a). The volume fraction of the ceramic constitutive $V_c(z)$ for Model I is obtained as

$$V_c(z) = \left(\frac{z}{h} + \frac{1}{2} \right)^k \quad (3.1)$$

where (k) is the non-negative variable parameter (gradient index) which presents the material changing across the thickness direction of the FG part micro-beam.

On the other hand for Model II as shown in Fig.(3.2b) with the core made of FG material and the skins are made from the metal and ceramic at the top and the bottom of the sandwich FG micro-beam respectively. Moreover, $V_c(z)$ of this Model can be obtained as bellow

$$V_c(z) = \begin{cases} 0 & \text{for } h_3 \leq z \leq h_4 \\ \left(\frac{z - h_2}{h_3 - h_2} \right)^k & \text{for } h_2 \leq z \leq h_3 \\ 1 & \text{for } h_1 \leq z \leq h_2 \end{cases} \quad (3.2)$$

where the thickness values (h_1, h_2, h_3, h_4) are shown on Fig. (3.1).

Finally the last Model with the core is ceramic and the skins are made from the FG material, the top skin of FG part the ceramic in the bottom and the metal in the top, Moreover, the

bottom FG part is conversely, it can be observed in Fig. (3.2c). $V_c(z)$ of Model III for both skins can be obtained as follow

$$V_c(z) = \begin{cases} \left(\frac{z-h_1}{h_2-h_1}\right)^k & \text{for } z \in (h_1, h_2) \\ 1 & \text{for } z \in (h_2, h_3) \\ \left(\frac{z-h_4}{h_3-h_4}\right)^k & \text{for } z \in (h_3, h_4) \end{cases} \quad (3.3)$$

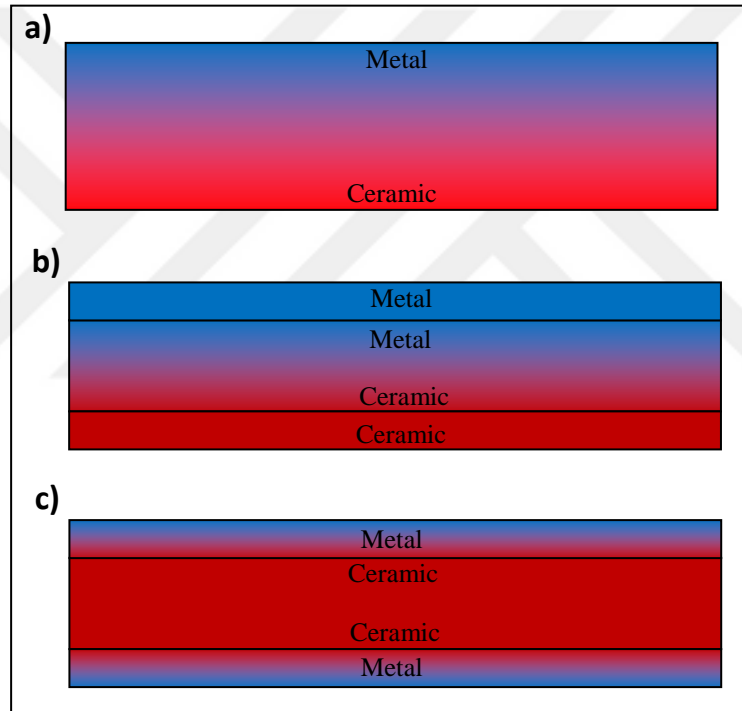


Figure 3.2 Sandwich FG micro-beam a. Model I, b. Model II, c. Model III

The ceramic and the metal of the FG part of the sandwich FG micro-beam for Model I and Model II in the bottom and the top surfaces respectively. on the other hand, for Model III there are two FG part, one of them of the top face is the same for Model I,II and conversely for bottom face with the top surface with ceramic and for bottom surfaces with metal. The local effective materials of sandwich FG micro-beam is consider with metal and ceramic, and the effective material properties for example Poisson's ratio (ν), Young's modulus (E), density (ρ), thermal expansion coefficient (α) and the shear modulus (G) vary smoothly a

cross the thickness direction can be calculated by using so called homogenization techniques here we consider two used: Mori-Tanaka homogenization and the rule of mixture method.

First of all Mori-Tanaka homogenization is used for calculating the effective material properties of sandwich FG micro-beam. The shear modulus G_r and the Bulk Modulus K_r are calculated with the Mori-Tanaka scheme

$$K_r = \frac{V_c (K_c - K_m)}{1 + V_m \left[(K_c - K_m) / (K_m + 4G_m / 3) \right]} + K_m \quad (3.4)$$

$$G_r = \frac{V_c (G_c - G_m)}{1 + V_m (G_c - G_m) / \left[G_m + G_m * (9 * K_m + 8 * G_m) / (6 * (K_m + 2 * G_m)) \right]} + G_m \quad (3.5)$$

where m indicate the metal and c indicate ceramic,

$$G_{(m,c)} = \frac{E_{(m,c)}}{2(1 + \nu_{(m,c)})} \quad (3.6)$$

$$K_{(m,c)} = \frac{E_{(m,c)}}{3(1 - 2\nu_{(m,c)})} \quad (3.7)$$

Where $V(z)$ is the volume fraction of the phase materials and $G_{m,c}$ is the shear modulus, $K_{m,c}$ is the bulk modulus of sandwich FG micro-beam. The relation between the volume fractions of the metal and the ceramic constituents as follows

$$V_m(z) + V_c(z) = 1 \quad (3.8)$$

The Young's modulus of sandwich FG micro-beam with the Mori-Tanaka homogenization is written as

$$E(z) = \frac{9K_r G_r}{3K_r + G_r} \quad (3.9)$$

Also, the poisson's ratio $\nu(z)$ of the sandwich FG micro-beam can be calculated as

$$\nu(z) = \frac{3K_r - 2G_r}{6K_r + 2G_r} \quad (3.10)$$

In case of the mass density $\rho(z)$ of FG part of the sandwich FG microbeam, the variation of mass density is expressed as

$$\rho(z) = \rho_m + V_c(z)(\rho_c - \rho_m) \quad (3.11)$$

The thermal expansion coefficient $\alpha(z)$

$$\alpha(z) = (\alpha_c - \alpha_m) \left(\frac{1}{K_e} - \frac{1}{K_m} \right) \Big/ \left(\frac{1}{K_c} - \frac{1}{K_m} \right) + \alpha_m \quad (3.12)$$

The second method for using to calculate the local effective properties of sandwich FG micro-beam is the rule of mixture method, the local effective properties of material R , can be written as follow

$$R = R_m V_m + R_c V_c \quad (3.13)$$

where R_m and R_c are the local effective properties of material with the metal and ceramic respectively.

The Young modulus and poisson's ratio, mass density and the thermal expansion coefficient can be calculate according to the classical rule of mixture in the following equations

$$E(z) = E_m + V_c(z)(E_c - E_m) \quad (3.14)$$

$$v(z) = v_m + V_c(z)(v_c - v_m) \quad (3.15)$$

$$\rho(z) = \rho_m + V_c(z)(\rho_c - \rho_m) \quad (3.16)$$

$$\alpha(z) = \alpha_m + V_c(z)(\alpha_c - \alpha_m) \quad (3.17)$$

The effect of the power law index on the volume fraction of the ceramic across the thickness of the sandwich FG micro-beam for each Model (I, II, III) is present in Fig. (3.3).

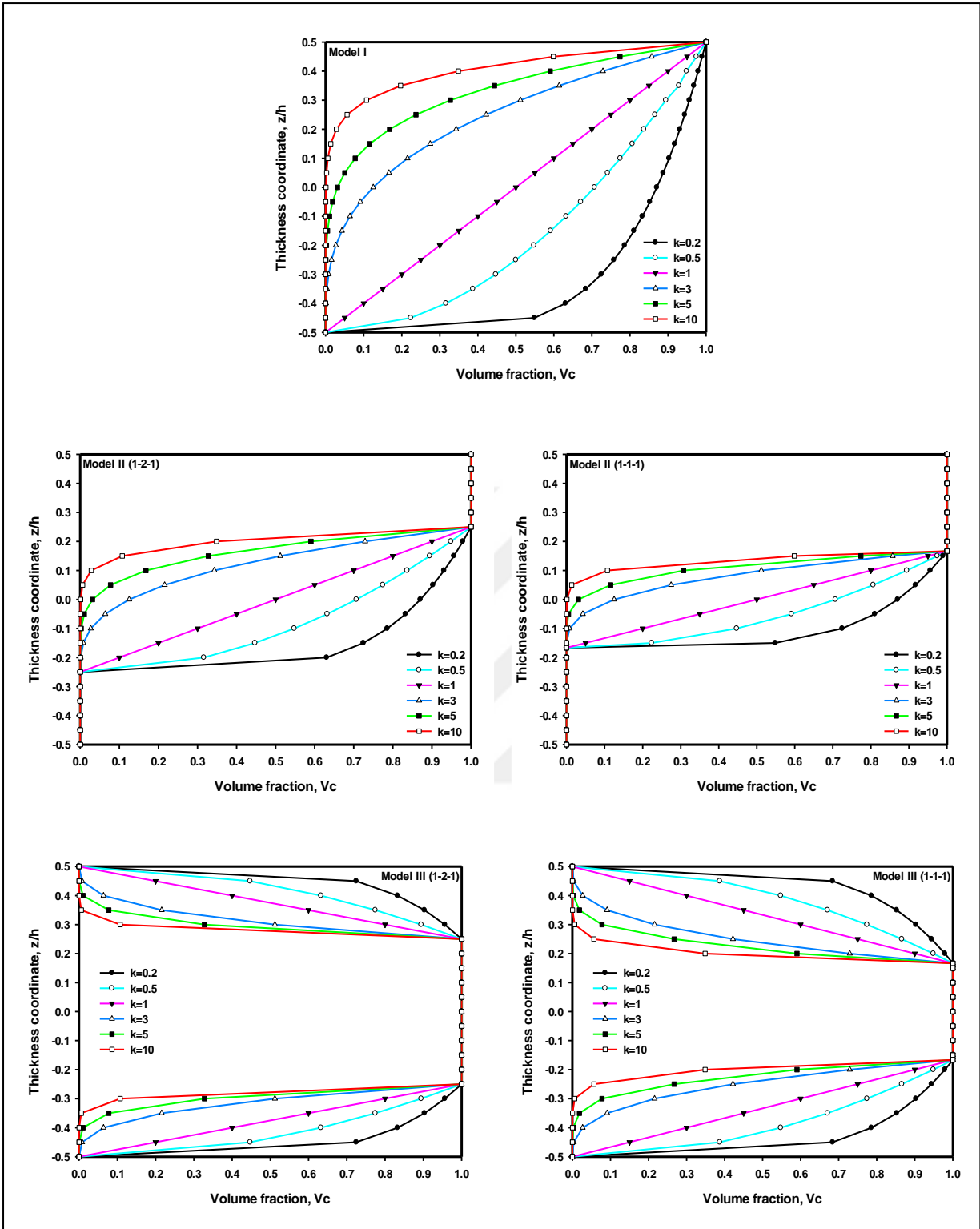


Figure 3.3 Variation of V_c cross the thickness of a FG micro-beam with different of gradient index (k) with cross-section types of (1,1,1) and (1,2,1) for Models II, III.

Various cross-sectional shapes type (1-1-1), (1-2-1), (1-8-1), (2-1-2) can be assumed for the thickness ratios of the core and skin regions. This representation can be directly given by dividing a region's (bottom skin, core, top skin) thickness with the greatest common divisor (GCD) of the regions' thicknesses. Thus according to Fig.1 if we denote the thicknesses of bottom skin, core and top skin with $\bar{h}_1 = h_2 - h_1$, $\bar{h}_2 = h_3 - h_2$ and $\bar{h}_3 = h_4 - h_3$ respectively then ratios (r_1, r_2, r_3) are simply obtained by $(\bar{h}_1, \bar{h}_2, \bar{h}_3) / GCD\{\bar{h}_1, \bar{h}_2, \bar{h}_3\}$.

The layer depth ratio of sandwich functionally graded microbeam from bottom to top, it is mean from $(z = h_1 = -h/2)$ to $(z = h_4 = h/2)$ is (1-1-1), (1-2-1), (1-8-1) and (2-1-2) respectively.

$h_2 = -h/6$; $h_3 = h/6$; with cross section (1-1-1) FG sandwich microbeam, in this type of cross section the core and the skins have the same thickness.

$h_2 = -h/4$; $h_3 = h/4$; with cross section (1-2-1) FG sandwich microbeam, it can be seen from this type, the core thickness is twice the face thickness.

$h_2 = -2h/5$; $h_3 = 2h/5$; with cross section (1-8-1) FG sandwich microbeam, the core depth is eight times as great than skin thickness.

$h_2 = -h/10$; $h_3 = h/10$; with cross section (2-1-2) FG sandwich microbeam, here the core thickness is half the face thickness of sandwich FG micro-beam.

3.2. Non-local sandwich FG micro-beam strain gradient Model (NLSGT)

The general NLSGT equations can be obtained as Lim et al. [47]

$$E(z) \left[1 - (e_1 a)^2 \nabla^2 \right] \varepsilon_{xx} - E(z) l_m^2 \left[1 - (e_0 a)^2 \nabla^2 \right] \nabla^2 \varepsilon_{xx} = \left[1 - (e_0 a)^2 \nabla^2 \right] \left[1 - (e_1 a)^2 \nabla^2 \right] t_{xx} \quad (3.18a)$$

$$G(z) \left[1 - (e_1 a)^2 \nabla^2 \right] \gamma_{xz} - G(z) l_m^2 \left[1 - (e_0 a)^2 \nabla^2 \right] \nabla^2 \gamma_{xz} = \left[1 - (e_0 a)^2 \nabla^2 \right] \left[1 - (e_1 a)^2 \nabla^2 \right] t_{xz} \quad (3.18b)$$

where $\nabla^2 = \frac{\partial^2}{\partial x^2}$,

the total stress tensor of the NLSGT is indicated as follow

$$t_{xz} = \sigma_{xz} - \nabla \sigma_{xz}^{(1)} \quad (3.19a)$$

$$t_{xx} = \sigma_{xx} - \nabla \sigma_{xx}^{(1)} \quad (3.19b)$$

where t_{xx} and t_{xz} are the total stress and total shear stress respectively, ∇ is defined as $\partial/\partial x$ is the one-dimensional differential operator, σ_{xz} and σ_{xx} is the shear and classical stress respectively, $\sigma_{xz}^{(1)}$ and $\sigma_{xx}^{(1)}$ is the higher-order shear stress and stress respectively, that is:

$$\sigma_{xx} = \int_0^L E(z) \alpha_0(x, x', e_0 a) \varepsilon'_{xx}(x') dx' \quad (3.20a)$$

$$\sigma_{xz} = \int_0^L G(z) \alpha_0(x, x', e_0 a) \gamma'_{xz}(x') dx' \quad (3.20b)$$

$$\sigma_{xx}^{(1)} = l_m^2 \int_0^L E(z) \alpha_1(x, x', e_1 a) \varepsilon'_{xx,x}(x') dx' \quad (3.20c)$$

$$\sigma_{xz}^{(1)} = l_m^2 \int_0^L G(z) \alpha_1(x, x', e_1 a) \gamma'_{xz,x}(x') dx' \quad (3.20d)$$

Here L is the length of the beam, $E(z)$ is the Young's modulus, $G(z)$ is the shear modulus, ε_{xx} and $\varepsilon_{xx,x}$ are the strain and the strain gradient, respectively, γ_{xz} and $\gamma_{xz,x}$ are the shear strain and the shear strain gradient, respectively, $e_0 a$ and $e_1 a$ denote the nonlocal parameters introduced to consider the significance of nonlocal elastic stress field, l_m is a material characteristic parameter (known as the material length scale parameter) introduced to consider the significance of higher-order strain gradient stress field.

The classical stress and shear stress and the higher-order stress and shear stress can be written as the form

$$\left[1 - (e_0 a)^2 \nabla^2\right] \sigma_{xx} = E(z) \varepsilon_{xx} \quad (3.21a)$$

$$\left[1 - (e_0 a)^2 \nabla^2\right] \sigma_{xz} = G(z) \gamma_{xz} \quad (3.21b)$$

$$\left[1 - (e_0 a)^2 \nabla^2\right] \sigma_{xx}^{(1)} = l_m^2 E(z) \nabla \varepsilon_{xx} \quad (3.22a)$$

$$\left[1 - (e_1 a)^2 \nabla^2\right] \sigma_{xz}^{(1)} = l_m^2 G(z) \nabla \gamma_{xz} \quad (3.22b)$$

The generalized NLSGT relation can be achieved as Lim et al.[47] by assuming that $e_0 = e_1 = e$,

$$\left[1 - (ea)^2 \nabla^2\right] t_{xx} = (1 - l_m^2 \nabla^2) E(z) \varepsilon_{xx} \quad (3.23a)$$

$$\left[1 - (ea)^2 \nabla^2\right] t_{xz} = (1 - l_m^2 \nabla^2) G(z) \gamma_{xz} \quad (3.23b)$$

first of all for the Eringen nonlocal theory can be achieved by setting $l_m = 0$ in Eqs.(3.23). That is:

$$\left[1 - (ea)^2 \nabla^2\right] t_{xx} = E(z) \varepsilon_{xx} \quad (3.24a)$$

$$\left[1 - (ea)^2 \nabla^2\right] t_{xz} = G(z) \gamma_{xz} \quad (3.24b)$$

Moreover, the Aifantis strain gradient theory can be achieved by letting $(ea) = 0$ in Eqs.(3.23), that is:

$$t_{xz} = (1 - l_m^2 \nabla^2) G(z) \gamma_{xz} \quad (3.25a)$$

$$t_{xx} = (1 - l_m^2 \nabla^2) E(z) \varepsilon_{xx} \quad (3.25b)$$

3.3 The governing equations for sandwich FG micro-beams

3.3.1 Higher-order beam theories (HOBTS)

Based on higher-order beam theory that contains different other theories is used, the displacement field takes the form:

$$u_x = u - z \frac{\partial w}{\partial x} + \Phi(z) \gamma \quad (3.26a)$$

$$u_y = 0 \quad (3.26b)$$

$$u_z = w \quad (3.26c)$$

Here (u) is the axial displacement, (w) is the transverse displacement on the neutral axis, γ is the transverse shear strain on the mid axis.

$$\gamma = \frac{\partial w}{\partial x} - \phi \quad (3.27)$$

where ϕ is the rotation of the cross-sections on the mid axis, $\Phi(z)$ is a function of z . $\Phi(z)$ is a function of z that characterizes the transverse shear and stress distribution along the

thickness of the beam. The displacement fields of different beam theories can be obtained by choosing $\Phi(z)$ as follows:

$$\text{EBBT: } \Phi(z) = 0 \quad (3.28a)$$

$$\text{FSDBT: } \Phi(z) = z \quad (3.28b)$$

$$\text{PSDBT: } \Phi(z) = z \left(1 - 4z^2/3h^2\right) \quad (3.28c)$$

$$\text{TSDBT: } \Phi(z) = \frac{h}{\pi} \sin\left(\frac{\pi z}{h}\right) \quad (3.28d)$$

$$\text{HSDBT: } \Phi(z) = h \sinh\left(\frac{z}{h}\right) - z \cosh\left(\frac{1}{2}\right) \quad (3.28e)$$

$$\text{ESDBT: } \Phi(z) = z e^{-2(z/h)^2} \quad (3.28f)$$

$$\text{ASDBT: } \Phi(z) = z \alpha^{\frac{-2(z/h)^2}{\ln \alpha}} \text{ with } \alpha = 3 \quad (3.28g)$$

The equations of motion and the corresponding boundary conditions are derived by using the Hamilton's principle and written as the form

$$\delta \int_0^t [U_k - (U_s + U_{ef} - W + U_{th})] dt = 0 \quad (3.29)$$

Where (U_k) is the kinetic energy, (U_s) is the strain energy, (U_{ef}) is the strain energy due to elastic foundations, (U_{th}) is the strain energy with effect of temperature change and (W) is the work done subjected to external applied loads. Thus, the formula of the strain of Higher-order micro-beam theories (HOBTs) can be written as

$$\varepsilon_{xx} = \frac{\partial u}{\partial x} - z \frac{\partial^2 w}{\partial x^2} + \Phi(z) \left(\frac{\partial^2 w}{\partial x^2} - \frac{\partial \phi}{\partial x} \right) \quad (3.30a)$$

$$\varepsilon_{yy} = \varepsilon_{zz} = \varepsilon_{xy} = \varepsilon_{yz} = 0 \quad (3.30b)$$

$$\gamma_{xz} = \frac{\partial \Phi(z)}{\partial z} \left(\frac{\partial w}{\partial x} - \phi \right) \quad (3.30c)$$

The strain energy of sandwich FG micro-beam can be written as follows

$$\delta \int_0^t U_s dt = \int_0^t \int \int_V \left(\sigma_{xx} \delta \varepsilon_{xx} + \sigma_{xz} \delta \gamma_{xz} + \sigma_{xx}^{(1)} \nabla \delta \varepsilon_{xx} + \sigma_{xz}^{(1)} \nabla \delta \gamma_{xz} \right) dv dt \quad (3.31)$$

using Eq. (3.19) and few mathematical operations that the Eq.(3.31) becomes

$$\delta \int_0^t U_S dt = \int_0^t \int_{0V} t_{xx} \delta \varepsilon_{xx} dv dt + \int_0^t \int_{0V} t_{xz} \delta \gamma_{xz} dv dt + \int_0^t \left[\int_A \sigma_{xx}^{(1)} \delta \varepsilon_{xx} dA + \int_A \sigma_{xz}^{(1)} \delta \gamma_{xz} dA \right] dt \quad (3.32)$$

The stress resultants of FG sandwich micro-beam can be obtained as follow

$$N = \int_A t_{xx} dA \quad (3.33a)$$

$$M = \int_A z t_{xx} dA \quad (3.33b)$$

$$M_h = \int_A \Phi(z) t_{xx} dA \quad (3.33c)$$

$$Q_h = \int_A \frac{\partial \Phi}{\partial z} t_{xz} dA \quad (3.33d)$$

$$N^{(1)} = \int_A \sigma_{xx}^{(1)} dA \quad (3.33e)$$

$$M^{(1)} = \int_A z \sigma_{xx}^{(1)} dA \quad (3.33f)$$

$$M_h^{(1)} = \int_A \Phi(z) \sigma_{xx}^{(1)} dA \quad (3.33g)$$

$$Q_h^{(1)} = \int_A \frac{\partial \Phi}{\partial z} \sigma_{xz}^{(1)} dA \quad (3.33h)$$

The Eq. (3.32) can be rewritten with the stress results in Eqs. (3.33) in the following form

$$\delta \int_0^t U_S dt = \int_0^t \int_0^L \left[N \frac{\partial \delta u}{\partial x} - M \frac{\partial^2 \delta w}{\partial x^2} + M_h \left(\frac{\partial^2 \delta w}{\partial x^2} - \frac{\partial \delta \phi}{\partial x} \right) + Q_h \left(\frac{\partial \delta w}{\partial x} - \delta \phi \right) \right] dx dt + \int_0^t \left[N^{(1)} \frac{\partial \delta u}{\partial x} - M^{(1)} \frac{\partial^2 \delta w}{\partial x^2} + M_h^{(1)} \left(\frac{\partial^2 \delta w}{\partial x^2} - \frac{\partial \delta \phi}{\partial x} \right) + Q_h^{(1)} \left(\frac{\partial \delta w}{\partial x} - \delta \phi \right) \right] dt \quad (3.34)$$

And the strain energy due to temperature change is given as

$$\delta \int_0^t U_{th} dt = - \int_0^t \int_0^L C^T \Delta T \frac{\partial w}{\partial x} \frac{\partial \delta w}{\partial x} dx dt \quad (3.35)$$

in which

$$C^T = \int_A \frac{E(z)}{1-2\nu} \alpha(z) dA$$

where ΔT is temperature change and $\alpha(z)$ is the thermal expansion coefficients.

Moreover, the strain energy with elastic foundations is given as

$$\delta \int_0^t U_{ef} dt = \int_0^t \int_0^L k_w w \delta w dx dt + \int_0^t \int_0^L k_p \frac{\partial w}{\partial x} \frac{\partial \delta w}{\partial x} dx dt \quad (3.36)$$

Here k_w is spring constant of the Winkler elastic foundation and k_p is the spring constant of the Pasternak elastic medium.

Also virtual work done by the external applied loads is given as follow

$$\delta \int_0^t W dt = \int_0^t \int_0^L (f \delta u + q \delta w) dx dt + \int_0^t \int_0^L \bar{P}(t) \left(\frac{\partial \delta u}{\partial x} + \frac{\partial w}{\partial x} \frac{\partial \delta w}{\partial x} \right) dx dt \quad (3.37)$$

Where (f) and (q) are the x and z components of the body forces per unit length respectively. And $\bar{P}(t)$ is an axial compressive excitation load.

The virtual kinetic energy δU_K can be obtained as follow

$$\delta \int_0^t U_K dt = \int_0^t \int_{0V} \rho(z) \frac{\partial u_x}{\partial t} \frac{\partial \delta u_x}{\partial t} dv dt + \int_0^t \int_{0V} \rho(z) \frac{\partial u_z}{\partial t} \frac{\partial \delta u_z}{\partial t} dv dt \quad (3.38)$$

$$\frac{\partial u_x}{\partial t} = \frac{\partial u}{\partial t} - z \frac{\partial^2 w}{\partial t \partial x} + \Phi(z) \left(\frac{\partial^2 w}{\partial t \partial x} - \frac{\partial \phi}{\partial t} \right) \quad (3.39a)$$

$$\frac{\partial u_z}{\partial t} = \frac{\partial w}{\partial t} \quad (3.39b)$$

Where $\rho(z)$ is the mass density of the functionally graded microbeam. By using Eqs.(3.39)

sub. in Eq.(3.38), the virtual kinetic energy δU_K is given as follow

$$\begin{aligned} \delta \int_0^t U_K dt = & \int_0^t \int_0^L \left[I_0 \left(\frac{\partial u}{\partial t} \frac{\partial \delta u}{\partial t} + \frac{\partial w}{\partial t} \frac{\partial \delta w}{\partial t} \right) - I_1 \left(\frac{\partial u}{\partial t} \frac{\partial^2 \delta w}{\partial x \partial t} + \frac{\partial^2 w}{\partial x \partial t} \frac{\partial \delta u}{\partial t} \right) \right. \\ & \left. + I_3 \frac{\partial^2 w}{\partial x \partial t} \frac{\partial^2 \delta w}{\partial x \partial t} + I_2 \left(\frac{\partial u}{\partial t} \left(\frac{\partial^2 \delta w}{\partial x \partial t} - \delta \dot{\phi} \right) + \frac{\partial \delta u}{\partial t} \left(\frac{\partial^2 w}{\partial x \partial t} - \frac{\partial \phi}{\partial t} \right) \right) \right. \\ & \left. - I_4 \left(\frac{\partial^2 w}{\partial x \partial t} \left(\frac{\partial^2 \delta w}{\partial x \partial t} - \frac{\partial \delta \phi}{\partial t} \right) + \frac{\partial^2 \delta w}{\partial x \partial t} \left(\frac{\partial^2 w}{\partial x \partial t} - \frac{\partial \phi}{\partial t} \right) \right) + I_5 \left(\left(\frac{\partial^2 w}{\partial x \partial t} - \frac{\partial \phi}{\partial t} \right) \left(\frac{\partial^2 \delta w}{\partial x \partial t} - \frac{\partial \delta \phi}{\partial t} \right) \right) \right] dx dt \end{aligned} \quad (3.40)$$

Where

$$(I_0, I_1, I_3) = \int_A \rho(z) (1, z, z^2) dA$$

$$(I_2, I_4, I_5) = \int_A \rho(z) \Phi(z) (1, z, \Phi(z)) dA \quad (3.41)$$

By substituting Eqs.(3.34-3.37) and (3.40) into equation (3.29) and implementing the integration and the coefficients of δu , δw and $\delta \phi$ are gathered, the governing equations with the higher-order micro-beam theory in conjunction with NLSGT can be obtained by ($0 \leq x \leq L$):

$$\frac{\partial N}{\partial x} - f = I_0 \frac{\partial^2 u}{\partial t^2} - (I_1 - I_2) \frac{\partial^3 w}{\partial x \partial t^2} - I_2 \frac{\partial^2 \phi}{\partial t^2} \quad (3.42)$$

$$\begin{aligned} \frac{\partial^2 M}{\partial x^2} - \frac{\partial^2 M_h}{\partial x^2} + \frac{\partial Q_h}{\partial x} - q - (P + C_0 \Delta T - k_p) \frac{\partial^2 w}{\partial x^2} - k_w w = I_0 \frac{\partial^2 w}{\partial t^2} \\ + (I_1 - I_2) \frac{\partial^3 u}{\partial x \partial t^2} - (I_5 - 2I_4 + I_3) \frac{\partial^4 w}{\partial x^2 \partial t^2} + (I_4 - I_5) \frac{\partial^3 \phi}{\partial x \partial t^2} \end{aligned} \quad (3.43)$$

$$Q_h - \frac{\partial M_h}{\partial x} = -I_2 \frac{\partial^2 u}{\partial t^2} + (I_4 - I_5) \frac{\partial^3 w}{\partial x \partial t^2} + I_5 \frac{\partial^2 \phi}{\partial t^2} \quad (3.44)$$

Moreover, the associated boundary conditions is given as follows with $x = 0$ and $x = L$

$$\begin{aligned} \delta w \left(\frac{\partial M}{\partial x} - \frac{\partial M_h}{\partial x} + Q_h + (P + C_0 \Delta T - k_p) \frac{\partial w}{\partial x} \right) = 0 &\Rightarrow \\ \frac{\partial M}{\partial x} - \frac{\partial M_h}{\partial x} + Q_h + (P + C_0 \Delta T - k_p) \frac{\partial w}{\partial x} &\quad \text{or } w = 0 \\ \delta u (N) = 0 &\Rightarrow N = 0 \quad \text{or } u = 0 \\ \frac{\partial \delta u}{\partial x} (N^{(1)}) = 0 &\Rightarrow N^{(1)} = 0 \quad \text{or } \frac{\partial u}{\partial x} = 0 \\ \frac{\partial \delta w}{\partial x} (M_h - M) = 0 &\Rightarrow M_h = M \quad \text{or } \frac{\partial w}{\partial x} = 0 \\ \delta \left(\frac{\partial^2 w}{\partial x^2} - \frac{\partial \phi}{\partial x} \right) (M_h^{(1)}) = 0 &\Rightarrow M_h^{(1)} = 0 \quad \text{or } \left(\frac{\partial^2 w}{\partial x^2} - \frac{\partial \phi}{\partial x} \right) = 0 \\ \frac{\partial^2 \delta w}{\partial x^2} (M^{(1)}) = 0 &\Rightarrow M^{(1)} = 0 \quad \text{or } \frac{\partial^2 w}{\partial x^2} = 0 \\ \delta \left(\frac{\partial w}{\partial x} - \phi \right) (Q_h^{(1)} + M_h) = 0 &\Rightarrow Q_h^{(1)} + M_h = 0 \quad \text{or } \left(\frac{\partial w}{\partial x} - \phi \right) = 0 \end{aligned}$$

the equations of motion can be written in term of the displacements, in Eqs.(3.33) the stress resultant can be expressed by displacement. Substituting Eq.(3.23) and (3.30) into Eqs.(3.33) we can obtains

$$N = b \int_{-h/2}^{h/2} t_{xx}(z) dz = (ea)^2 \frac{\partial^2 N}{\partial x^2} + \left(1 - l_m^2 \frac{\partial^2}{\partial x^2}\right) \left(A_0 \frac{\partial u}{\partial x} + (A_2 - A_1) \frac{\partial^2 w}{\partial x^2} - A_2 \frac{\partial \phi}{\partial x} \right) \quad (3.45)$$

$$M = b \int_{-h/2}^{h/2} z t_{xx}(z) dz = (ea)^2 \frac{\partial^2 M}{\partial x^2} + \left(1 - l_m^2 \frac{\partial^2}{\partial x^2}\right) \left(A_0 \frac{\partial u}{\partial x} + (A_4 - A_3) \frac{\partial^2 w}{\partial x^2} - A_4 \frac{\partial \phi}{\partial x} \right) \quad (3.46)$$

$$Q_h = b \int_{-h/2}^{h/2} \frac{\partial \Phi}{\partial z}(z) t_{xz} dz = (ea)^2 \frac{\partial^2 Q_h}{\partial x^2} + \left(1 - l_m^2 \frac{\partial^2}{\partial x^2}\right) G_0 \left(\frac{\partial w}{\partial x} - \phi \right) \quad (3.47)$$

$$M_h = b \int_{-h/2}^{h/2} \Phi(z) t_{xx}(z) dz = (ea)^2 \frac{\partial^2 M_h}{\partial x^2} + \left(1 - l_m^2 \frac{\partial^2}{\partial x^2}\right) \left(A_2 \frac{\partial u}{\partial x} - (A_5 - A_4) \frac{\partial^2 w}{\partial x^2} - A_5 \frac{\partial \phi}{\partial x} \right) \quad (3.48)$$

where

$$(A_0, A_1, A_3) = b \int_{-h/2}^{h/2} E(z) (1, z, z^2) dz$$

$$(A_2, A_4, A_5) = b \int_{-h/2}^{h/2} E(z) \Phi(z) (1, z, \Phi(z)) dz \quad (3.49)$$

$$G_0 = b \int_{-h/2}^{h/2} G(z) \left(\frac{\partial \Phi(z)}{\partial z} \right)^2 dz \quad (3.50)$$

Eqs.(3.44)-(3.48) can be rewritten in term of the displacement based on the Eqs.(3.42)-(3.44),

$$N = (ea)^2 \left(I_0 \frac{\partial^3 u}{\partial t^2 \partial x} + (I_1 - I_2) \frac{\partial^4 w}{\partial t^2 \partial x^2} - I_2 \frac{\partial^3 \phi}{\partial t^2 \partial x} - \frac{\partial f}{\partial x} \right) + \left(1 - l_m^2 \frac{\partial^2}{\partial x^2}\right) \left(A_0 \frac{\partial u}{\partial x} + (A_2 - A_1) \frac{\partial^2 w}{\partial x^2} - A_2 \frac{\partial \phi}{\partial x} \right) \quad (3.51)$$

$$M = (ea)^2 \left(I_0 \frac{\partial^2 w}{\partial t^2} + I_1 \frac{\partial^3 u}{\partial t^2 \partial x} + (I_4 - I_3) \frac{\partial^4 w}{\partial t^2 \partial x^2} - I_4 \frac{\partial^3 \phi}{\partial t^2 \partial x} - q + (P + C_0 \Delta T - k_p) \frac{\partial^2 w}{\partial x^2} + k_w w \right) + \left(1 - l_m^2 \frac{\partial^2}{\partial x^2}\right) \left(A_1 \frac{\partial u}{\partial x} + (A_4 - A_3) \frac{\partial^2 w}{\partial x^2} - A_4 \frac{\partial \phi}{\partial x} \right) \quad (3.52)$$

$$M_h = (ea)^2 \left(Q_h' + I_2 \frac{\partial^3 u}{\partial t^2 \partial x} + (I_5 - I_4) \frac{\partial^4 w}{\partial t^2 \partial x^2} - I_5 \frac{\partial^3 \phi}{\partial t^2 \partial x} \right) + \left(1 - l_m^2 \frac{\partial^2}{\partial x^2} \right) \left(A_2 \frac{\partial u}{\partial x} + (A_5 - A_4) \frac{\partial^2 w}{\partial x^2} - A_5 \frac{\partial \phi}{\partial x} \right) \quad (3.53)$$

$$Q_h - M_h' = (ea)^2 \left(-I_2 \frac{\partial^4 u}{\partial x^2 \partial t^2} - (I_5 - I_4) \frac{\partial^5 w}{\partial x^3 \partial t^2} + I_5 \frac{\partial^4 \phi}{\partial x^2 \partial t^2} \right) + \left(1 - l_m^2 \frac{\partial^2}{\partial x^2} \right) \left(-A_2 \frac{\partial^2 u}{\partial x^2} - (A_5 - A_4) \frac{\partial^3 w}{\partial x^3} + A_5 \frac{\partial^2 \phi}{\partial x^2} + G_0 \left(\frac{\partial w}{\partial x} w' - \phi \right) \right) \quad (3.54)$$

In view of Eqs.(3.42)-(3.44) and (3.51)-(3.54), it can be obtain the governing equations for a small size FG higher-order microbeam theory (HOBT) using NLSGT

$$\left(1 - (ea)^2 \frac{\partial^2}{\partial x^2} \right) \left(-I_0 \frac{\partial^2 u}{\partial t^2} + (I_1 - I_2) \frac{\partial^3 w}{\partial t^2 \partial x} + I_2 \frac{\partial^2 \phi}{\partial t^2} + f \right) + \left(1 - l_m^2 \frac{\partial^2}{\partial x^2} \right) \left(A_0 \frac{\partial^2 u}{\partial x^2} + (A_2 - A_1) \frac{\partial^3 w}{\partial x^3} - A_2 \frac{\partial^2 \phi}{\partial x^2} \right) = 0 \quad (3.55)$$

$$\left(1 - (ea)^2 \frac{\partial^2}{\partial x^2} \right) \left(-I_0 \frac{\partial^2 w}{\partial t^2} - I_1 \frac{\partial^3 u}{\partial x \partial t^2} - (I_4 - I_3) \frac{\partial^4 w}{\partial x^2 \partial t^2} + I_4 \frac{\partial^3 \phi}{\partial x \partial t^2} + q - (P + C_0 \Delta T - k_p) \frac{\partial^2 w}{\partial x^2} - k_w w \right) + \left(1 - l_m^2 \frac{\partial^2}{\partial x^2} \right) \left(A_1 \frac{\partial^3 u}{\partial x^3} + (A_4 - A_3) \frac{\partial^4 w}{\partial x^4} - A_4 \frac{\partial^3 \phi}{\partial x^3} \right) = 0 \quad (3.56)$$

$$\left(1 - (ea)^2 \frac{\partial^2}{\partial x^2} \right) \left(I_2 \frac{\partial^2 u}{\partial t^2} + (I_5 - I_4) \frac{\partial^3 w}{\partial x \partial t^2} - I_5 \frac{\partial^2 \phi}{\partial t^2} \right) + \left(1 - l_m^2 \frac{\partial^2}{\partial x^2} \right) \left(-A_2 \frac{\partial^2 u}{\partial x^2} - (A_5 - A_4) \frac{\partial^3 w}{\partial x^3} + A_5 \frac{\partial^2 \phi}{\partial x^2} + G_0 \left(\frac{\partial w}{\partial x} - \phi \right) \right) = 0 \quad (3.57)$$

It can be seen when putting the $l_m = 0$, in the equations (3.55-3.57), then can be obtained the Nonlocal continuum equations for nonlocal sandwich FG higher-order microbeam

$$\left(1 - (ea)^2 \frac{\partial^2}{\partial x^2} \right) \left(-I_0 \frac{\partial^2 u}{\partial t^2} + (I_1 - I_2) \frac{\partial^3 w}{\partial t^2 \partial x} + I_2 \frac{\partial^2 \phi}{\partial t^2} + f \right) + A_0 \frac{\partial^2 u}{\partial x^2} + (A_2 - A_1) \frac{\partial^3 w}{\partial x^3} - A_2 \frac{\partial^2 \phi}{\partial x^2} = 0 \quad (3.58)$$

$$\begin{aligned} & \left(1 - (ea)^2 \frac{\partial^2}{\partial x^2}\right) \left(-I_0 \frac{\partial^2 w}{\partial t^2} - I_1 \frac{\partial^3 u}{\partial x \partial t^2} - (I_4 - I_3) \frac{\partial^4 w}{\partial x^2 \partial t^2} + I_4 \frac{\partial^3 \phi}{\partial x \partial t^2} + q - (P + C_0 \Delta T - k_p) \frac{\partial^2 w}{\partial x^2} - k_w w \right) \\ & + A_1 \frac{\partial^3 u}{\partial x^3} + (A_4 - A_3) \frac{\partial^4 w}{\partial x^4} - A_4 \frac{\partial^3 \phi}{\partial x^3} = 0 \end{aligned} \quad (3.59)$$

$$\begin{aligned} & \left(1 - (ea)^2 \frac{\partial^2}{\partial x^2}\right) \left(I_2 \frac{\partial^2 u}{\partial t^2} + (I_5 - I_4) \frac{\partial^3 u}{\partial x \partial t^2} \ddot{w}' - I_5 \frac{\partial^2 \phi}{\partial t^2} \right) \\ & - A_2 \frac{\partial^2 u}{\partial x^2} - (A_5 - A_4) \frac{\partial^3 w}{\partial x^3} + A_5 \frac{\partial^2 \phi}{\partial x^2} + G_0 \left(\frac{\partial w}{\partial x} - \phi \right) = 0 \end{aligned} \quad (3.60)$$

Additionally, the governing equations of sandwich FG higher-order microbeam based on the Aiffantis theory, it given when the $ea = 0$ in Eqs.(3.55-3.57).

$$\begin{aligned} & \left(1 - (ea)^2 \frac{\partial^2}{\partial x^2}\right) \left(-I_0 \frac{\partial^2 u}{\partial t^2} + (I_1 - I_2) \frac{\partial^3 w}{\partial t^2 \partial x} + I_2 \frac{\partial^2 \phi}{\partial t^2} + f \right) \\ & + A_0 \frac{\partial^2 u}{\partial x^2} + (A_2 - A_1) \frac{\partial^3 w}{\partial x^3} - A_2 \frac{\partial^2 \phi}{\partial x^2} = 0 \end{aligned} \quad (3.61)$$

$$\begin{aligned} & \left(1 - (ea)^2 \frac{\partial^2}{\partial x^2}\right) \left(-I_0 \frac{\partial^2 w}{\partial t^2} - I_1 \frac{\partial^3 u}{\partial x \partial t^2} - (I_4 - I_3) \frac{\partial^4 w}{\partial x^2 \partial t^2} + I_4 \frac{\partial^3 \phi}{\partial x \partial t^2} + q - (P + C_0 \Delta T - k_p) \frac{\partial^2 w}{\partial x^2} \right. \\ & \left. - k_w w \right) + A_1 \frac{\partial^3 u}{\partial x^3} + (A_4 - A_3) \frac{\partial^4 w}{\partial x^4} - A_4 \frac{\partial^3 \phi}{\partial x^3} = 0 \end{aligned} \quad (3.62)$$

$$\begin{aligned} & \left(1 - (ea)^2 \frac{\partial^2}{\partial x^2}\right) \left(I_2 \frac{\partial^2 u}{\partial t^2} + (I_5 - I_4) \frac{\partial^3 u}{\partial x \partial t^2} \ddot{w}' - I_5 \frac{\partial^2 \phi}{\partial t^2} \right) \\ & - A_2 \frac{\partial^2 u}{\partial x^2} - (A_5 - A_4) \frac{\partial^3 w}{\partial x^3} + A_5 \frac{\partial^2 \phi}{\partial x^2} + G_0 \left(\frac{\partial w}{\partial x} - \phi \right) = 0 \end{aligned} \quad (3.63)$$

Whereas for the classical continuum theory, the governing equations is given by putting $ea = 0$ and $l_m = 0$ in Eqs.(3.55-3.57), as follow

$$\begin{aligned} & -I_0 \frac{\partial^2 u}{\partial t^2} + (I_1 - I_2) \frac{\partial^3 w}{\partial t^2 \partial x} + I_2 \frac{\partial^2 \phi}{\partial t^2} + f + A_0 \frac{\partial^2 u}{\partial x^2} + (A_2 - A_1) \frac{\partial^3 w}{\partial x^3} - A_2 \frac{\partial^2 \phi}{\partial x^2} = 0 \end{aligned} \quad (3.64)$$

$$\begin{aligned} & -I_0 \frac{\partial^2 w}{\partial t^2} - I_1 \frac{\partial^3 u}{\partial x \partial t^2} - (I_4 - I_3) \frac{\partial^4 w}{\partial x^2 \partial t^2} + I_4 \frac{\partial^3 \phi}{\partial x \partial t^2} + q - (P + C_0 \Delta T - k_p) \frac{\partial^2 w}{\partial x^2} \\ & - k_w w + A_1 \frac{\partial^3 u}{\partial x^3} + (A_4 - A_3) \frac{\partial^4 w}{\partial x^4} - A_4 \frac{\partial^3 \phi}{\partial x^3} = 0 \end{aligned} \quad (3.65)$$

$$\begin{aligned}
& I_2 \frac{\partial^2 u}{\partial t^2} + (I_5 - I_4) \frac{\partial^3 u}{\partial x \partial t^2} \ddot{w}' - I_5 \frac{\partial^2 \phi}{\partial t^2} \\
& - A_2 \frac{\partial^2 u}{\partial x^2} - (A_5 - A_4) \frac{\partial^3 w}{\partial x^3} + A_5 \frac{\partial^2 \phi}{\partial x^2} + G_0 \left(\frac{\partial w}{\partial x} - \phi \right) = 0
\end{aligned} \tag{3.66}$$

The non-classical counterparts of the stress resultants can be obtained by using Eqs.(3.23) ,(3.42)- (3.44), (3.51)-(3.53) and (3.54) together.

$$\begin{aligned}
N^{(1)} &= \frac{(ea)^4 l_m^2}{(ea)^2 - l_m^2} \left(I_0 \frac{\partial^4 u}{\partial x^2 \partial t^2} + (I_2 - I_1) \frac{\partial^5 w}{\partial x^3 \partial t^2} - I_2 \frac{\partial^4 \phi}{\partial x^2 \partial t^2} - \frac{\partial^2 f}{\partial x^2} \right) \\
&+ l_m^2 \left(1 - \frac{(ea)^2 l_m^2}{(ea)^2 - l_m^2} \frac{\partial^2}{\partial x^2} \right) \left(A_0 \frac{\partial^2 u}{\partial x^2} + (A_2 - A_1) \frac{\partial^3 w}{\partial x^3} - A_2 \frac{\partial^2 \phi}{\partial x^2} \right)
\end{aligned} \tag{3.67}$$

$$\begin{aligned}
M^{(1)} &= \frac{(ea)^4 l_m^4}{(ea)^2 - l_m^2} \left(I_0 \frac{\partial^3 w}{\partial x \partial t^2} + I_1 \frac{\partial^4 u}{\partial x^2 \partial t^2} + (I_4 - I_3) \frac{\partial^5 w}{\partial x^3 \partial t^2} - I_4 \frac{\partial^4 \phi}{\partial x^2 \partial t^2} \right. \\
&\left. - \frac{\partial^2 q}{\partial x^2} + (P + C_0 \Delta T - k_p) \frac{\partial^3 w}{\partial x^3} - k_w \frac{\partial w}{\partial x} \right) \\
&+ l_m^2 \left(1 - \frac{(ea)^2 l_m^2}{(ea)^2 - l_m^2} \frac{\partial^2}{\partial x^2} \right) \left(A_1 \frac{\partial^2 u}{\partial x^2} + (A_4 - A_3) \frac{\partial^3 w}{\partial x^3} - A_4 \frac{\partial^2 \phi}{\partial x^2} \right)
\end{aligned} \tag{3.68}$$

Stress resultants $M_h, Q_h, M_h^{(1)}, Q_h^{(1)}$ are inherently coupled and no feasible way seems to resolve them separately. In fact the number of equations are not enough for the number of undetermined resultants. Nevertheless we can still obtain some boundary conditions involving these coupled resultants. For example it is possible to obtain the following condition which is equivalent to the boundary condition $Q_h^{(1)} + M_h^{(1)} = 0$ by using Eqs. (3.19), Eq. (3.47), Eq.(3.48) and Eq. (3.54).

$$\begin{aligned}
& Q_h^{(1)} + M_h = 0 \Rightarrow \\
& \left(1 - (ea)^2 \frac{\partial^2}{\partial x^2} \right) \left(I_2 \frac{\partial^3 u}{\partial x \partial t^2} + (I_5 - I_4) \frac{\partial^4 w}{\partial x^2 \partial t^2} - I_5 \frac{\partial^3 \phi}{\partial x \partial t^2} \right) \\
& + \frac{l_m^2}{(ea)^2} G_0 \left(\frac{\partial^2 w}{\partial x^2} - \frac{\partial \phi}{\partial x} \right) + \left(1 - l_m^2 \frac{\partial^2}{\partial x^2} \right) G_0 \left(\frac{\partial^2 w}{\partial x^2} - \frac{\partial \phi}{\partial x} \right) \\
& + \frac{1}{(ea)^2} \left(1 - l_m^2 \frac{\partial^2}{\partial x^2} \right) \left(1 - (ea)^2 \frac{\partial^2}{\partial x^2} \right) \left(A_2 \frac{\partial u}{\partial x} + (A_5 - A_4) \frac{\partial^2 w}{\partial x^2} - A_5 \frac{\partial \phi}{\partial x} \right) = 0
\end{aligned} \tag{3.69}$$

Eqs. (3.55)-(3.57) can be written in term of the dimensionless quantities with the non-dimensional quantities as given as follow

$$\bar{x} = \frac{x}{L}, \quad \bar{u}, \bar{w} = \frac{(u, w)}{L}, \quad \phi = \bar{\phi}, \quad \lambda = \frac{h}{L}, \quad \alpha = \frac{ea}{L}, \quad \beta = \frac{l_m}{L}$$

$$(\bar{C}_0, \bar{G}_0, \bar{A}_0, \bar{A}_1, \bar{A}_2, \bar{A}_3, \bar{A}_4, \bar{A}_5) = \left(\frac{C_0}{E_m bh}, \frac{G_0}{G_m bh}, \frac{A_0}{E_m bh}, \frac{A_1}{E_m bh^2}, \frac{A_2}{E_m bh^2}, \frac{A_3}{E_m bh^3}, \frac{A_4}{E_m bh^3}, \frac{A_5}{E_m bh^3} \right)$$

$$(\bar{I}_0, \bar{I}_1, \bar{I}_2, \bar{I}_3, \bar{I}_4, \bar{I}_5) = \left(\frac{I_0}{\rho_m bh}, \frac{I_1}{\rho_m bh^2}, \frac{I_2}{\rho_m bh^2}, \frac{I_3}{\rho_m bh^3}, \frac{I_4}{\rho_m bh^3}, \frac{I_5}{\rho_m bh^3} \right)$$

$$\bar{t} = \frac{t}{L} \sqrt{\frac{E_m}{\rho_m}}, \quad \bar{P} = \frac{P}{E_m bh}, \quad (\bar{q}, \bar{f}) = \left(\frac{q}{E_m bh/L}, \frac{f}{E_m bh/L} \right), \quad (K_p, K_w) = \left(\frac{k_p}{E_m bh}, \frac{k_w L^2}{E_m bh} \right)$$

Here G_m is the shear modulus for metal part of sandwich FG micro-beam. The equations of motion can be rewritten by using the above dimensionless variables as

$$\begin{aligned} & \left(1 - \alpha^2 \frac{\partial^2}{\partial \bar{x}^2} \right) \left(-\bar{I}_0 \frac{\partial^2 \bar{u}}{\partial \bar{t}^2} + (\bar{I}_1 - \bar{I}_2) \lambda \frac{\partial^3 \bar{w}}{\partial \bar{x} \partial \bar{t}^2} + \bar{I}_2 \lambda \frac{\partial^2 \bar{\phi}}{\partial \bar{t}^2} + \bar{f} \right) \\ & + \left(1 - \beta^2 \frac{\partial^2}{\partial \bar{x}^2} \right) \left(\bar{A}_0 \frac{\partial^2 \bar{u}}{\partial \bar{x}^2} + (\bar{A}_2 - \bar{A}_1) \lambda \frac{\partial^3 \bar{w}}{\partial \bar{x}^3} - \bar{A}_2 \lambda \frac{\partial^2 \bar{\phi}}{\partial \bar{x}^2} \right) = 0 \end{aligned} \quad (3.70)$$

$$\begin{aligned} & \left(1 - \alpha^2 \frac{\partial^2}{\partial \bar{x}^2} \right) \left(-\bar{I}_0 \frac{\partial^2 \bar{w}}{\partial \bar{t}^2} - \bar{I}_1 \lambda \frac{\partial^3 \bar{u}}{\partial \bar{x} \partial \bar{t}^2} - (\bar{I}_4 - \bar{I}_3) \lambda^2 \frac{\partial^4 \bar{w}}{\partial \bar{x}^2 \partial \bar{t}^2} + \bar{I}_4 \lambda^2 \frac{\partial^3 \bar{\phi}}{\partial \bar{x} \partial \bar{t}^2} \right. \\ & \left. + \bar{q} - (\bar{P} + \bar{C}_0 \Delta T - K_p) \frac{\partial^2 \bar{w}}{\partial \bar{x}^2} - K_w \bar{w} \right) + \left(1 - \beta^2 \frac{\partial^2}{\partial \bar{x}^2} \right) \left(\bar{A}_1 \lambda \frac{\partial^3 \bar{u}}{\partial \bar{x}^3} + (\bar{A}_4 - \bar{A}_3) \lambda^2 \frac{\partial^4 \bar{w}}{\partial \bar{x}^4} - \bar{A}_4 \lambda^2 \frac{\partial^3 \bar{\phi}}{\partial \bar{x}^3} \right) = 0 \end{aligned} \quad (3.71)$$

$$\begin{aligned} & \left(1 - \alpha^2 \frac{\partial^2}{\partial \bar{x}^2} \right) \left(\bar{I}_2 \lambda \frac{\partial^2 \bar{u}}{\partial \bar{t}^2} + (\bar{I}_5 - \bar{I}_4) \lambda^2 \frac{\partial^3 \bar{w}}{\partial \bar{x} \partial \bar{t}^2} - \bar{I}_5 \lambda^2 \frac{\partial^2 \bar{\phi}}{\partial \bar{t}^2} \right) \\ & + \left(1 - \beta^2 \frac{\partial^2}{\partial \bar{x}^2} \right) \left(-\bar{A}_2 \lambda \frac{\partial^2 \bar{u}}{\partial \bar{x}^2} - (\bar{A}_5 - \bar{A}_4) \lambda^2 \frac{\partial^3 \bar{w}}{\partial \bar{x}^3} + \bar{A}_5 \lambda^2 \frac{\partial^2 \bar{\phi}}{\partial \bar{x}^2} + \bar{G}_0 \left(\frac{\partial \bar{w}}{\partial \bar{x}} - \bar{\phi} \right) \right) = 0 \end{aligned} \quad (3.72)$$

Similarly in dimensionless form classical stress resultants and non-classical counterparts of the stress resultants becomes

$$\begin{aligned}\bar{N} = & \alpha^2 \left(\bar{I}_0 \frac{\partial^3 \bar{u}}{\partial \bar{x} \partial \bar{t}^2} + (\bar{I}_2 - \bar{I}_1) \lambda \frac{\partial^4 \bar{w}}{\partial \bar{x}^2 \partial \bar{t}^2} - \bar{I}_2 \lambda \frac{\partial^3 \bar{\phi}}{\partial \bar{x} \partial \bar{t}^2} - \frac{\partial \bar{f}}{\partial \bar{x}} \right) \\ & + \left(1 - \beta^2 \frac{\partial^2}{\partial \bar{x}^2} \right) \left(\bar{A}_0 \frac{\partial \bar{u}}{\partial \bar{x}} + (\bar{A}_2 - \bar{A}_1) \lambda \frac{\partial^2 \bar{w}}{\partial \bar{x}^2} - \bar{A}_2 \lambda \frac{\partial \bar{\phi}}{\partial \bar{x}} \right)\end{aligned}\quad (3.73)$$

$$\begin{aligned}\bar{M} = & \alpha^2 \left(\bar{I}_0 \frac{\partial^2 \bar{w}}{\partial \bar{t}^2} + \bar{I}_1 \lambda \frac{\partial^3 \bar{u}}{\partial \bar{x} \partial \bar{t}^2} + (\bar{I}_4 - \bar{I}_3) \lambda^2 \frac{\partial^4 \bar{w}}{\partial \bar{x}^2 \partial \bar{t}^2} - \bar{I}_4 \lambda^2 \frac{\partial^3 \bar{\phi}}{\partial \bar{x} \partial \bar{t}^2} - \bar{q} + (\bar{P} + \bar{C}_0 \Delta T - K_p) \frac{\partial^2 \bar{w}}{\partial \bar{x}^2} + K_w \bar{w} \right) \\ & + \left(1 - \beta^2 \frac{\partial^2}{\partial \bar{x}^2} \right) \left(\bar{A}_1 \lambda \frac{\partial \bar{u}}{\partial \bar{x}} + (\bar{A}_4 - \bar{A}_3) \lambda^2 \frac{\partial^2 \bar{w}}{\partial \bar{x}^2} - \bar{A}_4 \lambda^2 \frac{\partial \bar{\phi}}{\partial \bar{x}} \right)\end{aligned}\quad (3.74)$$

$$\begin{aligned}\bar{N}^{(1)} = & \frac{\alpha^4 \beta^2}{\alpha^2 - \beta^2} \left(\bar{I}_0 \frac{\partial^4 \bar{u}}{\partial \bar{x}^2 \partial \bar{t}^2} + (\bar{I}_2 - \bar{I}_1) \lambda \frac{\partial^5 \bar{w}}{\partial \bar{x}^3 \partial \bar{t}^2} - \bar{I}_2 \lambda \frac{\partial^4 \bar{\phi}}{\partial \bar{x}^2 \partial \bar{t}^2} - \frac{\partial^2 \bar{f}}{\partial \bar{x}^2} \right) \\ & + \beta^2 \left(1 - \frac{\alpha^2 \beta^2}{\alpha^2 - \beta^2} \frac{\partial^2}{\partial \bar{x}^2} \right) \left(\bar{A}_0 \frac{\partial^2 \bar{u}}{\partial \bar{x}^2} + (\bar{A}_2 - \bar{A}_1) \frac{\partial^3 \bar{w}}{\partial \bar{x}^3} - \bar{A}_2 \frac{\partial^2 \bar{\phi}}{\partial \bar{x}^2} \right)\end{aligned}\quad (3.75)$$

$$\begin{aligned}\bar{M}^{(1)} = & \frac{\alpha^4 \beta^4}{\alpha^2 - \beta^2} \left(\bar{I}_0 \frac{\partial^3 \bar{w}}{\partial \bar{x} \partial \bar{t}^2} + \bar{I}_1 \frac{\partial^4 \bar{u}}{\partial \bar{x}^2 \partial \bar{t}^2} + (\bar{I}_4 - \bar{I}_3) \frac{\partial^5 \bar{w}}{\partial \bar{x}^3 \partial \bar{t}^2} - \bar{I}_4 \frac{\partial^4 \bar{\phi}}{\partial \bar{x}^2 \partial \bar{t}^2} \right. \\ & \left. - \frac{\partial^2 \bar{q}}{\partial \bar{x}^2} + (\bar{P} + \bar{C}_0 \Delta T - K_p) \frac{\partial^3 \bar{w}}{\partial \bar{x}^3} - K_w \frac{\partial \bar{w}}{\partial \bar{x}} \right) \\ & + \beta^2 \left(1 - \frac{\alpha^2 \beta^2}{\alpha^2 - \beta^2} \frac{\partial^2}{\partial \bar{x}^2} \right) \left(\bar{A}_1 \frac{\partial^2 \bar{u}}{\partial \bar{x}^2} + (\bar{A}_4 - \bar{A}_3) \frac{\partial^3 \bar{w}}{\partial \bar{x}^3} - \bar{A}_4 \frac{\partial^2 \bar{\phi}}{\partial \bar{x}^2} \right)\end{aligned}\quad (3.76)$$

The related boundary conditions involving the higher order stress resultant (3.69) can be given in dimensionless form as well

$$\begin{aligned}\bar{Q}_h^{(1)} + \bar{M}_h = & \left(1 - \alpha^2 \frac{\partial^2}{\partial \bar{x}^2} \right) \left(\bar{I}_2 \lambda \frac{\partial^3 \bar{u}}{\partial \bar{x} \partial \bar{t}^2} + (\bar{I}_5 - \bar{I}_4) \lambda^2 \frac{\partial^4 \bar{w}}{\partial \bar{x}^2 \partial \bar{t}^2} - \bar{I}_5 \lambda^2 \frac{\partial^3 \bar{\phi}}{\partial \bar{x} \partial \bar{t}^2} \right) \\ & + \frac{\beta^2}{\alpha^2} \bar{G}_0 \left(\frac{\partial^2 \bar{w}}{\partial \bar{x}^2} - \frac{\partial \bar{\phi}}{\partial \bar{x}} \right) + \left(1 - \beta^2 \frac{\partial^2}{\partial \bar{x}^2} \right) \bar{G}_0 \left(\frac{\partial^2 \bar{w}}{\partial \bar{x}^2} - \frac{\partial \bar{\phi}}{\partial \bar{x}} \right) \\ & + \frac{1}{\alpha^2} \left(1 - \beta^2 \frac{\partial^2}{\partial \bar{x}^2} \right) \left(1 - \alpha^2 \frac{\partial^2}{\partial \bar{x}^2} \right) \left(\bar{A}_2 \lambda \frac{\partial \bar{u}}{\partial \bar{x}} + (\bar{A}_5 - \bar{A}_4) \lambda^2 \frac{\partial^2 \bar{w}}{\partial \bar{x}^2} - \bar{A}_5 \lambda^2 \frac{\partial \bar{\phi}}{\partial \bar{x}} \right)\end{aligned}\quad (3.77)$$

With

$$(\bar{N}, \bar{M}) = \left(\frac{N}{E_m bh}, \frac{M}{E_m bhL} \right), (\bar{N}^{(1)}, \bar{Q}_h^{(1)} + \bar{M}_h, \bar{M}^{(1)}) = \left(\frac{N^{(1)}}{E_m bhL}, \frac{Q^{(1)} + M_h}{E_m bhL}, \frac{M^{(1)}}{E_m bhL^2} \right)$$

3.3.2 Timoshenko beam theory (TBT)

The equation of motion and corresponding boundary conditions of TBT can be obtained in the same procedure of HOBTS. It can be seen for TBT, the shape function $\Phi(z) = z$ in Eqs. (3.26). The displacement field with TBT in the following form

$$u_x = u(x, t) - z \phi(x, t) \quad (3.78a)$$

$$u_y = 0 \quad (3.78b)$$

$$u_z = w(x, t) \quad (3.78c)$$

The virtual strain energy and virtual kinetic energy for First order shear deformation beam theory are given explicitly in Appendix A1. The equations of motion for TBT as follow

$$\frac{\partial N}{\partial x} - f = I_0 \frac{\partial^2 u}{\partial t^2} - I_1 \frac{\partial^2 \phi}{\partial t^2} \quad (3.79)$$

$$\frac{\partial Q}{\partial x} - q - (P + C_0 \Delta T - k_p) \frac{\partial^2 w}{\partial x^2} - k_w w = I_0 \frac{\partial^2 w}{\partial t^2} \quad (3.80)$$

$$Q - \frac{\partial M}{\partial x} = I_2 \frac{\partial^2 \phi}{\partial t^2} - I_1 \frac{\partial^2 u}{\partial t^2} \quad (3.81)$$

for $(0 \leq x \leq L)$. The classical and non-classical boundary conditions at $x = 0$ and $x = L$

become

$$\delta u(N) = 0 \Rightarrow N = 0 \text{ or } u = 0$$

$$\delta \phi(M) = 0 \Rightarrow M = 0 \text{ or } \phi = 0$$

$$\delta w \left((P + C_0 \Delta T - K_p) \frac{\partial w}{\partial x} - Q \right) = 0 \Rightarrow Q = -(P + C_0 \Delta T - k_p) \frac{\partial w}{\partial x} \text{ or } w = 0$$

$$\frac{\partial \delta u}{\partial x} (N^{(1)}) = 0 \Rightarrow N^{(1)} = 0 \text{ or } \frac{\partial u}{\partial x} = 0$$

$$\delta \left(\frac{\partial w}{\partial x} - \phi \right) (Q^{(1)}) = 0 \Rightarrow Q^{(1)} = 0 \text{ or } \left(\frac{\partial w}{\partial x} - \phi \right) = 0$$

$$\delta \left(\frac{\partial \phi}{\partial x} \right) (M^{(1)}) = 0 \Rightarrow \quad M^{(1)} = 0 \text{ or } \frac{\partial \phi}{\partial x} = 0$$

The force and moment resultants of FSDBT are given below with (3.23), (3.30), and (3.33):

$$N = b \int_{-h/2}^{h/2} t_{xx}(z) dz = (ea)^2 \frac{\partial^2 N}{\partial x^2} + \left(1 - l_m^2 \frac{\partial^2}{\partial x^2} \right) \left(A_0 \frac{\partial u}{\partial x} - A_1 \frac{\partial \phi}{\partial x} \right) \quad (3.82)$$

$$M = b \int_{-h/2}^{h/2} z t_{xx}(z) dz = (ea)^2 \frac{\partial^2 M}{\partial x^2} + \left(1 - l_m^2 \frac{\partial^2}{\partial x^2} \right) \left(A_1 \frac{\partial u}{\partial x} - A_2 \frac{\partial \phi}{\partial x} \right) \quad (3.83)$$

$$Q = b \int_{-h/2}^{h/2} t_{xz}(z) dz = (ea)^2 \frac{\partial^2 Q}{\partial x^2} + k_s G_0 \left(1 - l_m^2 \frac{\partial^2}{\partial x^2} \right) \left(\frac{\partial w}{\partial x} - \phi \right) \quad (3.84)$$

The following rigidities are defined as

$$(A_0, A_1, A_2) = b \int_{-h/2}^{h/2} E(z) (1, z, z^2) dx$$

Also G_0 is the shear coefficient and can be calculated as

$$G_0 = b \int_{-h/2}^{h/2} G(z) dz$$

In view of Eqs.(79)- (81) classical normal force, classical moment and classical shear force can be written with the displacements and rotations

$$N = (ea)^2 \left(I_0 \frac{\partial^3 u}{\partial x \partial t^2} - I_1 \frac{\partial^3 \phi}{\partial x \partial t^2} + \frac{\partial f}{\partial x} \right) + \left(1 - l_m^2 \frac{\partial^2}{\partial x^2} \right) \left(A_0 \frac{\partial u}{\partial x} - A_1 \frac{\partial \phi}{\partial x} \right) \quad (3.85)$$

$$M = (ea)^2 \left(I_0 \frac{\partial^2 w}{\partial t^2} + I_1 \frac{\partial^3 u}{\partial x \partial t^2} - I_2 \frac{\partial^3 \phi}{\partial x \partial t^2} + q + (P + C_0 \Delta T - k_p) \frac{\partial^2 w}{\partial x^2} + k_w w \right) + \left(1 - l_m^2 \frac{\partial^2}{\partial x^2} \right) \left(A_1 \frac{\partial u}{\partial x} - A_2 \frac{\partial \phi}{\partial x} \right) \quad (3.86)$$

$$Q = (ea)^2 \left(I_0 \frac{\partial^3 w}{\partial x \partial t^2} + \frac{\partial q}{\partial x} + (P + C_0 \Delta T) \frac{\partial^3 w}{\partial x^3} \right) + k_s G_0 \left(1 - l_m^2 \frac{\partial^2}{\partial x^2} \right) \left(\frac{\partial w}{\partial x} - \phi \right)$$

(3.87)

The equations of motion for FSDBT in conjunction with the nonlocal strain gradient theory (NLSGT) can be given by utilize Eqs.(3.79), (3.80), (3.81) with Eqs. (3.85-3.87) in term of the displacements are written below

$$\left(1-l_m^2 \frac{\partial^2}{\partial x^2}\right) \left(A_0 \frac{\partial^2 u}{\partial x^2} - A_1 \frac{\partial^2 \phi}{\partial x^2}\right) - \left(1-(ea)^2 \frac{\partial^2}{\partial x^2}\right) \left(I_0 \frac{\partial^2 u}{\partial t^2} - I_1 \frac{\partial^2 \phi}{\partial t^2} + f\right) = 0$$

(3.88)

$$k_s G_0 \left(1-l_m^2 \frac{\partial^2}{\partial x^2}\right) \left(\frac{\partial^2 w}{\partial x^2} - \frac{\partial \phi}{\partial x}\right) - \left(1-(ea)^2 \frac{\partial^2}{\partial x^2}\right) \left(I_0 \frac{\partial^2 w}{\partial t^2} - q - (P + C_0 \Delta T - k_p) \frac{\partial^2 w}{\partial x^2} - k_w w\right) = 0$$

(3.89)

$$\left(1-(ea)^2 \frac{\partial^2}{\partial x^2}\right) \left(I_1 \frac{\partial^2 u}{\partial t^2} - I_2 \frac{\partial^2 \phi}{\partial t^2}\right) + \left(1-l_m^2 \frac{\partial^2}{\partial x^2}\right) \left(k_s G_0 \left(\frac{\partial w}{\partial x} - \phi\right) - A_1 \frac{\partial^2 u}{\partial x^2} + A_2 \frac{\partial^2 \phi}{\partial x^2}\right) = 0$$

(3.90)

When setting $l_m = 0$, in the equations (3.88-3.90), then can be obtained the Nonlocal continuum equations for nonlocal sandwich FG first shear deformation microbeam

$$A_0 \frac{\partial^2 u}{\partial x^2} - A_1 \frac{\partial^2 \phi}{\partial x^2} - \left(1-(ea)^2 \frac{\partial^2}{\partial x^2}\right) \left(I_0 \frac{\partial^2 u}{\partial t^2} - I_1 \frac{\partial^2 \phi}{\partial t^2} + f\right) = 0$$

(3.91)

$$k_s G_0 \left(\frac{\partial^2 w}{\partial x^2} - \frac{\partial \phi}{\partial x}\right) - \left(1-(ea)^2 \frac{\partial^2}{\partial x^2}\right) \left(I_0 \frac{\partial^2 w}{\partial t^2} - q - (P + C_0 \Delta T - k_p) \frac{\partial^2 w}{\partial x^2} - k_w w\right) = 0$$

(3.92)

$$\left(1-(ea)^2 \frac{\partial^2}{\partial x^2}\right) \left(I_1 \frac{\partial^2 u}{\partial t^2} - I_2 \frac{\partial^2 \phi}{\partial t^2}\right) + k_s G_0 \left(\frac{\partial w}{\partial x} - \phi\right) - A_1 \frac{\partial^2 u}{\partial x^2} + A_2 \frac{\partial^2 \phi}{\partial x^2} = 0$$

(3.93)

Additionally, the governing equations of sandwich FG microbeam with TBT based on the the Strain gradient (Aiffantis) theory, it given when the $ea = 0$ in Eqs.(3.88-3.90).

$$\left(1-l_m^2 \frac{\partial^2}{\partial x^2}\right) \left(A_0 \frac{\partial^2 u}{\partial x^2} - A_1 \frac{\partial^2 \phi}{\partial x^2}\right) - \left(I_0 \frac{\partial^2 u}{\partial t^2} - I_1 \frac{\partial^2 \phi}{\partial t^2} + f\right) = 0$$

(3.94)

$$k_s G_0 \left(1 - l_m^2 \frac{\partial^2}{\partial x^2} \right) \left(\frac{\partial^2 w}{\partial x^2} - \frac{\partial \phi}{\partial x} \right) - \left(I_0 \frac{\partial^2 w}{\partial t^2} - q - (P + C_0 \Delta T - k_p) \frac{\partial^2 w}{\partial x^2} - k_w w \right) = 0 \quad (3.95)$$

$$I_1 \frac{\partial^2 u}{\partial t^2} - I_2 \frac{\partial^2 \phi}{\partial t^2} + \left(1 - l_m^2 \frac{\partial^2}{\partial x^2} \right) \left(k_s G_0 \left(\frac{\partial w}{\partial x} - \phi \right) - A_1 \frac{\partial^2 u}{\partial x^2} + A_2 \frac{\partial^2 \phi}{\partial x^2} \right) = 0 \quad (3.96)$$

Whereas for the classical continuum theory, the governing equations is given by putting $ea = 0$ and $l_m = 0$ in Eqs.(3.88-3.90), as follow

$$A_0 \frac{\partial^2 u}{\partial x^2} - A_1 \frac{\partial^2 \phi}{\partial x^2} - I_0 \frac{\partial^2 u}{\partial t^2} + I_1 \frac{\partial^2 \phi}{\partial t^2} - f = 0 \quad (3.97)$$

$$k_s G_0 \left(\frac{\partial^2 w}{\partial x^2} - \frac{\partial \phi}{\partial x} \right) - I_0 \frac{\partial^2 w}{\partial t^2} + q + (P + C_0 \Delta T - k_p) \frac{\partial^2 w}{\partial x^2} + k_w w = 0 \quad (3.98)$$

$$I_1 \frac{\partial^2 u}{\partial t^2} - I_2 \frac{\partial^2 \phi}{\partial t^2} + k_s G_0 \left(\frac{\partial w}{\partial x} - \phi \right) - A_1 \frac{\partial^2 u}{\partial x^2} + A_2 \frac{\partial^2 \phi}{\partial x^2} = 0 \quad (3.99)$$

The non-classical counterparts of the stress resultants can be obtained by using Eqs.(3.23), (3.42)- (3.44), (3.51)-(3.53) and (3.54) together.

$$N^{(1)} = \frac{(ea)^4 l_m^2}{(ea)^2 - l_m^2} \left(I_0 \frac{\partial^4 u}{\partial x^2 \partial t^2} - I_1 \frac{\partial^4 \phi}{\partial x^2 \partial t^2} + \frac{\partial^2 f}{\partial x^2} \right) + l_m^2 \left(1 - \frac{(ea)^2 l_m^2}{(ea)^2 - l_m^2} \frac{\partial^2}{\partial x^2} \right) \left(A_0 \frac{\partial^2 u}{\partial x^2} - A_1 \frac{\partial^2 \phi}{\partial x^2} \right) \quad (3.100)$$

$$M^{(1)} = \frac{(ea)^4 l_m^2}{(ea)^2 - l_m^2} \left(I_0 \frac{\partial^3 w}{\partial x \partial t^2} + I_1 \frac{\partial^4 u}{\partial x^2 \partial t^2} - I_2 \frac{\partial^4 \phi}{\partial x^2 \partial t^2} + \frac{\partial q}{\partial x} + (P + C_0 \Delta T - k_p) \frac{\partial^3 w}{\partial x^3} + k_w \frac{\partial w}{\partial x} \right) + l_m^2 \left(1 - \frac{(ea)^2 l_m^2}{(ea)^2 - l_m^2} \frac{\partial^2}{\partial x^2} \right) \left(A_1 \frac{\partial^2 u}{\partial x^2} - A_2 \frac{\partial^2 \phi}{\partial x^2} \right) \quad (3.101)$$

$$\begin{aligned}
Q^{(1)} &= \frac{(ea)^4 l_m^2}{(ea)^2 - l_m^2} \left(I_0 \frac{\partial^4 w}{\partial x^2 \partial t^2} + \frac{\partial^2 q}{\partial x^2} + (P + C_0 \Delta T - k_p) \frac{\partial^4 w}{\partial x^4} + k_w w \right) \\
&+ k_s G_0 l_m^2 \left(1 - \frac{(ea)^2 l_m^2}{(ea)^2 - l_m^2} \frac{\partial^2}{\partial x^2} \right) \left(\frac{\partial^2 w}{\partial x^2} - \frac{\partial \phi}{\partial x} \right)
\end{aligned} \tag{3.102}$$

Eqs. (3.88)-(3.90) can be written in term of the dimensionless quantities with the non-dimensional quantities as given as follow

$$\bar{x} = \frac{x}{L}, \quad \bar{u}, \bar{w} = \frac{(u, w)}{L}, \quad \phi = \bar{\phi}, \quad \lambda = \frac{h}{L}, \quad \alpha = \frac{ea}{L}, \quad \beta = \frac{l_m}{L}$$

$$(\bar{C}_0, \bar{G}_0, \bar{A}_0, \bar{A}_1, \bar{A}_2) = \left(\frac{C_0}{E_m bh}, \frac{G_0}{G_m bh}, \frac{A_0}{E_m bh}, \frac{A_1}{E_m bh^2}, \frac{A_2}{E_m bh^3} \right)$$

$$(\bar{I}_0, \bar{I}_1, \bar{I}_2) = \left(\frac{I_0}{\rho_m bh}, \frac{I_1}{\rho_m bh^2}, \frac{I_2}{\rho_m bh^3} \right)$$

$$\bar{t} = \frac{t}{L} \sqrt{\frac{E_m}{\rho_m}}, \quad \kappa = \frac{k_s G_m}{E_m}, \quad \bar{P} = \frac{P}{E_m bh}, \quad (\bar{q}, \bar{f}) = \left(\frac{q}{E_m bh / L}, \frac{f}{E_m bh / L} \right)$$

$$(K_p, K_w) = \left(\frac{k_p}{E_m bh}, \frac{k_w L^2}{E_m bh} \right)$$

Here G_m is the shear modulus for metal part. The equations of motion can be rewritten by using the above dimensionless variables as

$$\left(1 - \beta^2 \frac{\partial^2}{\partial \bar{x}^2} \right) \left(\bar{A}_0 \frac{\partial^2 \bar{u}}{\partial \bar{x}^2} - \bar{A}_1 \lambda \frac{\partial^2 \bar{\phi}}{\partial \bar{x}^2} \right) - \left(1 - \alpha^2 \frac{\partial^2}{\partial \bar{x}^2} \right) \left(\bar{I}_0 \frac{\partial^2 \bar{u}}{\partial \bar{t}^2} - \bar{I}_1 \lambda \frac{\partial^2 \bar{\phi}}{\partial \bar{t}^2} + \bar{f} \right) = 0 \tag{3.103}$$

$$\begin{aligned}
& - \kappa \bar{A}_0 \left(1 - \beta^2 \frac{\partial^2}{\partial \bar{x}^2} \right) \left(\frac{\partial^2 \bar{w}}{\partial \bar{x}^2} - \frac{\partial \bar{\phi}}{\partial \bar{x}} \right) + \left(1 - \alpha^2 \frac{\partial^2}{\partial \bar{x}^2} \right) \left(\bar{I}_0 \frac{\partial^2 \bar{w}}{\partial \bar{t}^2} - \bar{q} - (\bar{P} + \bar{C}_0 \Delta T - K_p) \frac{\partial^2 \bar{w}}{\partial \bar{x}^2} - K_w \bar{w} \right) = 0
\end{aligned} \tag{3.104}$$

$$\begin{aligned}
& \left(1 - \beta^2 \frac{\partial^2}{\partial \bar{x}^2} \right) \left(\kappa \bar{A}_0 \left(\frac{\partial \bar{w}}{\partial \bar{x}} - \bar{\phi} \right) - \bar{A}_1 \lambda \frac{\partial^2 \bar{u}}{\partial \bar{x}^2} + \bar{A}_2 \lambda^2 \frac{\partial^2 \bar{\phi}}{\partial \bar{x}^2} \right) \\
& + \left(1 - \alpha^2 \frac{\partial^2}{\partial \bar{x}^2} \right) \left(\bar{I}_1 \lambda \frac{\partial^2 \bar{u}}{\partial \bar{t}^2} - \bar{I}_2 \lambda^2 \frac{\partial^2 \bar{\phi}}{\partial \bar{t}^2} \right) = 0
\end{aligned} \tag{3.105}$$

Similarly in dimensionless form classical stress resultants becomes

$$\bar{N} = \alpha^2 \left(\bar{I}_0 \frac{\partial^3 \bar{u}}{\partial \bar{x} \partial \bar{t}^2} - \bar{I}_1 \frac{\partial^3 \bar{\phi}}{\partial \bar{x} \partial \bar{t}^2} + \frac{\partial \bar{f}}{\partial \bar{x}} \right) + \left(1 - \beta^2 \frac{\partial^2}{\partial \bar{x}^2} \right) \left(\bar{A}_0 \frac{\partial \bar{u}}{\partial \bar{x}} - \bar{A}_1 \frac{\partial \bar{\phi}}{\partial \bar{x}} \right) \quad (3.106)$$

$$\begin{aligned} \bar{M} = & \alpha^2 \left(\bar{I}_0 \frac{\partial^2 \bar{w}}{\partial \bar{t}^2} + \bar{I}_1 \lambda \frac{\partial^3 \bar{u}}{\partial \bar{x} \partial \bar{t}^2} - \bar{I}_2 \lambda^2 \frac{\partial^3 \bar{\phi}}{\partial \bar{x} \partial \bar{t}^2} + \bar{q} + (\bar{P} + \bar{C}_0 \Delta T - K_p) \frac{\partial^2 \bar{w}}{\partial \bar{x}^2} + K_w \bar{w} \right) \\ & + \left(1 - \beta^2 \frac{\partial^2}{\partial \bar{x}^2} \right) \left(\bar{A}_1 \lambda \frac{\partial \bar{u}}{\partial \bar{x}} - \bar{A}_2 \lambda^2 \frac{\partial \bar{\phi}}{\partial \bar{x}} \right) \end{aligned} \quad (3.107)$$

$$\bar{Q} = \alpha^2 \left(\bar{I}_0 \frac{\partial^3 \bar{w}}{\partial \bar{x} \partial \bar{t}^2} + \frac{\partial \bar{q}}{\partial \bar{x}} + (\bar{P} + \bar{C}_0 \Delta T - K_p) \frac{\partial^3 \bar{w}}{\partial \bar{x}^3} + K_w \bar{w} \right) + \kappa \bar{A}_0 \left(1 - \beta^2 \frac{\partial^2}{\partial \bar{x}^2} \right) \left(\frac{\partial \bar{w}}{\partial \bar{x}} - \bar{\phi} \right) \quad (3.108)$$

$$\bar{N}^{(1)} = \frac{\alpha^4 \beta^2}{\alpha^2 - \beta^2} \left(\bar{I}_0 \frac{\partial^4 \bar{u}}{\partial \bar{x}^2 \partial \bar{t}^2} - \bar{I}_1 \lambda \frac{\partial^4 \bar{\phi}}{\partial \bar{x}^2 \partial \bar{t}^2} + \frac{\partial^2 \bar{f}}{\partial \bar{x}^2} \right) + \beta^2 \left(1 - \frac{\alpha^2 \beta^2}{\alpha^2 - \beta^2} \frac{\partial^2}{\partial \bar{x}^2} \right) \left(\bar{A}_0 \frac{\partial^2 \bar{u}}{\partial \bar{x}^2} - \bar{A}_1 \lambda \frac{\partial^2 \bar{\phi}}{\partial \bar{x}^2} \right) \quad (3.109)$$

$$\begin{aligned} \bar{M}^{(1)} = & \frac{\alpha^4 \beta^2}{\alpha^2 - \beta^2} \left(\bar{I}_0 \frac{\partial^3 \bar{w}}{\partial \bar{x} \partial \bar{t}^2} + \bar{I}_1 \lambda \frac{\partial^4 \bar{u}}{\partial \bar{x}^2 \partial \bar{t}^2} - \bar{I}_2 \lambda^2 \frac{\partial^4 \bar{\phi}}{\partial \bar{x}^2 \partial \bar{t}^2} + \frac{\partial \bar{q}}{\partial \bar{x}} + (\bar{P} + \bar{C}_0 \Delta T - K_p) \frac{\partial^3 \bar{w}}{\partial \bar{x}^3} + K_w \frac{\partial \bar{w}}{\partial \bar{x}} \right) \\ & + \beta^2 \left(1 - \frac{\alpha^2 \beta^2}{\alpha^2 - \beta^2} \frac{\partial^2}{\partial \bar{x}^2} \right) \left(\bar{A}_1 \lambda \frac{\partial^2 \bar{u}}{\partial \bar{x}^2} - \bar{A}_2 \lambda^2 \frac{\partial^2 \bar{\phi}}{\partial \bar{x}^2} \right) \end{aligned} \quad (3.110)$$

$$\begin{aligned} \bar{Q}^{(1)} = & \frac{\alpha^4 \beta^2}{\alpha^2 - \beta^2} \left(\bar{I}_0 \frac{\partial^4 \bar{w}}{\partial \bar{x}^2 \partial \bar{t}^2} + \frac{\partial^2 \bar{q}}{\partial \bar{x}^2} + (\bar{P} + \bar{C}_0 \Delta T - K_p) \frac{\partial^4 \bar{w}}{\partial \bar{x}^4} + K_w \bar{w} \right) \\ & + \kappa \bar{A}_0 \beta^2 \left(1 - \frac{\alpha^2 \beta^2}{\alpha^2 - \beta^2} \frac{\partial^2}{\partial \bar{x}^2} \right) \left(\frac{\partial^2 \bar{w}}{\partial \bar{x}^2} - \frac{\partial \bar{\phi}}{\partial \bar{x}} \right) \end{aligned} \quad (3.111)$$

With

$$(\bar{N}, \bar{Q}, \bar{M}) = \left(\frac{N}{E_m bh}, \frac{Q}{E_m bh}, \frac{M}{E_m bhL} \right), (\bar{N}^{(1)}, \bar{Q}^{(1)}, \bar{M}^{(1)}) = \left(\frac{N^{(1)}}{E_m bhL}, \frac{Q^{(1)}}{E_m bhL}, \frac{M^{(1)}}{E_m bhL^2} \right)$$

3.3.3 Euler- Bernoulli beam theory (EBBT)

For EBBT the shape function $\Phi(z) = 0$ in Eqs.(3.26), then the displacement equations can be taking in the following form

$$u_x(x, z) = u - z \frac{\partial w}{\partial x} \quad (3.112a)$$

$$u_y(x, z) = 0 \quad (3.112b)$$

$$u_z(x, z) = w \quad (3.112c)$$

The virtual of the U_s and U_k for Euler- Bernoulli micro-beam theory are obtained explicitly in Appendix A2. Therefore the governing equations EBBT can be derived as follows:

$$\frac{\partial N}{\partial x} - f - I_0 \frac{\partial^2 u}{\partial t^2} + I_1 \frac{\partial^3 w}{\partial x \partial t^2} = 0 \quad (3.113)$$

$$\frac{\partial^2 M}{\partial x^2} - q + (P + C_0 \Delta T - k_p) \frac{\partial^2 w}{\partial x^2} + k_w w + I_3 \frac{\partial^4 w}{\partial x^2 \partial t^2} - I_1 \frac{\partial^3 u}{\partial x \partial t^2} - I_0 \frac{\partial^2 w}{\partial t^2} = 0 \quad (3.114)$$

Moreover, the associated boundary conditions is given as follows with $x = 0$ and $x = L$

$$\delta u(N) = 0 \Rightarrow N = 0 \text{ or } u = 0$$

$$\delta w \left(\frac{\partial M}{\partial x} \right) = 0 \Rightarrow \frac{\partial M}{\partial x} = 0 \text{ or } w = 0$$

$$\frac{\partial \delta w}{\partial x} (M) = 0 \Rightarrow M = 0 \text{ or } \frac{\partial w}{\partial x} = 0$$

$$\frac{\partial \delta u}{\partial x} (N^{(1)}) = 0 \Rightarrow N^{(1)} = 0 \text{ or } \frac{\partial u}{\partial x} = 0$$

$$\frac{\partial^2 \delta w}{\partial x^2} (M^{(1)}) = 0 \Rightarrow M^{(1)} = 0 \text{ or } \frac{\partial^2 w}{\partial x^2} = 0$$

The force and moment resultants of EBBT are given below

$$N = b \int_{-h/2}^{h/2} t_{xx}(z) dz = (ea)^2 \frac{\partial^2 N}{\partial x^2} + \left(1 - l_m^2 \frac{\partial^2}{\partial x^2}\right) \left(A_0 \frac{\partial u}{\partial x} - A_1 \frac{\partial^2 w}{\partial x^2} \right) \quad (3.115)$$

$$M = b \int_{-h/2}^{h/2} z t_{xx}(z) dz = (ea)^2 \frac{\partial^2 M}{\partial x^2} + \left(1 - l_m^2 \frac{\partial^2}{\partial x^2}\right) \left(A_1 \frac{\partial u}{\partial x} - A_2 \frac{\partial^2 w}{\partial x^2} \right) \quad (3.116)$$

Where

$$(A_0, A_1, A_2) = b \int_{-h/2}^{h/2} E(z) (1, z, z^2) dx$$

In view of Eqs.(3.113)-(3.114) classical normal force, classical moment and classical shear force can be written with the displacements and rotations

$$N = (ea)^2 \left(I_0 \frac{\partial^3 u}{\partial x \partial t^2} - I_1 \frac{\partial^4 w}{\partial x^2 \partial t^2} + \frac{\partial f}{\partial x} \right) + \left(1 - l_m^2 \frac{\partial^2}{\partial x^2}\right) \left(A_0 \frac{\partial u}{\partial x} - A_1 \frac{\partial^2 w}{\partial x^2} \right) \quad (3.117)$$

$$M = (ea)^2 \left(I_0 \frac{\partial^2 w}{\partial t^2} - I_3 \frac{\partial^4 w}{\partial x^2 \partial t^2} + I_1 \frac{\partial^3 u}{\partial x \partial t^2} + q + (P + C_0 \Delta T - k_p) \frac{\partial^2 w}{\partial x^2} + k_w w \right) + \left(1 - l_m^2 \frac{\partial^2}{\partial x^2}\right) \left(A_1 \frac{\partial u}{\partial x} - A_2 \frac{\partial^2 w}{\partial x^2} \right) \quad (3.118)$$

The non-classical counterparts of the force and the moment are obtained by using Eqs.(3.23), (3.113)- (3.114), and (3.115)-(3.116) together

$$N^{(1)} = \frac{(ea)^4 l_m^2}{(ea)^2 - l_m^2} \left(I_0 \frac{\partial^4 u}{\partial x^2 \partial t^2} - I_1 \frac{\partial^5 w}{\partial x^3 \partial t^2} + \frac{\partial^2 f}{\partial x^2} \right) + l_m^2 \left(1 - \frac{(ea)^2 l_m^2}{(ea)^2 - l_m^2} \frac{\partial^2}{\partial x^2}\right) \left(A_0 \frac{\partial^2 u}{\partial x^2} - A_1 \frac{\partial^3 w}{\partial x^3} \right) \quad (3.119)$$

$$M^{(1)} = \frac{(ea)^4 l_m^2}{(ea)^2 - l_m^2} \left(I_0 \frac{\partial^3 w}{\partial x \partial t^2} + I_1 \frac{\partial^5 w}{\partial x^3 \partial t^2} - I_2 \frac{\partial^4 w}{\partial x^2 \partial t^2} + \frac{\partial q}{\partial x} + (P + C_0 \Delta T - k_p) \frac{\partial^3 w}{\partial x^3} + k_w \frac{\partial w}{\partial x} \right) + l_m^2 \left(1 - \frac{(ea)^2 l_m^2}{(ea)^2 - l_m^2} \frac{\partial^2}{\partial x^2}\right) \left(A_1 \frac{\partial^2 u}{\partial x^2} - A_2 \frac{\partial^3 w}{\partial x^3} \right) \quad (3.120)$$

The equations of motion for EBBT can be obtained in the same procedure as follow

$$\left(1-l_m^2 \frac{\partial^2}{\partial x^2}\right) \left(A_0 \frac{\partial^2 u}{\partial x^2} - A_1 \frac{\partial^3 w}{\partial x^3}\right) - \left(1-(ea)^2 \frac{\partial^2}{\partial x^2}\right) \left(I_0 \frac{\partial^2 u}{\partial t^2} - I_1 \frac{\partial^3 w}{\partial x \partial t^2} + f\right) = 0 \quad (3.121)$$

$$\left(1-l_m^2 \frac{\partial^2}{\partial x^2}\right) \left(A_1 \frac{\partial^3 u}{\partial x^3} - A_2 \frac{\partial^4 w}{\partial x^4}\right) - \left(1-(ea)^2 \frac{\partial^2}{\partial x^2}\right) \left(I_0 \frac{\partial^2 w}{\partial t^2} - I_3 \frac{\partial^4 u}{\partial x^2 \partial t^2} + I_1 \frac{\partial^3 u}{\partial x \partial t^2} + q - (P + C_0 \Delta T - k_p) \frac{\partial^2 w}{\partial x^2} - k_w w\right) = 0 \quad (3.122)$$

when putting $A_3 = A_4 = A_5 = G_0 = 0$ in the governing equations HOBTs, the governing equations EBBT is obtained .

When setting $l_m = 0$, in the Eq.(3.121) and Eq.(3.122), then can be obtained the Nonlocal continuum equations for nonlocal sandwich FG Euler- Bernoulli microbeam as follows

$$A_0 \frac{\partial^2 u}{\partial x^2} - A_1 \frac{\partial^3 w}{\partial x^3} - \left(1-(ea)^2 \frac{\partial^2}{\partial x^2}\right) \left(I_0 \frac{\partial^2 u}{\partial t^2} - I_1 \frac{\partial^3 w}{\partial x \partial t^2} + f\right) = 0 \quad (3.123)$$

$$- \left(1-(ea)^2 \frac{\partial^2}{\partial x^2}\right) \left(I_0 \frac{\partial^2 w}{\partial t^2} - I_3 \frac{\partial^4 u}{\partial x^2 \partial t^2} + I_1 \frac{\partial^3 u}{\partial x \partial t^2} + q - (P + C_0 \Delta T - k_p) \frac{\partial^2 w}{\partial x^2} - k_w w\right) + A_1 \frac{\partial^3 u}{\partial x^3} - A_2 \frac{\partial^4 w}{\partial x^4} = 0 \quad (3.124)$$

Additionally, the governing equations of sandwich FG microbeam with EBBT based on the Aiffantis theory, it given when the $ea = 0$ in Eqs.(3.121-3.122).

$$\left(1-l_m^2 \frac{\partial^2}{\partial x^2}\right) \left(A_0 \frac{\partial^2 u}{\partial x^2} - A_1 \frac{\partial^3 w}{\partial x^3}\right) - I_0 \frac{\partial^2 u}{\partial t^2} + I_1 \frac{\partial^3 w}{\partial x \partial t^2} - f = 0 \quad (3.125)$$

$$-I_0 \frac{\partial^2 w}{\partial t^2} + I_3 \frac{\partial^4 u}{\partial x^2 \partial t^2} - I_1 \frac{\partial^3 u}{\partial x \partial t^2} - q - (P + C_0 \Delta T - k_p) \frac{\partial^2 w}{\partial x^2} - k_w w + \left(1-l_m^2 \frac{\partial^2}{\partial x^2}\right) \left(A_1 \frac{\partial^3 u}{\partial x^3} - A_2 \frac{\partial^4 w}{\partial x^4}\right) = 0 \quad (3.126)$$

Whereas for the classical continuum theory, the governing equations is given by putting $ea = 0$ and $l_m = 0$ in Eqs.(3.121-3.122), as follow

$$A_0 \frac{\partial^2 u}{\partial x^2} - A_1 \frac{\partial^3 w}{\partial x^3} - I_0 \frac{\partial^2 u}{\partial t^2} + I_1 \frac{\partial^3 w}{\partial x \partial t^2} - f = 0 \quad (3.127a)$$

$$-I_0 \frac{\partial^2 w}{\partial t^2} + I_3 \frac{\partial^4 u}{\partial x^2 \partial t^2} - I_1 \frac{\partial^3 u}{\partial x \partial t^2} - q - (P + C_0 \Delta T - k_p) \frac{\partial^2 w}{\partial x^2} - k_w w + A_1 \frac{\partial^3 u}{\partial x^3} - A_2 \frac{\partial^4 w}{\partial x^4} = 0 \quad (3.127b)$$

The non-classical counterparts of the stress resultants can be obtained by using Eq.(3.23), Eqs.(3.113)- (3.114), and Eqs. (3.117-3.118) together

$$N^{(1)} = \frac{(ea)^4 l_m^2}{(ea)^2 - l_m^2} \left(I_0 \frac{\partial^4 u}{\partial x^2 \partial t^2} - I_1 \frac{\partial^5 w}{\partial x^3 \partial t^2} + \frac{\partial^2 f}{\partial x^2} \right) + l_m^2 \left(1 - \frac{(ea)^2 l_m^2}{(ea)^2 - l_m^2} \frac{\partial^2}{\partial x^2} \right) \left(A_0 \frac{\partial^2 u}{\partial x^2} - A_1 \frac{\partial^3 w}{\partial x^3} \right) \quad (3.128a)$$

$$M^{(1)} = \frac{(ea)^4 l_m^2}{(ea)^2 - l_m^2} \left(I_0 \frac{\partial^3 w}{\partial x \partial t^2} + I_1 \frac{\partial^5 w}{\partial x^3 \partial t^2} - I_2 \frac{\partial^4 w}{\partial x^2 \partial t^2} + \frac{\partial q}{\partial x} + (P + C_0 \Delta T - k_p) \frac{\partial^3 w}{\partial x^3} + k_w \frac{\partial w}{\partial x} \right) + l_m^2 \left(1 - \frac{(ea)^2 l_m^2}{(ea)^2 - l_m^2} \frac{\partial^2}{\partial x^2} \right) \left(A_1 \frac{\partial^2 u}{\partial x^2} - A_2 \frac{\partial^3 w}{\partial x^3} \right) \quad (3.128b)$$

Eqs. (3.121)-(3.122) can be written in term of the dimensionless quantities with the non-dimensional quantities as given as follow

$$\bar{x} = \frac{x}{L}, \quad \bar{u}, \bar{w} = \frac{(u, w)}{L}, \quad \lambda = \frac{h}{L}, \quad \alpha = \frac{ea}{L}, \quad \beta = \frac{l_m}{L}$$

$$(\bar{C}_0, \bar{G}_0, \bar{A}_0, \bar{A}_1, \bar{A}_2) = \left(\frac{C_0}{E_m bh}, \frac{G_0}{G_m bh}, \frac{A_0}{E_m bh}, \frac{A_1}{E_m bh^2}, \frac{A_2}{E_m bh^3} \right)$$

$$(\bar{I}_0, \bar{I}_1, \bar{I}_2) = \left(\frac{I_0}{\rho_m bh}, \frac{I_1}{\rho_m bh^2}, \frac{I_2}{\rho_m bh^3} \right)$$

$$\bar{t} = \frac{t}{L} \sqrt{\frac{E_m}{\rho_m}}, \quad \bar{P} = \frac{P}{E_m b h}, \quad (\bar{q}, \bar{f}) = \left(\frac{q}{E_m b h / L}, \frac{f}{E_m b h / L} \right)$$

$$(K_p, K_w) = \left(\frac{k_p}{E_m b h}, \frac{k_w L^2}{E_m b h} \right)$$

The Eqs. (121)- (122) can be rewritten in a dimensionless form

$$\left(1 - \beta^2 \frac{\partial^2}{\partial \bar{x}^2} \right) \left(\bar{A}_0 \frac{\partial^2 \bar{u}}{\partial \bar{x}^2} - \bar{A}_1 \lambda \frac{\partial^3 \bar{w}}{\partial \bar{x}^3} \right) - \left(1 - \alpha^2 \frac{\partial^2}{\partial \bar{x}^2} \right) \left(\bar{I}_0 \frac{\partial^2 \bar{u}}{\partial \bar{t}^2} - \bar{I}_1 \lambda \frac{\partial^3 \bar{w}}{\partial \bar{x} \partial \bar{t}^2} + \bar{f} \right) = 0 \quad (3.129)$$

$$\begin{aligned} & \left(1 - \beta^2 \frac{\partial^2}{\partial \bar{x}^2} \right) \left(\bar{A}_1 \lambda \frac{\partial^3 \bar{u}}{\partial \bar{x}^3} - \bar{A}_2 \lambda^2 \frac{\partial^4 \bar{w}}{\partial \bar{x}^4} \right) - \left(1 - \alpha^2 \frac{\partial^2}{\partial \bar{x}^2} \right) \left(\bar{I}_0 \frac{\partial^2 \bar{w}}{\partial \bar{t}^2} - \bar{I}_2 \lambda^2 \frac{\partial^4 \bar{u}}{\partial \bar{x}^2 \partial \bar{t}^2} + \bar{I}_1 \lambda \frac{\partial^3 \bar{u}}{\partial \bar{x} \partial \bar{t}^2} \right. \\ & \left. + \bar{q} - (\bar{P} + \bar{C}_0 \Delta T - \bar{K}_p) \frac{\partial^2 \bar{w}}{\partial \bar{x}^2} - \bar{K}_w \bar{w} \right) = 0 \end{aligned} \quad (3.130)$$

The stress resultants can be rewritten in dimensionless form

$$\bar{N} = \alpha^2 \left(\bar{I}_0 \frac{\partial^3 \bar{u}}{\partial \bar{x} \partial \bar{t}^2} - \bar{I}_1 \frac{\partial^4 \bar{w}}{\partial \bar{x}^2 \partial \bar{t}^2} + \frac{\partial \bar{f}}{\partial \bar{x}} \right) + \left(1 - \beta^2 \frac{\partial^2}{\partial \bar{x}^2} \right) \left(\bar{A}_0 \frac{\partial \bar{u}}{\partial \bar{x}} - \bar{A}_1 \frac{\partial^2 \bar{w}}{\partial \bar{x}^2} \right) \quad (3.131)$$

$$\begin{aligned} \bar{M} &= \alpha^2 \left(\bar{I}_0 \frac{\partial^2 \bar{w}}{\partial \bar{t}^2} + \bar{I}_1 \lambda \frac{\partial^3 \bar{u}}{\partial \bar{x} \partial \bar{t}^2} - \bar{I}_2 \lambda^2 \frac{\partial^4 \bar{u}}{\partial \bar{x}^2 \partial \bar{t}^2} + \bar{q} + (\bar{P} + \bar{C}_0 \Delta T - \bar{K}_p) \frac{\partial^2 \bar{w}}{\partial \bar{x}^2} + \bar{K}_w \bar{w} \right) \\ &+ \left(1 - \beta^2 \frac{\partial^2}{\partial \bar{x}^2} \right) \left(\bar{A}_1 \lambda \frac{\partial \bar{u}}{\partial \bar{x}} - \bar{A}_2 \lambda^2 \frac{\partial^2 \bar{w}}{\partial \bar{x}^2} \right) \end{aligned} \quad (3.132)$$

$$\begin{aligned} \bar{N}^{(1)} &= \frac{\alpha^4 \beta^2}{\alpha^2 - \beta^2} \left(\bar{I}_0 \frac{\partial^4 \bar{u}}{\partial \bar{x}^2 \partial \bar{t}^2} - \bar{I}_1 \lambda \frac{\partial^5 \bar{w}}{\partial \bar{x}^3 \partial \bar{t}^2} + \frac{\partial^2 \bar{f}}{\partial \bar{x}^2} \right) \\ &+ \beta^2 \left(1 - \frac{\alpha^2 \beta^2}{\alpha^2 - \beta^2} \frac{\partial^2}{\partial \bar{x}^2} \right) \left(\bar{A}_0 \frac{\partial^2 \bar{u}}{\partial \bar{x}^2} - \bar{A}_1 \lambda \frac{\partial^3 \bar{w}}{\partial \bar{x}^3} \right) \end{aligned} \quad (3.133)$$

$$\begin{aligned} \bar{M}^{(1)} = & \frac{\alpha^4 \beta^2}{\alpha^2 - \beta^2} \left(\bar{I}_0 \frac{\partial^3 \bar{w}}{\partial \bar{x} \partial \bar{t}^2} + \bar{I}_1 \lambda \frac{\partial^5 \bar{w}}{\partial \bar{x}^3 \partial \bar{t}^2} - I_2 \lambda^2 \frac{\partial^4 \bar{w}}{\partial \bar{x}^2 \partial \bar{t}^2} \right) \\ & + \frac{\partial \bar{q}}{\partial \bar{x}} + (\bar{P} + \bar{C}_0 \Delta T - K_P) \frac{\partial^3 \bar{w}}{\partial \bar{x}^3} + K_w \frac{\partial \bar{w}}{\partial \bar{x}} \\ & + \beta^2 \left(1 - \frac{\alpha^2 \beta^2}{\alpha^2 - \beta^2} \frac{\partial^2}{\partial \bar{x}^2} \right) \left(\bar{A}_1 \lambda \frac{\partial^2 \bar{u}}{\partial \bar{x}^2} - \bar{A}_2 \lambda^2 \frac{\partial^3 \bar{w}}{\partial \bar{x}^2} \right) \end{aligned} \quad (3.134)$$

With

$$(\bar{N}, \bar{M}) = \left(\frac{N}{E_m b h}, \frac{M}{E_m b h L} \right), (\bar{N}^{(1)}, \bar{M}^{(1)}) = \left(\frac{N^{(1)}}{E_m b h L}, \frac{M^{(1)}}{E_m b h L^2} \right)$$

3.4 Analytical Solution of sandwich FG micro-beam

The equations of motion are analytical solved for buckling analysis, static bending, and free behavior of a S-S sandwich functionally graded micro-beam based on the nonlocal strain gradient theory. In this thesis, the Navier approach is utilized to given the analytical solution. For this investigation, the displacement fields are explicit are result of the coefficients which are unknown and trigonometric functions, the displacement field for analytical solutions are assumed in the following as

$$u(x, t) = \sum_{n=1}^{\infty} U_n e^{i\omega t} \cos \beta x \quad (3.135)$$

$$w(x, t) = \sum_{n=1}^{\infty} W_n e^{i\omega t} \sin \beta x \quad (3.136)$$

$$\phi(x, t) = \sum_{n=1}^{\infty} G_n e^{i\omega t} \cos \beta x \quad (3.137)$$

(ω) is the fundamental frequency, the U_n, W_n, G_n are the coefficients which are undetermined, and $\beta = n \pi / L$. It can be seen in the EBBT that G_n is equal to zero.

3.4.1 Bending of the sandwich FG micro-beam

For the this section of the thesis, the derivatives of the time must be equal to zero and the external load represented by f vanish. On the other hand the transverse force represented by q is presented as follow

$$q(x) = \sum_{m=1}^N Q_m \sin \beta x \quad (3.138)$$

$$Q_m = \frac{2}{L} \int_0^L q(x) \sin \beta x dx \quad (3.139)$$

where Q_m coefficients are given for uniform forces is represented in the following equation

$$q(x) = q_o ; Q_m = \frac{4q_o}{m \pi} \quad m = 1, 3, 5, \dots$$

where q_o is the intensity of the uniformly distributed load.

3.4.1.1 Euler Bernoulli Beam Theory (EBBT)

Substituting Eqs.(3.135),(3.136) and (3.138) into Eqs.(3.121),(3.122) to obtain the following equations

$$\begin{bmatrix} CA_0 \beta^2 & -CA_1 \beta^2 \\ -CA_1 \beta^2 & CA_3 \beta^2 + (k_p - C_0 \Delta T) \beta^2 Z + k_w Z \end{bmatrix} \begin{Bmatrix} U_n \\ W_n \\ G_n \end{Bmatrix} = \begin{Bmatrix} 0 \\ (1 + \beta^2 (ea)^2) Q_n \\ 0 \end{Bmatrix} \quad (3.140)$$

$$\text{where } C = (1 + \beta^2 l_m^2) \quad Z = (1 + \beta^2 ea^2)$$

Equation (140) can be solved to obtain the Fourier coefficients for EBBT.

$$U_n = \frac{Q_n (A_1 \beta (\beta^2 (ea)^2 + 1))}{\beta^4 (\beta^2 l_m^2 + 1) (A_0 A_3 - A_1^2) + (\beta^2 (ea)^2 + 1) A_0 (k_w + k_p \beta^2 - C_0 \Delta T \beta^2)} \quad (3.141)$$

$$W_n = \frac{Q_n (A_0 (\beta^2 (ea)^2 + 1))}{\beta^4 (\beta^2 l_m^2 + 1) (A_0 A_3 - A_1^2) + (\beta^2 (ea)^2 + 1) A_0 (k_w + k_p \beta^2 - C_0 \Delta T \beta^2)} \quad (3.142)$$

3.4.1.2 Timoshenko Beam Theory (TBT)

Substituting Eqs.(3.135)-(3.137) and (3.138) into Eqs.(3.88)-(3.90) to obtain the following equations

$$\begin{bmatrix} CA_0\beta^2 & 0 & -CA_1\beta^2 \\ 0 & Ck_sG_0\beta^2 + (k_p - C_0\Delta T)\beta^2Z + k_wZ & Ck_sG_0\beta \\ -CA_1\beta^2 & Ck_sG_0\beta & CA_3\beta^2 + Ck_sG_0 \end{bmatrix} \begin{Bmatrix} U_n \\ W_n \\ G_n \end{Bmatrix} = \begin{Bmatrix} 0 \\ (1 + \beta^2(ea)^2)Q_n \\ 0 \end{Bmatrix} \quad (3.143)$$

$$\text{where } C = (1 + \beta^2l_m^2) \quad Z = (1 + \beta^2ea^2)$$

Eq.(3.143) can be solved to obtain the Fourier coefficients for Timoshenko micro-beam theory

$$U_n = \frac{Q_n \left(G_0 A_1 \beta k_s \left(\beta^2 (ea)^2 + 1 \right) \right)}{T} \quad (3.144)$$

$$W_n = \frac{Q_n \left(\beta^2 (ea)^2 + 1 \right) \left((A_0 A_3 - A_1^2) \beta^2 + k_s A_0 G_0 \right)}{T} \quad (3.145)$$

$$G_n = \frac{Q_n \left(G_0 A_0 \beta k_s \left(\beta^2 (ea)^2 + 1 \right) \right)}{T} \quad (3.146)$$

Where

$$T = \left(\beta^2 (ea)^2 + 1 \right) \left(k_p \beta^2 - C_0 \Delta T \beta^2 + k_w \right) \left(A_0 A_3 - A_2^2 + k_s \beta^2 A_0 G_0 \right) + \left(A_0 G_3 - A_1^2 \right) G_0 \left(\beta^2 l_m^2 + 1 \right) \beta^4 k_s$$

3.4.1.3 Higher order Beam Theories (HOBTs)

Substituting Eqs.(3.135)-(3.137) and (3.138) into Eqs.(3.55)-(3.57) lead to the following system of algebraic equations

$$\begin{bmatrix} CA_0\beta^2 & C\beta^3(A_2 - A_1) & -CA_2\beta^2 \\ -C\beta^3A_1 & \begin{pmatrix} C\beta^4(A_3 - A_4) \\ + \left(-(\bar{P} + C_0\Delta T)\beta^2 + k_p\beta^2 + k_w \right) Z \end{pmatrix} & CA_4\beta^3 \\ -CA_2\beta^2 & C\beta(A_4\beta^2 - A_5\beta^2 - G_0) & C(A_5\beta^2 + G_0) \end{bmatrix} \begin{Bmatrix} U_n \\ W_n \\ G_n \end{Bmatrix} = \begin{Bmatrix} 0 \\ (1 + \beta^2(ea)^2)Q_n \\ 0 \end{Bmatrix} \quad (3.147)$$

$$\text{where } C = (1 + \beta^2 l_m^2) \quad Z = (1 + \beta^2 ea^2)$$

Eq.(3.147) can be solved to obtain the Fourier coefficients for Higher order micro-beam theory

$$U_n = \frac{Q_n Z \beta (A_1 G_0 + A_1 A_5 \beta^2 - A_2 A_4 \beta^2)}{R} \quad (3.148)$$

$$W_n = \frac{Q_n Z (\beta^2 (A_0 A_5 - A_2^2) + A_0 G_0)}{R} \quad (3.149)$$

$$G_n = \frac{Q_n Z \beta (A_0 G_0 - A_2^2 \beta^2 - A_0 A_4 \beta^2 + B_1 A_2 \beta^2 + A_0 A_5 \beta^2)}{R} \quad (3.150)$$

Where

$$R = (\beta^2 l_m^2 + 1) \beta^4 \left(A_5 A_1^2 \beta^2 + G_0 A_1^2 - 2A_1 A_2 A_4 \beta^2 + A_3 A_2^2 \beta^2 \right) \\ + A_0 A_4^2 \beta^2 - A_0 A_3 A_5 \beta^2 + A_0 G_0 A_3 \\ - (\beta^2 (ea)^2 + 1) (A_0 G_0 + A_0 A_5 \beta^2 - A_2^2 \beta^2) (k_w + k_p \beta^2 - C_0 \Delta T)$$

3.4.2 Buckling Problem

For the buckling analysis, the external forces (f, q) is equal to zero and all time derivatives are set to zero. The critical buckling load of the FG sandwich micro-beam is calculated for the different beam theories with S-S boundary conditions according to the Navier solution approach.

3.4.2.1 Euler Bernoulli Beam Theory (EBBT)

By sub. Eq.(3.135) and Eq.(3.136) into the equations of Eqs.(3.121)-(3.122), it can be obtained the following equation as follow

$$\begin{bmatrix} C A_0 \beta^2 & -C A_1 \beta^3 \\ -C A_1 \beta^3 & C A_3 \beta^4 - (\bar{P} - K_p + C_0 \Delta T) \beta^2 Z + K_w Z \end{bmatrix} \begin{Bmatrix} U_n \\ W_n \end{Bmatrix} = \begin{Bmatrix} 0 \\ 0 \end{Bmatrix} \quad (3.151)$$

$$\text{where } C = (1 + \beta^2 l_m^2) \quad Z = (1 + \beta^2 ea^2)$$

the critical buckling load can be obtained by setting the determinant of the matrix in Eq.(151) is to be zero. The smallest value eigenvalue is the critical buckling load. On the other hand the formulation is used to find the critical buckling load for the Euler Bernoulli micro-beam as follow

$$\bar{P} = P_{cr}(n) = \frac{(1 + \beta^2 l_m^2) \beta^4 (A_0 A_3 - A_1^2) + (\beta^2 (ea)^2 + 1) A_0 (k_w + \beta^2 (k_p - C_0 \Delta T))}{A_0 \beta^2 (\beta^2 (ea)^2 + 1)} \quad (3.152)$$

3.4.2.2 Timoshenko Beam Theory (TBT)

The eigenvalue equation of the buckling analysis for sandwich FG microbeam with TBT can be obtained in the following equation

$$\begin{bmatrix} CA_0 \beta^2 & 0 & -CA_1 \beta^2 \\ 0 & Ck_s G_0 \beta^2 - (\bar{P} - k_p + C_0 \Delta T) \beta^2 Z + k_w Z & Ck_s G_0 \beta \\ -CA_1 \beta^2 & Ck_s G_0 \beta & CA_3 \beta^2 + Ck_s G_0 \end{bmatrix} \begin{Bmatrix} U_n \\ W_n \\ G_n \end{Bmatrix} = \begin{Bmatrix} 0 \\ 0 \\ 0 \end{Bmatrix} \quad (3.153)$$

$$\text{where } C = (1 + \beta^2 l_m^2) \quad Z = (1 + \beta^2 ea^2)$$

Also, the formulation is used to calculate the critical buckling load force is obtained as follow

$$\bar{P} = P_{cr}(n) = \frac{(1 + \beta^2 l_m^2) \beta^4 k_s G_0 (A_0 A_3 - A_1^2) + (k_w + \beta^2 (k_p - C_0 \Delta T)) (\beta^2 (ea)^2 + 1) T}{\beta^2 (\beta^2 (ea)^2 + 1) [\beta^2 (A_0 A_3 - A_1^2) + k_s G_0 A_0]} \quad (3.154)$$

$$\text{Where } T = [\beta^2 (A_0 A_3 - A_1^2) + k_s G_0 A_0]$$

3.4.2.3 Higher order Beam Theories (HOBTs)

Substituting Eqs.(3.135)-(3.137) into Eqs.(3.55)-(3.57), the following equations can be obtained

$$\begin{bmatrix} CA_0\beta^2 & C\beta^3(A_2 - A_1) & -CA_2\beta^2 \\ -C\beta^3A_1 & \begin{pmatrix} C\beta^4(A_3 - A_4) \\ +(-\bar{P}\beta^2 + k_p\beta^2 + k_w)Z \end{pmatrix} & CA_4\beta^3 \\ -CA_2\beta^2 & C\beta(A_4\beta^2 - A_5\beta^2 - G_0) & C(A_5\beta^2 + G_0) \end{bmatrix} \begin{Bmatrix} U_n \\ W_n \\ G_n \end{Bmatrix} = \begin{Bmatrix} 0 \\ 0 \\ 0 \end{Bmatrix} \quad (3.155)$$

$$\bar{P} = P_{cr}(n) = \frac{C \left[(\beta^4 G_0 S_1 - \beta^6 S_2) + (k_w + \beta^2 k_p) Z S_3 \right]}{Z \beta^2 \left[\beta^2 (A_0 A_5 - A_2^2) + A_0 G_0 \right]} \quad (3.156)$$

where

$$\text{where } Z = (1 + \beta^2 ea^2) \text{ and } C = (1 + \beta^2 l_m^2) \quad S_1 = A_1^2 - A_0 A_3$$

$$S_2 = (A_4^2 - A_0 A_5) A_0 - A_1 (2A_2 A_4 - A_5 A_1) + A_3 A_2^2 \quad S_3 = -A_0 G_0 - \beta^2 (A_0 A_5 - A_2^2)$$

3.4.3 Free vibration Analysis

For the free vibration analysis, the all external forces (f, q, P) is equal to zero. When substituting Eqs. (3.135)-(3.137) into Eqs.(3.55)-(3.57) for HOBTs, the eigenvalue equation can be obtained as follow

$$\left(\begin{bmatrix} K_{11} & K_{12} & K_{13} \\ K_{21} & K_{22} & K_{23} \\ K_{31} & K_{32} & K_{33} \end{bmatrix} - \omega_n^2 (1 + ea^2 \beta^2) \begin{bmatrix} M_{11} & M_{12} & M_{13} \\ M_{21} & M_{22} & M_{23} \\ M_{31} & M_{32} & M_{33} \end{bmatrix} \right) \begin{Bmatrix} U_n \\ W_n \\ G_n \end{Bmatrix} = \begin{Bmatrix} 0 \\ 0 \\ 0 \end{Bmatrix} \quad (3.157)$$

$$M_{11} = -I_0, \quad M_{12} = (I_1 - I_2)\beta, \quad M_{13} = M_{31} = I_2, \quad M_{21} = I_1\beta$$

$$M_{32} = (I_5 - I_4)\beta, \quad M_{23} = I_4, \quad M_{33} = -I_5, \quad M_{22} = -I_0 + (I_4 - I_3)\beta^2$$

The determinate of the coefficient matrix in Eq.(3.157) is equal to zero, then the characteristic values ω_n can be obtained. The smallest eigenvalues (ω_1) is the fundamental frequency. The eigenvalue free vibration equation for EBBT is given explicitly in Appendix B1 and TBT is given explicitly in Appendix B2.

3.4 Generalized differential quadrature method (GDQM)

The GDQM is an extension of the well-known differential quadrature method (DQM) which is commonly utilized for the numerical solution of differential equations, under various initial and boundary conditions (BCs). In the regular differential quadrature method (DQM) only the primary variables are discretized and the differential equations are represented as algebraic equations of the primary unknowns of the problem. The domain is discretized by dividing it into a grid and unknowns are defined as the values of primary variables at these pre-selected grid points. The approximation is based on Lagrange interpolation functions defined for the grid points. Corresponding algebraic equations are written for grid points inside the domain whereas grid points on the boundary are reserved for the implementation of the boundary conditions. Most of the time differential equations with higher order derivatives involve boundary conditions with the derivatives of primary variables (Neumann BCs), both primary variables and their derivatives (mixed Dirichlet-Neumann) or linear combinations of primary variables and their derivatives (Robin BCs). Thus speaking for a beam problem with two grid end points often requires additional interior points or some other extra points for the implementation of these kinds of BCs. Generalized differential quadrature method deals with these situations without involving other extra points. In this method approximation is not based on the primary variables only but also on their derivatives defined independently at the boundary points as well. This results in extra degrees of freedom (dof) for a boundary point which makes it sufficient to implement additional conditions involving the derivatives of the primary variables. A more robust system of equations are obtained albeit with a slightly larger linear system of unknown equations and sophisticated approximation functions of Hermite type. In the current study we opted to use the GDQM to determine the buckling and free vibration of sandwich functionally graded micro-beam. Here we briefly explain the utilization of the method for our problem. The primary variables of the system includes $u(x,t)$, $w(x,t)$ and $\phi(x,t)$. For the steady-state nature of the eigenvalue problems we assume that $u(x,t) = u(x)e^{i\omega t}$, $w(x,t) = w(x)e^{i\omega t}$, $\phi(x,t) = \phi(x)e^{i\omega t}$ with the natural frequency of ω . The beam's length L is divided into $N - 1$ regions with N grid points. The variables selected for the an interior point i for $1 < i < N$ can be represented with subscript i as $u_i = u(x_i)$, $w_i = w(x_i)$ and $\phi_i = \phi(x_i)$. Here x_i is the i^{th} grid point's coordinate with $0 \leq x \leq L$. The variables at the boundary points for $i = 1$ and $i = N$ are selected as $u_i^{(1)} = \partial u / \partial x|_{x=x_i}$, $\phi_i^{(1)} = \partial \phi / \partial x|_{x=x_i}$, $w_i^{(1)} = \partial w / \partial x|_{x=x_i}$, $w_i^{(2)} = \partial^2 w / \partial x^2|_{x=x_i}$. This selection makes the first derivatives of the axial displacement, rotation and first and second derivatives of the vertical

displacement independent variables of the numerical approximation. Thus at interior points we have defined three *dof* , and at the boundary points we have defined seven *dof* . Note that this is exactly the number of BCs we have at any boundary point. Also selections of the order of the derivatives for making independent variables are due to the nature of the boundary terms appeared at the end of the variational procedure. Following the procedure given in [50] closely, first we define the vector of unknowns d^u, d^w, d^ϕ as

$$\begin{aligned}
d^u &= \{u_1, u_1^{(1)}, u_2, \dots, u_N, u_N^{(1)}\} \\
d^w &= \{w_1, w_1^{(1)}, w_1^{(2)}, w_2, \dots, w_N, w_N^{(1)}, w_N^{(2)}\} \\
d^\phi &= \{\phi_1, \phi_1^{(1)}, \phi_2, \dots, \phi_N, \phi_N^{(1)}\} \\
d &= \{d^u, d^w, d^\phi\}
\end{aligned} \tag{3.158}$$

Now we can define the r^{th} derivative of a primary variable at i^{th} grid point as a linear combination of independent values at other points:

$$\begin{aligned}
\left. \frac{\partial^r u}{\partial x^r} \right|_{x=x_j} &= u_i^{(r)} = \sum_{j=1}^N G_{ij}^{(r)} d_j^u \quad j = 1, 2, \dots, N + 2 \\
\left. \frac{\partial^r w}{\partial x^r} \right|_{x=x_j} &= w_i^{(r)} = \sum_{j=1}^N H_{ij}^{(r)} d_j^w \quad j = 1, 2, \dots, N + 4 \\
\left. \frac{\partial^r \phi}{\partial x^r} \right|_{x=x_j} &= \phi_i^{(r)} = \sum_{j=1}^N G_{ij}^{(r)} d_j^\phi \quad j = 1, 2, \dots, N + 2
\end{aligned} \tag{3.159}$$

Here $G^{(r)}$ and $H^{(r)}$ are matrices with dimensions $N \times (N + 2)$ and $N \times (N + 4)$ respectively. They involve weight coefficients which are based on the modified Hermite interpolation functions. $G^{(0)}$ matrix's 1st , 2nd , N^{th} , $(N + 1)^{th}$ and other columns can be respectively obtained from functions $g_{10}(x)$, $g_{11}(x)$, $g_{N0}(x)$, $g_{N1}(x)$, $g_{i0}(x)$ for $i = 2, \dots, N - 1$ and for $j = 1, 2, \dots, N$ which satisfy the following set of conditions which are briefly dictating that a variable's "direct" influence to other points should be zero whereas should be unity for its own point:

$$\begin{array}{llll}
g_{10}(x_j) = \delta_{1j} & g_{10}^{(1)}(x_1) = 0 & g_{10}^{(1)}(x_N) = 0 & g_{10}(x) = (a_{10}x^2 + b_{10}x + c_{10})l_1(x) \\
g_{N0}(x_j) = \delta_{Nj} & g_{N0}^{(1)}(x_1) = 0 & g_{N0}^{(1)}(x_N) = 0 & g_{11}(x) = (a_{11}x^2 + b_{11}x + c_{11})l_1(x) \\
g_{11}(x_j) = 0 & g_{11}^{(1)}(x_1) = 1 & g_{11}^{(1)}(x_N) = 0 & \Rightarrow g_{N0}(x) = (a_{N0}x^2 + b_{N0}x + c_{N0})l_N(x) \\
g_{N1}(x_j) = 0 & g_{N1}^{(1)}(x_1) = 0 & g_{N1}^{(1)}(x_N) = 1 & g_{N1}(x) = (a_{N1}x^2 + b_{N1}x + c_{N1})l_N(x) \\
g_{i0}(x_j) = \delta_{ij} & g_{i0}^{(1)}(x_1) = 0 & g_{i0}^{(1)}(x_N) = 0 & g_{i0}(x) = (a_{i0}x^2 + b_{i0}x + c_{i0})l_i(x)
\end{array}
\tag{3.160}$$

Here $l_i(x_i)$ is the Lagrange interpolation functions and δ_{ij} is Kronecker's delta with $l_i(x_i) = \delta_{ij}$. These five set of conditions can be satisfied with the forms given next to them respectively for each set. The parameters inside functions are then found as:

$$\begin{aligned}
a_{10} &= -\frac{1}{(x_1 - x_N)^2} - \frac{l_1^{(1)}(x_1)}{(x_1 - x_N)}, \quad b_{10} = \frac{1}{(x_1 - x_N)} - a_{10}(x_1 + x_N), \quad c_{10} = 1 - a_{10}x_1^2 - b_{10}x_1 \\
a_{11} &= \frac{1}{(x_1 - x_N)}, \quad b_{11} = \frac{(x_1 + x_N)}{(x_N - x_1)}, \quad c_{11} = \frac{x_1x_N}{(x_1 - x_N)} \\
a_{N0} &= -\frac{1}{(x_1 - x_N)^2} - \frac{l_N^{(1)}(x_N)}{(x_1 - x_N)}, \quad b_{N0} = \frac{1}{(x_N - x_1)} - a_{N0}(x_1 + x_N), \quad c_{N0} = 1 - a_{N0}x_N^2 - b_{N0}x_N \\
a_{N1} &= \frac{1}{(x_N - x_1)}, \quad b_{N1} = \frac{(x_1 + x_N)}{(x_1 - x_N)}, \quad c_{N1} = \frac{x_1x_N}{(x_N - x_1)} \\
a_{i0} &= \frac{1}{(x_1 - x_i)(x_N - x_i)}, \quad b_{i0} = -\frac{x_1 + x_N}{(x_1 - x_i)(x_N - x_i)}, \quad c_{i0} = \frac{x_1x_N}{(x_1 - x_i)(x_N - x_i)}
\end{aligned}$$

A similar development can be given for $H^{(r)}$ matrix. $H^{(0)}$ matrix's 1^{st} , 2^{nd} , 3^{rd} , N^{th} , $N + 1^{th}$, $N + 2^{th}$ columns and the rest of the columns can be respectively obtained from functions $h_{10}(x)$, $h_{11}(x)$, $h_{12}(x)$, $h_{N0}(x)$, $h_{N1}(x)$, $h_{N2}(x)$, $h_{i0}(x)$ for $i = 2, \dots, N - 1$ and for $j = 1, 2, \dots, N$ which satisfy the following set of conditions with the similar reasoning:

$$\begin{array}{cccccc}
h_{10}(x_j) = \delta_{1j} & h_{10}^{(1)}(x_1) = 0 & h_{10}^{(2)}(x_1) = 0 & h_{10}^{(1)}(x_N) = 0 & h_{10}^{(2)}(x_N) = 0 \\
h_{N0}(x_j) = \delta_{Nj} & h_{N0}^{(1)}(x_1) = 0 & h_{N0}^{(2)}(x_1) = 0 & h_{N0}^{(1)}(x_N) = 0 & h_{N0}^{(2)}(x_N) = 0 \\
h_{11}(x_j) = 0 & h_{11}^{(1)}(x_1) = 1 & h_{11}^{(2)}(x_1) = 0 & h_{11}^{(1)}(x_N) = 0 & h_{11}^{(2)}(x_N) = 0 \\
h_{12}(x_j) = 0 & h_{12}^{(1)}(x_1) = 0 & h_{12}^{(2)}(x_1) = 1 & h_{12}^{(1)}(x_N) = 0 & h_{12}^{(2)}(x_N) = 0 \Rightarrow \\
h_{N1}(x_j) = 0 & h_{N1}^{(1)}(x_1) = 0 & h_{N1}^{(2)}(x_1) = 0 & h_{N1}^{(1)}(x_N) = 1 & h_{N1}^{(2)}(x_N) = 0 \\
h_{N2}(x_j) = 0 & h_{N2}^{(1)}(x_1) = 0 & h_{N2}^{(2)}(x_1) = 0 & h_{N2}^{(1)}(x_N) = 0 & h_{N2}^{(2)}(x_N) = 1 \\
h_{i0}(x_j) = \delta_{ij} & h_{i0}^{(1)}(x_1) = 0 & h_{i0}^{(2)}(x_1) = 0 & h_{i0}^{(1)}(x_N) = 0 & h_{i0}^{(2)}(x_N) = 0
\end{array} \tag{3.161}$$

$$h_{1s}(x) = \frac{(x-x_N)^2}{(x_1-x_N)^2} (\hat{a}_{1s}x^2 + \hat{b}_{1s}x + \hat{c}_{1s}) l_1(x) \quad \text{for } s=0,1,2$$

$$h_{Ns}(x) = \frac{(x-x_1)^2}{(x_1-x_N)^2} (\hat{a}_{Ns}x^2 + \hat{b}_{Ns}x + \hat{c}_{Ns}) l_1(x) \quad \text{for } s=0,1,2$$

$$h_{i0}(x) = \frac{(x-x_1)^2}{(x_i-x_1)^2} \frac{(x-x_N)^2}{(x_i-x_N)^2} l_i(x)$$

These conditions give the following parameters of the approximation functions

$$\hat{a}_{10} = \left(l_1^{(1)}(x_1) + \frac{2}{(x_1-x_N)} \right)^2 - \frac{1}{(x_1-x_N)^2} - \frac{2l_1^{(1)}(x_1)}{(x_1-x_N)} - \frac{l_1^{(2)}(x_1)}{2},$$

$$\hat{b}_{10} = - \left(l_1^{(1)}(x_1) + \frac{2}{(x_1-x_N)} \right) - 2\hat{a}_{10}x_1,$$

$$\hat{c}_{10} = 1 - \hat{a}_{10}x_1^2 - \hat{b}_{10}x_1,$$

$$\hat{a}_{11} = - \left(l_1^{(1)}(x_1) + \frac{2}{(x_1-x_N)} \right), \quad \hat{b}_{11} = 1 - 2\hat{a}_{11}x_1, \quad \hat{c}_{11} = x_1(\hat{a}_{11}x_1 - 1)$$

$$\hat{a}_{12} = \frac{1}{2}, \quad \hat{b}_{12} = -x_1, \quad \hat{c}_{12} = \frac{x_1^2}{2}$$

$$\hat{a}_{N0} = \left(l_N^{(1)}(x_N) - \frac{2}{(x_1-x_N)} \right)^2 - \frac{1}{(x_1-x_N)^2} + \frac{2l_N^{(1)}(x_N)}{(x_1-x_N)} - \frac{l_N^{(2)}(x_N)}{2},$$

$$\hat{b}_{N0} = - \left(l_N^{(1)}(x_N) - \frac{2}{(x_1-x_N)} \right) - 2\hat{a}_{N0}x_N,$$

$$\hat{c}_{N0} = 1 - \hat{a}_{N0}x_N^2 - \hat{b}_{N0}x_N,$$

$$\hat{a}_{N1} = - \left(l_N^{(1)}(x_N) - \frac{2}{(x_1-x_N)} \right), \quad \hat{b}_{N1} = 1 - 2\hat{a}_{N1}x_N, \quad \hat{c}_{N1} = x_N(\hat{a}_{N1}x_N - 1)$$

$$\hat{a}_{N2} = \frac{1}{2}, \quad \hat{b}_{N2} = -x_N, \quad \hat{c}_{N2} = \frac{x_N^2}{2}$$

Matrices $G^{(r)}$ and $H^{(r)}$ include calculations based on derivatives of these functions and these in turn are depending on the derivatives of the Lagrange interpolation functions $l_i(x)$. For the sake of completeness we also give the recurrence relations for the values of derivatives of Lagrange interpolation functions on grid points below.

$$l_i^{(1)}(x_j) = \frac{M(x_j)}{(x_j - x_i) \cdot M(x_i)} \quad \text{for } i, j = 1, 2, \dots, N \text{ and } i \neq j$$

$$l_i^{(r)}(x_j) = r \left(l_j^{(r-1)}(x_j) l_i^{(1)}(x_j) - \frac{l_i^{(r-1)}(x_j)}{(x_j - x_i)} \right) \quad \text{for } i, j = 1, 2, \dots, N; \quad i \neq j \text{ and } r \geq 2$$

$$l_i^{(r)}(x_i) = - \sum_{j=1, j \neq i}^N l_j^{(r)}(x_i) \quad \text{for } i, j = 1, 2, \dots, N \text{ and } r \geq 1$$

where

$$M(x_i) = \prod_{m=1, m \neq i}^N (x_i - x_m)$$

Now the components of $G^{(r)}$ and $H^{(r)}$ can be obtained by calculating the values of r^{th} derivative of the associated approximation functions' at grid points. Finally it is essential to know that the number and distribution of the sampling points are the key factors defining the accuracy of the numerical results. In the present study, these interpolation points are being considered as Chebyshev-Gauss-Lobatto points:

$$x_i = \frac{L}{2} \left(1 - \cos \left(\frac{(i-1)\pi}{N-1} \right) \right) \quad \text{for } i = 1, \dots, N \quad (3.162)$$

Applying the relationships in (60) and assuming the steady-state response for Eqs. (3.70), (3.71) and (3.72) one obtains the following eigenvalue system:

$$\{ [K] - \bar{\omega}^2 [M] + \bar{P} [S] \} \{ \bar{d} \} \quad (3.163)$$

Here $\bar{\omega} = \omega L \sqrt{\rho_m / E_m}$ is the dimensionless natural frequency. Eq. (3.163) can be explicitly written for the K , M and S matrices which carry terms related with the stiffness, mass and stability respectively. One obtains a set of ordinary differential equations for higher order beam theories (HOBTs)

$$\left\{ \begin{array}{ccc} {}^b K^{uu} & {}^b K^{uw} & {}^b K^{\phi} \\ K^{uu} & K^{uw} & K^{u\phi} \\ K^{wu} & K^{ww} & K^{w\phi} \\ K^{\phi u} & K^{\phi w} & K^{\phi\phi} \end{array} \right\} - \bar{\omega}^2 \left\{ \begin{array}{ccc} {}^b M^{uu} & {}^b M^{uw} & {}^b M^{\phi} \\ M^{uu} & M^{uw} & M^{u\phi} \\ M^{wu} & M^{ww} & M^{w\phi} \\ M^{\phi u} & M^{\phi w} & M^{\phi\phi} \end{array} \right\} + \bar{P} \left\{ \begin{array}{ccc} {}^b S^{uu} & {}^b S^{uw} & {}^b S^{\phi} \\ S^{uu} & S^{uw} & S^{u\phi} \\ S^{wu} & S^{ww} & S^{w\phi} \\ S^{\phi u} & S^{\phi w} & S^{\phi\phi} \end{array} \right\} \left\{ \begin{array}{c} \bar{d}^u \\ \bar{d}^w \\ \bar{d}^{\phi} \end{array} \right\} = 0 \quad (3.164)$$

Components of the above matrices are then become

$$K_{ij}^{uu} = \bar{A}_0 \left(G_{ij}^{(2)} - \beta^2 G_{ij}^{(4)} \right), \quad K_{ij}^{uw} = \lambda \left(\bar{A}_2 - \bar{A}_1 \right) \left(H_{ij}^{(3)} - \beta^2 H_{ij}^{(5)} \right), \quad K_{ij}^{u\phi} = -\lambda \bar{A}_2 \left(G_{ij}^{(2)} - \beta^2 G_{ij}^{(4)} \right),$$

$$K_{ij}^{wu} = \lambda \bar{A}_1 \left(G_{ij}^{(3)} - \beta^2 G_{ij}^{(5)} \right), \quad K_{ij}^{w\phi} = -\lambda^2 \bar{A}_4 \left(G_{ij}^{(3)} - \beta^2 G_{ij}^{(5)} \right),$$

$$K_{ij}^{ww} = \lambda^2 \left(\bar{A}_4 - \bar{A}_3 \right) \left(H_{ij}^{(4)} - \beta^2 H_{ij}^{(6)} \right) - \left(\bar{C}_0 \Delta T - \bar{K}_p \right) \left(H_{ij}^{(2)} - \alpha^2 H_{ij}^{(4)} \right) - \bar{K}_w \left(H_{ij}^{(0)} - \alpha^2 H_{ij}^{(2)} \right),$$

$$K_{ij}^{\phi u} = -\lambda \bar{A}_2 \left(G_{ij}^{(2)} - \beta^2 G_{ij}^{(4)} \right), \quad K_{ij}^{\phi w} = -\lambda^2 \left(\bar{A}_5 - \bar{A}_4 \right) \left(H_{ij}^{(3)} - \beta^2 H_{ij}^{(5)} \right) + G_0 \left(H_{ij}^{(1)} - \beta^2 H_{ij}^{(3)} \right),$$

$$K_{ij}^{\phi\phi} = \lambda^2 \bar{A}_5 \left(G_{ij}^{(2)} - \beta^2 G_{ij}^{(4)} \right) - G_0 \left(G_{ij}^{(0)} - \alpha^2 G_{ij}^{(2)} \right)$$

$$M_{ij}^{uu} = -\bar{I}_0 \left(G_{ij}^{(0)} - \alpha^2 G_{ij}^{(2)} \right), \quad M_{ij}^{uw} = \lambda \left(\bar{I}_1 - \bar{I}_2 \right) \left(H_{ij}^{(1)} - \alpha^2 H_{ij}^{(3)} \right), \quad M_{ij}^{u\phi} = \lambda \bar{I}_2 \left(G_{ij}^{(0)} - \alpha^2 G_{ij}^{(2)} \right),$$

$$M_{ij}^{wu} = -\lambda \bar{I}_1 \left(G_{ij}^{(1)} - \alpha^2 G_{ij}^{(3)} \right), \quad M_{ij}^{w\phi} = \lambda^2 \bar{I}_4 \left(G_{ij}^{(1)} - \alpha^2 G_{ij}^{(3)} \right),$$

$$M_{ij}^{ww} = -\lambda^2 \left(\bar{I}_4 - \bar{I}_3 \right) \left(H_{ij}^{(2)} - \alpha^2 H_{ij}^{(4)} \right) - \bar{I}_0 \left(H_{ij}^{(0)} - \alpha^2 H_{ij}^{(2)} \right),$$

$$M_{ij}^{\phi u} = \lambda \bar{I}_2 \left(G_{ij}^{(0)} - \alpha^2 G_{ij}^{(2)} \right), \quad M_{ij}^{\phi w} = \lambda^2 \left(\bar{I}_5 - \bar{I}_4 \right) \left(H_{ij}^{(1)} - \alpha^2 H_{ij}^{(3)} \right),$$

$$M_{ij}^{\phi\phi} = -\lambda^2 \bar{I}_5 \left(G_{ij}^{(0)} - \alpha^2 G_{ij}^{(2)} \right)$$

$$S_{ij}^{uu} = S_{ij}^{uw} = S_{ij}^{u\phi} = S_{ij}^{wu} = S_{ij}^{w\phi} = S_{ij}^{\phi u} = S_{ij}^{\phi w} = S_{ij}^{\phi\phi} = 0,$$

$$S_{ij}^{ww} = -\left(H_{ij}^{(2)} - \alpha^2 H_{ij}^{(4)} \right)$$

Here $i = 2, \dots, (N-1)$ and $j = 1, 2, \dots, (N+2)$ for \bar{d}^u and \bar{d}^ϕ . $j = 1, 2, \dots, (N+4)$ for \bar{d}^w .

The sub-system written for interior points has a dimension of $(3N-6) \times (3N+8)$. Remaining 14 equations due to BCs are gathered in the terms with a left upper script "b" denoting boundary.

For a simply supported (S) end the nature of the BCs can be deduced from a Navier type solution suggestion:

$$u(x) \square \cos(x\pi/L) \Rightarrow N = 0, \quad \partial u / \partial x = 0$$

$$w(x) \square \sin(x\pi/L) \Rightarrow w = 0, \quad M = 0, \quad \partial^2 w / \partial x^2 = 0 \quad (3.165)$$

$$\phi(x) \square \cos(x\pi/L) \Rightarrow \partial^2 w / \partial x^2 - \partial \phi / \partial x = 0, \quad Q_h^{(1)} + M_h = 0$$

For a clamped (C) end we will assume that all geometrical type constraints are activated thus

$$u=0, \quad \partial u/\partial x=0, \quad w=0, \quad \partial w/\partial x=0, \quad \partial^2 w/\partial x^2=0, \quad \phi=0, \quad \partial \phi/\partial x=0$$

(3.166)

Discretization of the corresponding boundary conditions can be handled in the same way. For

example a beam with C-S type supports, for the clamped end ($i=1$) we have from Eq. (3.166)

$${}^b K_{1j}^u = G_{1j}^{(0)}, {}^b K_{2j}^u = G_{1j}^{(1)}, {}^b K_{3j}^w = H_{1j}^{(0)}, {}^b K_{4j}^w = G_{1j}^{(1)}, {}^b K_{5j}^w = G_{1j}^{(2)}, {}^b K_{6j}^\phi = G_{1j}^{(0)}, {}^b K_{7j}^\phi = G_{1j}^{(1)}$$

and for the simply supported end ($i=N$) we have from Eq. (165)

$$\begin{aligned} {}^b K_{8j}^u &= \bar{A}_0 G_{Nj}^{(3)}, {}^b K_{8j}^w = \lambda (\bar{A}_2 - \bar{A}_1) H_{Nj}^{(4)}, {}^b K_{8j}^\phi = -\lambda \bar{A}_2 G_{Nj}^{(3)}, {}^b K_{9j}^u = G_{Nj}^{(1)}, {}^b K_{10j}^w = H_{Nj}^{(0)}, \\ {}^b K_{11j}^u &= \lambda \bar{A}_1 \beta^2 G_{Nj}^{(3)}, {}^b K_{11j}^w = \lambda^2 (\bar{A}_4 - \bar{A}_3) \beta^2 H_{Nj}^{(4)}, {}^b K_{11j}^\phi = -\lambda^2 \bar{A}_4 \beta^2 G_{Nj}^{(3)}, \\ {}^b K_{12j}^w &= H_{Nj}^{(2)}, {}^b K_{13j}^\phi = G_{Nj}^{(1)}, {}^b K_{14j}^u = \lambda \bar{A}_2 (\beta^2 G_{Nj}^{(5)} - (\alpha^2 + \beta^2) / \alpha^2 G_{Nj}^{(3)}), \\ {}^b K_{14j}^w &= \lambda^2 (\bar{A}_5 - \bar{A}_4) (\beta^2 H_{Nj}^{(6)} - (\alpha^2 + \beta^2) / \alpha^2 H_{Nj}^{(4)}) - \bar{G}_0 \beta^2 H_{Nj}^{(4)}, \\ K_{14j}^\phi &= -\lambda^2 \bar{A}_5 (\beta^2 G_{Nj}^{(5)} - (\alpha^2 + \beta^2) / \alpha^2 G_{Nj}^{(3)}) + \bar{G}_0 \beta^2 G_{Nj}^{(3)} \end{aligned}$$

All the remaining components of boundary related sub K matrices are zero. Also

$${}^b M^u = {}^b M^\phi = {}^b S^u = {}^b S^\phi = 0, {}^b M^w = {}^b S^w = 0$$

On the other hand, for FSDBT, the Eqs. (3.88)-(3.90) can be given with the following set

$$\begin{aligned} &\left(\bar{A}_0 \left(\sum_{j=1}^N C_{ij}^{(2)} - \beta^2 \sum_{j=1}^N C_{ij}^{(4)} \right) + \bar{\omega}^2 \bar{I}_0 \left(\sum_{j=1}^N C_{ij}^{(2)} - \alpha^2 \sum_{j=1}^N C_{ij}^{(4)} \right) \right) \bar{u}_j \\ &- \lambda \left(\bar{A}_1 \left(\sum_{j=1}^N C_{ij}^{(2)} - \beta^2 \sum_{j=1}^N C_{ij}^{(4)} \right) + \bar{\omega}^2 \bar{I}_1 \left(\sum_{j=1}^N C_{ij}^{(2)} - \alpha^2 \sum_{j=1}^N C_{ij}^{(4)} \right) \right) \bar{\phi}_j = 0 \end{aligned} \quad (3.167)$$

$$\begin{aligned} &\left[\begin{aligned} &\kappa \bar{A}_0 \left(\sum_{j=1}^N C_{ij}^{(2)} - \beta^2 \sum_{j=1}^N C_{ij}^{(4)} \right) + \bar{\omega}^2 \bar{I}_0 \left(\sum_{j=1}^N C_{ij}^{(0)} - \alpha^2 \sum_{j=1}^N C_{ij}^{(2)} \right) - \\ &\left\{ (\eta_s \pm \frac{\eta_d}{2}) \bar{P}_{cr} + \bar{C}_0 \Delta T - K_P \right\} \left(\sum_{j=1}^N C_{ij}^{(2)} - \alpha^2 \sum_{j=1}^N C_{ij}^{(4)} \right) - K_W \sum_{j=1}^N C_{ij}^{(0)} \end{aligned} \right] \bar{w}_j \\ &+ \kappa \bar{A}_0 \left(\sum_{j=1}^N C_{ij}^{(1)} - \beta^2 \sum_{j=1}^N C_{ij}^{(3)} \right) \bar{\phi}_j = 0 \end{aligned} \quad (3.168)$$

$$\begin{aligned}
& -\lambda \left(\bar{A}_1 \left(\sum_{j=1}^N C_{ij}^{(2)} - \beta^2 \sum_{j=1}^N C_{ij}^{(4)} \right) + \bar{\omega}^2 \bar{I}_1 \left(\sum_{j=1}^N C_{ij}^{(2)} - \alpha^2 \sum_{j=1}^N C_{ij}^{(4)} \right) \right) \bar{u}_j + \kappa \bar{A}_0 \left(\sum_{j=1}^N C_{ij}^{(1)} - \beta^2 \sum_{j=1}^N C_{ij}^{(3)} \right) \bar{w}_j \\
& + \left(\bar{A}_2 \lambda^2 \left(\sum_{j=1}^N C_{ij}^{(2)} - \beta^2 \sum_{j=1}^N C_{ij}^{(4)} \right) - \kappa \bar{A}_0 \left(\sum_{j=1}^N C_{ij}^{(1)} - \beta^2 \sum_{j=1}^N C_{ij}^{(3)} \right) + \right. \\
& \left. \bar{\omega}^2 \bar{I}_2 \lambda^2 \left(\sum_{j=1}^N C_{ij}^{(2)} - \alpha^2 \sum_{j=1}^N C_{ij}^{(4)} \right) \right) \bar{\phi}_j = 0
\end{aligned} \tag{3.169}$$

For N nodes there will be 3xN unknowns. There are always 6 boundary conditions at each end of the beam and 3 degrees of freedoms per node. Thus the first two and the last two nodes will be used to write the boundary conditions and remaining nodes will be used to write the governing equations (3.167, 3.168, 3.169). Thus $i=3,4,\dots,N-2$ and at the end there will be 3xN equations. For example for a simply supported end at $i=1$ or N boundary conditions can be discretized as below:

$$\bar{N}^c = 0 \Rightarrow \bar{A}_0 \left(\left(\sum_{j=1}^N C_{ij}^{(1)} - \beta^2 \sum_{j=1}^N C_{ij}^{(3)} \right) \bar{u}_j - \bar{A}_1 \left(\sum_{j=1}^N C_{ij}^{(1)} - \beta^2 \sum_{m=1}^N C_{im}^{(3)} \right) \bar{\phi}_j \right) = 0$$

$$w_i = 0 \Rightarrow \bar{w}_i = 0$$

$$\bar{M}^c = 0 \Rightarrow \bar{A}_1 \lambda \left(\left(\sum_{j=1}^N C_{ij}^{(1)} - \beta^2 \sum_{j=1}^N C_{ij}^{(3)} \right) \bar{u}_j - \bar{A}_2 \lambda^2 \left(\sum_{j=1}^N C_{ij}^{(1)} - \beta^2 \sum_{m=1}^N C_{im}^{(3)} \right) \bar{\phi}_j \right) = 0$$

$$\frac{\partial \bar{u}}{\partial \bar{x}} = 0 \Rightarrow \sum_{j=1}^N C_{ij}^{(1)} \bar{u}_j = 0$$

$$\frac{\partial \bar{\phi}}{\partial \bar{x}} = 0 \Rightarrow \sum_{j=1}^N C_{ij}^{(1)} \bar{\phi}_j = 0$$

$$\bar{Q}^{nc} = 0 \Rightarrow \kappa \beta^2 \bar{A}_0 \left(\left(\sum_{j=1}^N C_{ij}^{(2)} - \frac{\beta^2 \alpha^2}{\alpha^2 - \beta^2} \sum_{j=1}^N C_{ij}^{(4)} \right) \bar{w}_j - \bar{A}_2 \lambda^2 \left(\sum_{j=1}^N C_{ij}^{(1)} - \frac{\beta^2 \alpha^2}{\alpha^2 - \beta^2} \sum_{m=1}^N C_{im}^{(3)} \right) \bar{\phi}_j \right) = 0$$

Other type of boundary conditions like C-C and C-S can be generated in the same manner easily.

and for Euler Bernoulli Beam Theory (EBBT)

$$\begin{aligned} & \left(\bar{A}_0 \left(\sum_{j=1}^N C_{ij}^{(2)} - \beta^2 \sum_{j=1}^N C_{ij}^{(4)} \right) + \bar{\omega}^2 \bar{I}_0 \left(\sum_{j=1}^N C_{ij}^{(0)} - \alpha^2 \sum_{j=1}^N C_{ij}^{(2)} \right) \right) \bar{u}_j \\ & - \lambda \left(\bar{A}_1 \left(\sum_{j=1}^N C_{ij}^{(3)} - \beta^2 \sum_{j=1}^N C_{ij}^{(5)} \right) - \bar{\omega}^2 \bar{I}_1 \lambda \left(\sum_{j=1}^N C_{ij}^{(1)} - \alpha^2 \sum_{j=1}^N C_{ij}^{(3)} \right) \right) \bar{w}_j = 0 \end{aligned} \quad (3.170)$$

$$\begin{aligned} & - \left(\bar{A}_2 \lambda^2 \left(\sum_{j=1}^N C_{ij}^{(4)} - \beta^2 \sum_{j=1}^N C_{ij}^{(6)} \right) + \bar{\omega}^2 \bar{I}_0 \left(\sum_{j=1}^N C_{ij}^{(0)} - \alpha^2 \sum_{j=1}^N C_{ij}^{(2)} \right) - \right. \\ & \left. \left\{ (\eta_s \pm \frac{\eta_d}{2}) \bar{P}_{cr} + \bar{C}_0 \Delta T - K_p \right\} \left(\sum_{j=1}^N C_{ij}^{(2)} - \alpha^2 \sum_{j=1}^N C_{ij}^{(4)} \right) - K_w \sum_{j=1}^N C_{ij}^{(0)} \right) \bar{w}_j \\ & + \left(\bar{A}_1 \lambda \left(\sum_{j=1}^N C_{ij}^{(3)} - \beta^2 \sum_{j=1}^N C_{ij}^{(5)} \right) - \bar{\omega}^2 \bar{I}_2 \lambda^2 \left(\sum_{j=1}^N C_{ij}^{(2)} - \alpha^2 \sum_{j=1}^N C_{ij}^{(4)} \right) \right) \bar{u}_j = 0 \\ & + \left(\bar{\omega}^2 \bar{I}_1 \lambda \left(\sum_{j=1}^N C_{ij}^{(1)} - \alpha^2 \sum_{j=1}^N C_{ij}^{(3)} \right) \right) \bar{u}_j \end{aligned} \quad (3.171)$$

The equations from (3.167) to (3.169) for FSDBT and (3.170) to (3.171) for EBBT can be rewritten also in matrix form the equation (3.163).

$$\{ [K] - \bar{\omega}^2 [M] + \bar{P} [S] \} \{ \bar{d} \} \quad (3.163)$$

where M is the mass matrix, K is the stiffness matrix and S is the geometric stiffness matrix. M , K and S are $3N \times 3N$ matrices for FSDBT and $2N \times 2N$ matrices for EBBT.

The general eigenvalue problem of (3.163) can be modified to give results for free vibration frequency with setting $\bar{P} = 0$ Eq. (3.172) or for static buckling load with setting $\bar{\omega} = 0$ Eq. (3.173):

$$[K - \bar{\omega}^2 M] \bar{d} = 0 \quad (3.172)$$

$$[K + \bar{P} S] \bar{d} = 0 \quad (3.173)$$

Extracting eigenvalues can be carried out with any suitable method.

3.6 Dynamic Stability

In order to find the instability conditions we assume a classical case where axial excitation force, $P(t)$ can be taken as harmonic in the following form

$$P(t) = [\eta_s + \eta_d \cos(\Omega t)] P_{cr} \quad (3.174)$$

where η_s is the static and η_d is the dynamic load ratios of $P(t)$ with respect to the fundamental static buckling load P_{cr} , Ω is the excitation frequency. Using dimensionless form with

$$\bar{P}_{cr} = \frac{P_{cr}}{E_m b h}, \quad \bar{\Omega} = \Omega L \sqrt{\frac{\rho_m}{E_m}}$$

And denoting the vector of primary unknowns as (d)

$$\bar{d} = [\bar{u}, \bar{w}, \bar{\phi}]^T$$

If static and dynamic parts of the axial excitation load are applied in the same manner, the governing equations can be given in vector form

$$([\mathbf{K}] - \{(\eta_s + \eta_d \cos \bar{\Omega} \bar{t}) \bar{P}_{cr} + \bar{C}_0 \Delta T\} [\mathbf{S}]) \bar{d} + [\mathbf{M}] \ddot{\bar{d}} = 0 \quad (3.175)$$

Where $[\mathbf{M}]$ is the mass matrix, $[\mathbf{S}]$ is stability matrix and $[\mathbf{K}]$ stiffness matrix and they can be expressed explicitly as below

(a) higher order beam theories (HOBTs)

$$[\mathbf{M}] = \left(1 - \alpha^2 \frac{\partial^2}{\partial \bar{x}^2}\right) \begin{bmatrix} -\bar{I}_0 & (\bar{I}_1 - \bar{I}_2) \lambda \frac{\partial}{\partial \bar{x}} & \bar{I}_2 \lambda \\ -\bar{I}_1 \lambda \frac{\partial}{\partial \bar{x}} & -\bar{I}_0 - (\bar{I}_4 - \bar{I}_3) \lambda^2 \frac{\partial^2}{\partial \bar{x}^2} & \bar{I}_4 \lambda^2 \frac{\partial}{\partial \bar{x}} \\ \lambda \bar{I}_1 & (\bar{I}_5 - \bar{I}_4) \lambda^2 \frac{\partial}{\partial \bar{x}} & -\lambda^2 \bar{I}_5 \end{bmatrix},$$

$$[\mathbf{S}] = \left(1 - \alpha^2 \frac{\partial^2}{\partial \bar{x}^2}\right) \begin{bmatrix} 0 & 0 & 0 \\ 0 & \frac{\partial^2}{\partial \bar{x}^2} & 0 \\ 0 & 0 & 0 \end{bmatrix}$$

$$[\mathbf{K}] = \left(1 - \beta^2 \frac{\partial^2}{\partial \bar{x}^2}\right) \begin{bmatrix} \bar{A}_0 \frac{\partial^2}{\partial \bar{x}^2} & (\bar{A}_2 - \bar{A}_1) \lambda \frac{\partial^3}{\partial \bar{x}^3} & -\bar{A}_2 \lambda \frac{\partial^2}{\partial \bar{x}^2} \\ \bar{A}_1 \lambda \frac{\partial^3}{\partial \bar{x}^3} & (\bar{A}_4 - \bar{A}_3) \lambda^2 \frac{\partial^4}{\partial \bar{x}^4} + K_P \frac{\partial^2}{\partial \bar{x}^2} - K_W & -\bar{A}_4 \lambda^2 \frac{\partial^3}{\partial \bar{x}^3} \\ -\bar{A}_2 \lambda \frac{\partial^2}{\partial \bar{x}^2} & -(\bar{A}_5 - \bar{A}_4) \lambda^2 \frac{\partial^3}{\partial \bar{x}^3} + \bar{G}_0 \frac{\partial}{\partial \bar{x}} & \bar{A}_5 \lambda^2 \frac{\partial^2}{\partial \bar{x}^2} - \bar{G}_0 \end{bmatrix}$$

(b) First shear deformation theory (FSDBT)

$$[\mathbf{M}] = \left(1 - \alpha^2 \frac{\partial^2}{\partial \bar{x}^2}\right) \begin{bmatrix} -\bar{I}_0 & 0 & \lambda \bar{I}_1 \\ 0 & \bar{I}_0 & 0 \\ \lambda \bar{I}_1 & 0 & -\lambda^2 \bar{I}_2 \end{bmatrix}, \quad [\mathbf{S}] = \left(1 - \alpha^2 \frac{\partial^2}{\partial \bar{x}^2}\right) \begin{bmatrix} 0 & 0 & 0 \\ 0 & \frac{\partial^2}{\partial \bar{x}^2} & 0 \\ 0 & 0 & 0 \end{bmatrix}$$

$$[\mathbf{K}] = \left(1 - \beta^2 \frac{\partial^2}{\partial \bar{x}^2}\right) \begin{bmatrix} \bar{A}_0 \frac{\partial^2}{\partial \bar{x}^2} & 0 & -\lambda \bar{A}_1 \frac{\partial^2}{\partial \bar{x}^2} \\ 0 & -\kappa \bar{A}_0 \frac{\partial^2}{\partial \bar{x}^2} + K_P \frac{\partial^2 \bar{w}}{\partial \bar{x}^2} - K_W \bar{w} & \kappa \bar{A}_0 \frac{\partial}{\partial \bar{x}} \\ -\lambda \bar{A}_1 \frac{\partial^2}{\partial \bar{x}^2} & \kappa \bar{A}_0 \frac{\partial}{\partial \bar{x}} & \lambda^2 \bar{A}_2 \frac{\partial^2}{\partial \bar{x}^2} - \kappa \bar{A}_0 \end{bmatrix}$$

(c) Euler- Bernoulli beam theory (EBBT)

$$[\mathbf{M}] = \left(1 - \alpha^2 \frac{\partial^2}{\partial \bar{x}^2}\right) \begin{bmatrix} -\bar{I}_0 & \bar{I}_1 \lambda \frac{\partial}{\partial \bar{x}} \\ \bar{I}_2 \lambda^2 \frac{\partial^2}{\partial \bar{x}^2} - \bar{I}_1 \lambda \frac{\partial}{\partial \bar{x}} & \bar{I}_0 \end{bmatrix}, \quad [\mathbf{S}] = \left(1 - \alpha^2 \frac{\partial^2}{\partial \bar{x}^2}\right) \begin{bmatrix} 0 & 0 \\ 0 & \frac{\partial^2}{\partial \bar{x}^2} \end{bmatrix}$$

$$[\mathbf{K}] = \left(1 - \beta^2 \frac{\partial^2}{\partial \bar{x}^2}\right) \begin{bmatrix} \bar{A}_0 \frac{\partial^2}{\partial \bar{x}^2} & -\lambda \bar{A}_1 \frac{\partial^3}{\partial \bar{x}^3} \\ \lambda \bar{A}_1 \frac{\partial}{\partial \bar{x}} & \bar{A}_2 \lambda^2 \frac{\partial^4}{\partial \bar{x}^4} + K_P \frac{\partial^2 \bar{w}}{\partial \bar{x}^2} - K_W \bar{w} \end{bmatrix}$$

It is seen that Eq.(3.175) illustrates a system of second-order coupled differential equations which has periodic coefficients of the Mathieu-Hill type. Theory of linear equations with periodic coefficients dictates that the stable and unstable regions are separated by the periodic solutions of period T and $2T$ such that the relation with excitation frequency is $T=2\pi/\Omega$. [69]

Of T and $2T$ periodic solutions, regions determined with $2T$ periodic solutions have more practical importance since they produce primary resonance behavior which is usually more dominant when compared to the periodic solutions with T as the beam vibrates laterally.

Now if we assume a steady state response with dimensionless natural frequency of $\bar{\omega} = \bar{\Omega} / 2$

$$\bar{d}(\bar{x}, \bar{t}) = \bar{d}(\bar{x})e^{i\bar{\omega}\bar{t}}$$

a first approximation for the instability problem can be formulated as a general eigenvalue problem of the following form

$$\left([\mathbf{K}] - \left\{ (\eta_s \pm \frac{\eta_d}{2}) \bar{P}_{cr} + \bar{C}_0 \Delta T \right\} [\mathbf{S}] - \frac{\bar{\Omega}^2}{4} [\mathbf{M}] \right) \bar{d} = 0 \quad (3.176)$$

This general eigenvalue formulation includes static buckling (with buckling load \bar{P}_{cr}) when one sets $\eta_s = 1, \eta_d = 0, \bar{\Omega} = 0$, free vibration (with natural frequency $\bar{\omega}$) when one sets $\eta_s = 0, \eta_d = 0, \bar{\Omega} = 2\bar{\omega}$ and dynamic stability in original form. In the solution for the dynamic stability, two conditions with plus-minus sign correspond to the two different sets of frequency values which defines the boundaries of the unstable regions.

4.1 Verification of the present results

Before the extensive parametric analysis, result of the present formulation are validated by comparing with existing literature.

4.1.1 Static and Buckling analysis

The transverse deflection and the critical buckling loads analysis of the nanobeam Modal I responses are obtained and compared with the reference [16]. In [16] the following material properties of functionally graded nano-beam were used

$$E_1 = 1 \text{ TPa}, \quad \nu_1 = 0.3,$$

$$E_2 = 0.25 \text{ TPa}, \quad \nu_2 = 0.3,$$

$$k_s = 5/6.$$

The results of Ref.[16] were obtained by using Timoshenko beam theories according to the nonlocal elasticity theory with different of aspect ratio, power law index and nonlocal parameter (ea). The nonlocal elasticity Eringen theory can be obtained from the nonlocal gradient strain theory when the material length scale parameter (l_m) equal to zero.

The following dimensionless for transverse deflection and critical buckling loads are used in this section, can be defined as

$$\bar{w} = 100 E_m I / q L^4 w$$

$$\bar{P} = PL^2 / E_m I$$

The results of the dimensionless transverse deflection and the dimensionless critical buckling forces based on Timoshenko beam theory are given in table (4.1) and table (4.2) respectively.

Fairly well agreement between the present results and the results in Ref.[16] are observed. This clearly shows the reliability of the present solution method for the analysis of sandwich FG microbeam.

Table 4.1 Non-Dimensional transverse deflection, ($\bar{w} = 100 E_m I / q L^4 w$) of the functionally graded nano-beam Model I with the distributed load

		ea (nm)									
L/h	k	0		0.5		1		1.5		2	
		ref. 16	present	ref. 16	present	ref. 16	present	ref. 16	present	ref. 16	present
10	0	5.3383	5.3383	5.4659	5.4659	5.8487	5.8487	6.4867	6.4866	7.3798	7.3798
	0.3	3.2169	3.2155	3.2938	2.2923	3.5245	3.5229	3.9090	3.9072	4.4472	4.4452
	1	2.4194	2.4194	2.4772	2.4772	2.6508	2.6508	2.9401	2.9401	3.3451	3.3451
	3	1.9249	1.9249	1.9710	1.9710	2.1091	2.1091	2.3393	2.3393	2.6615	2.6615
	10	1.5799	1.5799	1.6176	1.6176	1.7310	1.7310	1.9199	1.9199	2.1843	2.1843
30	0	5.2227	5.2227	5.2366	5.2367	5.2784	5.2784	5.3480	5.3480	5.4455	5.4455
	0.3	3.1486	3.1472	3.1570	3.1556	3.1822	3.1807	3.2241	3.2227	3.2829	3.2814
	1	2.3732	2.3732	2.3795	2.3795	2.3985	2.3985	2.4301	2.4101	2.4744	2.4744
	3	1.8894	1.8894	1.8944	1.8944	1.9095	1.9095	1.9347	1.9347	1.9700	1.9700
	10	1.5489	1.5489	1.5530	1.5530	1.5654	1.5654	1.5860	1.5860	1.6149	1.6149
100	0	5.2096	5.2096	5.2108	5.2105	5.2146	5.2146	5.2208	5.2208	5.2296	5.2296
	0.3	3.1408	3.1394	3.1416	3.1402	3.1438	3.1424	3.1476	3.1462	3.1529	3.1515
	1	2.3679	2.3679	2.3685	2.3685	2.3702	2.3702	2.3730	2.3730	2.3770	2.3770
	3	1.8853	1.8853	1.8858	1.8858	1.8871	1.8871	1.8894	1.8894	1.8926	1.8926
	10	1.5453	1.5453	1.5457	1.5457	1.5468	1.5468	1.5487	1.5487	1.5513	1.5513

Table 4.2 Dimensionless buckling load ($P = \bar{P}L^2/E_m I$) of the functionally graded nano-beam Model I

		ea (nm)									
L/h	k	0		0.5		1		1.5		2	
		ref. 16	present	ref. 16	present	ref. 16	present	ref. 16	present	ref. 16	present
10	0	2.4056	2.4056	2.3477	2.3477	2.1895	2.1895	1.9685	1.9686	1.7247	1.7247
	0.3	3.9928	3.9921	3.8977	3.8959	3.6351	3.6335	3.2667	3.2667	2.8621	2.8621
	1	5.3084	5.3084	5.1805	5.1805	4.8315	4.8315	4.3438	4.3437	3.8059	3.8059
	3	6.6720	6.6720	6.5114	6.5113	6.0727	6.0727	5.4596	5.4596	4.7835	4.7835
	10	8.1289	8.1289	7.9332	7.9332	7.3987	7.3987	6.5518	6.6518	5.8281	5.8281
30	0	2.4603	2.4603	2.4536	2.4536	2.4336	2.4337	2.4011	2.4011	2.3569	2.3569
	0.3	4.0811	4.0829	4.0699	4.0718	4.0368	4.0386	3.9828	3.9846	3.9096	3.9114
	1	5.4146	5.4147	5.3998	5.3998	5.3559	5.3559	5.2843	5.2843	5.1871	5.1871
	3	6.8011	6.8011	6.7825	6.7825	6.7273	6.7273	6.6373	6.6373	6.5153	6.5153
	10	8.2962	8.2962	8.2735	8.2735	8.2062	8.2062	8.0964	8.0964	7.9476	7.9476
100	0	2.4667	2.4667	2.4661	2.4661	2.4643	2.4643	2.4613	2.4613	2.4570	2.4570
	0.3	4.0915	4.0933	4.0905	4.0923	4.0874	4.0893	4.0824	4.0842	4.0754	4.0772
	1	5.4270	5.4270	5.4257	5.4257	5.4217	5.4217	5.4150	5.4150	5.4057	5.4057
	3	6.8161	6.8161	6.8144	6.8144	6.8094	6.8094	6.8010	6.8010	6.7893	6.7893
	10	8.3157	8.3157	8.3136	8.3136	8.3075	8.3075	8.2972	8.2972	8.2830	8.2830

4.1.2 Elastic foundation and cross-section shape

The influence of the elastic foundation on the dimensionless buckling loads is presented in table (4.3) with different cross-section types, the aspect ratio (L/h) with classical theory ($\alpha = \beta = 0$), without thermal effect ($\Delta T = 0$) and power law index ($k = 0.5$) with using the different homogenization techniques. The following material properties are used :

Aluminum (Al): $E_m = 70$ GPa, $\rho_m = 2702$ kg/m³, $\nu_m = 0.3$

Alumina(Al₂O₃): $E_c = 380$ GPa, $\rho_c = 3960$ kg/m³, $\nu_c = 0.3$

The following dimensionless are used

$$K_w = \frac{k_w L^2}{E_m h}, \quad K_p = \frac{k_p}{E_m h}$$

$$\bar{P} = \frac{P}{E_m b h}$$

From this comparison a good agreement for the results in this thesis and the results in [6].

On the other hand, for the dimensionless fundamental frequency ($\bar{\omega}$) results with elastic foundation are obtained and can be compared with same properties of reference above [6], in table (4.4) dimensionless natural frequencies ($\bar{\omega}$) are shown for Timoshenko beam theory (TBT) and parabolic shear deformation beam theory (PSDBT) with generalized differential quadrature method (GDQM) and compared with Ref.(6) with Chebyshev collection method (CCM) for different boundary conditions.

The dimensionless fundamental frequency can be given as follow

$$\bar{\omega} = \omega L \sqrt{\frac{\rho_m}{E_m}}$$

Again, fairly well agreement also between the thesis results and the results in Ref.[6] are observed.

Table 4.3 Dimensionless critical buckling load ($\bar{P} = P/E_m bh$) of sandwich FG beam Model III with $K_w, K_p, L/h = 10, k = 0.5, \beta = 0, \alpha = 0$ and $\Delta T = 0$

B.Cs	K_w	K_p	Method	Mori-Tanaka homogenization scheme			The simple rule of mixture		
				1-1-1	2-1-2	1-5-1	1-1-1	2-1-2	1-5-1
S-S Boundary Condition	0	0	Ref.(6)	0.0205	0.0186	0.0304	0.0280	0.0263	0.0351
			TBT(GDQM)	0.0205	0.0186	0.0303	0.0279	0.0263	0.0351
			PSDBT(GDQM)	0.0205	0.0186	0.0304	0.0280	0.0263	0.0351
	0.2	0	Ref.(6)	0.0408	0.0389	0.0506	0.0482	0.0466	0.0554
			TBT(DQM)	0.0408	0.0388	0.0506	0.0482	0.0465	0.0553
			PSDBT(DQM)	0.0408	0.0389	0.0506	0.0482	0.0466	0.0554
	0.2	0.2	Ref.(6)	0.2408	0.2389	0.2506	0.2482	0.2466	0.2554
			TBT(GDQM)	0.2408	0.2388	0.2506	0.2482	0.2465	0.2553
			PSDBT(GDQM)	0.2408	0.2389	0.2506	0.2482	0.2466	0.2554
C-S Boundary Condition	0	0	Ref.(6)	0.0412	0.0373	0.0607	0.0559	0.0526	0.0699
			TBT(GDQM)	0.0412	0.0373	0.0606	0.0558	0.0525	0.0699
			PSDBT(GDQM)	0.0421	0.0382	0.0619	0.0571	0.0537	0.0713
	0.2	0	Ref.(6)	0.0574	0.0535	0.0770	0.0722	0.0689	0.0863
			TBT(GDQM)	0.0574	0.0535	0.0770	0.0722	0.0688	0.0863
			PSDBT(GDQM)	0.0581	0.0541	0.0780	0.0731	0.0698	0.0874
	0.2	0.2	Ref.(6)	0.2574	0.2535	0.2770	0.2722	0.2688	0.2863
			TBT(GDQM)	0.2574	0.2535	0.2770	0.2722	0.2688	0.2863
			PSDBT(GDQM)	0.2581	0.2541	0.2780	0.2731	0.2698	0.2874
C-C Boundary Condition	0	0	Ref.(6)	0.0783	0.0709	0.1147	0.1057	0.0995	0.1318
			TBT(GDQM)	0.0785	0.0711	0.1150	0.1060	0.0998	0.1322
			PSDBT(GDQM)	0.0819	0.0743	0.1193	0.1102	0.1038	0.1370
	0.2	0	Ref.(6)	0.0933	0.0859	0.1297	0.1207	0.1145	0.1469
			TBT(GDQM)	0.0934	0.0860	0.1300	0.1209	0.1147	0.1472
			PSDBT(GDQM)	0.0964	0.0888	0.1339	0.1248	0.1184	0.1515
	0.2	0.2	Ref.(6)	0.2933	0.2859	0.3297	0.3207	0.3145	0.3469
			TBT(GDQM)	0.2934	0.2860	0.3300	0.3209	0.3147	0.3472
			PSDBT(GDQM)	0.2988	0.2964	0.3339	0.3248	0.3184	0.3515

Table 4.4 Dimensionless natural frequency ($\bar{\omega} = \omega L \sqrt{\rho_m / E_m}$) of sandwich FG beam III
with $K_w, K_p, L/h = 10, k = 0.5, \beta = 0, \alpha = 0$ and $\Delta T = 0$

			Mori-Tanaka homogenization scheme			The simple rule of mixture			
B.Cs	K_w	K_p	Method	1-1-1	2-1-2	1-5-1	1-1-1	2-1-2	1-5-1
S-S Boundary Condition	0	0	Ref.(6)	0.4486	0.4384	0.4920	0.3845	0.3687	0.4577
			TBT(GDQM)	0.4486	0.4384	0.4920	0.3844	0.3687	0.4577
			PSDBT(GDQM)	0.4490	0.4389	0.4923	0.3850	0.3692	0.4580
	0.2	0	Ref.(6)	0.5891	0.5833	0.6178	0.5418	0.5329	0.5909
			TBT(DQM)	0.5890	0.5832	0.6178	0.5418	0.5328	0.5909
			PSDBT(DQM)	0.5894	0.5836	0.6180	0.5422	0.5332	0.5911
	0.2	0.2	Ref.(6)	1.3363	1.3420	1.3267	1.3161	1.3209	1.3144
			TBT(GDQM)	1.3362	1.3420	1.3267	1.3161	1.3208	1.3144
			PSDBT(GDQM)	1.3364	1.3421	1.3268	1.3162	1.3210	1.3145
C-S Boundary Condition	0	0	Ref.(6)	0.6887	0.6732	0.7539	0.5917	0.5676	0.7025
			TBT(GDQM)	0.6890	0.6736	0.7542	0.5922	0.5680	0.7030
			PSDBT(GDQM)	0.7028	0.6871	0.7683	0.6043	0.5798	0.7162
	0.2	0	Ref.(6)	0.7874	0.7753	0.8414	0.7041	0.6856	0.7956
			TBT(GDQM)	0.7878	0.7756	0.8419	0.7045	0.6859	0.7961
			PSDBT(GDQM)	0.7997	0.7874	0.8543	0.7147	0.6957	0.8077
	0.2	0.2	Ref.(6)	1.4844	1.4855	1.4937	1.4387	1.4368	1.4673
			TBT(GDQM)	1.4847	1.4858	1.4939	1.4397	1.4377	1.4683
			PSDBT(GDQM)	1.5016	1.5028	1.5109	1.4552	1.4532	1.4840
C-C Boundary Condition	0	0	Ref.(6)	0.9787	0.9570	1.0690	0.8434	0.8091	0.9980
			TBT(GDQM)	0.9790	0.9575	1.0694	0.8461	0.8118	1.0012
			PSDBT(GDQM)	1.0178	0.9957	1.1093	0.8785	0.8433	1.0362
	0.2	0	Ref.(6)	1.0505	1.0314	1.1324	0.9257	0.8959	1.0656
			TBT(GDQM)	1.0509	1.0317	1.1328	0.9282	0.8982	1.0686
			PSDBT(GDQM)	1.0870	1.0674	1.1705	0.9578	0.9268	1.1015
	0.2	0.2	Ref.(6)	1.6622	1.6572	1.6962	1.5837	1.5728	1.6519
			TBT(GDQM)	1.6627	1.6575	1.6966	1.5869	1.5759	1.6554
			PSDBT(GDQM)	1.7055	1.7003	1.7400	1.6128	1.6240	1.6938

4.1.3 Free vibration analysis

The final verification with the present results with the free vibration, the fundamental frequency analysis responses obtained is compared with the reference [49]. The following material properties are utilized

$$E_1 = 14.4 \text{ GPa}, \quad \rho_1 = 12.2 \times 10^3 \text{ kg/m}^3$$

$$E_2 = 1.44 \text{ GPa}, \quad \rho_2 = 1.22 \times 10^3 \text{ kg/m}^3$$

$$h = 17.6 \times 10^{-6} \text{ m}, \quad b = 2h, \quad L = 20h$$

$$k_s G_1 = E_1/13.6, \quad k_s G_2 = E_2/13.6$$

The functionally graded micro-beam is used with Model I, ($ea = 0.1h$), ($l_m = h$) without temperature change $\Delta T = 0$, without elastic foundations $K_p = K_w = 0$ and various power-law index (k) by using the rule of mixture method. In Fig.(4.1) and table (4.5) show that the first three fundamental frequencies with different values of the nonlocal parameter (ea) and the material length scale parameter (l_m). It can be seen from Fig.(4.1) and table (4.5) that the frequencies increase with decrease the nonlocal parameter (ea) at certain length scale parameter (l_m). This is due to the FG microbeam when (ea) is greater than (l_m) exerts softening effect and on the other hand, when (l_m) is greater than (ea) FG sandwich micro-beam exerts stiffness hardening effect. Good agreement for compared the present results of the thesis and the relate results in Ref.[49].

Table 4.5 First three natural frequency of FG micro-beam with various B.Cs under the effect of gradient index, k with $ea = 0.1h$ and $l_m = h$

k	ω	S-S		C-C	C-S
		Present	Ref. (49)		
0	ω_1	0.4431	0.4426	1.2199	0.7630
	ω_2	1.8120	1.8089	3.3945	2.5145
	ω_3	4.2125	4.2095	6.7668	5.1190
2	ω_1	0.3785	0.3779	1.0469	0.6530
	ω_2	1.5531	1.5524	2.9329	2.1627
	ω_3	3.6292	3.6282	5.8941	4.6606
4	ω_1	0.4006	0.4001	1.1064	0.6908
	ω_2	1.6421	1.6416	3.0928	2.2840
	ω_3	3.8307	3.8295	6.1988	4.9112
6	ω_1	0.4285	0.4281	1.1811	0.7382
	ω_2	1.7538	1.7532	3.2917	2.4357
	ω_3	4.0822	4.0816	6.5743	5.2223
8	ω_1	0.4494	0.4489	1.2368	0.7738
	ω_2	1.8373	1.8368	3.4390	2.5486
	ω_3	4.2690	4.2681	6.8498	5.4520
10	ω_1	0.4640	0.4638	1.2754	0.7984
	ω_2	1.8951	1.8945	3.5403	2.6266
	ω_3	4.3979	4.3972	7.0381	5.6098

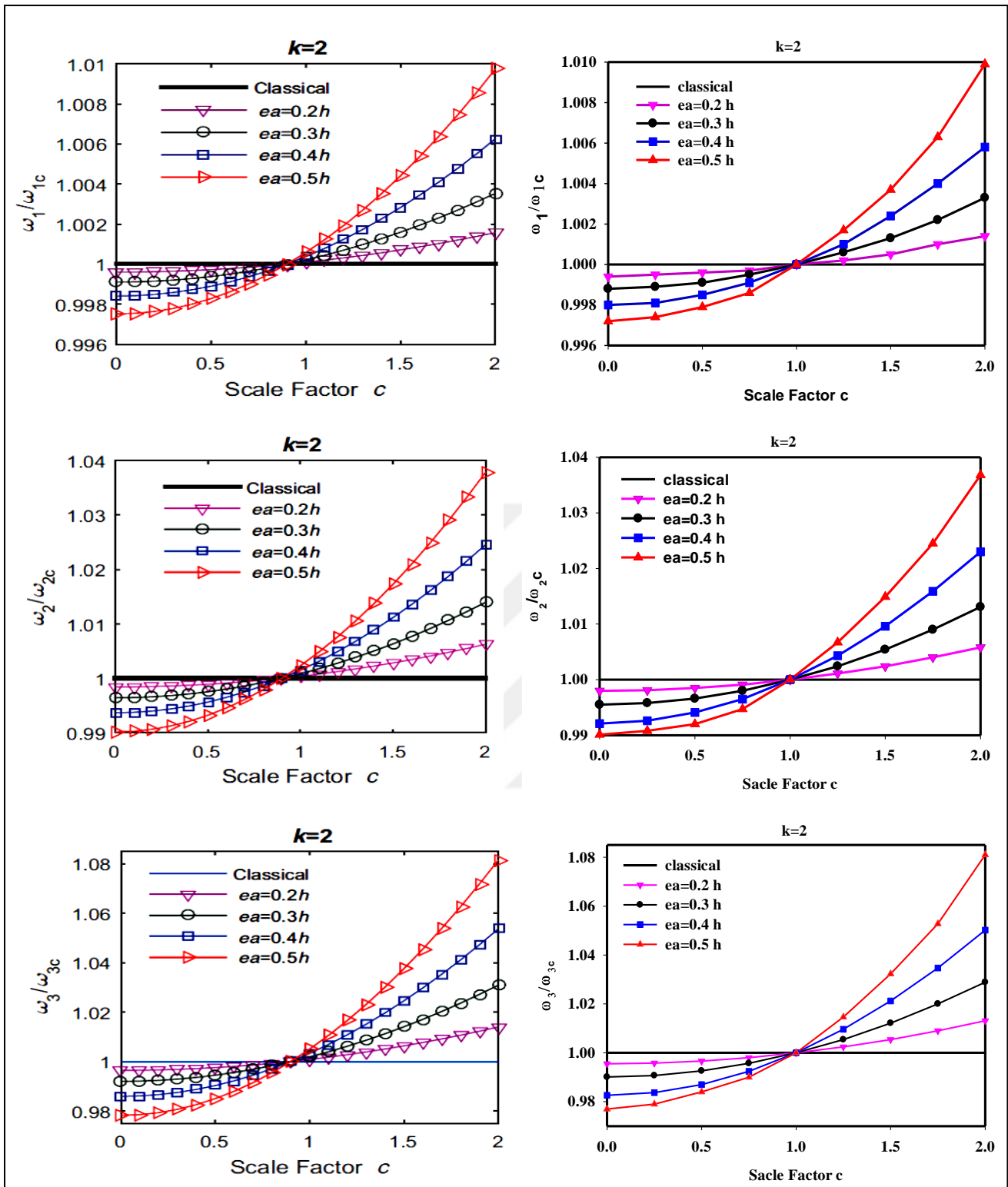


Figure 4.1 First three natural frequencies (MHz) as a function of different scale factor c Comparison with [49] (left) and present results (right).

4.2 Dynamic stability of Sandwich FG micro-beam

In this section, numerical results of dynamic stability of FG sandwich micro-beam with various cross section shapes (1-1-1), (1-2-1), (1-8-1), (1-3-2), (3-2-1), (2-1-3) and (2-1-2) based on nonlocal strain gradient theory (NLSGT) in conjunction with higher-order beam theories (HOBTs) resting on Winkler and Pasternak elastic foundation and temperature change effect. There are three kinds of sandwich FG microbeam in this study (a.) Homogeneous (FGM) micro-beam (Model I), (b.) The core is made of FG material and the top skin with metal and the bottom skin with ceramic (Model II), (c.) The core is made from the ceramic and the two skins are FG material (Model III). It is assumed the constituents of the FG material part of the sandwich micro-beam used in this section of the present thesis composed of Aluminum (Al) and alumina (Al_2O_3). Their properties are

$$\text{Aluminum (Al):} \quad E_m = 70 \text{ GPa}, \quad \rho_m = 2700 \text{ kg/m}^3, \quad \nu_m = 0.23, \quad \alpha_m = 23 \times 10^{-6}$$

$$\text{Alumina(Al}_2\text{O}_3\text{):} \quad E_c = 380 \text{ GPa}, \quad \rho_c = 3800 \text{ kg/m}^3, \quad \nu_c = 0.23, \quad \alpha_c = 7.4 \times 10^{-6}$$

The following dimensionless can be used in the present thesis

$$\text{Dimensionless material length scale parameter} \quad \beta = l_m / L .$$

$$\text{Dimensionless nonlocal parameter} \quad \alpha = ea / L .$$

$$\text{Dimensionless Pasternak elastic foundation} \quad K_p = k_p / E_m h b .$$

$$\text{Dimensionless Winkler elastic foundation} \quad K_w = k_w L^2 / E_m h b .$$

$$\text{Dimensionless buckling load is} \quad P = \bar{P} / E_m h b .$$

Fig. (4.2) plots the effect of aspect ratio ($\lambda = L/h$) on the instability region for size dependent sandwich FG micro-beam (Modal III) for cross-section types (1-1-1) and (1-8-1) with $\eta_s = 0.5$, $k = 2$, $\Delta T = 0$, $ea = 0.5h$, $K_p = K_w = 0$ and $l_m = h$ and for simply-supported boundary conditions.

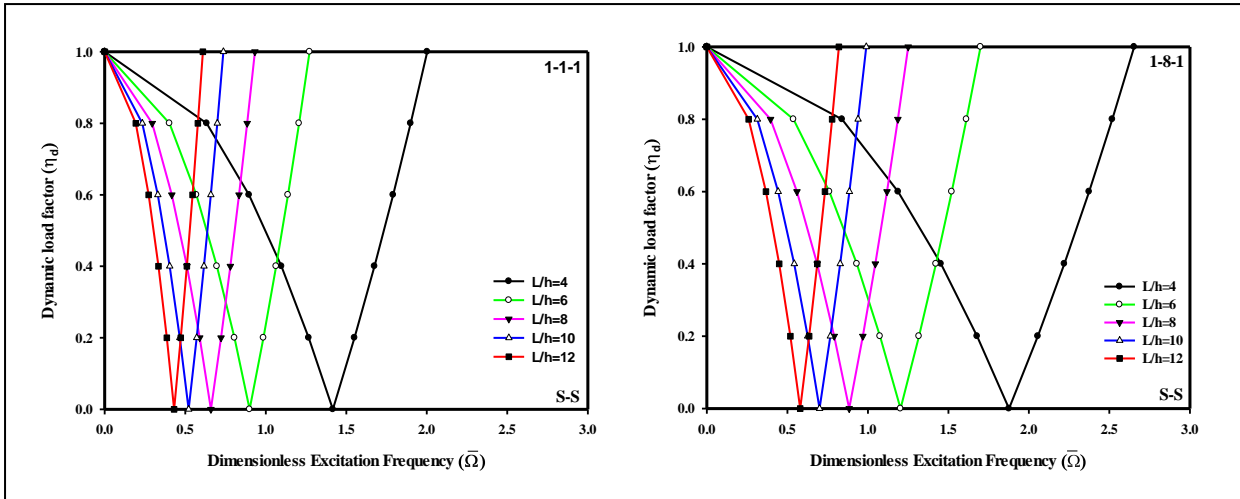


Figure 4.2 Effect of (L/h) on the instability region for sandwich FG micro beam (Modal III) for cross-section types (1-1-1) and (1-8-1) with $\eta_s = 0.5$, $k = 2$, $\Delta T = 0$, $ea = 0.5h$
 $K_p = K_w = 0$ and $l_m = h$ and for S-S boundary conditions.

It can be seen from Fig. (4.2) at given dynamic load factor (η_d) when the aspect ratio decrease leads to a larger dimensionless excitation frequency $(\bar{\Omega})$ and It is also noticed when the decrease in aspect ratio, the width of the instability region increase (broader instability region). On the other hand for FG sandwich microbeam is more sensitive to dynamic instability in conjunction with a larger aspect ratio when comparing with a smaller aspect ratio at a lower value of $(\bar{\Omega})$ due to the sandwich FG microbeam has lower bending resistance to bending deformation with larger slenderness ratios. It is observed also in Fig. (4.2) that the dimensionless excitation frequency is smaller with (1-1-1) comparison with (1-8-1) and for FG sandwich microbeam with Model III the width of the instability region is larger for (1-8-1) comparison with (1-1-1), due to the (1-8-1) for model III with ceramic core and it occupies 80 percent thickness of the sandwich FG micro-beam. Then it has larger effective elasticity modulus than for (1-1-1).

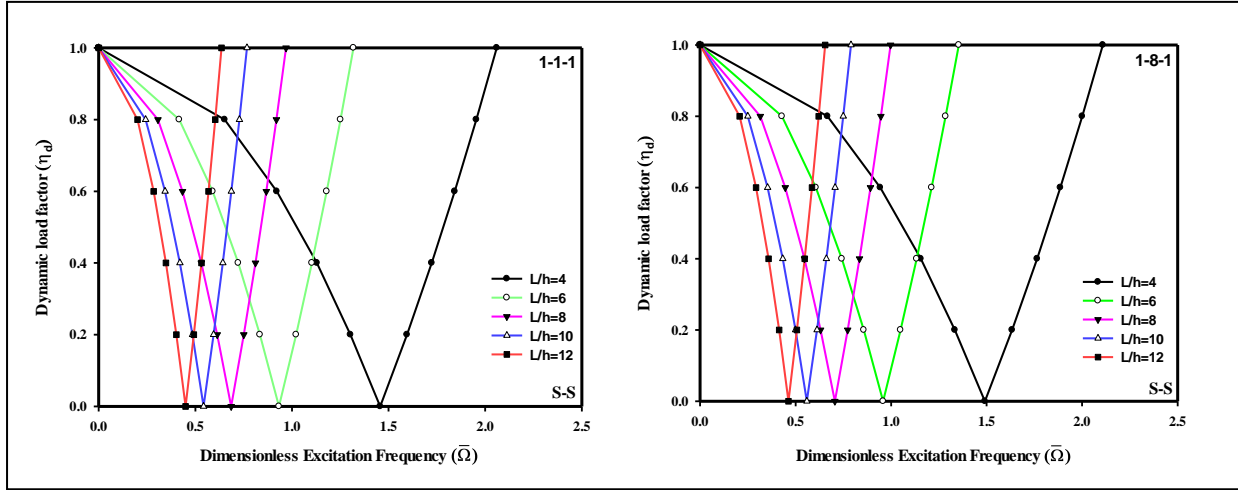


Figure 4.3 Effect of (L/h) on the instability region for sandwich FG micro beam (Modal II) for cross-section types (1-1-1) and (1-8-1) with $\eta_s = 0.5$, $k = 2$, $\Delta T = 0$, $ea = 0.5h$, $K_p = K_w = 0$ and $l_m = h$ and for S-S boundary conditions.

Moreover, it can be seen in Fig. (4.3) and Fig. (4.2) when the comparison between Model III and Model II, Model III have a greater of the dimensionless excitation frequency ($\bar{\Omega}$) than Model II at certain dynamic load factor. This due to the ceramic constitute of Model III is greater than of Model II at lower value of power law index ($k = 2$), and it can be seen the core of Model III is fully ceramic. Moreover, the modulus of elasticity of Model II is less than that of Model III.

For other boundary conditions for Model II, III in Figs. (4.4), (4.5) respectively. It can be observed that for C-C B.C, the dimensionless excitation frequencies ($\bar{\Omega}$) is more than for S-S boundary conditions. Also, it can be observed for S-S boundary condition the width of the instability regions is lower than these for the other B.Cs (i.e. C-S, C-C) because the sandwich FG microbeam with S-S boundary condition more flexible compared to the other boundary conditions.

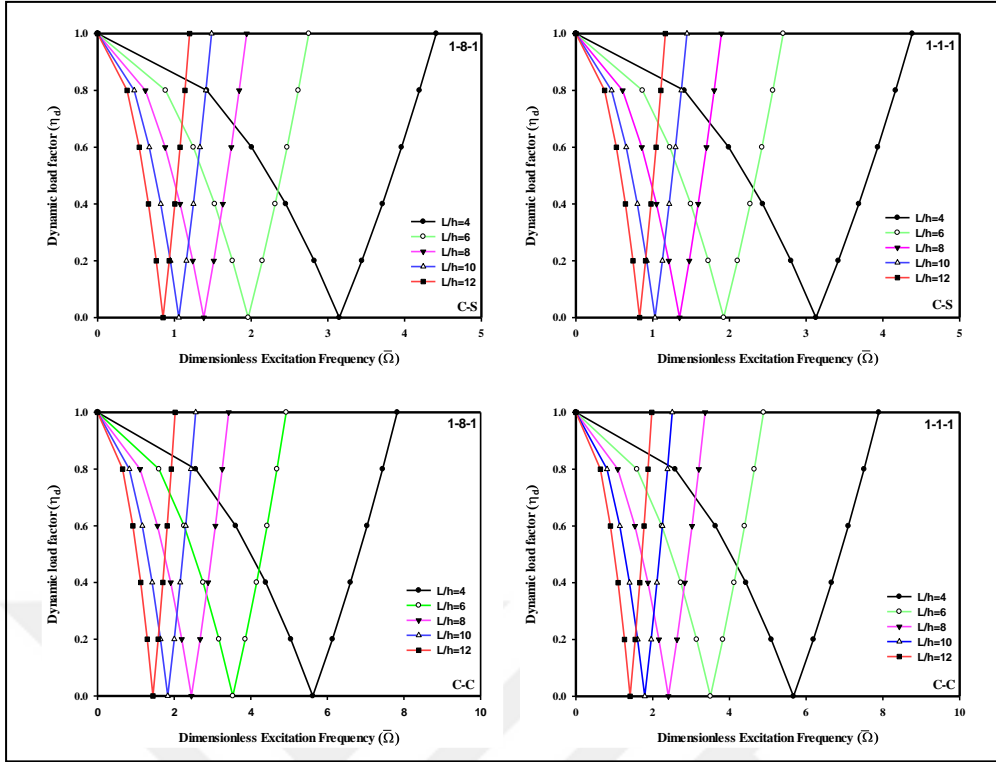


Figure 4.4 Effect of (L/h) on the instability region for sandwich FG micro beam (Modal II) with $\eta_s = 0.5$, $k = 2$, $\Delta T = 0$, $ea = 0.5h$, $K_p = K_w = 0$ and $l_m = h$ for various B.Cs.

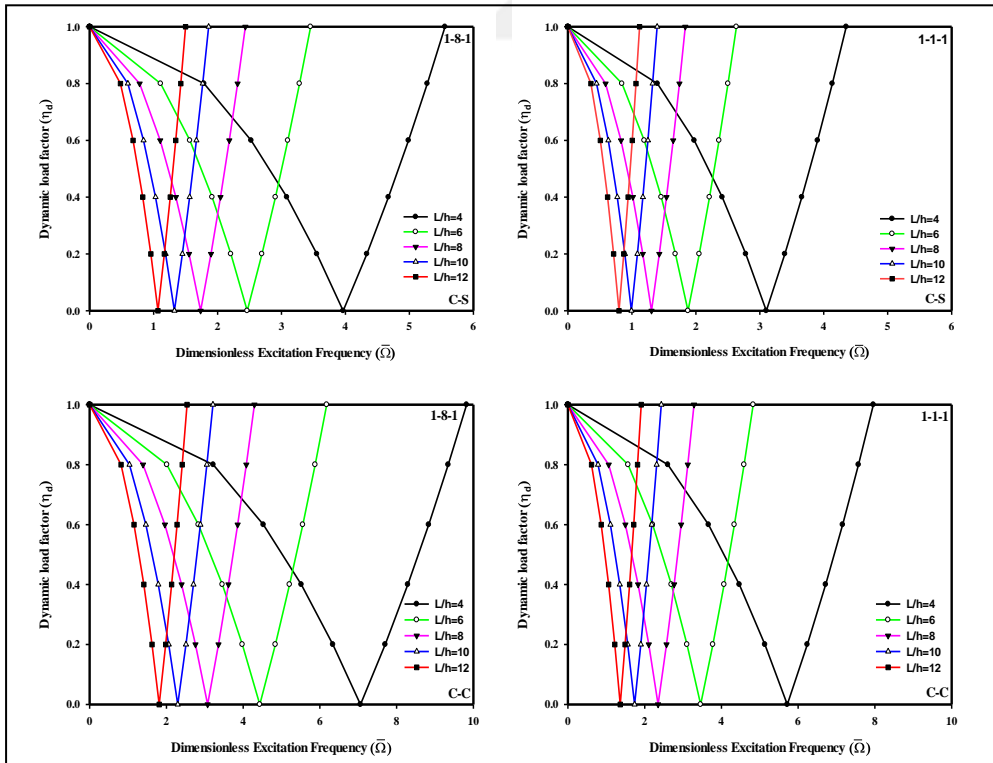


Figure 4.5 Effect of (L/h) on the instability region for sandwich FG micro beam (Modal III) with $\eta_s = 0.5$, $k = 2$, $\Delta T = 0$, $ea = 0.5h$, $K_p = K_w = 0$ and $l_m = h$ for various B.Cs.

The effect of gradient index (k) on the instability regions of sandwich functionally graded micro-beams Model III for (1-1-1) and (1-8-1) with $L/h=10$, $\eta_s = 0.5$, $\Delta T = 0$, $ea = 0.5h$, $K_p = K_w = 0$ and $l_m = h$ for S-S supported boundary conditions is depicted in Fig.(4.6).

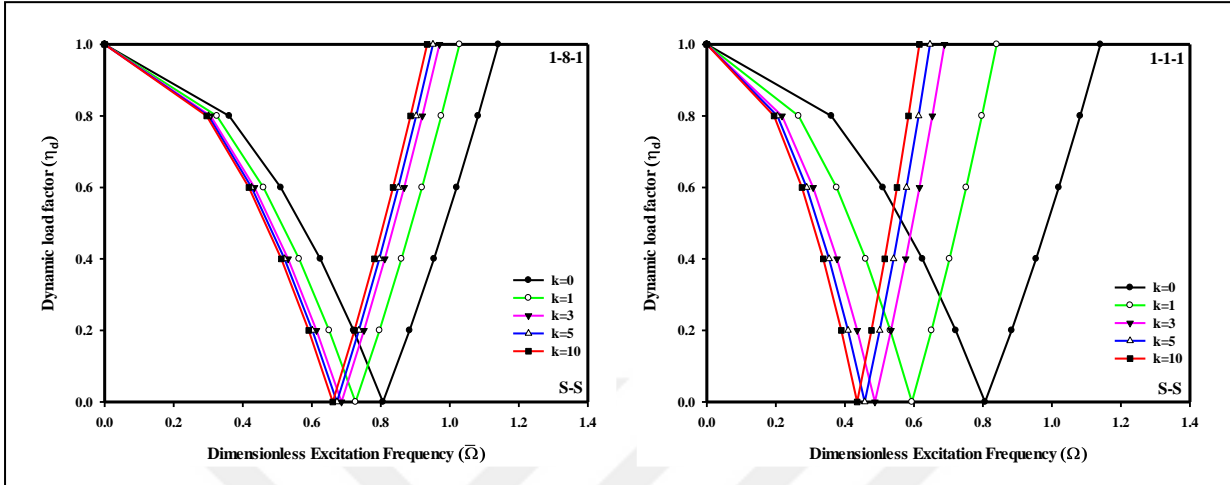


Figure 4.6 Effect of power law index (k) on the instability region for sandwich FG micro-beam Modal III with $\eta_s = 0.5$, $L/h = 10$, $\Delta T = 0$, $ea = 0.5h$, $K_p = K_w = 0$ and $l_m = h$ for S-S B.Cs.

It is indicated that at given dynamic load factor (η_d), the dimensionless excitation frequency ($\bar{\Omega}$) increase when the power law index (k) decrease. Also, it can be seen that the width of the instability region with small the gradient index is larger than that in the higher gradient index. It is noticed also from Fig. (4.6) when $k = 0$, the FG part of the sandwich FG microbeam is full ceramic then the whole sandwich FG microbeam become also ceramic for all cross section shape, therefore the dimensionless excitation frequency for both (1-1-1), (1-8-1) is equal.

The effect of gradient index (k) on the instability regions of sandwich FG micro-beams Model III with different B.Cs, it can be seen in Fig. (4.7). It is noted that the excitation frequencies of C-C sandwich FG micro-beam are higher than those of their C-S boundary condition this is due to the C-C is less flexible compared to a C-S configuration.

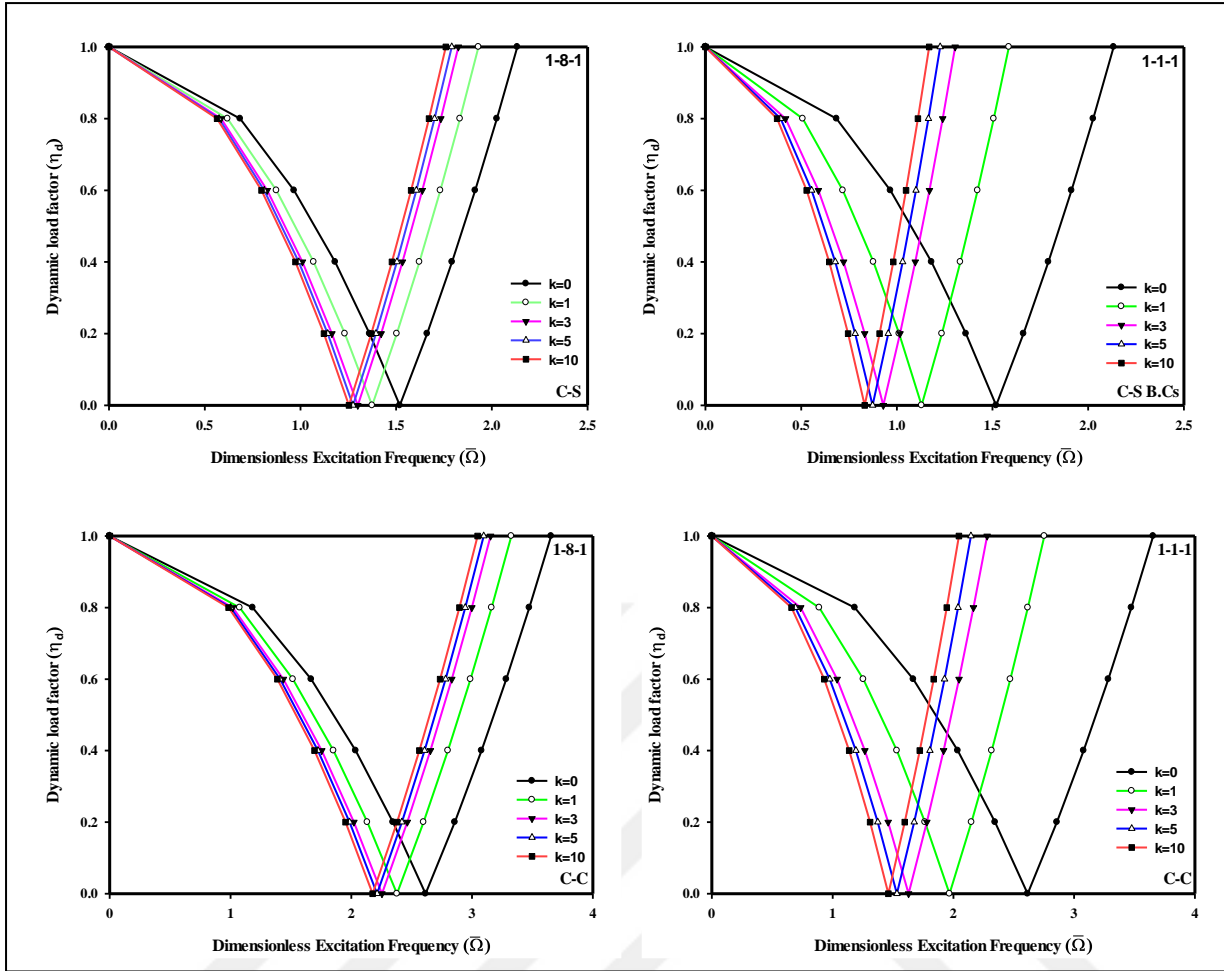


Figure 4.7 Effect of (k) on the instability region for sandwich FG micro beam Modal III with $\eta_s = 0.5, L/h = 10, \Delta T = 0, ea = 0.5h, K_p = K_w = 0$ and $l_m = h$ for C-S and C-C B.Cs.

Fig.(4.8) demonstrates the influence of the static load factor (η_s) on the instability region for S-S B.C and cross section type (1-8-1) sandwich FG microbeam Model II, III, for $k = 2, L/h = 10, \Delta T = 0, ea = 0.5h, K_p = K_w = 0$ and $l_m = h$. It can be noticed that when increasing the value of static load factor (η_s) from 0 (without static axial force component) to $\eta_s = 0.5$ tends to the instability region more wider and shifts closer to the coordinate origin. This is because an axial compressive force give rise to a compressive prestress in the sandwich FG microbeam and therefore weaken the microbeam stiffness. It is noted also from Fig.(4.8) that the excitation frequencies of Model III sandwich FG microbeam are higher than those of their Model II sandwich FG microbeam this is due to the Model III has much greater bending rigidity than Model II.

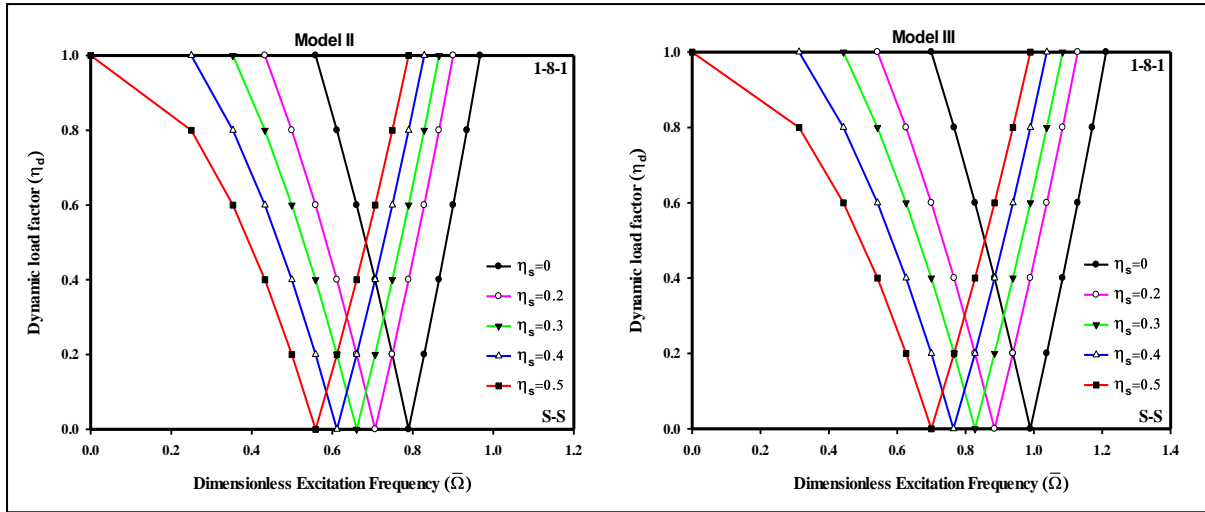


Figure 4.8 Effect of static load factor (η_s) on the instability region for sandwich FG micro beam Modal III, II with $k = 2$, $L/h = 10$, $\Delta T = 0$, $ea = 0.5h$, $K_p = K_w = 0$ and $l_m = h$ for S-S B.Cs.

It can be seen in Fig. (4.9) the effect of (η_s) on the instability region for sandwich FG micro-beam Modal III for other boundary conditions (C-S) and (C-C).

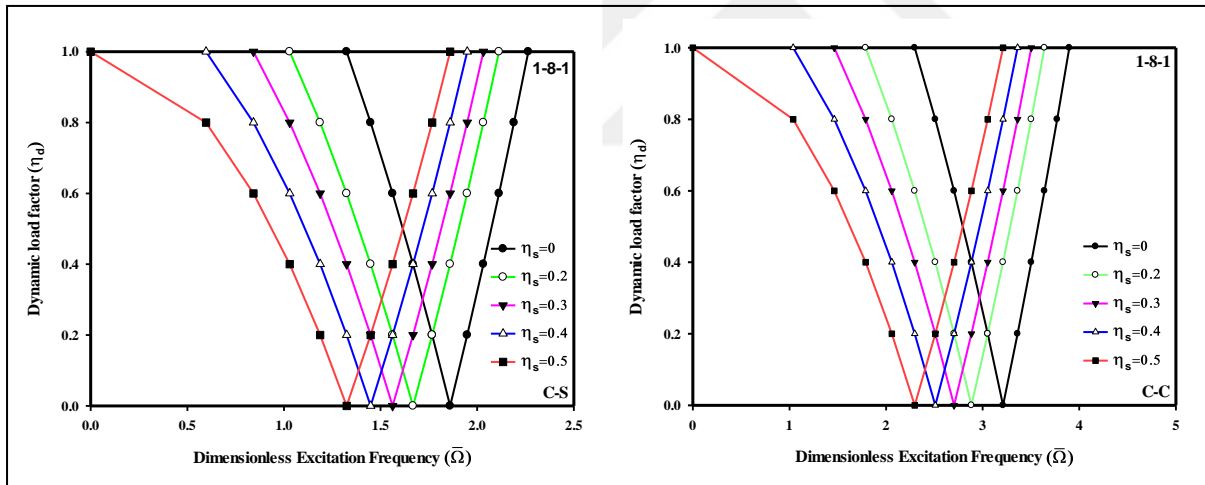


Figure 4.9 Effect of static load factor (η_s) on the instability region for sandwich FG micro beam Modal III with $k = 2$, $L/h = 10$, $\Delta T = 0$, $ea = 0.5h$, $K_p = K_w = 0$ and $l_m = h$ for different B.Cs.

Fig. (4.10) presents the effect the different temperature gradients (ΔT) on the instability region for sandwich FG micro-beam with cross section shapes (1-1-1) and (1-8-1) for $\eta_s = 0.5$, $L/h = 10$, $k = 2$, $ea = 0.5h$ and $l_m = h$. It is seen that an increase in the change of the temperature moves the origins of the instability regions to lower excitation frequencies and decrease the width of the instability region of sandwich FG microbeams at a certain (η_d)

for both (1-1-1) and (1-8-1) cross section shapes ,which is due to an increase in temperature change leads to a negative value of the axial resultant force due to the thermal loading. This mean the sandwich FG microbeam has higher stiffness with lower temperature.

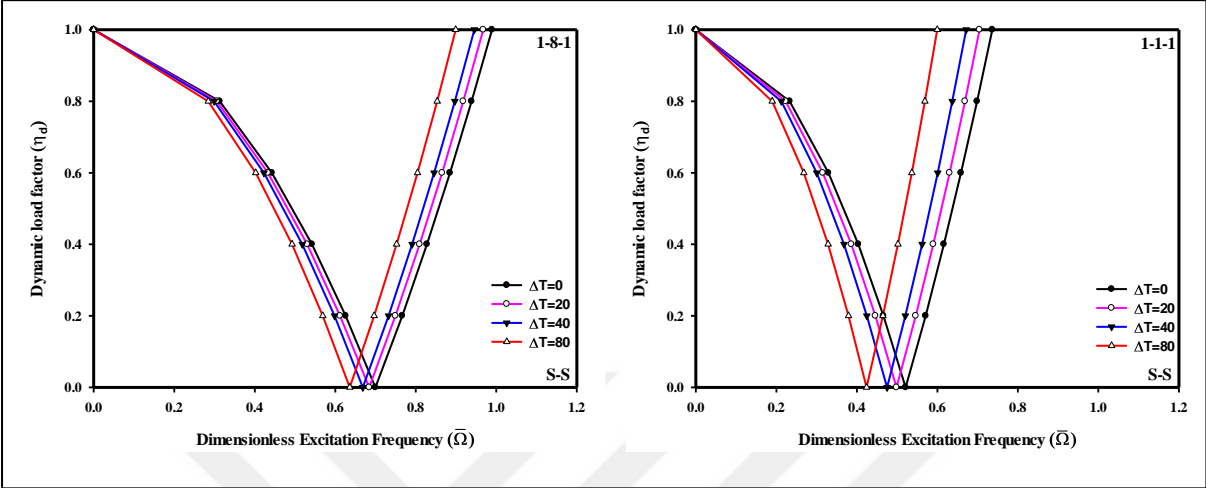


Figure 4.10 Effect of Temperature change (ΔT) on the instability region for sandwich FG micro beam Modal III with $k = 2, L/h = 10, l_m = h, \eta_s = 0.5, K_p = K_w = 0$ and $ea = 0.5h$ for S-S B.Cs.

Moreover, it can be noticed in Fig. (4.11), that the dimensionless excitation frequencies of C-C sandwich FG microbeam are larger than the dimensionless excitation frequencies of C-S boundary condition and wide of the instability region of C-C is close the each other than C-S for different temperature change because in C-C leads harder structure.

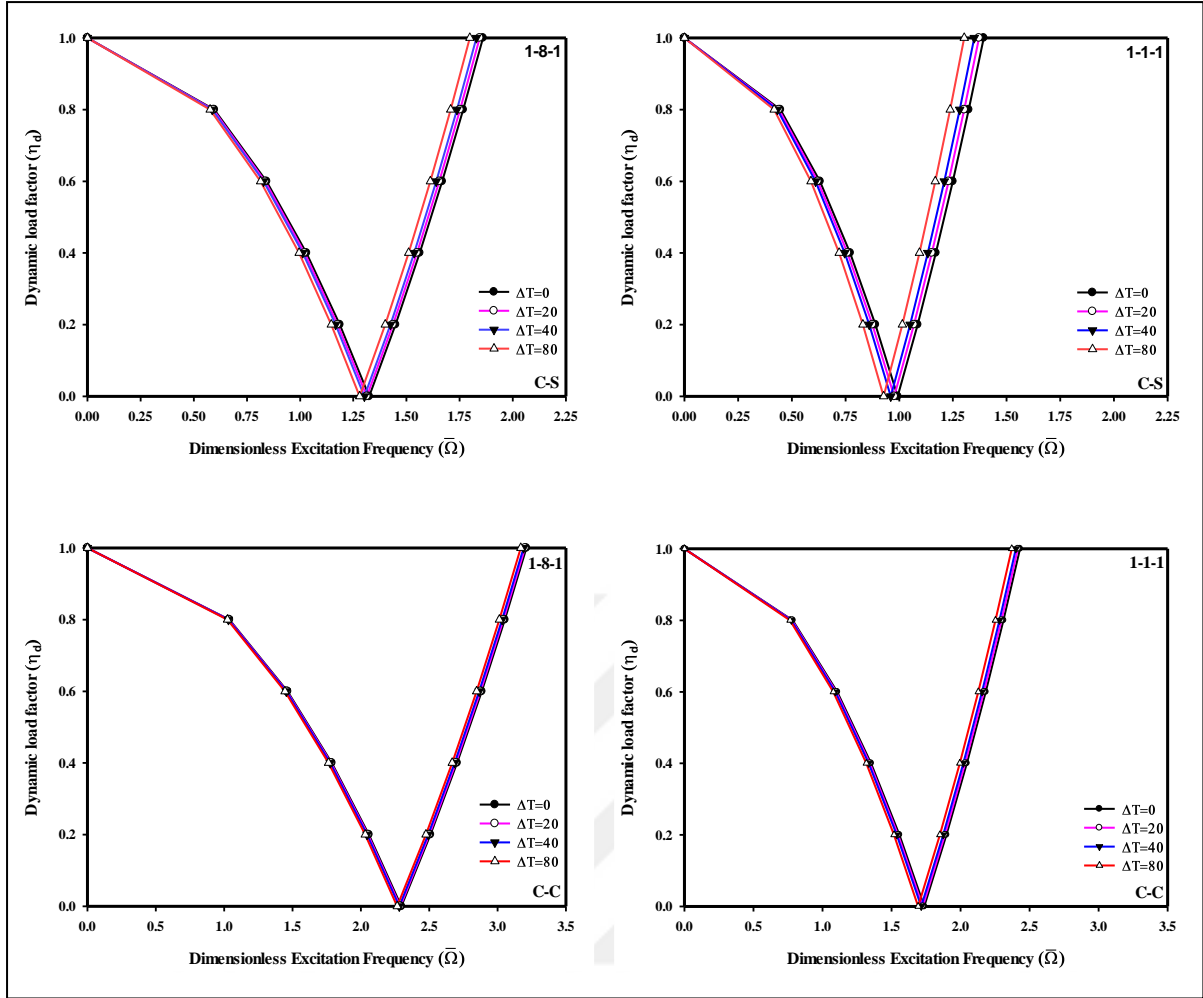


Figure 4.11 Effect of Temperature change (ΔT) on the instability region for sandwich FG micro beam (Modal III) with $k = 2$, $L/h = 10$, $l_m = h$, $\eta_s = 0.5$, $K_p = K_w = 0$ and $ea = 0.5h$ for C-S and C-C B.Cs.

The effect of temperature change (ΔT) on the instability regions of sandwich FG micro-beams Model II for (1-1-1) and (1-8-1) with $\eta_s = 0.5$, $L/h = 10$, $k = 2$, $ea = 0.5h$, $K_p = K_w = 0$ and $l_m = h$ for S supported boundary condition is depicted in Fig.(4.12).

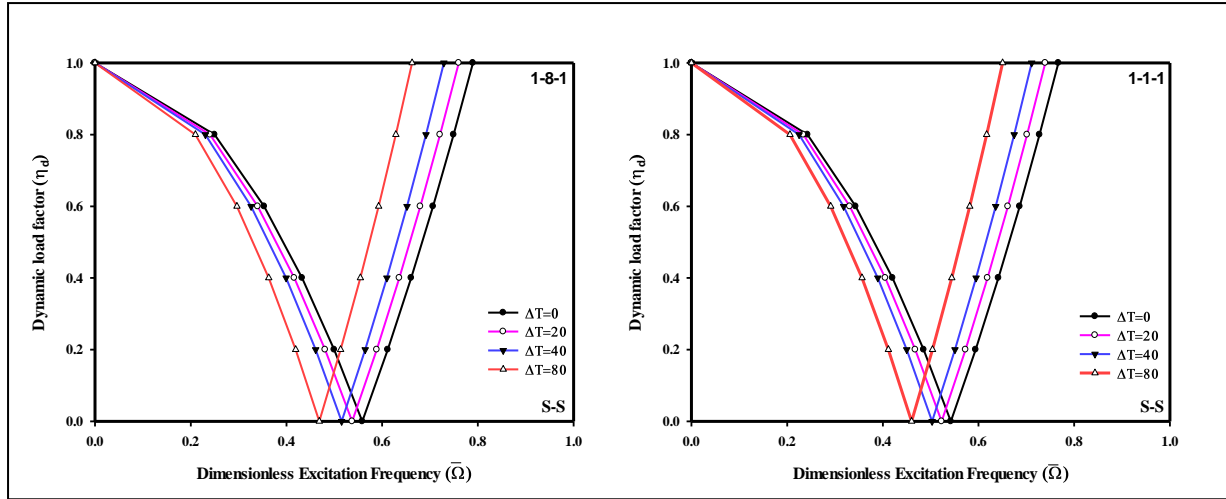


Figure 4.12 Effect of temperature change (ΔT) on the instability region for sandwich FG micro beam Modal II with $k = 2$, $L/h = 10$, $l_m = h$, $\eta_s = 0.5$, $K_p = K_w = 0$ and $ea = 0.5h$ for S-S B.Cs.

The effect of dimensionless material length scale parameter ($\beta = l_m/L$) on the dynamic instability region of for (1-1-1) and (1-8-1) sandwich FG microbeam with a certain dimensionless nonlocal parameter ($\alpha = ea/L = 0.1$), $\alpha = 0.5$, $L/h = 10$, without elastic foundation $K_p = K_w = 0$ and $\Delta T = 0$ for both cross section types (1-1-1) and (1-8-1) is shown in Fig.(4.13). Also can be noted from this figure that with increase in the $\beta = l_m/L$ leads to higher dimensionless excitation frequencies and also the width of the instability regions will be wider with increase the $\beta = l_m/L$ because the strain gradient effect makes sandwich FG micro-beam stiffer. It means when the dimensionless material length scale parameter ($\beta = l_m/L$) is larger than the dimensionless nonlocal parameter ($\alpha = ea/L$), the size dependent sandwich functionally graded micro-beam exerts a stiffness-hardening effect (Aifantis theory). Moreover, when the $\alpha = ea/L$, is larger than $\beta = l_m/L$ (Eringen theory), the sandwich functionally graded micro-beam exerts a stiffness-softening effect.

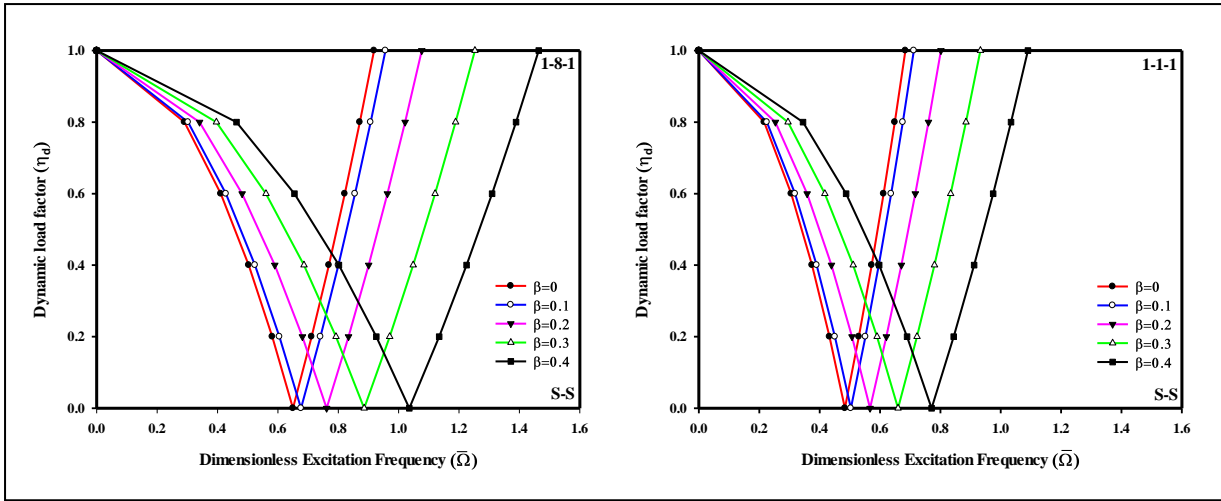


Figure 4.13 Effect of (β) on the instability region for sandwich FG micro beam (Modal III) with $\Delta T = 0$, $k = 2$, $L/h = 10$, $\eta_s = 0.5$, $K_p = K_w = 0$ and $\alpha = 0.1$ for S-S boundary conditions.

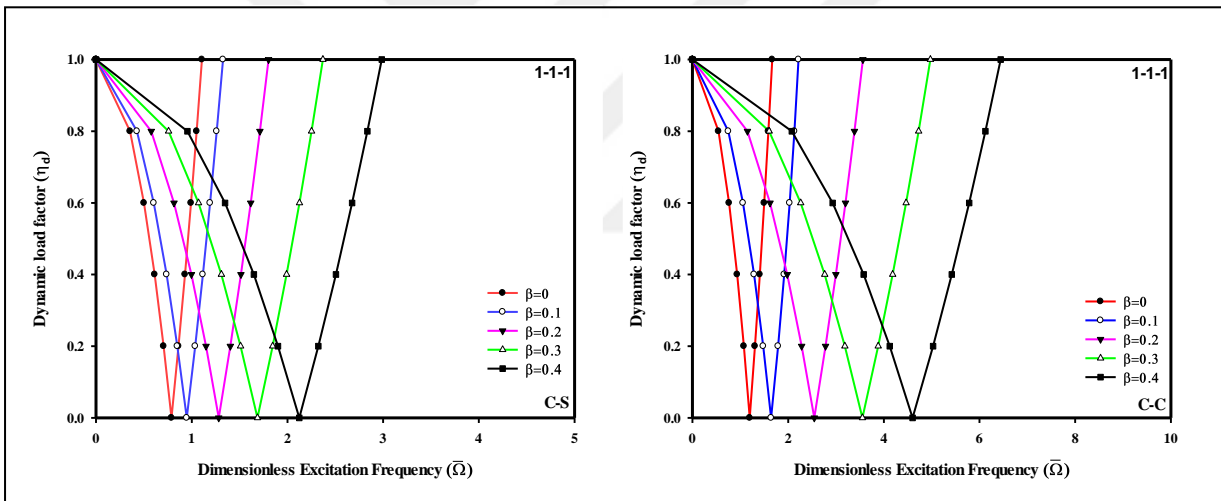


Figure 4.14 Effect of (β) on the instability region for sandwich FG micro beam (Modal III) with $\Delta T = 0$, $k = 2$, $L/h = 10$, $\eta_s = 0.5$, $K_p = K_w = 0$ and $\alpha = 0.1$ for various boundary conditions.

The effect of dimensionless material length scale parameter (β) on the instability regions of sandwich FG micro-beams Model III for cross-section shape (1-1-1) with $\eta_s = 0.5$, $L/h = 10$, $k = 2$, $K_p = K_w = 0$ and $\alpha = 0.1$ for C-S and C-C boundary conditions is seen in Fig.(4.14). On the other hand, for size dependent sandwich FG microbeam Model II with

various boundary conditions, the effect of (β) on the instability regions with $L/h=10$, $\Delta T = 0$, $\eta_s = 0.5$, $K_p = K_w = 0$ and $\alpha = 0.1$, is observed in Fig. (4.15)

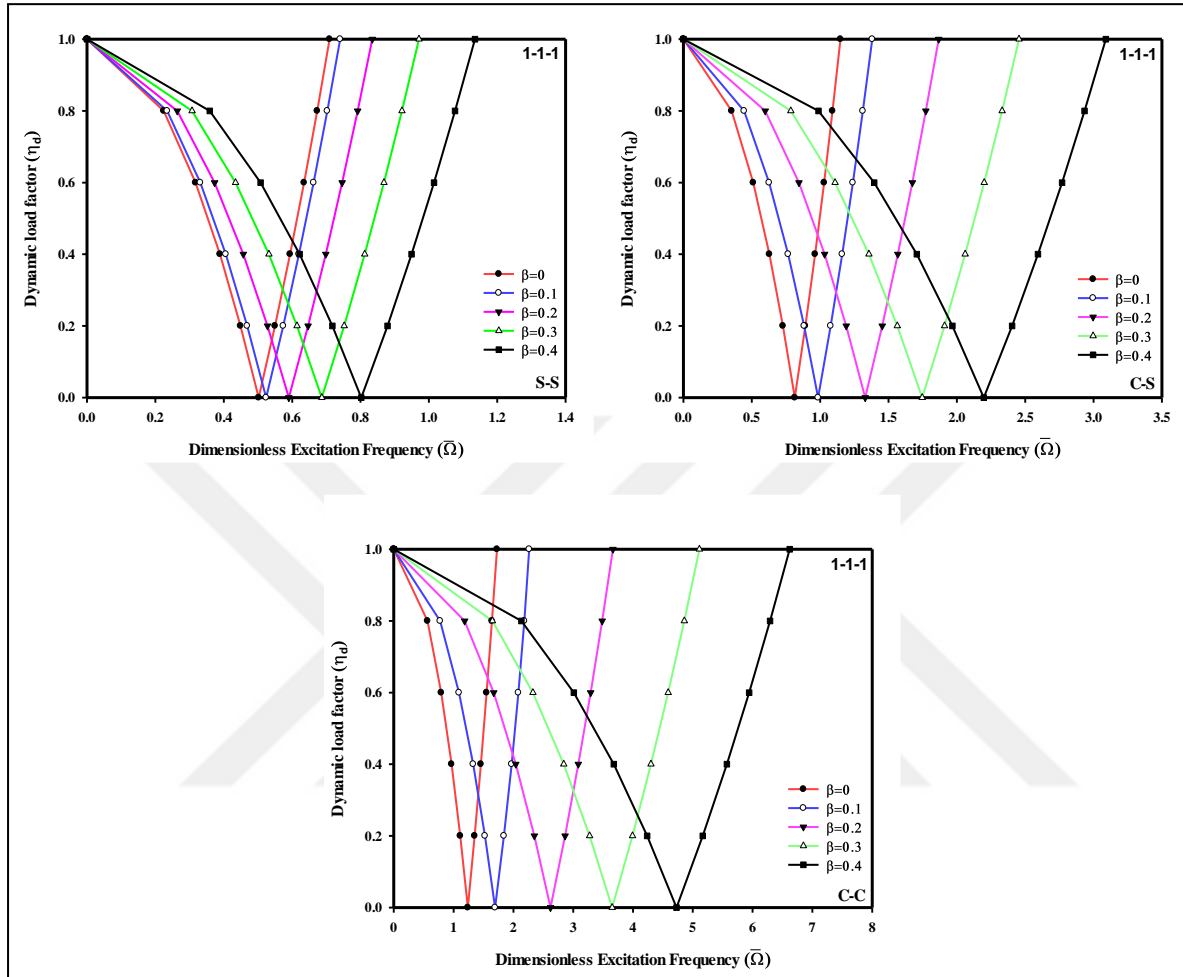


Figure 4.15 Effect of (β) on the instability region for sandwich FG micro beam (Modal II) with $\Delta T = 0$, $k = 2$, $L/h = 10$, $\eta_s = 0.5$, $K_p = K_w = 0$ and $\alpha = 0.1$ for various boundary conditions.

The effect of dimensionless nonlocal parameter $(\alpha = ea/L)$ on the dynamic instability region of for (1-1-1) and (1-8-1) sandwich FG microbeam with a certain dimensionless nonlocal parameter $\beta = l_m/L = 0.1$, $\alpha = 0.5$, $L/h = 10$, $K_p = K_w = 0$ and without temperature change $\Delta T = 0$ for both (1-1-1) and (1-8-1) is shown in Fig.(4.16). Also it can be noticed from this figure that with increase in the $\alpha = ea/L$ leads to lower dimensionless excitation frequencies and as well as the width of the instability regions will be decrease with increase the

dimensionless nonlocal parameter due to when the $\alpha = ea/L$ is larger than $\beta = l_m/L$ (the nonlocal Eringen elasticity theory), the sandwich FG micro-beam exerts a stiffness-softening effect.

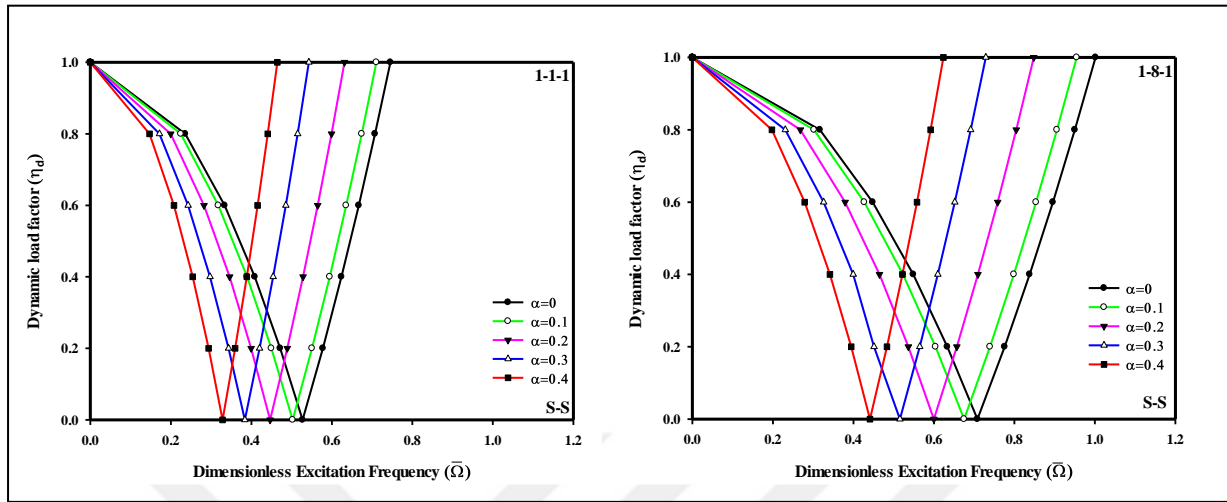


Figure 4.16 Effect of $\alpha = ea/L$ on the instability region for sandwich FG micro beam (Modal III) with $\Delta T = 0$, $k = 2$, $L/h = 10$, $\eta_s = 0.5$, $K_p = K_w = 0$ & $\beta = 0.1$ for S-S boundary conditions.

The effect dimensionless nonlocal parameter ($\alpha = ea/L$) on the instability regions of sandwich FG micro-beams Model III for cross section shape (1-1-1) with $\eta_s = 0.5$, $k = 2$, $L/h = 10$, $K_p = K_w = 0$ and $\beta = 0.1$ for C-S and C-C boundary conditions is seen in Fig.(4.17).

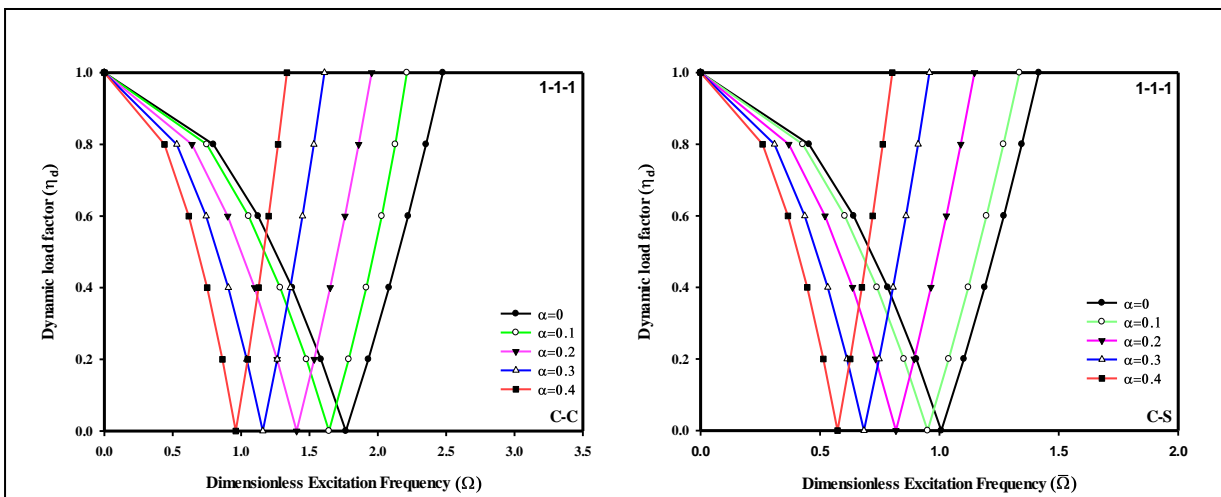


Figure 4.17 Effect of $\alpha = ea/L$ on the instability region for sandwich FG micro beam (Modal III) with $\Delta T = 0$, $L/h = 10$, $\eta_s = 0.5$, $K_p = K_w = 0$ and $\beta = 0.1$ for various boundary conditions.

Fig. (4.18) gives the influence of the dimensionless nonlocal parameter ($\alpha = ea/L$) on the instability region for sandwich FG micro beam (Modal II) with different boundary conditions at certain dynamic load factor with fixed $\Delta T = 0, L/h = 10, \eta_s = 0.5, K_p = K_w = 0$ and $\beta = 0.1$. Fig.(4.19) examines the effect of the various cross sectional shapes (1-1-1), (1-2-1), (1-8-1) and (2-1-2) on the instability region of sandwich FG microbeam with a certain dynamic load factor and fixed the parameters $\eta_s = 0.5, k = 2, K_p = K_w = 0, \Delta T = 0, ea = 0.5h, L/h = 10$, and $l_m = h$ for various B.Cs. It is noticed that the dimensionless excitation frequency for sandwich FG microbeam (Model III) in the left side is larger with cross sectional shape (1-8-1) and smaller for (2-1-2), and the width region decrease with the decrease the ratio of the core height to the total height of the sandwich FG microbeam for B.Cs. The reason for the (1-8-1) has the higher dimensionless excitation frequency is the core is ceramic and its occupy (8/10) from the height of the sandwich FG microbeam.

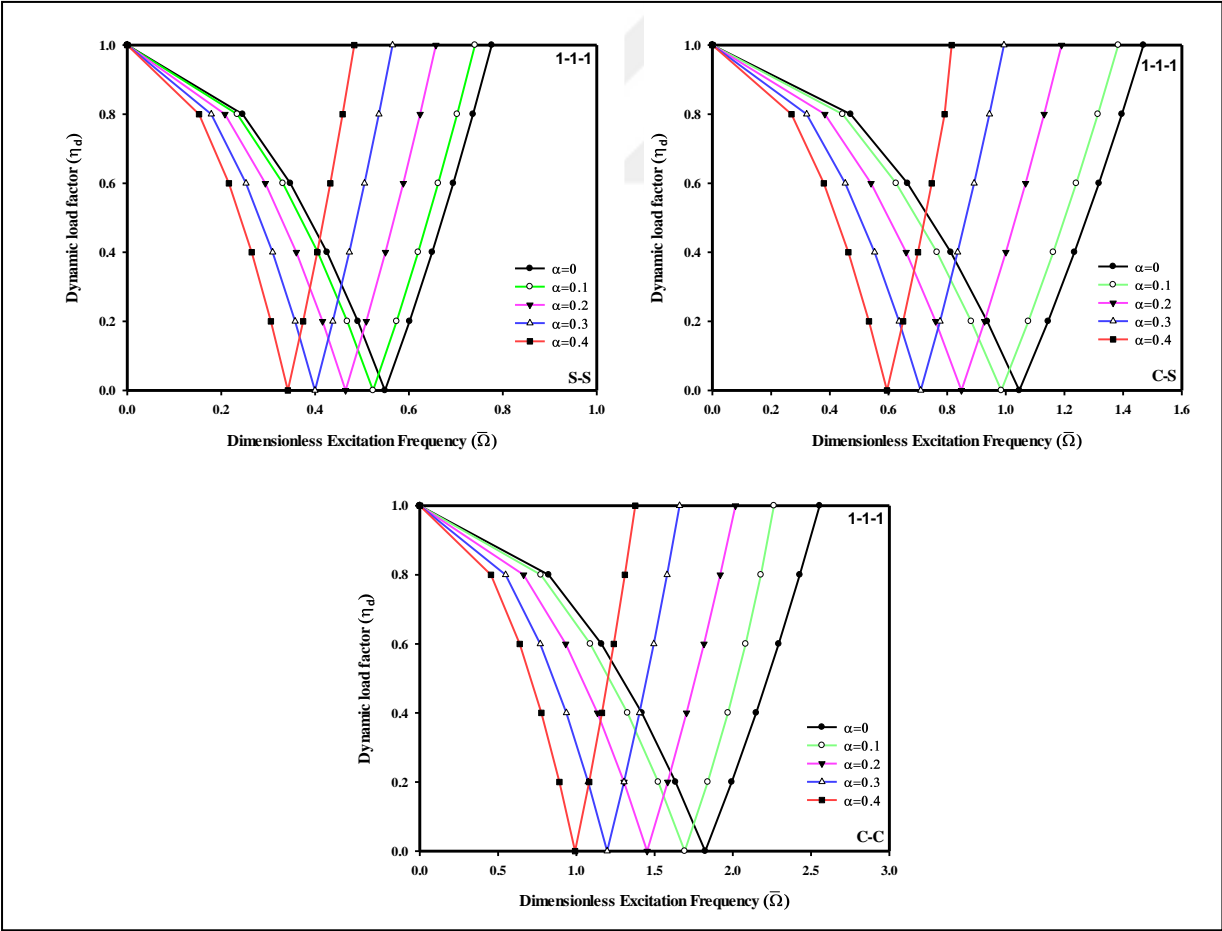


Figure 4.18 Effect of ($\alpha = ea/L$) on the instability region for sandwich FG micro beam (Modal II) with $k = 2, \eta_s = 0.5, L/h = 10, \Delta T = 0, K_p = K_w = 0$ and $\beta = 0.1$

Thus effective elasticity modulus is larger for this cross sectional shape (1-8-1) than the other. It can be noticed from Fig.(4.19) that the value of the dimensionless excitation frequency are the highest for (1-8-1) cross sectional shape whereas they are lowest for sandwich FG micro-beam with (2-1-2) cross sectional shape. On the other hand the figures in the right side for size dependent sandwich FG micro-beam with Model II, it can be noticed the dimensionless excitation frequency for each cross section shapes are close to each other when compare with Model III.

Fig. (4.20) depicts the influence of various boundary conditions on the instability region for sandwich FG micro-beam with Model I,II,III of (1-1-1) and (1-8-1) at $\eta_s = 0.5$, $k = 2$, $\Delta T = 0$, $ea = 0.5h$, $K_p = K_w = 0$ and $l_m = h$. It is observed from Fig. (4.20) that the dimensionless excitation frequencies of C-C boundary condition is much more the other B.Cs. Moreover, the width of the instability regions of C-C sandwich FG microbeam is larger than those of the C-S and S- S. This is due to the fact that sandwich FG microbeam with C-C has more rigidity stiffness than those in C-S and S-S sandwich FG microbeam respectively. It is observed at a lower results for excitation frequency for S-S supported B.C for the size dependent sandwich FG micro-beam is more sensitive to the dynamic instability than the other boundary conditions with C-S and C-C respectively.

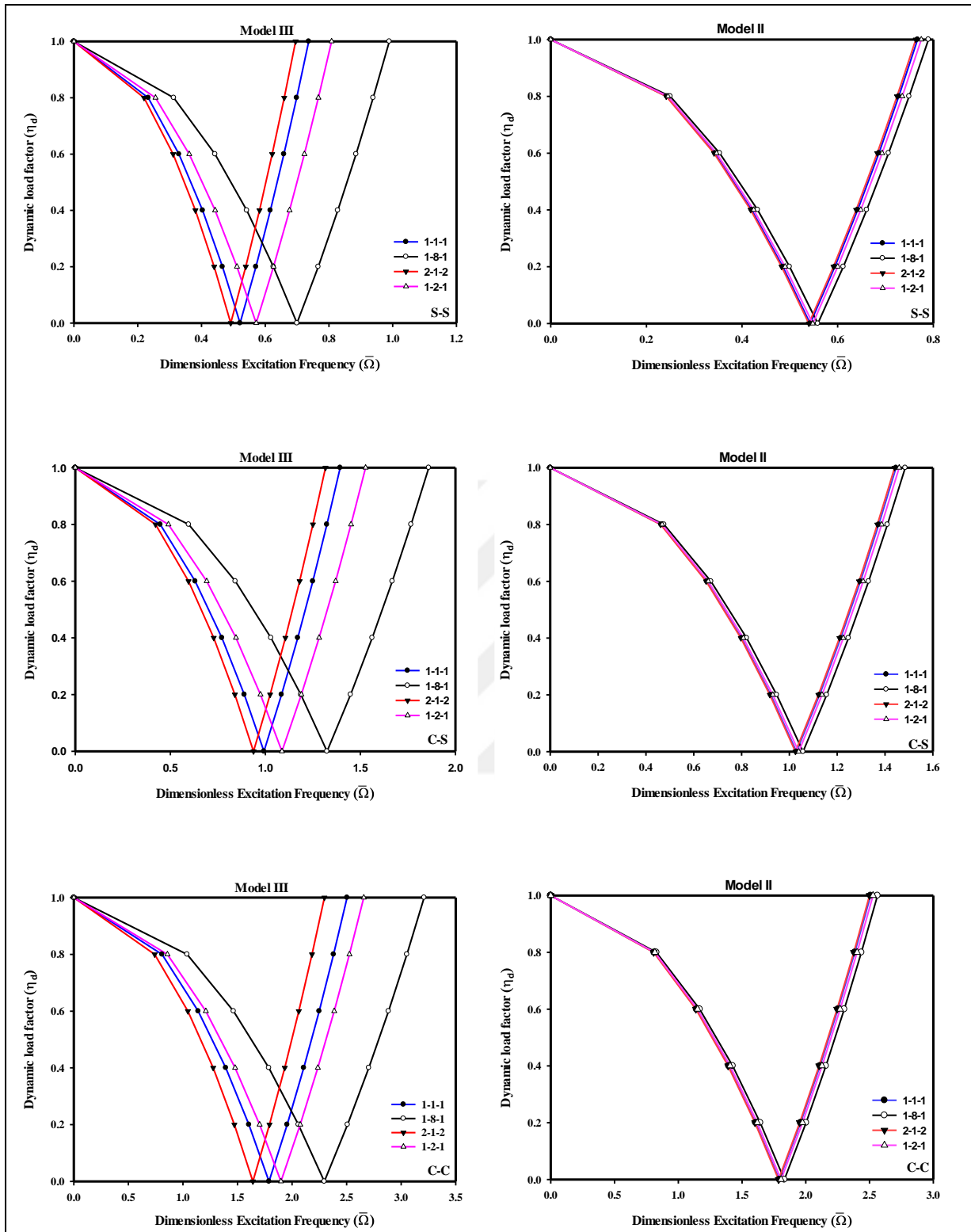


Figure 4.19 Effect of cross sectional types on the instability region for sandwich FG micro beam (Modal II,III) with $k = 2$, $\eta_s = 0.5$, $L/h = 10$, $l_m = h$, $\Delta T = 0$, $K_p = K_w = 0$ and $ea = 0.5h$ for various boundary conditions.

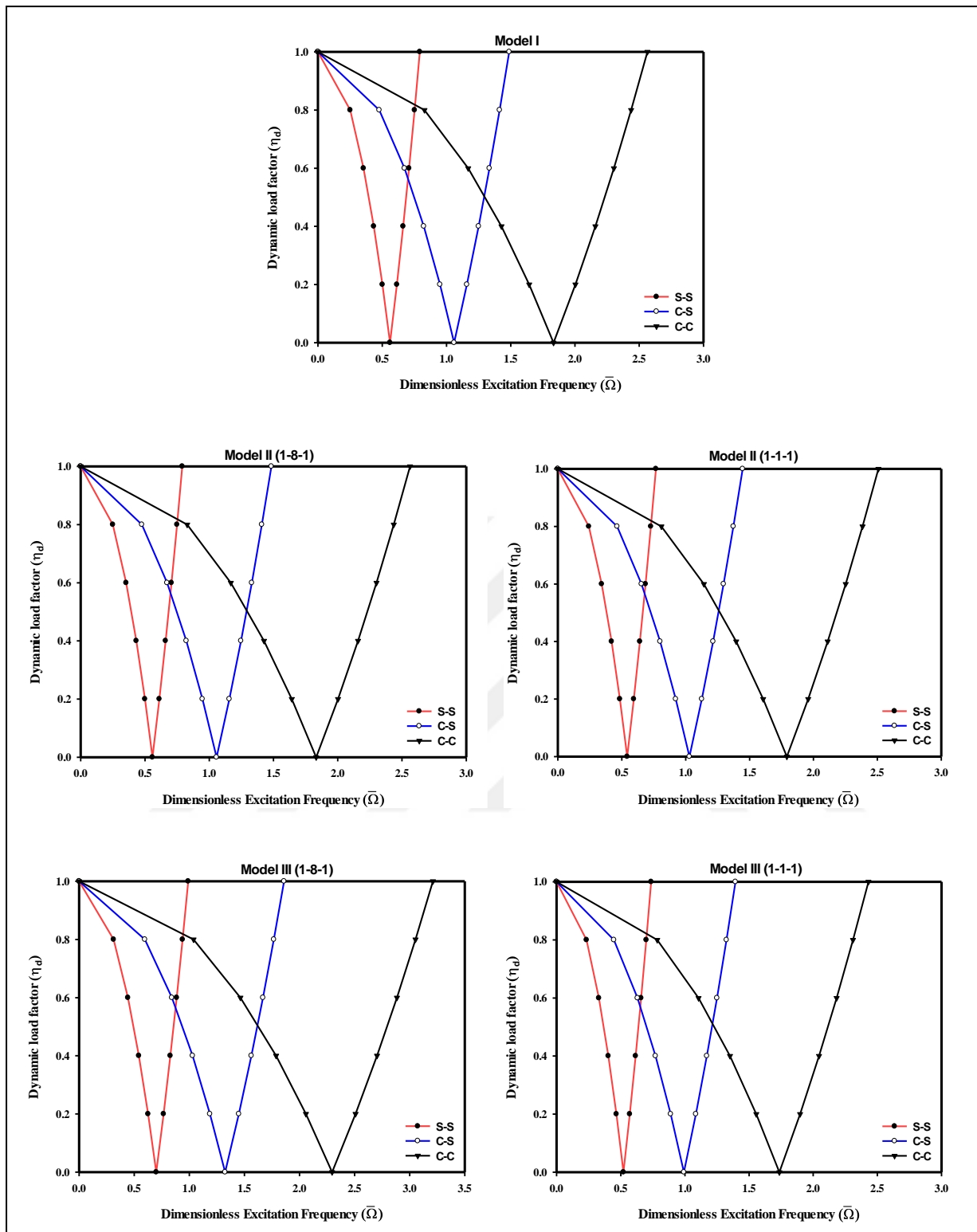


Figure 4.20 Effect of B.Cs various on the instability region for sandwich FG micro beam (Modals I, II, III) for (1-1-1) and (1-8-1) with $k = 2, \Delta T = 0, L/h = 10, \eta_s = 0.5,$

$$K_p = K_w = 0 \text{ } ea = 0.5h, \text{ and } l_m = h .$$

The effect of dimensionless Pasternak shear parameter (K_p) and dimensionless Winkler parameter (K_w) on the instability region for size dependent sandwich FG micro beam with (Modal II, III) for cross section shape (1-1-1) at certain dynamic load factor (η_d) for fixed $k = 2$, $\Delta T = 0$, $ea = 0.5h$, $\eta_s = 0.5$, $L/h = 10$ and $l_m = h$ with various boundary conditions (i.e. S-S, C-S, and C-C) is shown in Figs. (4.21) and (4.22) respectively. It is noticed from Figs. (4.21) and (4.22) the increase of dimensionless Winkler and Pasternak shear parameters leads to higher excitation frequencies ($\bar{\Omega}$) and the width of the instability region for all types of sandwich FG micro-beam is increase with the increasing of (K_p) and (K_w) at given dynamic load factor. It can be seen also when sandwich FG micro-beam with soften elastic foundation is susceptible to the dynamic instability at the lower value of dimensionless excitation frequency ($\bar{\Omega}$). This is due to the lower bending resistance to bending deformation. Also it can be observed that the effect of dimensionless Pasternak shear parameter on the instability region of sandwich FG micro-beam is the same influence for the dimensionless Winkler parameter . However the excitation frequency on dimensionless Pasternak shear parameter is larger than that on the dimensionless Winkler parameter with all kinds of sandwich FG micro-beam.

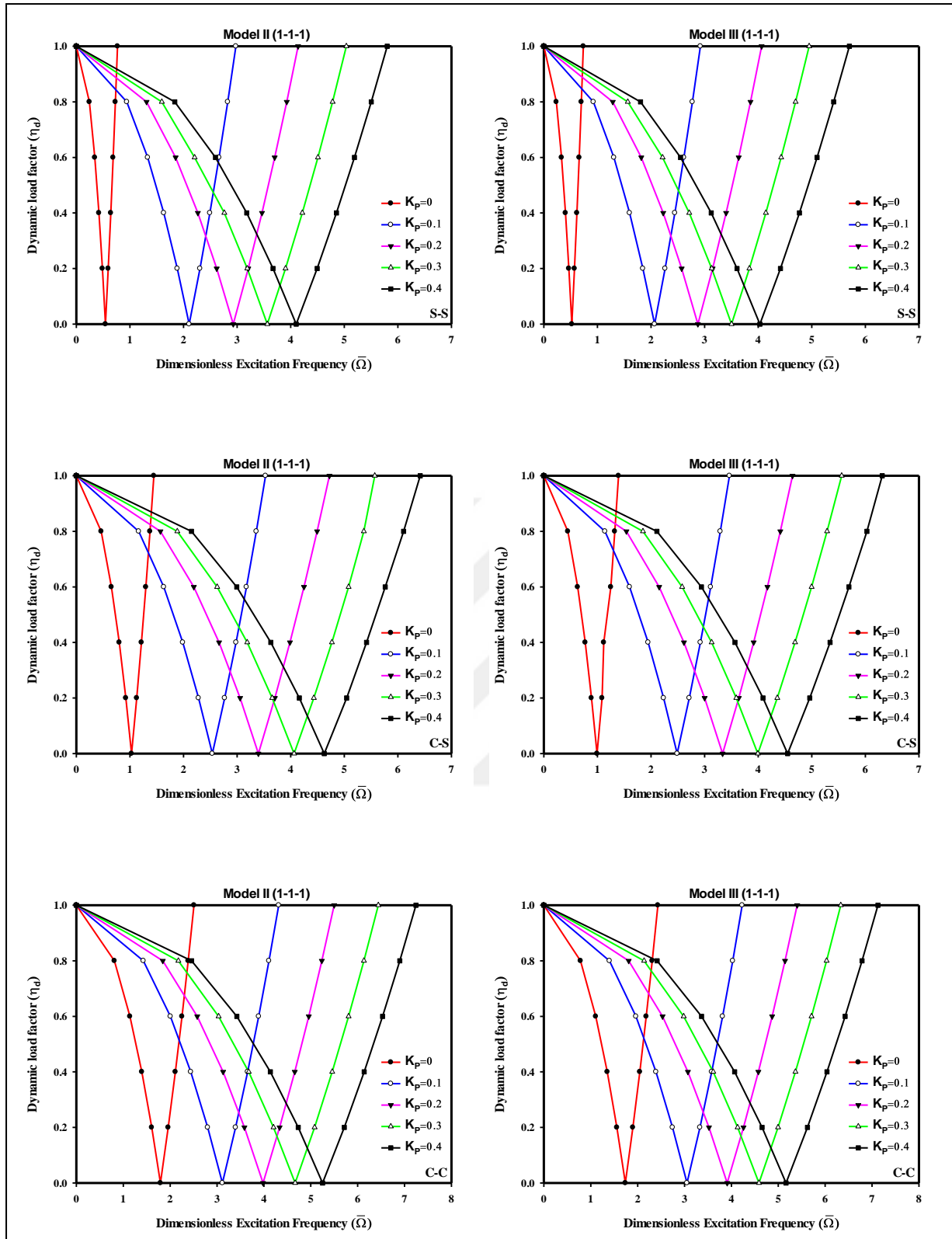


Figure 4.21 Effect of dimensionless Pasternak shear parameter (K_p) on the instability region for sandwich FG micro beam (Modal II, III) for cross section shapes (1-1-1) with $k = 2$, $\Delta T = 0$, $L/h = 10$, $l_m = h$, $\eta_s = 0.5$, $K_W = 0$ and $ea = 0.5h$ for various boundary conditions.

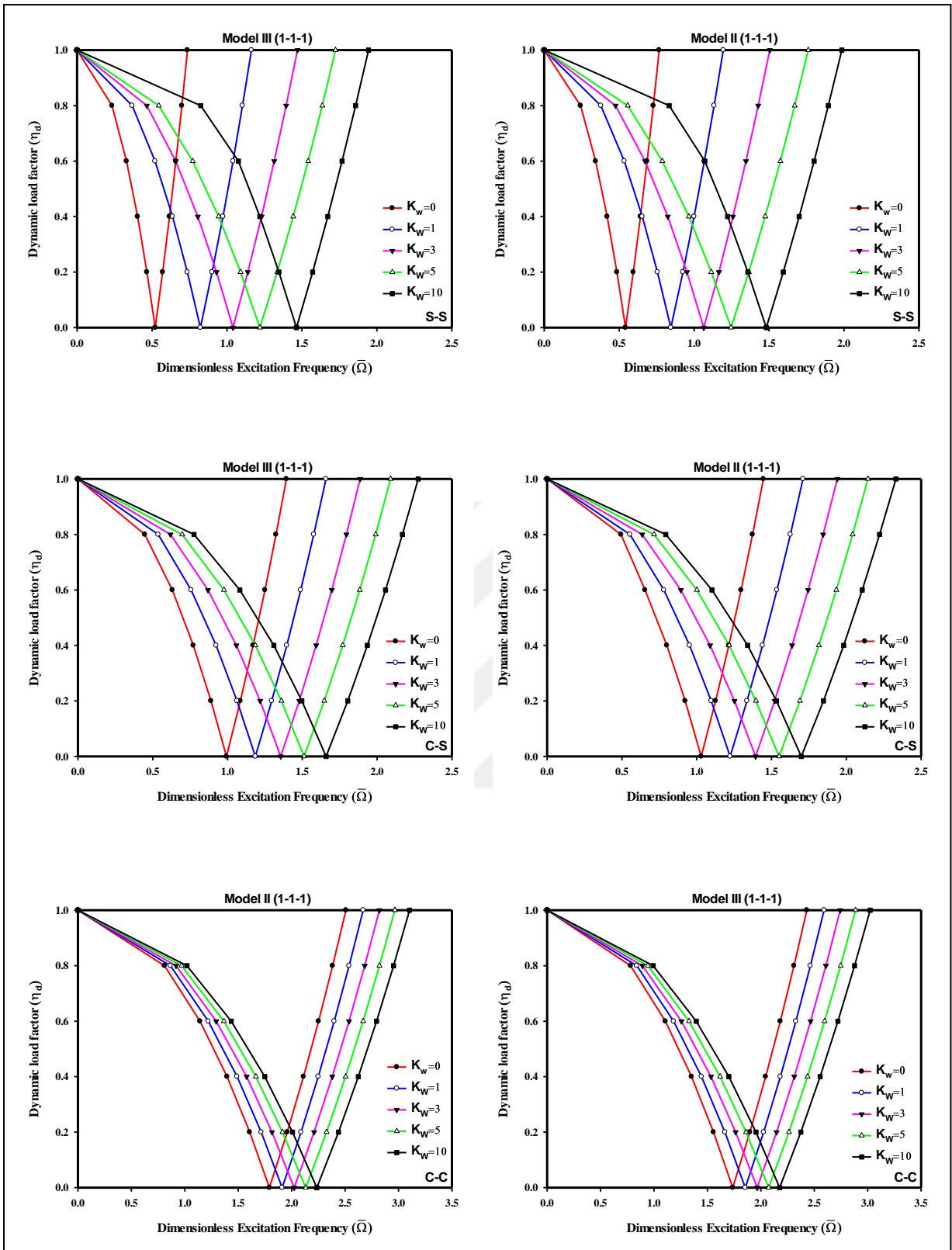


Figure 4.22 Effect of dimensionless Winkler shear parameter (K_W) on the instability region for sandwich FG micro beam (Modal II, III) for cross section shapes (1-1-1) with $k = 2$, $\Delta T = 0$, $L/h = 10$, $l_m = h$, $\eta_s = 0.5$, $K_p = 0$ and $ea = 0.5h$ for various boundary conditions.

4.3 Static bending, Free and buckling analysis of Sandwich functionally graded micro-beam

The numerical results of static bending, buckling behavior and free vibration of small scale sandwich FG micro-beam with higher-order beam theories in conjunction with the nonlocal strain gradient theory (NLSGT) under the action of temperature change with elastic foundation (Winkler and Pasternak elastic foundation) is presented in this section of thesis. For sandwich FG micro-beam, there are many cross section shapes with different Models I,II, III. In this part of the thesis, the FG material part of the sandwich micro-beam is made of SuS304 constituent and alumina (Al_2O_3) constituent. Their properties are collected and presented in table (4.6).

Table (4.6) Material properties of the FGM microbeam constituent

Material Properties	SuS304	alumina (Al_2O_3)
Young's modulus (E) GPa	210 GPa	380 GPa
thermal expansion coefficient (α_T)	12.33×10^{-6}	7.4×10^{-6}
mass density (ρ) kg/m^3	8166	3960
Poisson's ratio (ν)	0.3177	0.3

The following non-dimension are used in this section

dimensionless nonlocal parameter

$$\alpha = ea/L$$

dimensionless material length scale parameter

$$\beta = l_m/L$$

dimensionless Winkler elastic foundation

$$K_w = k_w L^2 / E_m bh$$

dimensionless Pasternak elastic foundation

$$K_p = k_p / E_m bh$$

dimensionless transverse deflection for uniform load

$$\bar{w} = 100wE_m I / q_o L^4$$

dimensionless critical buckling load is

$$\bar{P} = PL^2/E_m I$$

Dimensionless natural frequency

$$\bar{\omega} = \omega L^2/h \sqrt{\rho_m/E_m}$$

In the first aspect of this part of the present thesis is the static bending of size dependent sandwich FG micro-beam. In table 4.7. a comparison of the dimensionless transverse deflection ($\bar{w} = 100 w E_m I / q_0 L^4$) of size dependent FG microbeam for model II,III with cross section shape (1-1-1) and different dimensionless material length scale parameter (β) (0, 0.05, 0.1, 0.15, 0.2), dimensionless nonlocal parameter (α) (0, 0.1, 0.2), various gradient index $k = (1, 5)$, aspect ratio $L/h = 10$ and different estimate method (Mori-Tanaka scheme and the rule of mixture) of the effective material properties. It is can be noted from this table that the dimensionless transverse deflection obtained by the Mori-Tanaka scheme are greater than that the results obtained by the rule of mixture. This is due to the size dependent FG sandwich microbeam becomes more flexible according to Mori-Tanaka scheme than with respect to classical rule of mixture for a constant material property gradient index and the different estimation of the effective material properties.

Table 4.7 Dimensionless transverse deflection $\bar{w} = 100 E_m I / q L^4 w$ of sandwich beams subject to distributed load for $L / h = 10$, $\Delta T = 0$, $K_w = K_p = 0$ and Model II,III (1-1-1)

Model	k	β	The rule of mixture			Mori Tanaka scheme		
			$\alpha = 0$	$\alpha = 0.1$	$\alpha = 0.2$	$\alpha = 0$	$\alpha = 0.1$	$\alpha = 0.2$
Model II	1	$\beta = 0$	1.0068	1.1031	1.3920	1.0096	1.1065	1.3956
		$\beta = 0.05$	0.9832	1.0776	1.3608	0.9864	1.0803	1.3642
		$\beta = 0.1$	0.9180	1.0068	1.2733	0.9205	1.0105	1.2784
		$\beta = 0.15$	0.8260	0.9064	1.1475	0.8295	0.9098	1.1512
		$\beta = 0.2$	0.7240	0.7947	1.0068	0.7284	0.7986	1.0103
	5	$\beta = 0$	1.0160	1.1131	1.4044	1.0193	1.1175	1.4089
		$\beta = 0.05$	0.9922	1.0874	1.3730	0.9965	1.0912	1.3772
		$\beta = 0.1$	0.9264	1.0160	1.2847	0.9289	1.0199	1.2883
		$\beta = 0.15$	0.8335	0.9146	1.1579	0.8364	0.9187	1.1612
		$\beta = 0.2$	0.7307	0.8020	1.0160	0.7348	0.8056	1.0197
Model III	1	$\beta = 0$	1.0214	1.1192	1.4124	1.0252	1.1225	1.4153
		$\beta = 0.05$	0.9975	1.0933	1.3807	1.0025	1.0975	1.3849
		$\beta = 0.1$	0.9313	1.0214	1.2918	0.9357	1.0262	1.2965
		$\beta = 0.15$	0.8379	0.9195	1.1641	0.8412	0.9246	1.1685
		$\beta = 0.2$	0.7345	0.8062	1.0214	0.7387	0.8095	1.0248
	5	$\beta = 0$	1.2252	1.3425	1.6944	1.2295	1.3478	1.6985
		$\beta = 0.05$	1.1965	1.3115	1.6564	1.1999	1.3166	1.6596
		$\beta = 0.1$	1.0761	1.1802	1.4927	1.0789	1.1853	1.4987
		$\beta = 0.15$	0.9682	1.0624	1.3452	0.9723	1.0654	1.3495
		$\beta = 0.2$	0.8487	0.9316	1.1802	0.8523	0.9368	1.1835

Table 4.8 contains the influences of the various beam theories on the dimensionless transverse deflection of size dependent sandwich FG micro-beam for different boundary conditions (i.e. S-S, C-S, C-C) with various values of the dimensionless material length scale parameter ($\beta = 0.1, 0.2, 0.3$), aspect ratio ($L/h = 10, 20$), both Models (II,III) and cross section shape (1-1-1) with certain dimensionless nonlocal parameter ($\alpha = 0.1$), without the elastic foundation ($K_w = K_p = 0$) and no thermal effect ($\Delta T = 0$). It can be observed from table (4.8) the dimensionless transverse deflection with the higher order beam theories (HOBTs) is

greater than those in Euler theory (EBBT) and less than the dimensionless transverse deflection for First shear deformation theory (FSDBT). It mean the Euler Bernoulli beam theory is more stiffer than the other theories because neglect the shear deformation effect and the Timoshenko beam theory is the most flexible with constant shear $5/6$. It can be observed as well as, the effect of shear deformation is decrease with increase the aspect ratio from 10 to 20 then the dimensionless transverse deflection is close each to other for all beam theory for aspect ratio 20 than aspect ratio 10. Moreover, the results for higher order deformation beam theories (HOBTs) are almost the same and for ASDBT and ESDBT theory the dimensionless transverse deflection are the same. Also the sandwich FG microbeam become more stiffer with C-C boundary condition, it can be seen for example with PSDBT, C-C B.Cs, Model III and ($\beta = 0.1, L/h = 10$) the dimensionless transverse deflection is 0.0909 whereas for C-S is 0.2881 and for S-S is 1.0214.

Table 4.8 Dimensionless transverse deflection $\bar{w} = 100 w E_m I / q_0 L^4$ of sandwich micro-beams

with B.Cs with a cross-section shape (1-1-1) for $\alpha = 0.1, \Delta T = 0, k = 1, K_w = K_p = 0$

B.Cs		Model II						Model III						
		Beam theory	$L/h = 10$			$L/h = 20$			$L/h = 10$			$L/h = 20$		
			$\beta = 0.1$	$\beta = 0.2$	$\beta = 0.3$	$\beta = 0.1$	$\beta = 0.2$	$\beta = 0.3$	$\beta = 0.1$	$\beta = 0.2$	$\beta = 0.3$	$\beta = 0.1$	$\beta = 0.2$	$\beta = 0.3$
S-S Boundary Condition	EBBT	1.0060	0.7941	0.5859	0.9891	0.7805	0.5767	1.0209	0.8055	0.5947	1.0062	0.7942	0.5870	
	FSDBT	1.0071	0.7950	0.5869	0.9895	0.7809	0.5771	1.0229	0.8074	0.5961	1.0066	0.7947	0.5872	
	PSDBT	1.0068	0.7947	0.5864	0.9893	0.7808	0.5769	1.0214	0.8062	0.5951	1.0064	0.7944	0.5869	
	TSDBT	1.0068	0.7947	0.5864	0.9894	0.7806	0.5769	1.0213	0.8061	0.5950	1.0064	0.7944	0.5869	
	ASDBT	1.0067	0.7946	0.5863	0.9892	0.7807	0.5769	1.0212	0.8060	0.5950	1.0064	0.7943	0.5869	
	ESDBT	1.0067	0.7946	0.5863	0.9892	0.7807	0.5769	1.0212	0.8060	0.5950	1.0064	0.7943	0.5869	
	HSDBT	1.0067	0.7947	0.5864	0.9893	0.7808	0.5769	1.0214	0.8062	0.5951	1.0064	0.7944	0.5869	
C-S Boundary Condition	EBBT	0.2618	0.1411	0.0801	0.2470	0.1302	0.0738	0.2872	0.1538	0.0799	0.2740	0.1452	0.0747	
	FSDBT	0.2631	0.1420	0.0810	0.2472	0.1305	0.0742	0.2892	0.1551	0.0811	0.2745	0.1455	0.0752	
	PSDBT	0.2622	0.1411	0.0805	0.2471	0.1304	0.0740	0.2881	0.1543	0.0805	0.2743	0.1454	0.0750	
	TSDBT	0.2622	0.1411	0.0804	0.2471	0.1304	0.0740	0.2879	0.1542	0.0805	0.2743	0.1453	0.0750	
	ASDBT	0.2621	0.1410	0.0804	0.2471	0.1304	0.0740	0.2877	0.1541	0.0804	0.2742	0.1453	0.0749	
	ESDBT	0.2621	0.1410	0.0804	0.2471	0.1304	0.0740	0.2877	0.1541	0.0804	0.2742	0.1453	0.0749	
	HSDBT	0.2622	0.1411	0.0805	0.2471	0.1304	0.0740	0.2881	0.1543	0.0805	0.2743	0.1454	0.0750	
C-C Boundary Condition	EBBT	0.0910	0.0387	0.0198	0.0810	0.0335	0.0170	0.0900	0.0378	0.0190	0.0819	0.0339	0.0171	
	FSDBT	0.0921	0.0399	0.0208	0.0813	0.0338	0.0173	0.0915	0.0395	0.0208	0.0822	0.0342	0.0174	
	PSDBT	0.0915	0.0391	0.0202	0.0812	0.0337	0.0171	0.0909	0.0386	0.0199	0.0821	0.0340	0.0173	
	TSDBT	0.0914	0.0390	0.0201	0.0812	0.0337	0.0171	0.0908	0.0386	0.0199	0.0821	0.0340	0.0173	
	ASDBT	0.0912	0.0389	0.0201	0.0812	0.0336	0.0171	0.0907	0.0385	0.0198	0.0821	0.0340	0.0173	
	ESDBT	0.0912	0.0389	0.0201	0.0812	0.0336	0.0171	0.0907	0.0385	0.0198	0.0821	0.0340	0.0173	
	HSDBT	0.0915	0.0391	0.0202	0.0812	0.0337	0.0171	0.0909	0.0386	0.0199	0.0821	0.0340	0.0173	

Fig.(4.23) shows the variation of the dimensionless transverse deflection with respect to material property gradient index (k) for different boundary conditions (i.e. S-S, C-S, C-C) of size dependent sandwich FG micro-beam with various cross section shapes (1-1-1, 1-2-1, 1-8-1, 2-1-2) at fixed dimensionless nonlocal parameter ($\alpha = 0.1$), dimensionless material length scale parameter ($\beta = 0.2$) without elastic foundation $K_w = K_p = 0$, no temperature change ($\Delta T = 0$) and $L/h = 10$. One can observe that the increase dimensionless deflection with increase power law index (k) for both Models II,III with various cross-section types. It can be seen from this figure the sandwich FG microbeam with shape (2-1-2) has the Max. value of transverse deflection and (1-8-1) represented Min. value of these for Model III. Moreover the dimensionless transverse deflection for Model II is different, it can be observed from this when the gradient index is less than 1.53 for example simply support boundary condition, the (\bar{w}) of (1-8-1) is less than (\bar{w}) for (2-1-2). In the other word, when the power law index is greater than 1.53 the dimensionless of transverse deflection for (1-8-1) is greater than the other cross section shapes and the results for (2-1-2) is lower than the other cross section shapes. This is due to the ceramic portion for (1-8-1) with increase gradient index (k) is lower than for (2-1-2) then the sandwich FG microbeam become more flexible with (1-8-1) than (2-1-2) for (k) greater than 1.53.

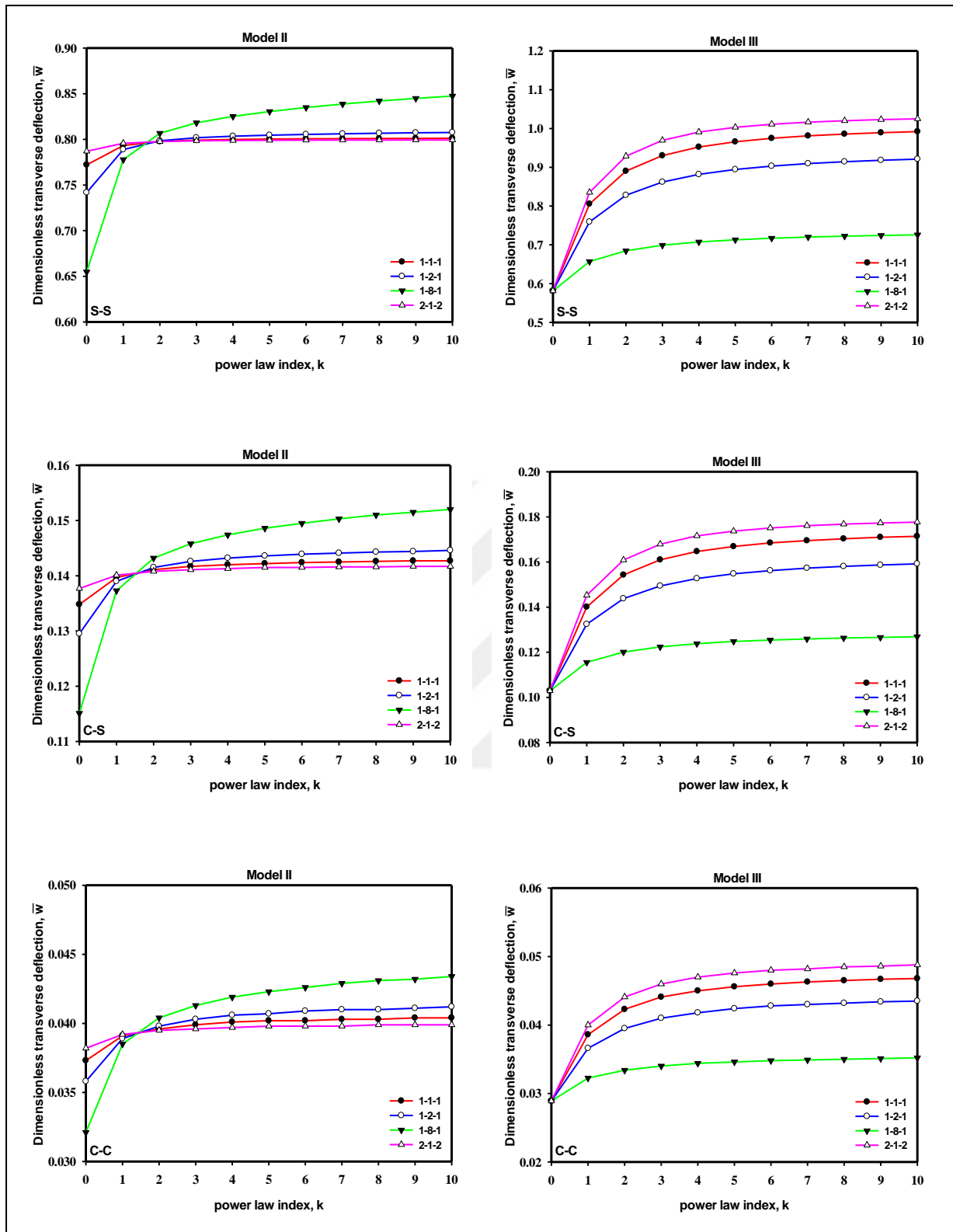


Figure 4.23 Variation of the dimensionless transverse deflection (\bar{w}) with the power-law exponent k for different cross-section shape sandwich FG microbeam, $L/h = 10$, $\alpha = 0.1$, $\beta = 0.2$, and for different boundary conditions.

The effect of power law index (k) with different symmetrical (1-1-1),(1-2-1),(1-8-1) and (2-1-2) and un-symmetrical (1-2-3), (2-3-1) and (3-1-2) cross section shapes on the dimensionless transverse deflection of sandwich FG micro-beam is presented in table 4.9 at fixed $L/h=10$, $\beta=0.2$, $\alpha=0.1$ and $K_w = K_p = 0$. It can be noticed that the dimensionless transverse deflection for Model III is less than these with Model II at lower value of power law index. On the other hand, with larger value of (k) the dimensionless transverse deflection of Model II is larger than of these results with Model III except shape (1-8-1). The reason of this phenomena is that for the Model III the core is full ceramic then the ceramic portion in this model is more than the ceramic portion for Model II with low values of gradient index (k), for example when $k=0$ this means the volume fraction of ceramic $V_c=1$ and $V_m=0$ then that the FG part of sandwich microbeam is made of whole ceramic then the sandwich FG microbeam have more effective elasticity modulus therefore the deflection is the smallest. On the other hand, when gradient index k goes to infinity the FG part of sandwich microbeam is becomes full metal then the results is conversely. This is due to the Model III have effective elasticity modulus is more than its for Model II for lower k and the results is different when power law index (k) increase the Model II have effective elasticity modulus is more than Model III except shape (1-8-1).

Table 4.9 Dimensionless transverse deflection ($\bar{w} = 100 w E_m I / q_0 L^4$) of sandwich FG microbeams (PSDBT) for various power law index $L / h = 10$, $\beta = 0.2$, $\alpha = 0.1$, and $K_w = K_p = 0$

B.Cs		Model	k	Symmetrical cross section				Un-symmetrical cross section		
				1-1-1	1-2-1	1-8-1	2-1-2	1-2-3	2-3-1	3-1-2
S-S Boundary Condition	Model II	0 (ceramic)	0.7732	0.7427	0.6558	0.7882	0.6990	0.7732	0.7984	
		1	0.7947	0.7903	0.7793	0.7971	0.7624	0.8023	0.8011	
		3	0.8008	0.8035	0.8200	0.7997	0.7869	0.8148	0.8025	
		5	0.8020	0.8064	0.8324	0.8005	0.7925	0.8208	0.8030	
		(metal) ∞	0.8043	0.8152	0.8868	0.8014	0.7983	0.8435	0.8044	
	Model III	0 (ceramic)	0.5821	0.5821	0.5821	0.5821	0.5821	0.5821	0.5821	
		1	0.8062	0.7602	0.6580	0.8365	0.7863	0.7547	0.8389	
		3	0.9316	0.8632	0.6999	0.9709	0.8911	0.8521	0.9702	
		5	0.9671	0.8956	0.7140	1.0046	0.9182	0.8819	1.0016	
		(metal) ∞	1.0137	0.9468	0.7400	1.0401	0.9514	0.9276	1.0339	
C-S Boundary Condition	Model II	0 (ceramic)	0.1348	0.1295	0.1151	0.1377	0.1222	0.1348	0.1403	
		1	0.1397	0.1390	0.1373	0.1401	0.1332	0.1418	0.1417	
		3	0.1417	0.1426	0.1458	0.1411	0.1377	0.1453	0.1425	
		5	0.1422	0.1436	0.1486	0.1415	0.1388	0.1468	0.1428	
		(metal) ∞	0.1433	0.1459	0.1584	0.1420	0.1403	0.1511	0.1433	
	Model III	0 (ceramic)	0.1029	0.1029	0.1029	0.1029	0.1029	0.1029	0.1029	
		1	0.1401	0.1324	0.1155	0.1453	0.1370	0.1315	0.1458	
		3	0.1610	0.1494	0.1224	0.1679	0.1548	0.1477	0.1681	
		5	0.1669	0.1548	0.1248	0.1737	0.1595	0.1527	0.1736	
		(metal) ∞	0.1751	0.1633	0.1291	0.1806	0.1657	0.1604	0.1801	
C-C Boundary Condition	Model II	0 (ceramic)	0.0373	0.0358	0.0321	0.0382	0.0339	0.0373	0.0392	
		1	0.0391	0.0389	0.0385	0.0392	0.0369	0.0399	0.0399	
		3	0.0399	0.0403	0.0413	0.0396	0.0383	0.0413	0.0403	
		5	0.0402	0.0407	0.0423	0.0398	0.0386	0.0418	0.0404	
		(metal) ∞	0.0407	0.0417	0.0451	0.0401	0.0392	0.0432	0.0407	
	Model III	0 (ceramic)	0.0289	0.0289	0.0289	0.0289	0.0289	0.0289	0.0289	
		1	0.0386	0.0366	0.0322	0.0400	0.0379	0.0364	0.0402	
		3	0.0441	0.0410	0.0340	0.0460	0.0426	0.0406	0.0461	
		5	0.0456	0.0424	0.0346	0.0476	0.0439	0.0419	0.0477	
		(metal) ∞	0.0479	0.0446	0.0357	0.0497	0.0458	0.0439	0.0498	

The effects of the both dimensionless nonlocal parameter ($\alpha = ea/L$) and the dimensionless material length scale parameter ($\beta = l_m/L$) with fixed $\Delta T = 0$, $L/h = 10$, $k = 1$, and $K_w = K_p = 0$ on the dimensionless transverse deflection for Modal II (1-1-1) and Modal III (1-1-1) for various B.Cs, ($\beta = 0, 0.05, 0.1, 0.15, 0.2$) and ($\alpha = 0, 0.05, 0.1, 0.15, 0.2$) presented in table (4.10). It is clear that the dimensionless deflection can decrease with increase dimensionless material length scale parameter (β) because the strain gradient effect makes sandwich FG microbeam stiffness-hardening and they increase with increase the dimensionless nonlocal parameter (α) due to softening effect observed in the nonlocal elasticity theory. It should be noted, the dimensionless transverse deflection of the classical elasticity theory can be obtained by setting $\alpha = \beta = 0$ and when $\alpha = \beta$ for simply support boundary condition. On the other hand for other B.Cs (i.e. C-C, C-S) the classical theory can be achieved only when $\alpha = \beta = 0$. Depending on the dimensionless nonlocal and material length scale parameters, the dimensionless transverse deflection value may be larger or smaller than that of classical values.

Table 4.10 Dimensionless transverse deflection ($\bar{w} = 100 w E_m I / q_0 L^4$) of sandwich FG micro-beams Model II,III with various B.Cs with a cross-section shape (1-1-1) for $L/h = 10$, $\Delta T = 0$, $k = 1$, $K_w = K_p = 0$

Model II

B.Cs	β	$\alpha = 0$	$\alpha = 0.05$	$\alpha = 0.1$	$\alpha = 0.15$	$\alpha = 0.2$
S-S	0	1.0068	1.0309	1.1031	1.2235	1.3920
	0.05	0.9832	1.0068	1.0776	1.1956	1.3608
	0.1	0.9180	0.9402	1.0068	1.1178	1.2733
	0.15	0.8260	0.8461	0.9064	1.0068	1.1475
	0.2	0.7240	0.7417	0.7947	0.8831	1.0068
C-S	0	0.4030	0.4088	0.4264	0.4556	0.4965
	0.05	0.3284	0.3337	0.3486	0.3739	0.4072
	0.1	0.2438	0.2478	0.2600	0.2798	0.3078
	0.15	0.1777	0.1808	0.1899	0.2053	0.2264
	0.2	0.1305	0.1329	0.1397	0.1512	0.1673
C-C	0	0.2043	0.2043	0.2043	0.2043	0.2043
	0.05	0.1450	0.1450	0.1450	0.1450	0.1450
	0.1	0.0914	0.0914	0.0914	0.0914	0.0914
	0.15	0.0584	0.0584	0.0584	0.0584	0.0584
	0.2	0.0391	0.0391	0.0391	0.0391	0.0391

Model III

B.Cs	β	$\alpha = 0$	$\alpha = 0.05$	$\alpha = 0.1$	$\alpha = 0.15$	$\alpha = 0.2$
S-S	0	1.0214	1.0458	1.1192	1.2413	1.4124
	0.05	0.9975	1.0214	1.0933	1.2131	1.3807
	0.1	0.9313	0.9538	1.0214	1.1341	1.2918
	0.15	0.8379	0.8583	0.9195	1.0214	1.1641
	0.2	0.7345	0.7524	0.8062	0.8959	1.0214
C-S	0	0.4060	0.4119	0.4297	0.4594	0.5009
	0.05	0.3305	0.3356	0.3510	0.3767	0.4125
	0.1	0.2450	0.2491	0.2612	0.2815	0.3098
	0.15	0.1783	0.1814	0.1907	0.2060	0.2276
	0.2	0.1308	0.1332	0.1401	0.1517	0.1679
C-C	0	0.2044	0.2044	0.2044	0.2044	0.2044
	0.05	0.1448	0.1448	0.1448	0.1448	0.1448
	0.1	0.0908	0.0908	0.0908	0.0908	0.0908
	0.15	0.0578	0.0578	0.0578	0.0578	0.0578
	0.2	0.0386	0.0386	0.0386	0.0386	0.0386

Figs.(4.24 and 4.25) examine dimensionless nonlocal parameter ($\alpha = ea/L$) and dimensionless material length scale parameter ($\beta = l_m/L$) of sandwich FG microbeam with a certain $\Delta T = 0$, $L/h = 10$, and $K_w = K_p = 0$ on the dimensionless transverse deflection for Modal II (1-2-1) and Modal III (1-2-1) for various B.Cs (i.e. S-S, C-S, C-C) and different gradient index (i.e. $k = 0, 1, 3, 5, 10$) respectively. It can be observed from Fig.(4.24) the influence of the dimensionless nonlocal parameter ($\alpha = ea/L$) on the dimensionless transverse deflection (\bar{w}) of sandwich FG micro-beam with certain the dimensionless material length scale parameter ($\beta = l_m/L = 0.2$). It is explicit that when the dimensionless nonlocal parameter ($\alpha = ea/L$) increase the dimensionless transverse deflection increase for both S-S and C-S boundary conditions because the sandwich FG micro-beam become more flexible with increase dimensionless nonlocal parameter (nonlocal elasticity theory). On the other hand for C-C boundary condition the dimensionless transverse deflection remain without change with increase the dimensionless nonlocal parameter.

Fig.(4.25) depicts the effect of dimensionless material length scale parameter ($\beta = l_m/L$) on the dimensionless transverse deflection of sandwich FG micro-beam with certain the dimensionless nonlocal parameter ($\alpha = ea/L = 0.2$). It can be noticed that the dimensionless transverse deflection decrease with increase the dimensionless material length scale parameter (β) for various gradient index (k) and different boundary conditions because the sandwich FG micro-beam become more stiffer with increase dimensionless material length scale parameter (pure strain gradient theory).

From Fig.(4.26) it can be shows the three dimension plot of dimensionless transverse deflection of simply supported sandwich FG micro-beams with Model II, III for (1-1-1) cross section shape with the change of the dimensionless material length scale parameter ($\beta = l_m/L$) and the dimensionless nonlocal parameter ($\alpha = ea/L$).

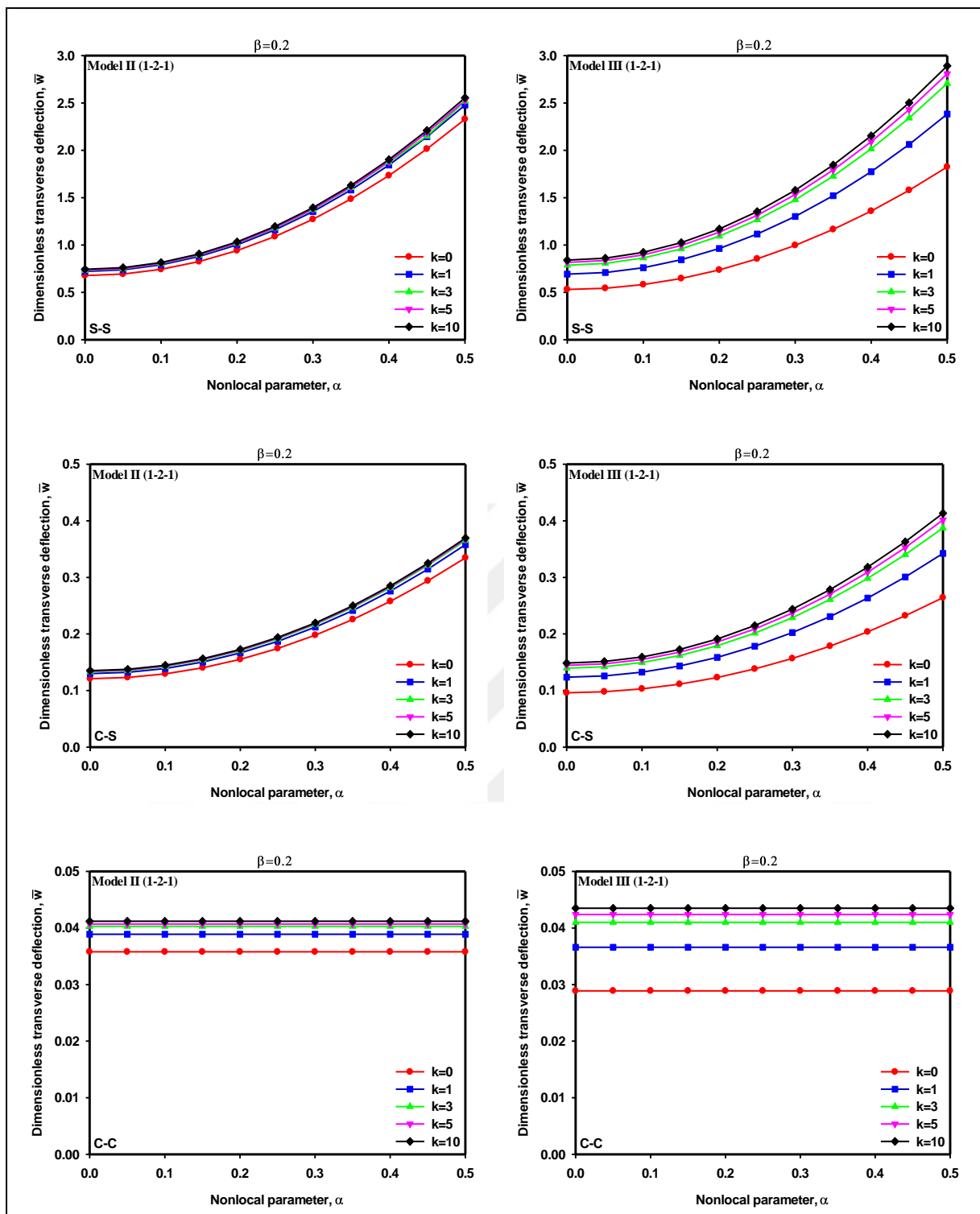


Figure 4.24 Effect of the nonlocal parameter (α) on the dimensionless transverse deflection \bar{w} of sandwich FG microbeam with a various boundary conditions (S-S, C-S, C-C) for different power law index (k) with $L/h = 10$, $K_p = K_w = 0$, $\Delta T = 0$, $\beta = 0.2$ and cross section shape (1-2-1).

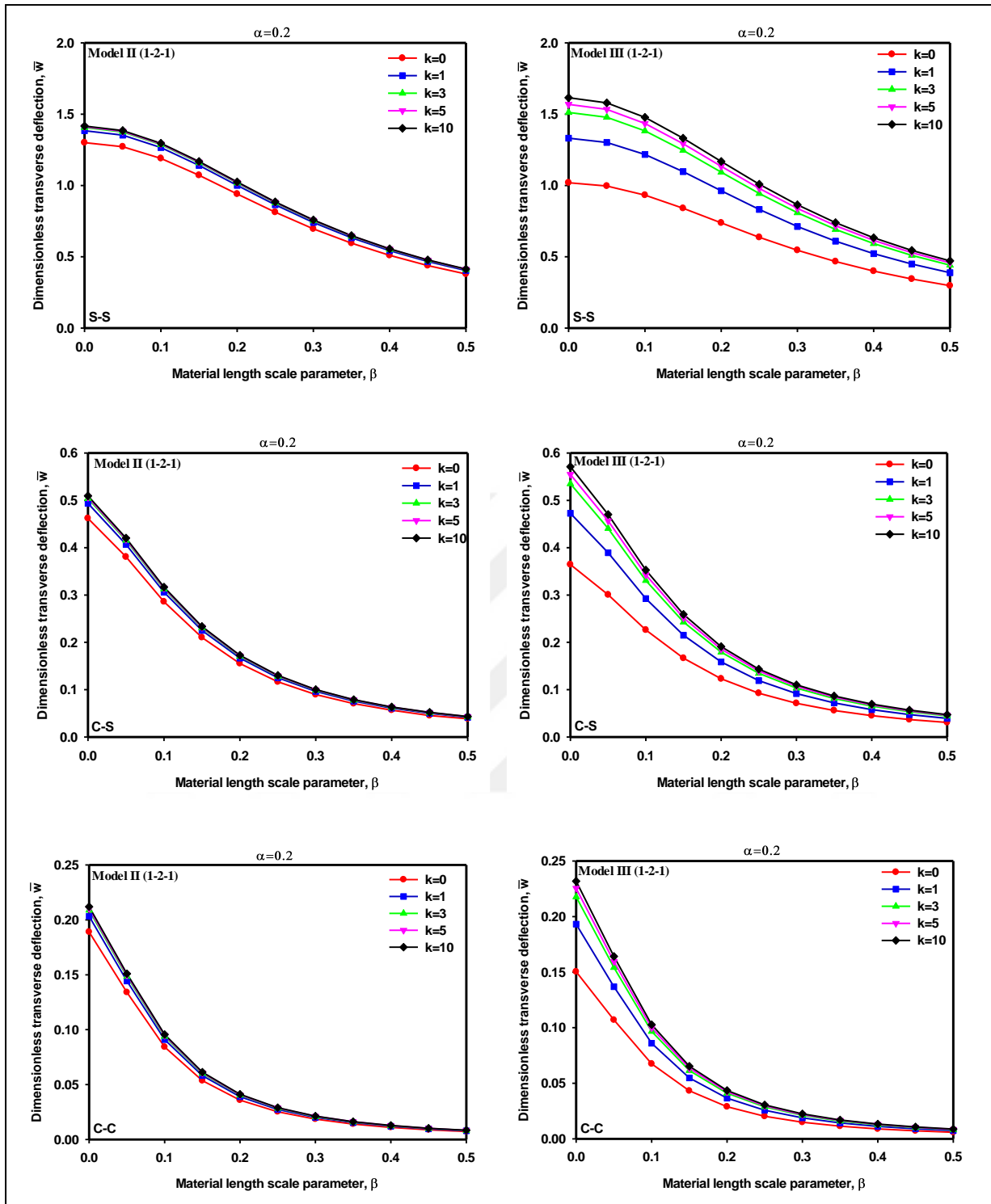


Figure 4.25 Effect of the material length scale parameter (β) on the dimensionless transverse deflection \bar{w} of sandwich FG microbeam with a various boundary conditions (S-S, C-S, C-C) for different power law index (k) with $L/h = 10, K_p = K_w = 0, \Delta T = 0, \alpha = 0.2$ and cross section shape (1-2-1).

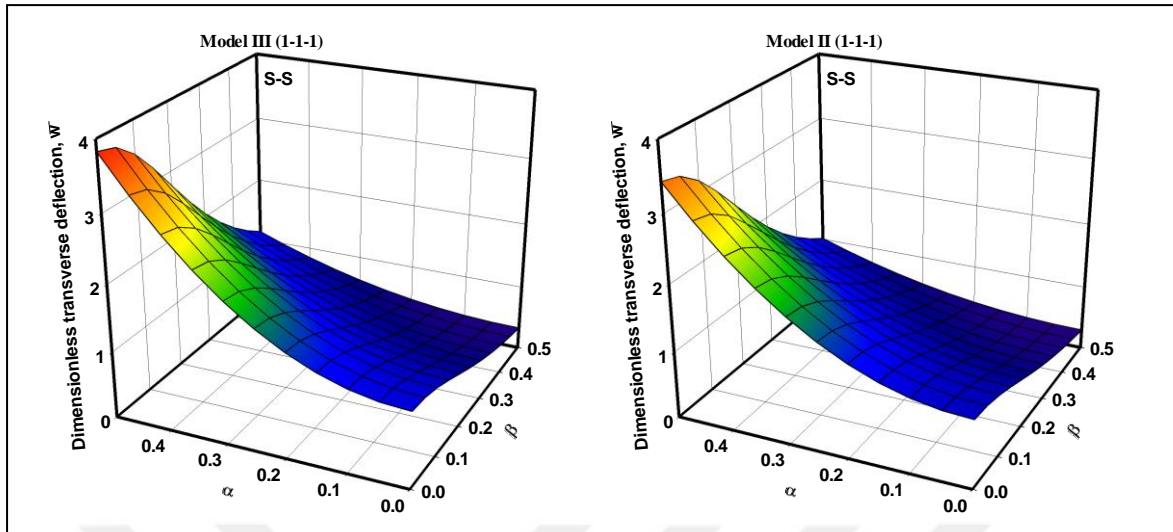


Figure 4.26 Effect of the nonlocal parameter (α) and the dimensionless material length scale parameter on the dimensionless transverse deflection \bar{w} of sandwich FG microbeam with a cross section shape (1-1-1) and S-S boundary conditions for $k = 2$, $L/h = 10$, $K_w = K_p = 0$ and $\Delta T = 0$.

Table 4.11 present thermal effect on the dimensionless transverse deflection (\bar{w}) for various boundary conditions (i.e. S-S, C-S, C-C) with different (symmetrical and un-symmetrical) cross section shapes of size dependent sandwich Model II, III FG micro-beam at certain dimensionless nonlocal and material length scale parameters ($\beta = 0.2$, $\alpha = 0.1$) without elastic foundations $K_w = K_p = 0$ and $k = 1$ with various values of temperature change ($\Delta T = 0, 20, 40, 80$). The dimensionless transverse deflection increase when the temperature change increase from 0 to 20,40 and 80. This is due to when the temperature change ΔT increase make the sandwich FG microbeam stiffness decrease, lead to increase dimensionless transverse deflection for all cross section shapes and various boundary conditions.

Figs.(4.27) depicts also the effect of temperature change (ΔT) on the dimensionless transverse deflection as a function of the various power law index (k) with fixed aspect ratio $L/h = 10$, $\alpha = 0.1$, $\beta = 0.2$, Model III with cross section shape (1-2-1) and various boundary conditions (i.e. S-S, C-S, C-C) for sandwich FG micro-beam. For given value of a gradient index (k), the dimensionless transverse deflection increase with increase the

temperature change (ΔT) due to with larger thermal effect (temperature change) make sandwich FG microbeam with less stiffness and it is explicit that the temperature change is more significant for S-S boundary condition and insensitive to thermal effect for C-C boundary condition. It can be noticed also when the gradient index is less than 1 the thermal effect is slight on the dimensionless transverse deflection, while become more pronounced when ($k \geq 1$).

Table 4.11 Dimensionless transverse deflection ($\bar{w} = 100 w E_m I / q_0 L^4$) of sandwich FG microbeams (PSDBT) with $k = 1$, $L/h = 10$, $\beta = 0.2$, $\alpha = 0.1$ and $K_w = K_p = 0$

B.Cs		Model	ΔT	Symmetrical cross section				Un-symmetrical cross section		
				1-1-1	1-2-1	1-8-1	2-1-2	1-2-3	2-3-1	3-1-2
S-S Boundary Condition	Model II	0	0.7947	0.7903	0.7793	0.7971	0.7624	0.8023	0.8011	
		20	0.8595	0.8556	0.8450	0.8612	0.8164	0.8727	0.8686	
		40	0.9332	0.9299	0.9194	0.9343	0.8746	0.9548	0.9475	
		80	1.1300	1.1291	1.1208	1.1283	1.0254	1.1787	1.1595	
	Model III	0	0.8062	0.7602	0.6580	0.8365	0.7863	0.7547	0.8389	
		20	0.8698	0.8124	0.6914	0.9091	0.8466	0.8061	0.9129	
		40	0.9383	0.8671	0.7248	0.9891	0.9115	0.8600	0.9949	
		80	1.1219	1.0089	0.8066	1.2097	1.0838	0.9993	1.2220	
C-S Boundary Condition	Model II	0	0.1397	0.1390	0.1373	0.1401	0.1332	0.1418	0.1417	
		20	0.1429	0.1422	0.1405	0.1432	0.1358	0.1452	0.1451	
		40	0.1462	0.1456	0.1438	0.1465	0.1385	0.1488	0.1485	
		80	0.1533	0.1527	0.1511	0.1536	0.1444	0.1567	0.1561	
	Model III	0	0.1401	0.1324	0.1155	0.1453	0.1370	0.1315	0.1458	
		20	0.1432	0.1349	0.1172	0.1487	0.1399	0.1340	0.1493	
		40	0.1463	0.1376	0.1189	0.1523	0.1430	0.1366	0.1530	
		80	0.1463	0.1376	0.1189	0.1523	0.1430	0.1366	0.1530	
C-C Boundary Condition	Model II	0	0.0391	0.0389	0.0385	0.0392	0.0369	0.0399	0.0399	
		20	0.0394	0.0392	0.0388	0.0395	0.0372	0.0402	0.0402	
		40	0.0397	0.0395	0.0391	0.0398	0.0374	0.0406	0.0406	
		80	0.0403	0.0402	0.0397	0.0404	0.0380	0.0413	0.0413	
	Model III	0	0.0386	0.0366	0.0322	0.0400	0.0379	0.0364	0.0402	
		20	0.0389	0.0368	0.0324	0.0404	0.0382	0.0366	0.0405	
		40	0.0392	0.0371	0.0325	0.0407	0.0385	0.0369	0.0409	
		80	0.0398	0.0376	0.0329	0.0414	0.0390	0.0374	0.0416	

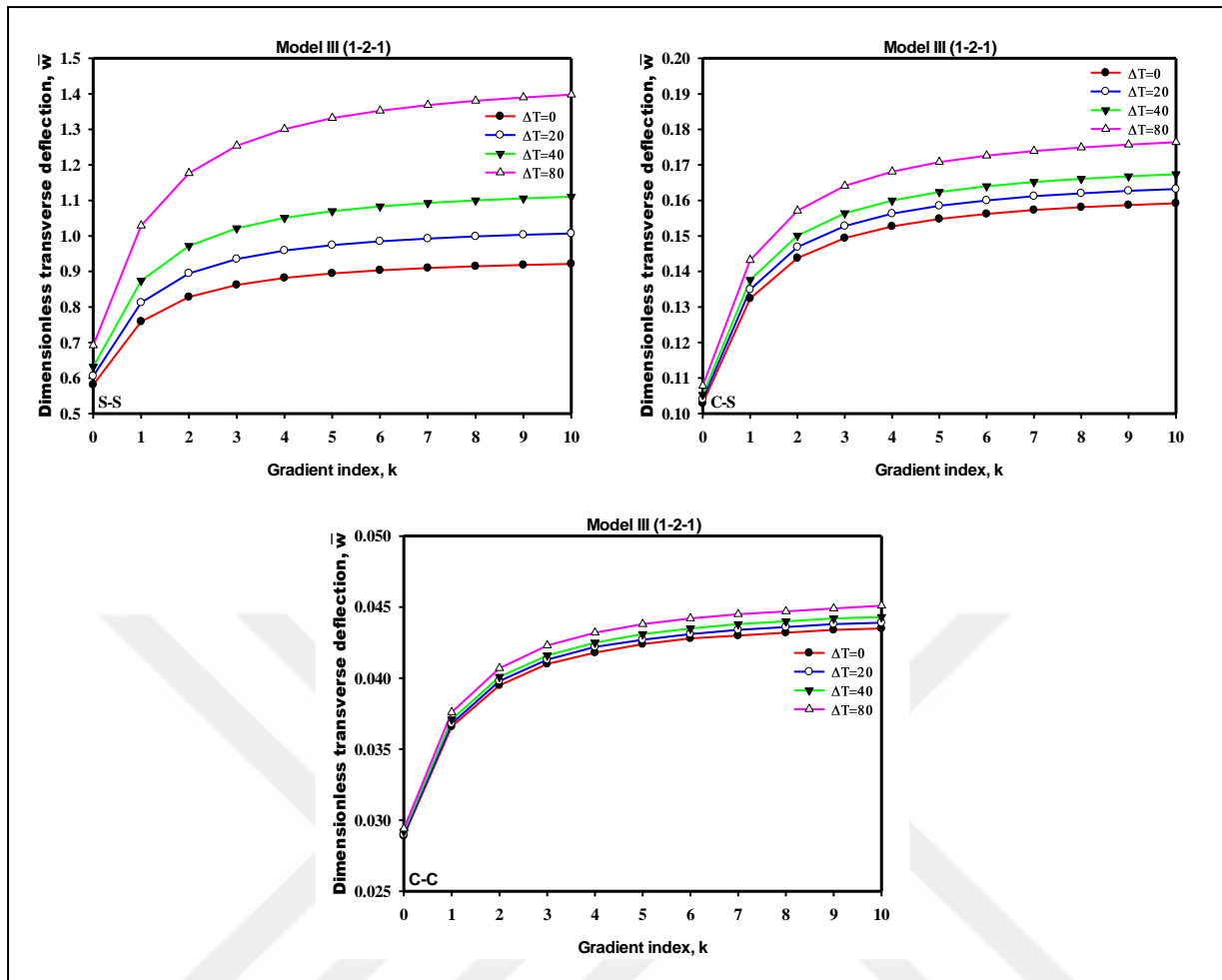


Figure 4.27 Thermal effect on the dimensionless transverse deflection, (\bar{w}) with $L/h = 10$, $K_W = K_P = 0$, $\alpha = 0.1$, $\beta = 0.2$, and cross section shape (1-2-1) sandwich FG micro-beam Model III.

In table 4.12, the effect of the dimensionless elastic foundation parameters on the dimensionless transverse deflection of size dependent sandwich FG micro-beam are given for different value of aspect ratio (L/h) , various cross section shapes, dimensionless Winkler and Pasternak parameters constant $(K_P = K_W = 0, 0.2)$ and different boundary conditions for Models II, III. It can be observed that when \bar{K}_P and \bar{K}_W increase from 0 to 0.2 the dimensionless transverse deflection of sandwich FG microbeam with Models II, III decrease for all cross-section shapes and consider models. This is due to the fact that the sandwich FG microbeam becomes more stiffer when both K_W and K_P increase. It can be seen from this table when $K_W = K_P = 0$ with $L/h = 10$ and cross section shape (1-2-1) for Model III with S-S boundary condition, the value of dimensionless transverse deflection is 0.8904

and decrease to 0.3304 when $K_w = 0.2$ and $K_p = 0$, finally the dimensionless transverse deflection increase more when $K_w = K_p = 0.2$. As well as according to this results, it can be seen that the boundary condition with C-C sandwich FG microbeam has largest value than other boundary conditions S-S and C-S of dimensionless transverse deflection. Another results from these figures is that the effect of the Pasternak shear modulus (\bar{K}_p) on the dimensionless transverse deflection is more significant than that of the Winkler elastic modulus (\bar{K}_w).

Figs.(4.28) shows of the dimensionless elastic foundations parameters on the dimensionless transverse deflection of size dependent sandwich FG micro-beam for various value of power law index ($k = 0, 1, 3, 5$) with fixed the aspect ratio ($L/h = 10$), $\alpha = 0.1, \beta = 0.2$, Model III with cross section shape (1-1-1) and various boundary conditions (i.e. S-S, C-S, C-C). The left side of figure is for various (K_p) with constant ($K_w = 0$) and the right side for various (K_w) with constant ($K_p = 0$). It can be noticed from Fig. (4.28) the dimensionless transverse deflection decrease with increase the dimensionless Winkler and Pasternak shear parameters. It is observed that for S-S boundary conditions the dimensionless transverse deflection is decrease rapidly with increase (K_w) and (K_p) when ($K_w \leq 0.5$) and ($K_p \leq 0.05$).

Table 4.12 Dimensionless transverse deflection $\bar{w} = 100 w E_m I / q_0 L^4$ of sandwich FG microbeams for $\Delta T = 0$, $\beta = 0.2$, $\alpha = 0.1$, and $k = 2$, with different cross section, aspect ratio, various B.Cs and elastic foundations.

B.Cs			Cross-section shape	Model II				Model III			
				$L/h = 5$	$L/h = 10$	$L/h = 20$	$L/h = 50$	$L/h = 5$	$L/h = 10$	$L/h = 20$	$L/h = 50$
S-S Boundary Condition	0	0	1-1-1	0.8525	0.7977	0.7841	0.7803	0.9358	0.8904	0.8790	0.8759
			1-8-1	0.8647	0.8067	0.7923	0.7883	0.7267	0.6847	0.6743	0.6713
			2-1-2	0.8512	0.7977	0.7844	0.7807	0.9761	0.9286	0.9167	0.9134
	0	0.2	1-1-1	0.6056	0.3167	0.1118	0.0193	0.6469	0.3304	0.1134	0.0193
			1-8-1	0.6117	0.3180	0.1119	0.0193	0.5394	0.2973	0.1094	0.0194
			2-1-2	0.6050	0.3167	0.1118	0.0193	0.6659	0.3355	0.1140	0.0192
	0.2	0.2	1-1-1	0.1562	0.0450	0.0116	0.0018	0.1590	0.0453	0.0116	0.0018
			1-8-1	0.1565	0.0450	0.0116	0.0018	0.1516	0.0446	0.0116	0.0018
			2-1-2	0.1562	0.0450	0.0116	0.0018	0.1601	0.0453	0.0116	0.0018
C-S Boundary Condition	0	0	1-1-1	0.1827	0.1411	0.1304	0.1273	0.1892	0.1543	0.1454	0.1428
			1-8-1	0.1872	0.1432	0.1319	0.1287	0.1523	0.1201	0.1119	0.1095
			2-1-2	0.1816	0.1408	0.1304	0.1274	0.1975	0.1609	0.1516	0.1489
	0	0.2	1-1-1	0.1664	0.1079	0.0607	0.0158	0.1717	0.1154	0.0638	0.0160
			1-8-1	0.1701	0.1091	0.0611	0.0158	0.1407	0.0951	0.0564	0.0155
			2-1-2	0.1654	0.1077	0.0607	0.0158	0.1784	0.1190	0.0649	0.0160
	0.2	0.2	1-1-1	0.0774	0.0268	0.0079	0.0014	0.0814	0.0288	0.0086	0.0015
			1-8-1	0.0783	0.0269	0.0080	0.0014	0.0738	0.0273	0.0084	0.0015
			2-1-2	0.0771	0.0268	0.0079	0.0014	0.0829	0.0291	0.0086	0.0015
C-C Boundary Condition	0	0	1-1-1	0.0614	0.0396	0.0339	0.0323	0.0607	0.0423	0.0375	0.0361
			1-8-1	0.0634	0.0404	0.0344	0.0326	0.0504	0.0334	0.0290	0.0277
			2-1-2	0.0608	0.0395	0.0339	0.0323	0.0634	0.0441	0.0391	0.0377
	0	0.2	1-1-1	0.0595	0.0366	0.0264	0.0119	0.0588	0.0384	0.0285	0.0123
			1-8-1	0.0614	0.0372	0.0266	0.0119	0.0491	0.0312	0.0233	0.0112
			2-1-2	0.0589	0.0364	0.0264	0.0119	0.0613	0.0404	0.0294	0.0125
	0.2	0.2	1-1-1	0.0389	0.0155	0.0053	0.0010	0.0384	0.0158	0.0054	0.0010
			1-8-1	0.0397	0.0156	0.0053	0.0010	0.0340	0.0144	0.0051	0.0010
			2-1-2	0.0386	0.0154	0.0053	0.0010	0.0395	0.0160	0.0054	0.0010

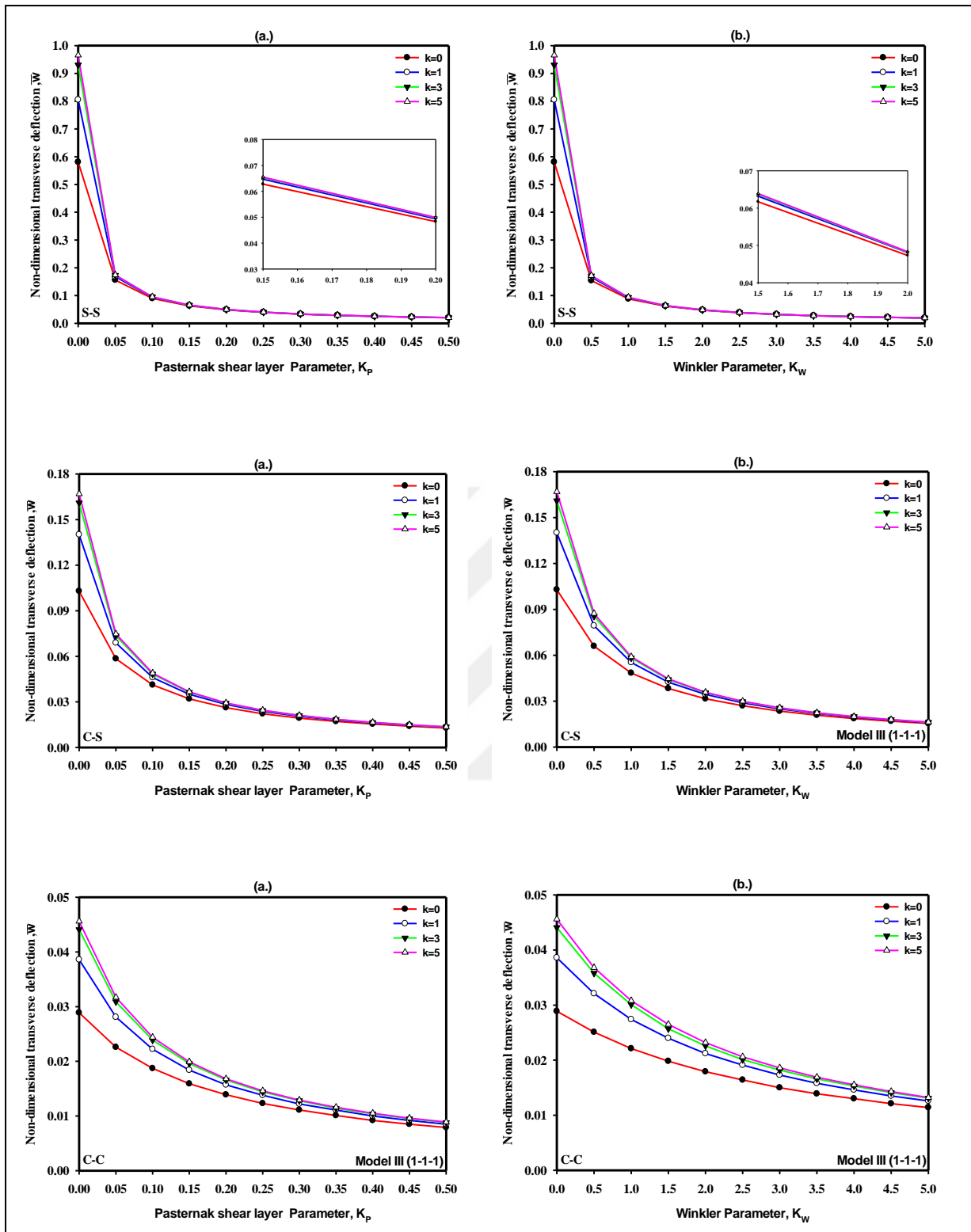


Figure 4.28 Effect of the Winkler and Pasternak shear parameter on the dimensionless transverse deflection, (\bar{w}) for $L/h = 10$, and $\alpha = 1, \beta = 2$ of SS sandwich microbeam for Model III (1-1-1). (a) $K_w = 0$ (b) $K_p = 0$ with various boundary conditions.

In the second aspect of this part of the present thesis is the buckling and free vibration analysis of small scale sandwich FG micro-beam. Tables 4.13 and 4.14 contain the effect of the various beam theories on the dimensionless fundamental frequency and critical buckling load of sandwich FG micro-beam for various boundary conditions (i.e. S-S, C-S, C-C) with different values of the dimensionless material length scale parameter ($\beta = 0.1, 0.2, 0.3$), aspect ratio ($L/h = 10, 20$), Models II and Model III and cross-section types (1-1-1) with certain dimensionless nonlocal parameter ($\alpha = 0.1$) without the elastic foundation ($K_w = K_p = 0$) and no temperature change ($\Delta T = 0$). It can be observed from tables 4.13 and 4.14 the dimensionless fundamental frequency and buckling load with the higher order beam theories (HOBTs) are less than these in Euler theory (EBBT) and greater than these for Timoshenko beam theory (TBT). Also as expected the Euler Bernoulli beam theory is more stiffer than the other theories because neglect the shear deformation effect and the Timoshenko beam theory is most flexible with constant shear $5/6$. It can be explicit also the effect of shear deformation is decrease with increase the aspect ratio from 10 to 20 then the dimensionless fundamental frequency and critical buckling load is close each to other for all beam theory for aspect ratio 20 than aspect ratio 10. Moreover, the results for higher order deformation beam theories are almost the same and for ASDBT and ESDBT theory the dimensionless fundamental frequency and critical buckling load are the same. Also the sandwich FG microbeam become more stiffer with C-C boundary condition, it can be seen for example with PSDBT, C-C B.Cs, Model III and ($\beta = 0.1, L/h = 10$) the dimensionless natural frequency and critical buckling load is $\bar{\omega} = 12.5915$, $\bar{P} = 66.6820$ whereas for C-S is $\bar{\omega} = 6.7038$, $\bar{P} = 27.3493$ and for S-S is $\bar{\omega} = 3.9494$, $\bar{P} = 12.5753$.

Table 4.13 Dimensionless natural frequency $\bar{\omega} = \omega L^2/h \sqrt{\rho_m/E_m}$ of sandwich micro-beams

with various B.Cs with a cross-section shape (1-1-1) for $\Delta T = 0$, $k = 1$, $K_w = K_p = 0$.

B.Cs	Beam theory	Model II						Model III					
		$L/h = 10$			$L/h = 20$			$L/h = 10$			$L/h = 20$		
		$\beta = 0.1$	$\beta = 0.2$	$\beta = 0.3$	$\beta = 0.1$	$\beta = 0.2$	$\beta = 0.3$	$\beta = 0.1$	$\beta = 0.2$	$\beta = 0.3$	$\beta = 0.1$	$\beta = 0.2$	$\beta = 0.3$
S-S Boundary Condition	EBBT	3.7873	4.2735	4.9053	3.7951	4.4722	4.9615	3.9848	4.4939	5.2283	3.9999	4.5108	5.2489
	FSDBT	3.7400	4.2140	4.9040	3.7877	4.2679	4.9656	3.9426	4.4462	5.1734	3.9891	4.4985	5.2343
	PSDBT	3.7413	4.2154	4.9044	3.7880	4.2680	4.9659	3.9494	4.4498	5.1769	3.9934	4.4995	5.2352
	TSDBT	3.7414	4.2155	4.9044	3.7881	4.2680	4.9659	3.9495	4.4500	5.1771	3.9935	4.4995	5.2352
	ASDBT	3.7416	4.2157	4.9048	3.7881	4.2681	4.9660	3.9498	4.4503	5.1774	3.9935	4.4996	5.2352
	ESDBT	3.7416	4.2157	4.9048	3.7881	4.2681	4.9660	3.9498	4.4503	5.1774	3.9935	4.4996	5.2352
	HSDBT	3.7413	4.2154	4.9043	3.7880	4.2680	4.9659	3.9494	4.4498	5.1769	3.9934	4.4995	5.2352
C-S Boundary Condition	EBBT	6.7854	9.1325	12.2935	6.9905	9.5030	12.7971	6.7215	9.0684	13.0265	6.8902	9.3499	13.5116
	FSDBT	6.7677	9.1241	12.2592	6.9869	9.5018	12.7959	6.6989	9.0486	13.0085	6.8885	9.3481	13.5101
	PSDBT	6.7680	9.1256	12.2614	6.9873	9.5021	12.7963	6.7023	9.0539	13.0185	6.8896	9.3492	13.5121
	TSDBT	6.7680	9.1256	12.2635	6.9873	9.5021	12.7970	6.7038	9.0563	13.0214	6.8900	9.3499	13.5129
	ASDBT	6.7687	9.1269	12.2674	6.9875	9.5024	12.7980	6.7057	9.0595	13.0257	6.8906	9.3508	13.5141
	ESDBT	6.7687	9.1269	12.2674	6.9875	9.5024	12.7980	6.7057	9.0595	13.0257	6.8906	9.3508	13.5141
	HSDBT	6.7680	9.1256	12.2613	6.9873	9.5021	12.7964	6.7022	9.0537	13.0183	6.8896	9.3492	13.5129
C-C Boundary Condition	EBBT	11.8725	18.1624	25.2358	12.6024	19.5567	27.3984	12.6958	19.3758	26.9939	13.3157	20.7012	28.9954
	FSDBT	11.7336	18.0302	25.0750	12.5762	19.5392	27.3785	12.4588	19.1802	26.6978	13.2879	20.6664	28.9578
	PSDBT	11.8097	18.0899	25.1747	12.5849	19.5487	27.3844	12.5865	19.3303	26.9337	13.3049	20.6854	28.9893
	TSDBT	11.8138	18.0989	25.1894	12.5859	19.5509	27.3881	12.5915	19.3408	26.9505	13.3062	20.6882	29.9939
	ASDBT	11.8206	18.1130	25.2117	12.5877	19.5547	27.3941	12.5985	19.3552	26.9732	13.3081	20.6922	29.0002
	ESDBT	11.8206	18.1130	25.2117	12.5877	19.5547	27.3941	12.5985	19.3552	26.9732	13.3081	20.6922	29.0002
	HSDBT	11.8095	18.0893	25.1738	12.5849	19.5485	27.3842	12.5862	19.3295	26.9325	13.3048	20.6852	28.9890

Table 4.14 Dimensionless critical buckling load $\bar{P} = PL^2/(E_m I)$ of sandwich micro-beams with various B.Cs with a cross-section shape (1-1-1) for $\Delta T = 0$, $k = 1$, $K_w = K_p = 0$.

B.Cs		Model II						Model III					
		$L/h = 10$			$L/h = 20$			$L/h = 10$			$L/h = 20$		
		$\beta = 0.1$	$\beta = 0.2$	$\beta = 0.3$	$\beta = 0.1$	$\beta = 0.2$	$\beta = 0.3$	$\beta = 0.1$	$\beta = 0.2$	$\beta = 0.3$	$\beta = 0.1$	$\beta = 0.2$	$\beta = 0.3$
S-S Boundary Condition	Beam theory												
	EBBT	13.0412	16.5860	22.4544	13.0404	16.5825	22.4337	12.8058	16.2859	22.0486	12.8058	16.2859	22.0486
	FSDBT	12.7492	16.1878	21.9151	12.9829	16.4835	22.3154	12.5306	15.9360	21.5742	12.7359	16.1971	21.9276
	PSDBT	12.7552	16.1926	21.9174	12.9853	16.4847	22.3160	12.5743	15.9630	21.6054	12.7542	16.2040	21.9357
	TSDBT	12.7558	16.1933	21.9185	12.9855	16.4849	22.3163	12.5753	15.9642	21.6071	12.7544	16.2043	21.9361
	ASDBT	12.7573	16.1953	21.9212	12.9859	16.4854	22.3170	12.5770	15.9664	21.6099	12.7548	16.2048	21.9368
	ESDBT	12.7573	16.1953	21.9212	12.9859	16.4854	22.3170	12.5770	15.9664	21.6099	12.7548	16.2048	21.9368
HSDBT	12.7552	16.1926	21.9174	12.9853	16.4847	22.3160	12.5743	15.9629	21.6054	12.7541	16.2040	21.9356	
C-S Boundary Condition	EBBT	30.1968	53.0568	91.5864	31.5898	56.2687	97.2103	27.3403	48.1848	90.8051	28.4095	50.3902	95.7856
	FSDBT	30.1705	53.0206	91.2710	31.5858	56.2594	97.1310	27.3308	48.1712	90.7924	28.3921	50.3624	95.6958
	PSDBT	30.1771	53.0295	91.2970	31.5866	56.2609	97.1368	27.3403	48.1848	90.8051	28.3968	50.3756	95.7084
	TSDBT	30.1750	53.0253	91.2939	31.5860	56.2599	97.1320	27.3496	48.2040	90.8311	28.3967	50.3809	95.7158
	ASDBT	30.1787	53.0328	91.3339	31.5870	56.2622	97.1436	27.3621	48.2300	90.8728	28.4001	50.3880	95.7275
	ESDBT	30.1787	53.0328	91.3339	31.5870	56.2622	97.1436	27.3621	48.2300	90.8728	28.4001	50.3880	95.7275
	HSDBT	30.1777	53.0309	91.2913	31.5866	56.2610	97.1364	27.3397	48.1836	90.8041	28.3941	50.3752	95.7080
C-C Boundary Condition	EBBT	66.7958	153.587	296.654	73.4120	172.213	335.768	66.6998	155.021	299.254	72.5624	170.235	332.256
	FSDBT	65.9797	152.653	294.554	73.2783	172.015	335.468	66.6427	152.287	294.242	71.7245	169.664	331.019
	PSDBT	66.5526	152.859	295.109	73.3847	172.057	335.574	66.6820	153.775	297.463	72.4624	170.105	331.972
	TSDBT	66.5723	152.922	295.530	73.3899	172.074	335.611	66.7115	153.864	297.659	72.4706	170.130	332.027
	ASDBT	66.6180	153.056	295.548	73.4029	172.112	335.696	66.7598	154.005	297.965	72.4843	170.170	332.115
	ESDBT	66.6180	153.056	295.548	73.4029	172.112	335.696	66.7598	154.005	297.965	72.4843	170.170	332.115
	HSDBT	66.5520	152.857	295.103	73.3846	172.057	335.573	66.6802	153.770	297.450	72.4619	170.103	331.968

Figs.(4.29 and 4.30) show the variation of the dimensionless buckling load and fundamental frequency for different boundary conditions (i.e. S-S, C-S, C-C) with respect to gradient index (k) of sandwich FG micro-beam with different cross section shapes (1-1-1, 1-2-1, 1-8-1, 2-1-2) at certain dimensionless nonlocal parameter ($\alpha = 0.1$), dimensionless material length scale parameter ($\beta = 0.2$) without elastic foundation ($K_w = K_p = 0$), no temperature change ($\Delta T = 0$) and aspect ratio ($L/h = 10$). It is explicit that dimensionless buckling load and fundamental frequency will be decrease with increase material property gradient index (k) for all cross section shapes with both Model II and Model III. It can seen also from this figures the sandwich FG microbeam with shape (1-8-1) and (2-1-2) represented maximum and minimum values of dimensionless critical buckling load and natural frequency respectively for Model III. In addition the dimensionless buckling load and fundamental frequency for Model II, it can be seen when the gradient index is less than 1.53 for example simply support boundary condition, the $(\bar{P}, \bar{\omega})$ of (1-8-1) is greater than $(\bar{P}, \bar{\omega})$ for (2-1-2). Moreover when the gradient index is greater than 1.53 the dimensionless of $(\bar{P}, \bar{\omega})$ for (1-8-1) is less than the other cross section shapes and the results for (2-1-2) is greater than the other cross section shapes. This is due to the ceramic portion for (1-8-1) with increase gradient index (k) is lower than for (2-1-2) then the sandwich FG microbeam become more flexible with (1-8-1) than (2-1-2) for (k) greater than 1.53.

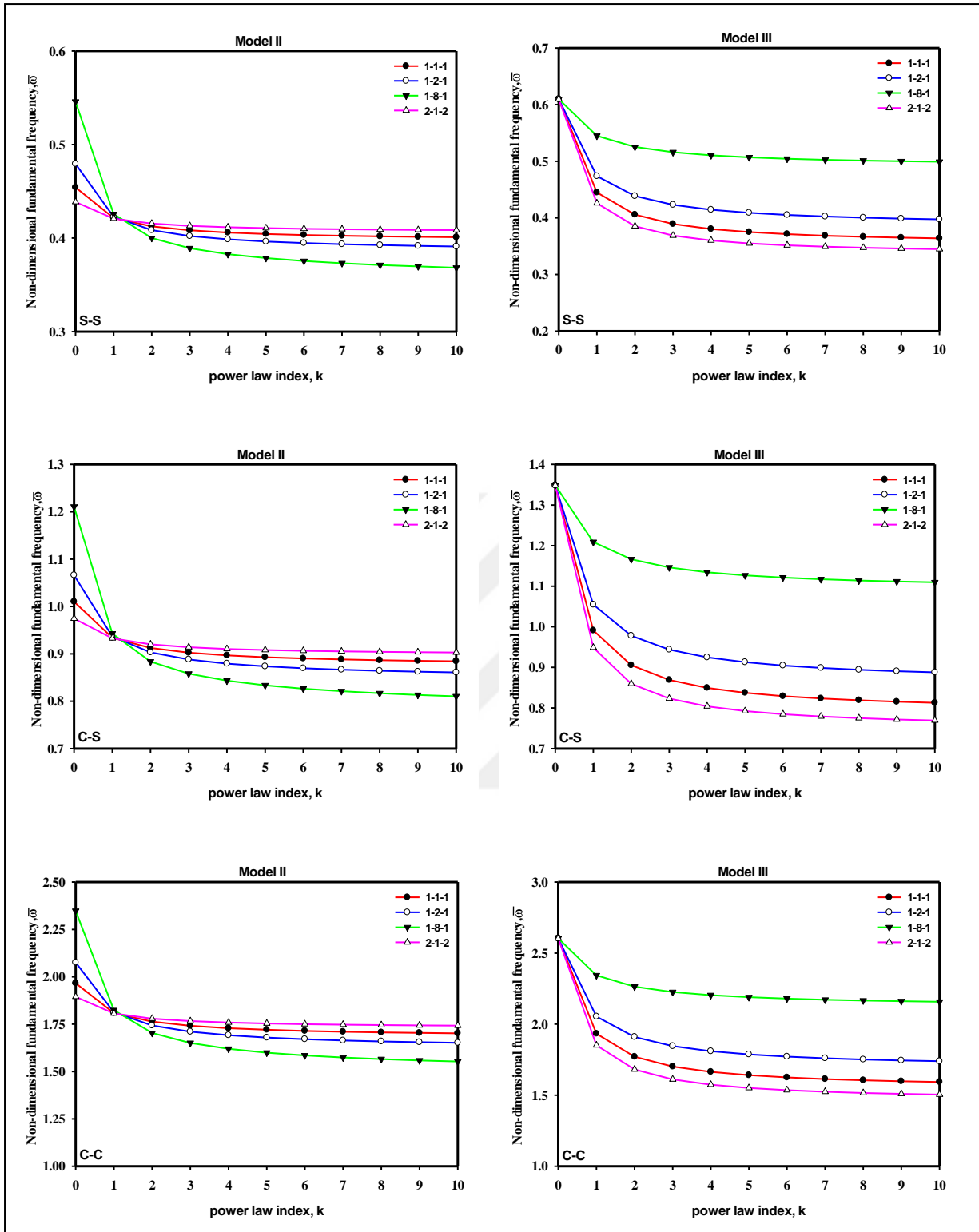


Figure 4.29 Variation of the dimensionless fundamental frequency ($\bar{\omega}$) with the power-law exponent k for different cross-section shape sandwich FG microbeam, $L / h = 10$, $\alpha = 0.1$, $\beta = 0.2$ and for different boundary conditions.

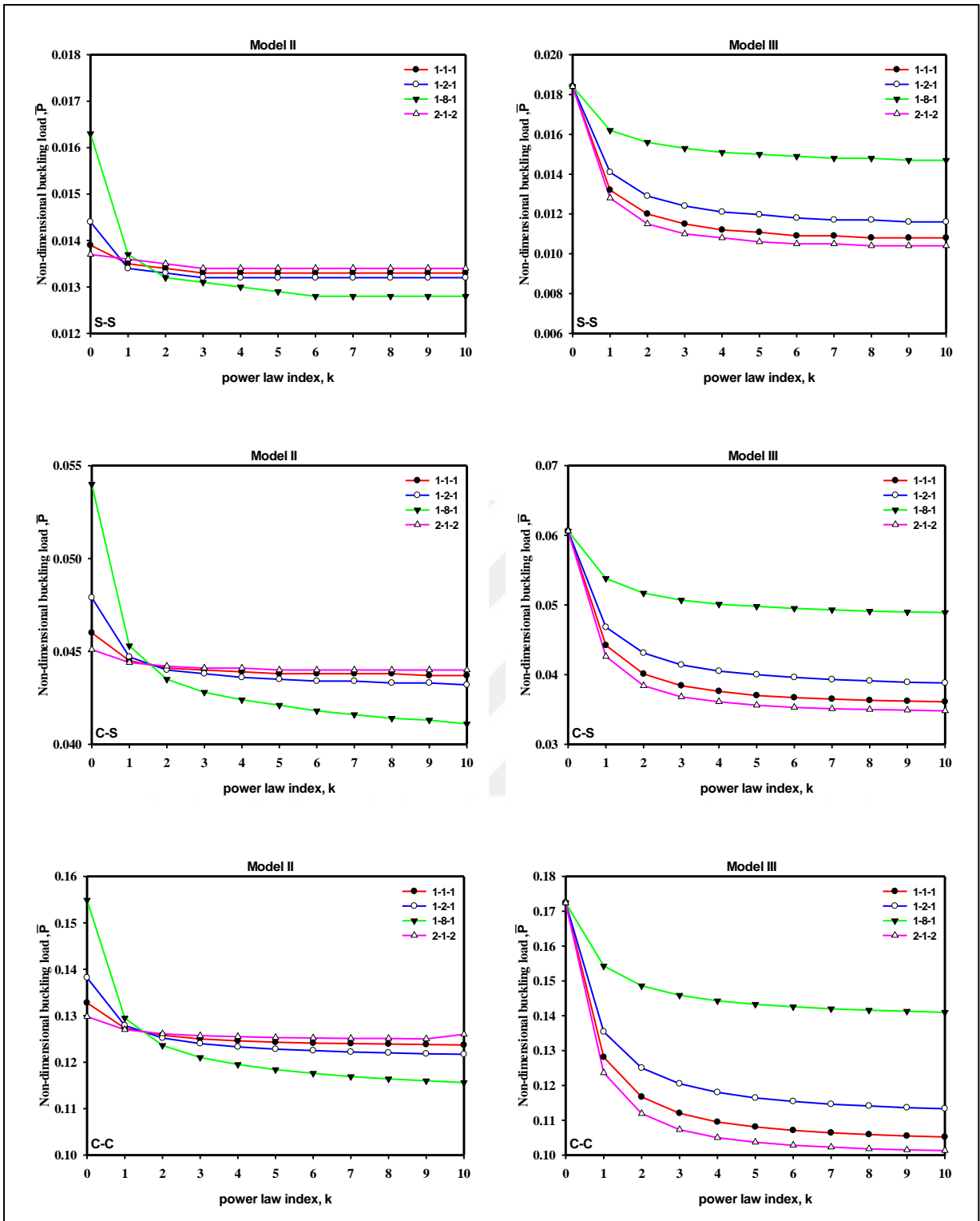


Figure 4.30 Variation of the dimensionless buckling load (\bar{P}) with the power-law exponent k for different cross-section shape sandwich FG microbeam, $L/h = 10$, $\alpha = 0.1$, $\beta = 0.2$, and for different boundary conditions.

Tables (4.15), and (4.16) show the influence of power law index (k) on the dimensionless critical buckling load (\bar{P}) and fundamental frequency ($\bar{\omega}$) of size dependent sandwich FG micro-beam with various cross section shapes (symmetrical and un-symmetrical) and different boundary conditions (i.e. S-S, C-S, C-C) at certain aspect ratio $L/h = 10$, dimensionless nonlocal parameter ($\alpha = 0.1$), dimensionless material length scale parameter ($\beta = 0.2$), ($K_w = K_p = 0$) and $\Delta T = 0$. It can be observed at lower values of power law index (k) the dimensionless critical buckling load (\bar{P}) and fundamental frequency ($\bar{\omega}$) for Model III is greater than the dimensionless of ($\bar{P}, \bar{\omega}$) of Model II. Moreover, when the power law index (k) increase for example with cross section shape (1-1-1) the dimensionless of ($\bar{P}, \bar{\omega}$) with Model II is greater than the dimensionless of ($\bar{P}, \bar{\omega}$) at ($k \geq 1$) except with cross section shape (1-8-1). This is due to the core of the Model III is full ceramic, then with cross section shape (1-8-1) has ceramic portion is greater than for the (1-8-1) of Model II with FG core until with greater value of power law index (k). Moreover the size dependent of FG sandwich micro-beam with Model III becomes more stiffer than with Model II for lower values of the gradient index (k) but when increasing the gradient index (k) the ceramic portion of sandwich FG micro-beam decrease and then the Model II have effective elasticity modulus is more than Model III except shape (1-8-1). Therefore the sandwich FG micro-beam with Model II has more rigidity stiffness than those Model III with higher value of (k).

Table 4.15 Dimensionless natural frequency $\bar{\omega} = \omega L^2 / h \sqrt{\rho_m / E_m}$ of sandwich FG microbeams (PSDBT) for different gradient index $L / h = 10$, $\alpha = 0.1$, $\beta = 0.2$, $\Delta T = 0$ and $K_p = K_w = 0$.

B.Cs	Model	k	Symmetrical cross section				Un-symmetrical cross section		
			1-1-1	1-2-1	1-8-1	2-1-2	1-2-3	2-3-1	3-1-2
S-S Boundary Condition	Model II	0 (ceramic)	4.5429	4.7946	5.4600	4.3866	5.1258	4.5429	4.2053
		1	4.2154	4.2274	4.2580	4.2090	4.5756	4.0804	4.0830
		3	4.0839	4.0230	3.8913	4.1310	4.3634	3.8937	4.0254
		5	4.0445	3.9638	3.7865	4.1067	4.3044	3.8319	4.0064
		(metal) ∞	3.9729	3.8505	3.5416	4.0629	4.2106	3.6959	3.9706
	Model III	0 (ceramic)	6.0991	6.0991	6.0991	6.0991	6.0991	6.0991	6.0991
		1	4.4498	4.7401	5.4510	4.2589	4.5059	4.7573	4.2268
		3	3.8928	4.2311	5.1618	3.6880	3.9805	4.2586	3.6600
		5	3.7494	4.0896	5.0716	3.5501	3.8481	4.1213	3.5252
		(metal) ∞	3.5412	3.8677	4.9122	3.3612	3.6556	3.9077	3.3399
C-S Boundary Condition	Model II	0 (ceramic)	10.1017	10.6615	12.1090	9.7458	11.3853	10.1017	9.3197
		1	9.3404	9.3653	9.4286	9.3273	10.1668	9.0225	9.0231
		3	9.0252	8.8801	8.5813	9.1396	9.685	8.5765	8.8820
		5	8.9289	8.7364	8.3365	9.0804	9.5531	8.4305	8.8357
		(metal) ∞	8.7540	8.4667	7.7959	8.9731	9.3323	8.1244	8.7484
	Model III	0 (ceramic)	13.4889	13.4889	13.4889	13.4889	13.4889	13.4889	13.4889
		1	9.9096	10.5460	12.0884	9.4869	10.0226	10.5812	9.4128
		3	8.6910	9.4379	11.4626	8.2316	8.8672	9.4943	8.1634
		5	8.3745	9.1287	11.2673	7.9239	8.5721	9.1935	7.8610
		(metal) ∞	7.9089	8.6408	10.9222	7.4906	8.1340	8.7219	7.4318
C-C Boundary Condition	Model II	0 (ceramic)	19.6659	20.7555	23.4785	18.9499	22.1272	19.6659	18.0548
		1	18.0899	18.1321	18.2405	18.0676	19.7701	17.4205	17.4086
		3	17.4129	17.1027	16.5035	17.6626	18.8218	16.4673	17.0984
		5	17.2020	16.7906	15.9946	17.5333	18.5458	16.1598	16.9967
		(metal) ∞	16.8186	16.2169	14.9520	17.2970	18.0819	15.5526	16.8066
	Model III	0 (ceramic)	26.0465	26.0465	26.0465	26.0465	26.0465	26.0465	26.0465
		1	19.3303	20.5432	23.4350	18.5125	19.5162	20.6030	18.3601
		3	17.0166	18.4561	22.2665	16.1093	17.3044	18.5516	15.9588
		5	16.4078	17.8700	21.9018	15.5070	16.7279	17.9793	15.3620
		(metal) ∞	15.4916	16.9361	21.2567	14.6236	15.8456	17.0709	14.4763

Table 4.16 Dimensionless critical buckling load $\bar{P} = P L^2 / E_m I$ of sandwich FG microbeams (PSDBT) for different power law index $L / h = 10$, $\alpha = 0.1$, $\beta = 0.2$, $\Delta T = 0$ and $K_p = K_w = 0$.

B.Cs	Model	k	Symmetrical cross section				Un-symmetrical cross section		
			1-1-1	1-2-1	1-8-1	2-1-2	1-2-3	2-3-1	3-1-2
S-S Boundary Condition	Model II	0 (ceramic)	16.6435	17.3267	19.6233	16.3270	18.4117	16.6435	16.1174
		1	16.1926	16.2828	16.5129	16.1447	16.8804	16.0404	16.0630
		3	16.0699	16.0159	15.6936	16.0871	16.3531	15.7927	16.0352
		5	16.0456	15.9576	15.4584	16.0746	16.2386	15.6780	16.0243
		(metal) ∞	15.9983	15.7845	14.5097	16.0575	16.1209	15.2550	15.9960
	Model III	0 (ceramic)	22.1051	22.1051	22.1051	22.1051	22.1051	22.1051	22.1051
		1	15.9630	16.9297	19.5570	15.3850	15.3660	17.0521	15.3411
		3	13.8155	14.9092	18.3873	13.2555	14.4427	15.1033	13.2651
		5	13.3085	14.3698	18.0236	12.8114	14.0167	14.5928	12.8488
		(metal) ∞	12.6968	13.5930	17.3903	12.3728	13.5268	13.8751	12.4473
C-S Boundary Condition	Model II	0 (ceramic)	55.2714	57.5394	64.8864	54.1483	61.0329	55.2714	53.2388
		1	53.4719	53.7515	54.4662	53.3237	55.9894	52.7923	52.8209
		3	52.8444	52.5653	51.4283	52.9964	54.1830	51.6581	52.5999
		5	52.6788	52.2513	50.5244	52.9050	53.7629	51.1872	52.5208
		(metal) ∞	52.3629	51.4904	47.4060	52.7505	53.2893	49.7360	52.3507
	Model III	0 (ceramic)	72.7518	72.7518	72.7518	72.7518	72.7518	72.7518	72.7518
		1	53.1315	56.2668	64.6622	51.2272	54.3706	56.6477	51.0579
		3	46.1639	49.7551	60.9318	44.2701	48.0939	50.3614	44.2523
		5	44.5000	48.0068	59.7702	42.7862	46.6727	48.7030	42.8468
		(metal) ∞	42.4433	45.4700	57.7459	41.2200	44.9576	46.3458	41.3657
C-C Boundary Condition	Model II	0 (ceramic)	159.409	165.952	185.894	155.842	175.537	159.409	152.264
		1	152.859	153.575	155.417	152.481	161.168	150.131	150.018
		3	150.087	148.850	145.278	150.940	155.705	145.522	148.826
		5	149.244	147.430	142.150	150.459	154.316	143.786	148.415
		(metal) ∞	147.655	144.452	133.291	149.592	152.362	139.404	147.601
	Model III	0 (ceramic)	206.941	206.941	206.941	206.941	206.941	206.941	206.941
		1	153.775	162.480	185.225	148.348	156.896	163.463	147.752
		3	134.434	144.605	175.147	128.809	139.290	146.176	128.525
		5	129.728	139.763	172.003	124.488	135.160	141.562	124.363
		(metal) ∞	123.675	132.646	166.519	119.442	129.809	134.885	119.409

Tables (4.17) and (4.18) show the effects of the dimensionless nonlocal parameter ($\alpha = ea/L$) and the dimensionless material length scale parameter ($\beta = l_m/L$) on the dimensionless buckling load and fundamental frequency for Modal II (1-1-1) and Modal III (1-1-1) of size dependent sandwich FG micro-beams for different boundary conditions (i.e. S-S, C-S, C-C), without elastic foundation ($K_p = K_w = 0$) different dimensionless material length scale parameter (β), various dimensionless nonlocal parameter (α) and without thermal effect ($\Delta T = 0$). It is observed that the dimensionless buckling load and fundamental frequency increase when the material length scale parameter (β) increase due to the size dependent sandwich FG microbeam have more stiffness-hardening with the strain gradient influence (strain gradient theory). On the other hand the size dependent sandwich FG microbeam with more stiffness-softening with the increase the dimensionless nonlocal parameter (α) (nonlocal elasticity theory). Similar to the bending static analysis, the dimensionless critical buckling load and fundamental frequency of sandwich FG micro-beam with the classical elasticity theory can be achieved by putting $\alpha = \beta = 0$ and also when $\alpha = \beta$ for simply supported boundary condition. On the other hand the classical elasticity theory can be obtained only when $\alpha = \beta = 0$ with other boundary conditions (i.e. C-C, C-S). The value of the dimensionless buckling load and fundamental frequency of sandwich FG micro-beams may be larger or smaller than that the values of the dimensionless buckling load and fundamental frequency with the classical theory.

Table 4.17 Dimensionless critical buckling load $\bar{P} = PL^2/(E_m I)$ of sandwich micro-beams with various B.Cs with a cross-section shape (1-1-1) for $\Delta T = 0$, $k = 1$, $K_p = K_w = 0$

Model II

B.Cs	β	$\alpha = 0$	$\alpha = 0.05$	$\alpha = 0.1$	$\alpha = 0.15$	$\alpha = 0.2$
S-S	0	12.7552	12.4480	11.6094	10.4374	9.1449
	0.05	13.0699	12.7552	11.8958	10.6949	9.3705
	0.1	14.0141	13.6766	12.7552	11.4675	10.0475
	0.15	15.5877	15.2123	14.1874	12.7552	11.1757
	0.2	17.7907	17.3623	16.1926	14.5579	12.7552
C-S	0	25.8789	24.6149	21.4028	17.5496	13.9933
	0.05	29.3223	27.8544	24.2196	19.8593	15.8350
	0.1	37.0033	35.1341	30.4112	24.8420	19.7343
	0.15	48.9449	46.4188	40.1249	32.6712	25.9219
	0.2	65.2120	61.9253	53.4719	43.5211	34.4649
C-C	0	49.5896	45.0072	34.7363	25.0095	17.8565
	0.05	63.2802	57.1786	44.1302	31.7730	22.6855
	0.1	96.3064	86.7388	66.6527	47.8057	34.1343
	0.15	148.8720	133.983	102.778	73.8001	52.6977
	0.2	221.475	199.292	152.859	109.722	78.501

Model III

B.Cs	β	$\alpha = 0$	$\alpha = 0.05$	$\alpha = 0.1$	$\alpha = 0.15$	$\alpha = 0.2$
S-S	0	12.5743	12.2715	11.4448	10.2894	9.0152
	0.05	12.8846	12.5743	11.7271	10.5433	9.2376
	0.1	13.8153	13.4827	12.5743	11.3049	9.9050
	0.15	15.3666	14.9966	13.9863	12.5743	11.0172
	0.2	17.5385	17.1161	15.9630	14.3515	12.5743
C-S	0	25.6289	24.3839	21.1882	17.3742	13.8567
	0.05	29.0704	27.6223	24.0022	19.6817	15.6971
	0.1	36.7443	34.8548	30.1922	24.6392	18.5731
	0.15	48.6321	46.0941	39.8372	32.4647	25.7294
	0.2	64.9507	61.5342	53.1315	43.2346	34.2683
C-C	0	49.4274	44.8682	34.6380	24.9649	17.8546
	0.05	63.2243	57.1259	44.1010	31.7852	22.7324
	0.1	96.8573	86.9226	66.7825	47.9087	34.2246
	0.15	149.613	134.614	103.218	74.1045	52.9205
	0.2	223.002	200.6010	153.775	110.341	78.9375

Table 4.18 Dimensionless natural frequency $\bar{\omega} = \omega L^2/h \sqrt{\rho_m/E_m}$ of sandwich micro-beams with various B.Cs with a cross-section shape (1-1-1) for $\Delta T = 0$, $k = 1$, $K_p = K_w = 0$

Model II

B.Cs	β	$\alpha = 0$	$\alpha = 0.05$	$\alpha = 0.1$	$\alpha = 0.15$	$\alpha = 0.2$
S-S	0	3.7413	3.7413	3.5693	3.3843	3.1678
	0.05	3.7872	3.7413	3.6131	3.4258	3.2067
	0.1	3.9216	3.8741	3.7413	3.5474	3.3205
	0.15	4.1359	4.0858	3.9458	3.7413	3.5019
	0.2	4.4186	4.3650	4.2154	3.9969	3.7413
C-S	0	5.8409	5.7575	5.5271	5.1967	4.8187
	0.05	6.4073	6.3087	6.0437	5.6643	5.2345
	0.1	7.3251	7.2461	6.9248	6.4756	5.9682
	0.15	8.5642	8.4246	8.0450	7.5083	6.9122
	0.2	9.9512	9.7867	9.3404	8.7134	8.0110
C-C	0	8.4284	8.2985	7.9405	7.4318	6.8564
	0.05	8.4284	8.2985	7.9405	7.4618	6.8564
	0.1	12.6593	12.4342	11.8168	10.9586	10.0162
	0.15	15.8700	15.5798	14.7931	13.7072	12.5123
	0.2	19.4164	19.0587	18.0899	16.7518	15.2908

Model III

B.Cs	β	$\alpha = 0$	$\alpha = 0.05$	$\alpha = 0.1$	$\alpha = 0.15$	$\alpha = 0.2$
S-S	0	3.9494	3.9015	3.7678	3.5725	3.3440
	0.05	3.9978	3.9494	3.8140	3.6163	3.3850
	0.1	4.1397	4.0895	3.9494	3.7447	3.5051
	0.15	4.3659	4.3130	4.1652	3.9494	3.6967
	0.2	4.6643	4.6078	4.4498	4.2192	3.9494
C-S	0	6.1843	6.0959	5.8514	5.5009	5.1001
	0.05	6.7873	6.6847	6.4012	5.9985	5.5424
	0.1	7.8041	7.6801	7.3416	6.8615	6.3228
	0.15	9.0827	8.9345	8.5308	7.9639	7.3270
	0.2	10.5593	10.3846	9.9096	9.2426	8.4999
C-C	0	8.9575	8.8186	8.4361	7.8931	7.2798
	0.05	10.6510	10.4694	9.9711	9.2750	8.5021
	0.1	13.4983	13.2545	12.5941	11.6746	10.6663
	0.15	16.9483	16.6361	15.7903	14.6246	13.3440
	0.2	20.7586	20.3732	19.3303	17.8920	16.3241

Figs.(4.31 and 4.32) examine dimensionless nonlocal parameter ($\alpha = ea/L$) on the dimensionless critical buckling load (\bar{P}) and fundamental frequency ($\bar{\omega}$) respectively of sandwich FG microbeam with a various gradient index (i.e. $k = 0, 1, 3, 5, 10$) and different boundary conditions (i.e. S-S, C-S, C-C) at certain aspect ratio ($L/h = 10$), without elastic foundation ($K_w = K_p = 0$) and no temperature change ($\Delta T = 0$) for Modal II (1-2-1) and Modal III (1-2-1). It is observed from Figs. (4.31 and 4.32) that when the dimensionless nonlocal parameter (α) increase with fixed the dimensionless material length scale parameter ($\beta = l_m/L = 0.2$), the dimensionless buckling load and natural frequency of sandwich FG microbeam decrease for all cross section shapes and different boundary conditions due to the sandwich FG micro-beam become more flexible with increase dimensionless nonlocal parameter (nonlocal elasticity theory).

On the other hand for Figs. (4.33-4.34) present the effect of ($\beta = l_m/L$) on the dimensionless buckling load (\bar{P}) and natural frequency ($\bar{\omega}$) of size dependent sandwich FG micro-beam with fixed the dimensionless nonlocal parameter ($\alpha = ea/L = 0.2$) aspect ratio ($L/h = 10$), ($K_w = K_p = 0$) and ($\Delta T = 0$) for Modal II and Modal III with cross section (1-2-1). It can be noticed that the dimensionless critical buckling load (\bar{P}) and natural frequency ($\bar{\omega}$) decrease with decrease the (β) for different power law index (k) and different boundary conditions.

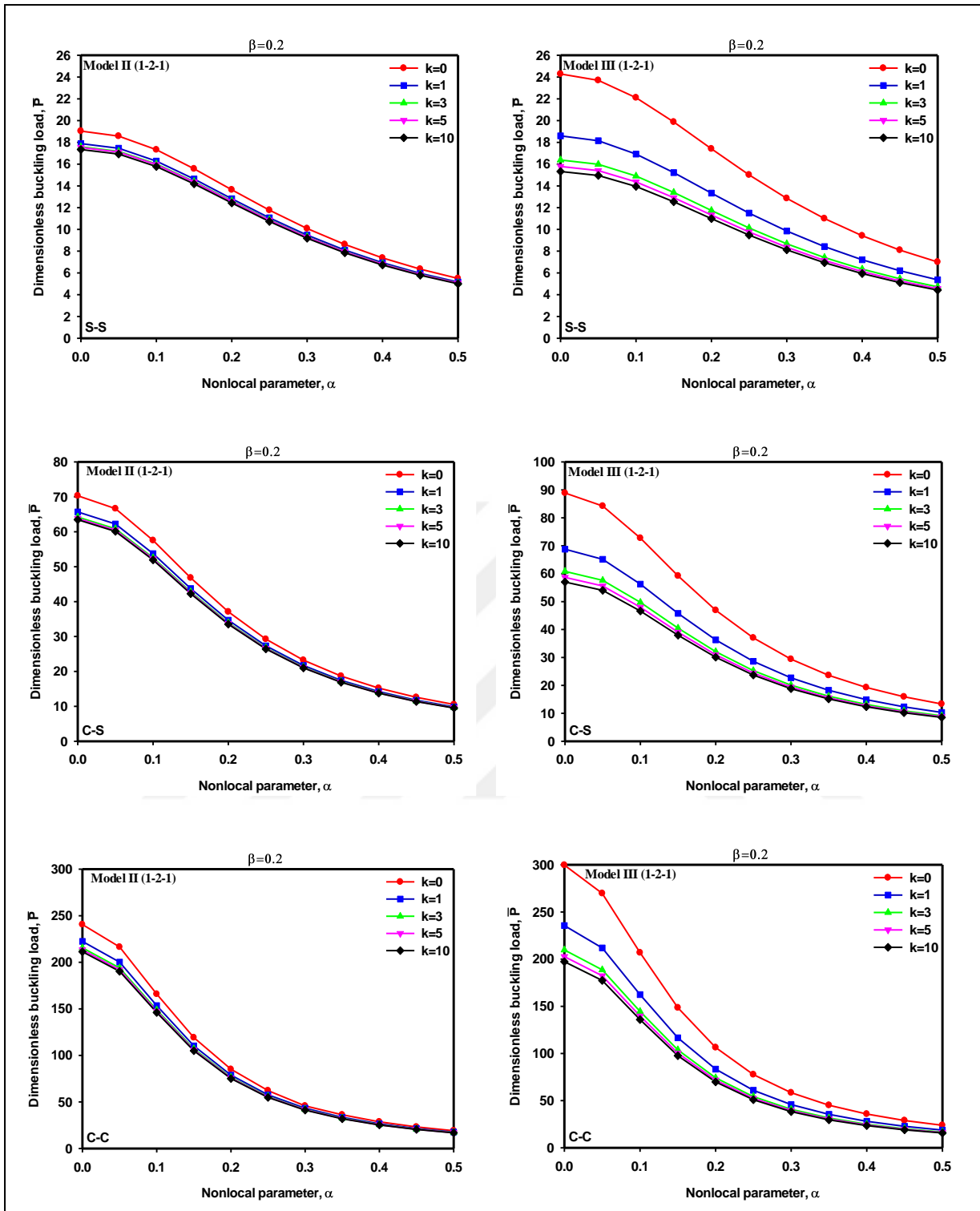


Figure 4.31 Effect of the nonlocal parameter (α) on the dimensionless buckling load \bar{P} of sandwich FG microbeam with a various boundary conditions (S-S, C-S, C-C) for different power law index (k) with $L/h = 10, K_p = K_w = 0, \Delta T = 0, \beta = 0.2$ and cross section shape (1-2-1).

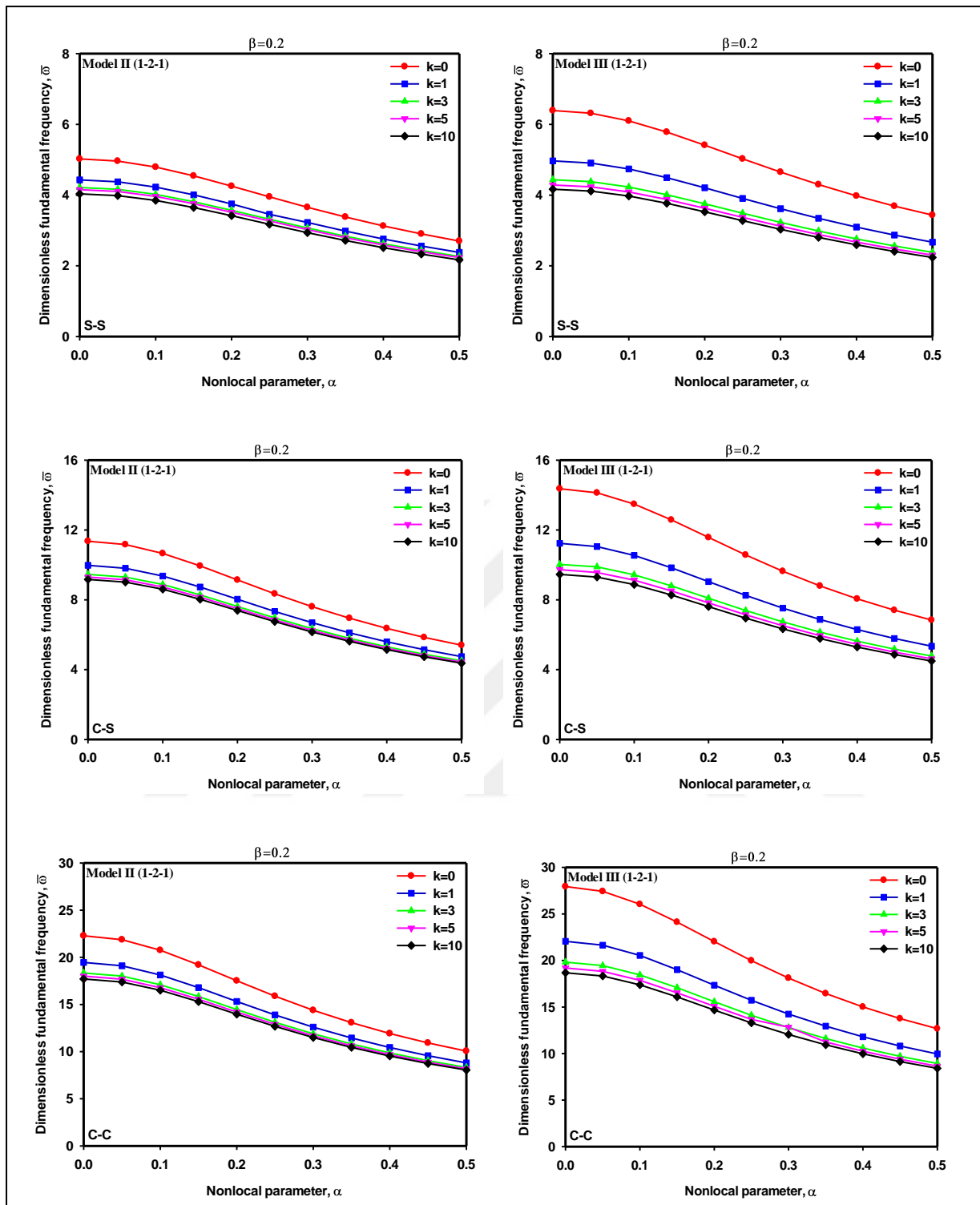


Figure 4.32 Effect of the nonlocal parameter (α) on the dimensionless fundamental frequency $\bar{\omega}$ of sandwich FG microbeam with a various boundary conditions (S-S, C-S, C-C) for different power law index (k) with $L/h = 10$, $K_p = K_w = 0$, $\Delta T = 0$, $\beta = 0.2$ and cross section shape (1-2-1).

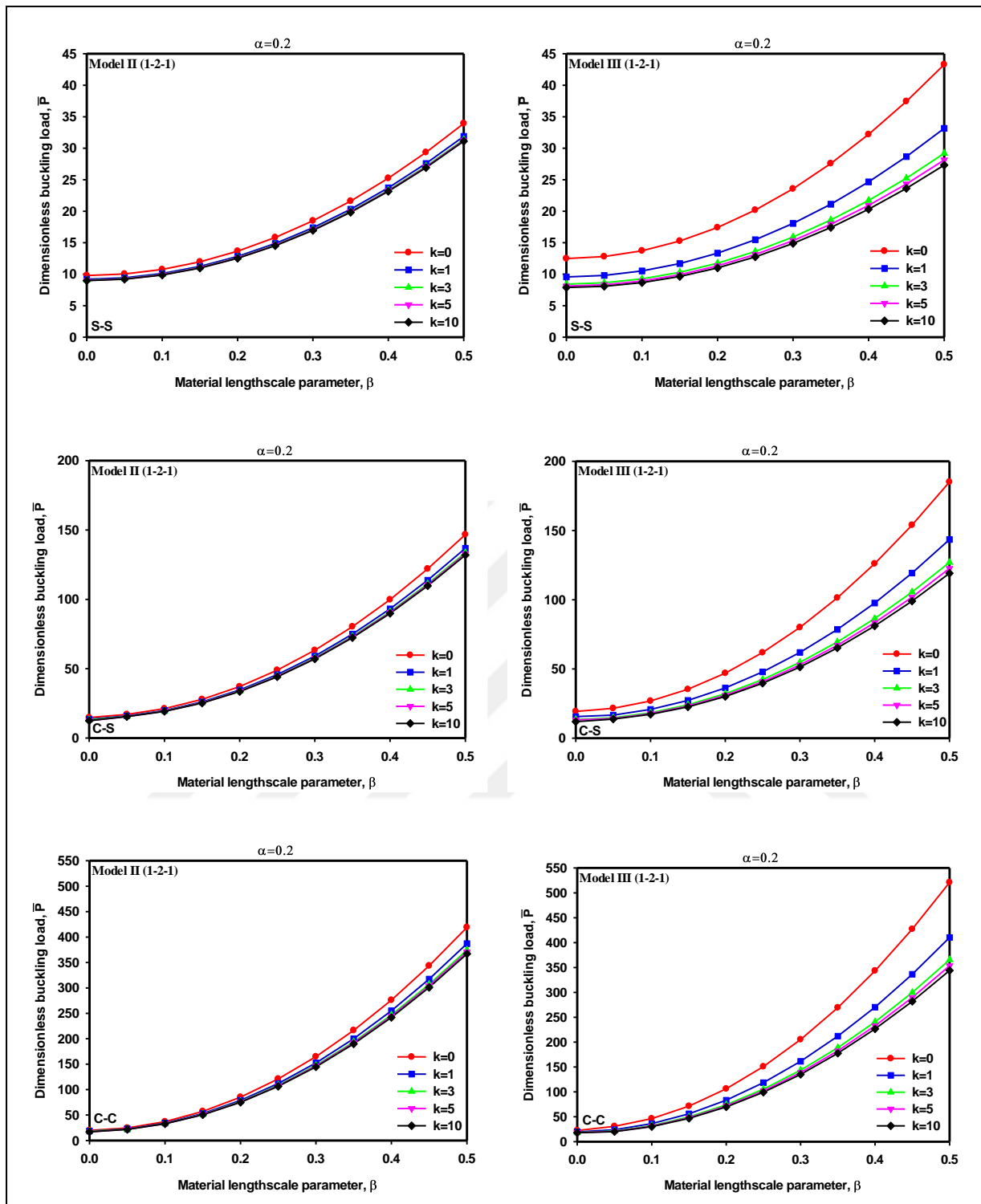


Figure 4.33 Effect of the material length scale parameter (β) on the dimensionless buckling load \bar{P} of sandwich FG microbeam with a various boundary conditions (S-S, C-S, C-C) for different power law index (k) with $L/h = 10$, $K_p = K_w = 0$, $\Delta T = 0$, $\alpha = 0.2$ and cross section shape (1-2-1).

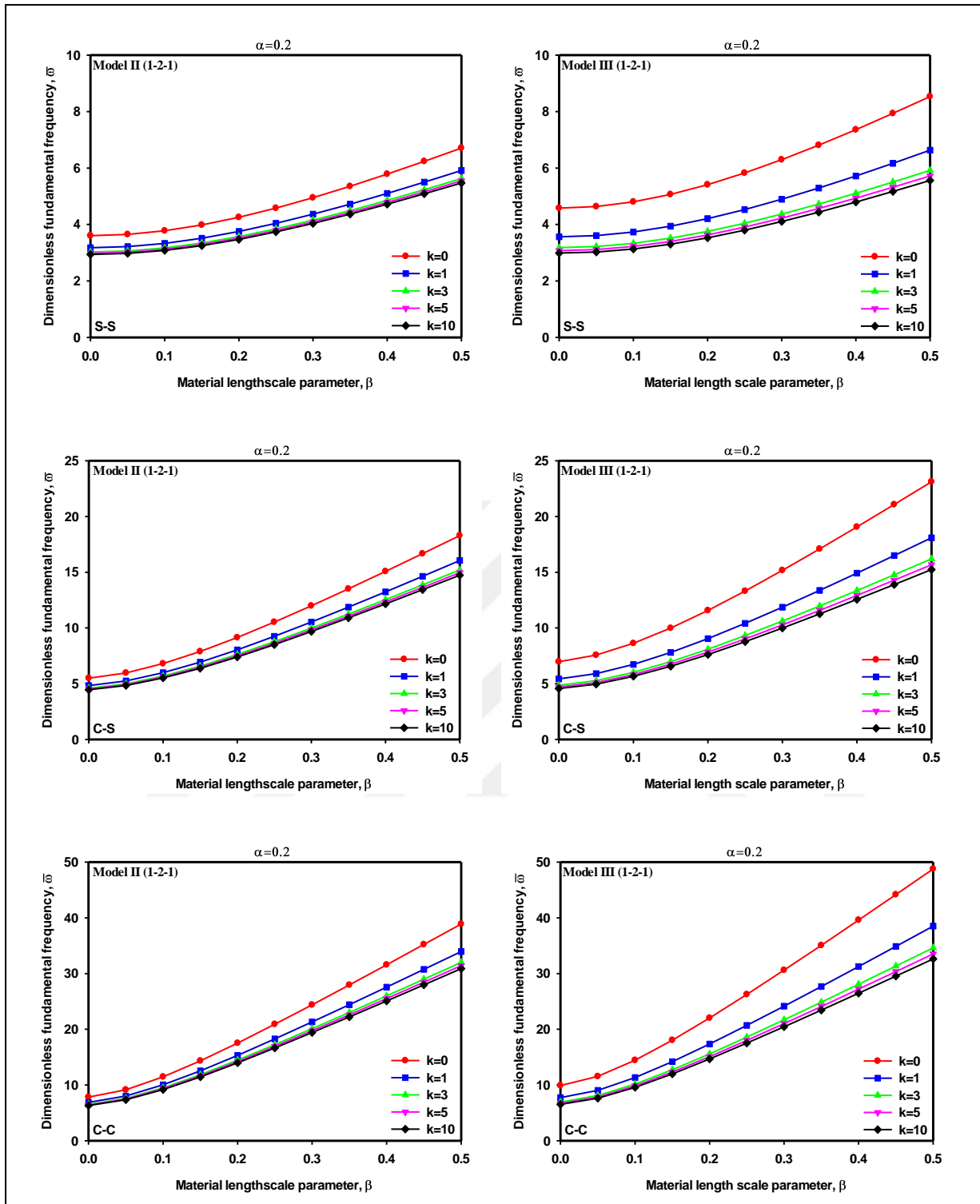


Figure 4.34 Effect of the material length scale parameter (β) on the dimensionless fundamental frequency $\bar{\omega}$ of sandwich FG microbeam with a various boundary conditions (S-S, C-S, C-C) for different power law index (k) with $L/h = 10$, $K_p = K_w = 0$, $\Delta T = 0$, $\alpha = 0.2$ and cross section shape (1-2-1).

From Fig.(4.35 and 4.36) it can be shows the three dimension plot of the dimensionless buckling load \bar{P} and the dimensionless fundamental frequency ($\bar{\omega}$) of simply supported sandwich FG micro-beams with Model II, III for (1-1-1) cross section shape with the change of the dimensionless material length scale parameter ($\beta = l_m/L$) and the dimensionless nonlocal parameter ($\alpha = ea/L$).

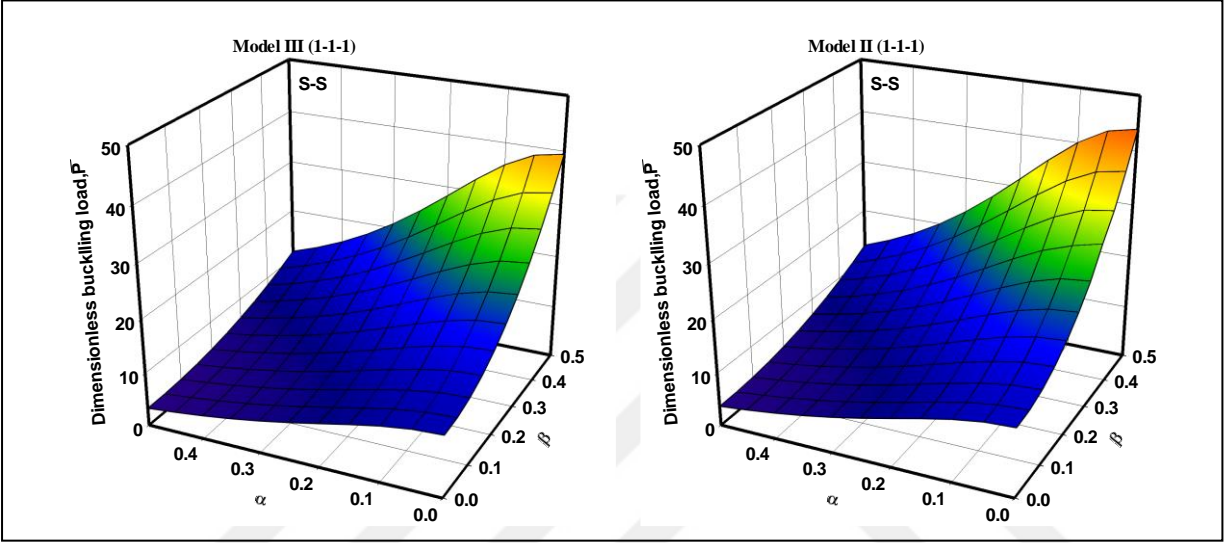


Figure 4.35 The nonlocal parameter (α) and the dimensionless material length scale parameter on the dimensionless buckling load \bar{P} of sandwich FG microbeam with a cross section shape (1-1-1) and S-S boundary conditions for $k = 2, L/h = 10, K_p = K_w = 0$ and $\Delta T = 0$.

In Tables 4.19 and 4.20, the first three dimensionless frequencies of the size dependent sandwich micro-beams are given for various values of material property gradient index (k), symmetrical and un- symmetrical cross section shapes, various boundary conditions (i.e. S-S, C-S, C-C) and length to thickness ratio ($L/h = 10$) for Model II and Model III. It can be observed that the dimensionless frequency of sandwich FG micro-beams decrease when the gradient index(k) increase for all model with different cross section shapes.

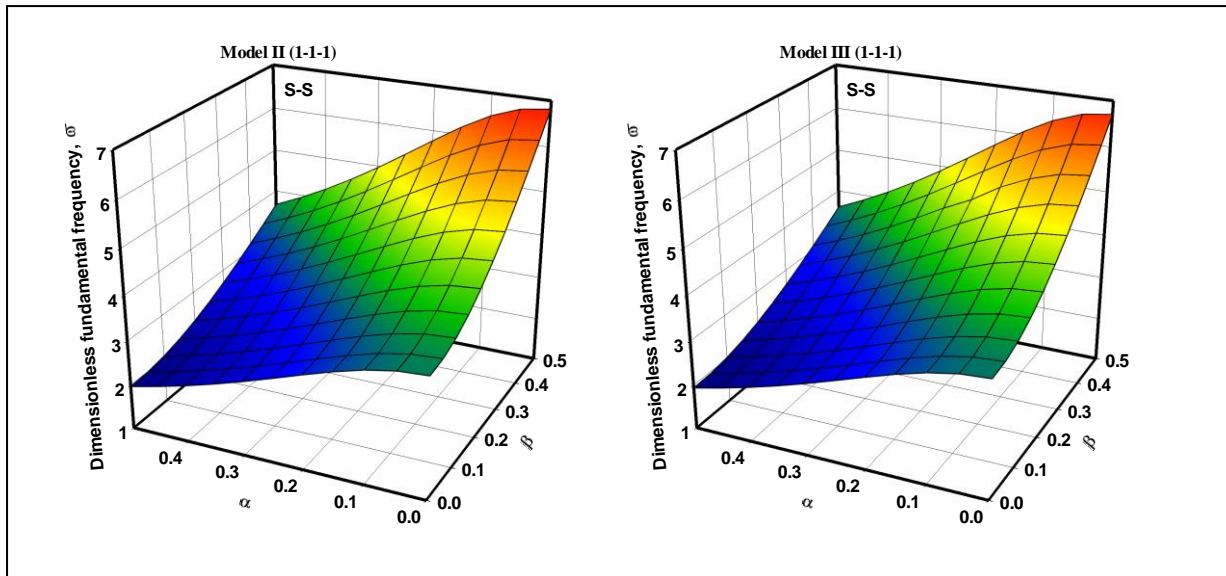


Figure 4.36 The nonlocal parameter (α) and the dimensionless material length scale parameter on the dimensionless fundamental frequency $\bar{\omega}$ of sandwich FG microbeam with a cross section shape (1-1-1) and S-S boundary conditions for $k = 2$, $L/h = 10$, $\bar{K}_p = \bar{K}_w = 0$ and $\Delta T = 0$.

The reason of this, the size dependent sandwich FG microbeams become more stiffer with increase of effective elasticity modulus with decrease of gradient index (k). It can be seen from tables (4.19 and 4.20) The Model II gives the dimensionless fundamental frequency smaller than Model III of sandwich FG micro-beams due to the core of the Model III is fully ceramic then the ceramic fraction of Model II is less than the ceramic fraction of Model III. Moreover the Model III of sandwich FG micro-beam has the effective elasticity modulus is larger than that of the effective elasticity modulus Model II.

Table 4.19 The three dimensionless natural frequency $\bar{\omega} = \omega L^2 / h \sqrt{\rho_m / E_m}$ of sandwich FG microbeams Model II with C-C B.C for $L/h = 10$, $\beta = 0.2$, $\alpha = 0.1$, and $K_p = K_w = 0$.

B.Cs	k	$\bar{\omega}$	Symmetrical cross section				Un-symmetrical cross section		
			1-1-1	1-2-1	1-8-1	2-1-2	1-2-3	2-3-1	3-1-2
S-S Boundary Condition	0	1	4.5424	4.7941	5.4592	4.3861	5.1252	4.5424	4.2050
		2	20.9987	22.1632	25.1987	20.2631	23.6776	20.9987	19.3880
		3	54.0852	57.1970	63.5204	51.7682	60.5832	54.0852	48.5424
	1	1	4.2151	4.2271	4.2577	4.2086	4.5751	4.0801	4.0827
		2	19.4337	19.4886	19.6284	19.4046	21.1398	18.7843	18.7831
		3	48.5557	48.5709	48.6063	48.5473	54.0943	46.0821	46.0572
	3	1	4.0836	4.0228	3.8911	4.1307	4.3629	3.8936	4.0251
		2	18.7879	18.4925	17.8800	19.0206	20.1473	17.8710	18.4955
		3	46.0599	44.8817	42.8481	47.0316	51.2158	42.7379	44.8705
	5	1	4.0442	3.9636	3.7864	4.1064	4.3040	3.8318	4.0062
		2	18.5913	18.1988	17.3768	18.8998	19.8674	17.5719	18.4012
		3	45.2630	43.7259	41.0952	46.5396	50.3026	41.9745	44.4828
	∞	1	3.9727	3.8504	3.5416	4.0626	4.2102	3.6959	3.9704
		2	18.2348	17.6473	16.2582	18.6811	19.4137	16.9414	18.2235
		3	43.6111	42.1245	38.8878	45.6319	48.6446	40.4455	43.7645
C-S Boundary Condition	0	1	10.1017	10.6615	12.1090	9.7458	11.3853	10.1017	9.3197
		2	33.8480	35.7221	40.4444	32.6224	38.0943	33.8480	31.0973
		3	69.6876	73.5553	83.0866	67.0966	78.3622	69.6876	63.7740
	1	1	9.3404	9.3653	9.4286	9.3273	10.1668	9.0225	9.0231
		2	31.1616	31.2390	31.4380	31.1207	34.0355	30.0262	30.0018
		3	63.9021	64.0570	64.4596	63.8205	70.0218	61.4464	61.3353
	3	1	9.0252	8.8801	8.5813	9.1396	9.685	8.5765	8.8820
		2	30.0098	29.4847	28.4667	30.4323	32.4068	28.4050	29.4759
		3	61.3543	60.2096	58.1011	62.2929	66.6102	57.8845	60.1574
	5	1	8.9289	8.7364	8.3365	9.0804	9.5531	8.4305	8.8357
		2	29.6516	28.9544	27.5989	30.2127	31.9344	27.882	29.3034
		3	60.5524	59.0302	56.2330	61.8016	65.6012	56.7509	59.7717
	∞	1	8.7540	8.4667	7.7959	8.9731	9.3323	8.1244	8.7484
		2	29.0015	27.9799	25.8132	29.8122	31.1434	26.8459	28.9811
		3	59.1014	56.9068	52.6205	60.9031	63.8760	54.6132	59.0566
C-C Boundary Condition	0	1	19.6659	20.7555	23.4785	18.9499	22.1272	19.6659	18.0548
		2	50.1759	52.9665	59.7187	48.2825	56.3889	50.1759	45.8253
		3	91.2935	96.3657	108.3970	87.7805	102.4830	91.2935	83.1161
	1	1	18.0899	18.1321	18.2405	18.0676	19.7701	17.4205	17.4086
		2	45.9098	46.0118	46.2772	45.8560	50.3907	44.0888	44.0072
		3	83.2618	83.4389	83.9050	83.1690	91.6226	79.8200	79.6147
	3	1	17.4129	17.1027	16.5035	17.6626	18.8218	16.4673	17.0984
		2	44.0202	43.1686	41.6244	44.7210	47.9147	41.4532	43.1294
		3	79.6404	78.0220	75.1934	80.9884	87.0644	74.7933	77.9192
	5	1	17.2020	16.7906	15.9946	17.5333	18.5458	16.1598	16.9967
		2	43.4235	42.2934	40.2529	44.3551	47.1758	40.6175	42.8421
		3	78.4883	76.3403	72.6148	80.2820	85.6826	73.2144	77.3651
	∞	1	16.8186	16.2169	14.9520	17.2970	18.0819	15.5526	16.8066
		2	42.3433	40.7231	37.6485	43.6852	45.9012	39.0617	42.3101
		3	76.4073	73.3616	67.9383	78.9865	83.2617	70.3748	76.3437

Table 4.20 The three dimensionless natural frequency $\bar{\omega} = \omega L^2 / h \sqrt{\rho_m / E_m}$ of sandwich FG microbeams Model III (PSDBT) for $L/h = 10$, $\beta = 0.2$, $\alpha = 0.1$, and $K_p = K_w = 0$.

B.Cs	k	$\bar{\omega}$	Symmetrical cross section				Un-symmetrical cross section		
			1-1-1	1-2-1	1-8-1	2-1-2	1-2-3	2-3-1	3-1-2
S-S Boundary Condition	0	1	6.0981	6.0981	6.0981	6.0981	6.0981	6.0981	6.0981
		2	28.1141	28.1141	28.1141	28.1141	28.1141	28.1141	28.1141
		3	67.6113	67.6113	67.6113	67.6113	67.6113	67.6113	67.6113
	1	1	4.4493	4.7395	5.4502	4.2584	4.5055	4.7567	4.2263
		2	20.6059	21.9293	25.1582	19.7299	20.8449	22.0038	19.5776
		3	49.8501	52.9864	60.5987	47.7566	50.3618	53.1501	47.3759
	3	1	3.8925	4.2307	5.1611	3.6877	3.9801	4.2582	3.658
		2	18.0684	19.6158	23.8424	17.1203	18.4392	19.7343	16.9814
		3	43.8440	47.5272	57.4878	41.5511	44.6283	47.7852	41.1848
	5	1	3.7490	4.0892	5.0709	3.5498	3.8478	4.1208	3.5250
		2	17.4118	18.9722	23.4325	16.4836	17.8279	19.1082	16.3562
		3	42.2816	46.0074	56.5207	40.0177	43.1548	46.3024	39.6692
	∞	1	3.5410	3.8673	4.9116	3.3610	3.6553	3.9074	3.3397
		2	16.4501	17.9599	22.7091	15.5919	16.9249	18.1304	15.4736
		3	39.9611	43.6077	54.8162	37.8053	40.9331	43.9728	37.4557
C-S Boundary Condition	0	1	13.4889	13.4889	13.4889	13.4889	13.4889	13.4889	13.4889
		2	44.9433	44.9433	44.9433	44.9433	44.9433	44.9433	44.9433
		3	92.1600	92.1600	92.1600	92.1600	92.1600	92.1600	92.1600
	1	1	9.9096	10.5460	12.0884	9.4869	10.0226	10.5812	9.4128
		2	33.2736	35.3598	40.3708	31.8719	33.6010	35.4653	31.6129
		3	68.7075	72.9128	82.9431	35.3595	35.3595	35.3595	65.2955
	3	1	8.6910	9.4379	11.4626	8.2316	8.8672	9.4943	8.1634
		2	29.2881	31.7538	38.3345	27.7398	29.7918	31.9214	27.4856
		3	60.6913	65.6895	78.8547	57.4901	61.5391	65.9844	56.9134
	5	1	8.3745	9.1287	11.2673	7.9239	8.5721	9.1935	7.8610
		2	28.2440	30.7450	37.7003	26.7091	28.8036	30.9366	26.4648
		3	58.5762	63.6668	77.5845	55.3706	59.5058	64.0012	54.7984
	∞	1	7.9089	8.6408	10.9222	7.4906	8.1340	8.7219	7.4318
		2	26.6791	29.1432	36.5809	25.2038	27.2977	29.3791	24.9559
		3	55.3501	60.4375	75.3465	52.1676	56.3352	60.8406	51.5530
C-C Boundary Condition	0	1	26.0465	26.0465	26.0465	26.0465	26.0465	26.0465	26.0465
		2	66.0697	66.0697	66.0697	66.0697	66.0697	66.0697	66.0697
		3	119.7690	119.7690	119.7690	119.7690	119.7690	119.7690	119.7690
	1	1	19.3303	20.5432	23.4350	18.5125	19.5162	20.6030	18.3601
		2	49.4930	52.5071	59.6095	47.4303	49.8648	52.6333	47.0198
		3	90.2223	95.5942	108.1870	86.5099	90.7796	95.7957	85.7392
	3	1	17.0166	18.4561	22.2665	16.1093	17.3044	18.5516	15.9588
		2	43.7644	47.3733	56.7330	41.4290	44.3256	47.5712	40.9950
		3	80.0365	86.4970	103.0600	75.7780	80.8430	86.8031	74.9275
	5	1	16.4078	17.8700	21.9018	15.5070	16.7279	17.9793	15.3620
		2	42.2401	45.9277	55.8376	39.8908	42.8537	46.1519	39.4565
		3	77.3096	83.9361	101.4700	72.9864	78.1702	84.2780	72.1165
	∞	1	15.4916	16.9361	21.2567	14.6236	15.8456	17.0709	14.4763
		2	39.8901	43.6041	54.2574	37.5341	40.5329	43.8726	37.0641
		3	73.0348	79.7997	98.6710	68.5798	73.8717	80.1936	67.6067

The effect of the dimensionless Winkler (K_w) and Pasternak shear parameters (K_p) on the dimensionless buckling load and fundamental frequency of sandwich FG micro-beam are given in table (4.21) for various values of aspect ratio ($L/h = 5, 10, 20, 50$), different cross section shapes, and various boundary conditions (i.e. S-S, C-S, C-C) for Model II and Model III. It can be seen from these tables that the dimensionless buckling load and fundamental frequency increase with increase the Winkler and Pasternak shear parameters from 0 to 0.2 for consider models of sandwich FG microbeam for Model II , III because the fact that the size dependent sandwich FG microbeam have more effective elasticity modulus and make sandwich FG microbeam more stiffer when increase the (K_w) and (K_p). It is observed that for example when the dimensionless Winkler (K_w) and Pasternak shear parameters (K_p) equal to zero (without elastic foundation) with Model III (1-2-1) cross section shape and simply supported boundary condition. The value of dimensionless critical buckling load (\bar{P}) is 0.0120 when sandwich FG micro-beam without elastic foundation and increase to 0.2322 when the $K_p = K_w = 0.2$. As well as for dimensionless fundamental frequency ($\bar{\omega}$) is 0.4057 when sandwich FG micro-beam without elastic foundation and increase to 1.7832 when the $K_p = K_w = 0.2$. Also it is explicit that the effect of the Pasternak shear modulus (K_p) is more pronounced than that of the Winkler elastic modulus (K_w) on the dimensionless buckling load and fundamental frequency the size dependent of sandwich FG microbeams. Also as expected C-C sandwich FG micro-beam has greatest value of dimensionless buckling load and natural frequency when compared with other boundary conditions with S-S and C-S.

Table 4.21 Dimensionless natural frequency $\bar{\omega} = \omega L \sqrt{\rho_m / E_m}$ of sandwich FG microbeams for $\Delta T = 0$, $\beta = 0.2$, $\alpha = 0.1$, and $k = 2$ with different cross section, aspect ratio, different B.Cs and elastic foundations.

			Model II				Model III				
B.Cs	K_P	K_W	Cross-section shape	$L/h = 5$	$L/h = 10$	$L/h = 20$	$L/h = 50$	$L/h = 5$	$L/h = 10$	$L/h = 20$	$L/h = 50$
S-S Boundary Condition	0	0	1-1-1	0.7868	0.4125	0.2089	0.0838	0.7797	0.4057	0.2050	0.0822
			1-8-1	0.7625	0.4000	0.2026	0.0813	1.0053	0.5254	0.2658	0.1067
			2-1-2	0.7931	0.4155	0.2104	0.0844	0.7405	0.38522	0.1946	0.0781
	0	0.2	1-1-1	0.9329	0.6535	0.5499	0.5165	0.9373	0.6648	0.5670	0.5355
			1-8-1	0.9060	0.6360	0.5358	0.5038	1.1663	0.7962	0.6565	0.6103
			2-1-2	0.9401	0.6584	0.5540	0.5199	0.8960	0.6396	0.5482	0.5189
	0.2	0.2	1-1-1	1.8293	1.7213	1.6899	1.6808	1.8833	1.7832	1.7549	1.7466
			1-8-1	1.7837	1.6783	1.6477	1.6388	2.1929	2.0411	1.9969	1.9841
			2-1-2	1.8426	1.7340	1.7026	1.6934	1.8202	1.7271	1.7007	1.6931
C-S Boundary Condition	0	0	1-1-1	1.5985	0.9125	0.4751	0.1923	1.6245	0.9053	0.4674	0.1887
			1-8-1	1.5427	0.8837	0.4606	0.1865	2.0631	1.1664	0.6052	0.2447
			2-1-2	1.6147	0.9200	0.4786	0.1937	1.5427	0.8595	0.4437	0.1791
	0	0.2	1-1-1	1.6749	1.0435	0.6958	0.5442	1.7054	1.0469	0.7054	0.5618
			1-8-1	1.6182	1.0123	0.6767	0.5303	2.1459	1.3105	0.8522	0.6488
			2-1-2	1.6914	1.0519	0.7010	0.5483	1.6227	0.9993	0.6776	0.5433
	0.2	0.2	1-1-1	2.4707	2.1380	1.9782	1.8944	2.5629	2.2066	2.0484	1.9658
			1-8-1	2.4008	2.0816	1.9275	1.8465	3.0535	2.5701	2.3519	2.2412
			2-1-2	2.4924	2.1546	1.9932	1.9086	2.4644	2.1308	1.9823	1.9044
C-C Boundary Condition	0	0	1-1-1	2.8206	1.7630	0.9557	0.3923	2.9362	1.7708	0.9440	0.3853
			1-8-1	2.7093	1.7036	0.9260	0.3805	3.6690	2.2644	1.2194	0.4994
			2-1-2	2.8554	1.7794	0.9632	0.3952	2.7877	1.6811	0.8962	0.3657
	0	0.2	1-1-1	2.8652	1.8342	1.0824	0.6427	2.9821	1.8471	1.0817	0.6545
			1-8-1	2.7536	1.7737	1.0503	0.6254	3.7166	2.3418	1.3589	0.7812
			2-1-2	2.9001	1.8510	1.0908	0.6475	2.8332	1.7566	1.0321	0.6299
	0.2	0.2	1-1-1	3.5421	2.8131	2.3940	2.1730	3.6879	2.8923	2.4699	2.2519
			1-8-1	3.4209	2.7318	2.3305	2.1175	4.4567	3.4456	2.8735	2.5802
			2-1-2	3.5797	2.8369	2.4126	2.1895	3.5287	2.7813	2.3852	2.1799

Table 4.22 Dimensionless critical buckling load ($\bar{P} = P/E_m bh$) of sandwich FG microbeams for $\Delta T = 0$, $\beta = 0.2$, $\alpha = 0.1$, and $k = 2$ with different cross section, aspect ratio, different B.Cs and elastic foundations.

B.Cs	K_p	K_w	Cross-section shape	Model II				Model III			
				$L/h = 5$	$L/h = 10$	$L/h = 20$	$L/h = 50$	$L/h = 5$	$L/h = 10$	$L/h = 20$	$L/h = 50$
S-S Boundary Condition	0	0	1-1-1	0.0499	0.0134	0.0034	0.0005	0.0455	0.0120	0.0030	0.0004
			1-8-1	0.0491	0.0132	0.0033	0.0005	0.0585	0.0156	0.0039	0.0006
			2-1-2	0.0499	0.0134	0.0034	0.0005	0.0436	0.0115	0.0029	0.0004
	0	0.2	1-1-1	0.0701	0.0336	0.0236	0.0082	0.0658	0.0322	0.0225	0.0079
			1-8-1	0.0694	0.0335	0.0236	0.0082	0.0788	0.0358	0.0242	0.0087
			2-1-2	0.0702	0.0336	0.0236	0.0082	0.0639	0.0317	0.0218	0.0077
	0.2	0.2	1-1-1	0.2701	0.2336	0.2236	0.2082	0.2658	0.2322	0.2225	0.2079
			1-8-1	0.2694	0.2335	0.2236	0.2082	0.2788	0.2358	0.2242	0.2087
			2-1-2	0.2702	1.7340	1.7026	1.6934	0.2639	0.2317	0.2218	0.2077
C-S Boundary Condition	0	0	1-1-1	0.1437	0.0441	0.0117	0.0019	0.1368	0.0401	0.0104	0.0017
			1-8-1	0.1406	0.0435	0.0115	0.0018	0.1716	0.0517	0.0136	0.0022
			2-1-2	0.1445	0.0442	0.0117	0.0019	0.1311	0.0384	0.0100	0.0016
	0	0.2	1-1-1	0.1572	0.0572	0.0242	0.0098	0.1502	0.0531	0.0229	0.0092
			1-8-1	0.1542	0.0566	0.0240	0.0097	0.1851	0.0648	0.0262	0.0107
			2-1-2	0.1580	0.0572	0.0242	0.0098	0.1445	0.0514	0.0224	0.0090
	0.2	0.2	1-1-1	0.3572	0.2572	0.2242	0.2098	0.3502	0.2531	0.2229	0.2092
			1-8-1	0.3542	0.2566	0.2240	0.2097	0.3851	0.2648	0.2262	0.2107
			2-1-2	0.3580	0.2572	0.2242	0.2098	0.3445	0.2514	0.2224	0.2090
C-C Boundary Condition	0	0	1-1-1	0.3437	0.1258	0.0356	0.0059	0.3434	0.1167	0.0320	0.0052
			1-8-1	0.3336	0.1236	0.0351	0.0058	0.4181	0.1486	0.0415	0.0068
			2-1-2	0.3469	0.1261	0.0356	0.0059	0.3291	0.1119	0.0307	0.0050
	0	0.2	1-1-1	0.3539	0.1355	0.0451	0.0147	0.3535	0.1264	0.0415	0.0139
			1-8-1	0.3438	0.1333	0.0447	0.0146	0.4282	0.1584	0.0511	0.0158
			2-1-2	0.3571	0.1359	0.0451	0.0147	0.3391	0.1216	0.0402	0.0136
	0.2	0.2	1-1-1	0.5539	0.3355	0.2451	0.2147	0.5535	0.3264	0.2415	0.2139
			1-8-1	0.5438	0.3333	0.2447	0.2146	0.6282	0.3584	0.2511	0.2158
			2-1-2	0.5571	0.3359	0.2451	0.2147	0.5391	0.3216	0.2402	0.2136

The effect of the dimensionless Winkler and Pasternak shear parameters (K_p, K_w) on the dimensionless buckling load and fundamental frequency of sandwich FG micro-beam with different gradient index ($k = 0, 1, 3, 5$) are presented in Figs.(4.37 and 4.38) respectively for a certain the aspect ratio ($L/h = 10$), dimensionless nonlocal parameter $\alpha = 0.1$, dimensionless material length scale parameter $\beta = 0.2$ and cross section type (1-1-1) of Model III with different boundary conditions (i.e. S-S, C-S, C-C). It can be observed that the dimensionless buckling load and fundamental frequency increase with increasing the dimensionless Winkler parameter (K_w) and Pasternak shear parameter (K_p) in the right when ($K_p = 0$) and left side when ($K_w = 0$) of figure respectively.



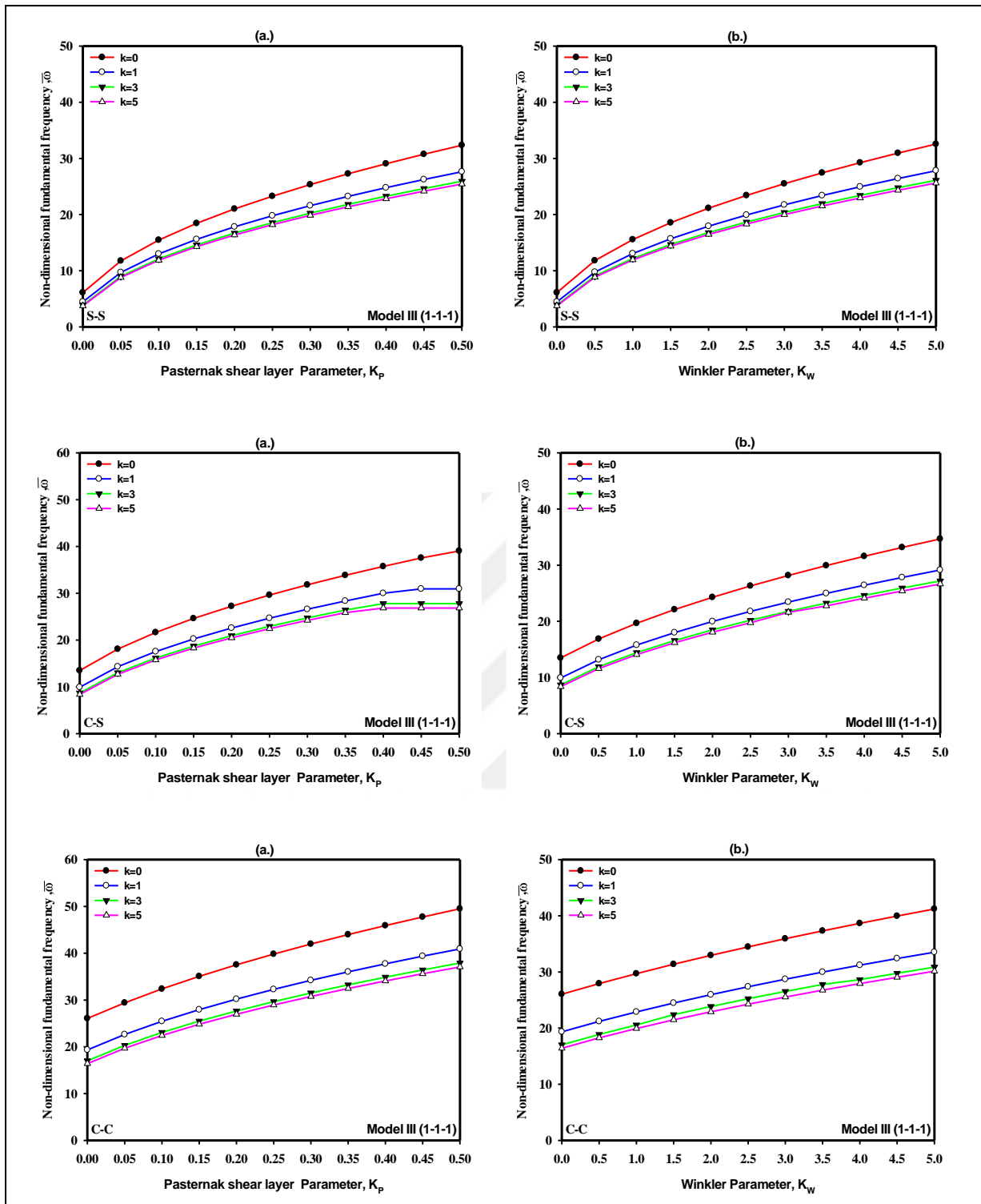


Figure 4.37 Effect of the Winkler and Pasternak shear parameter on the dimensionless fundamental frequency, $(\bar{\omega})$ for $L/h = 10$ and $\alpha = 0.1$, $\beta = 0.2$ of S-S sandwich microbeam for Model III (1-1-1). (a) $K_w = 0$ (b) $K_p = 0$ with various boundary conditions.

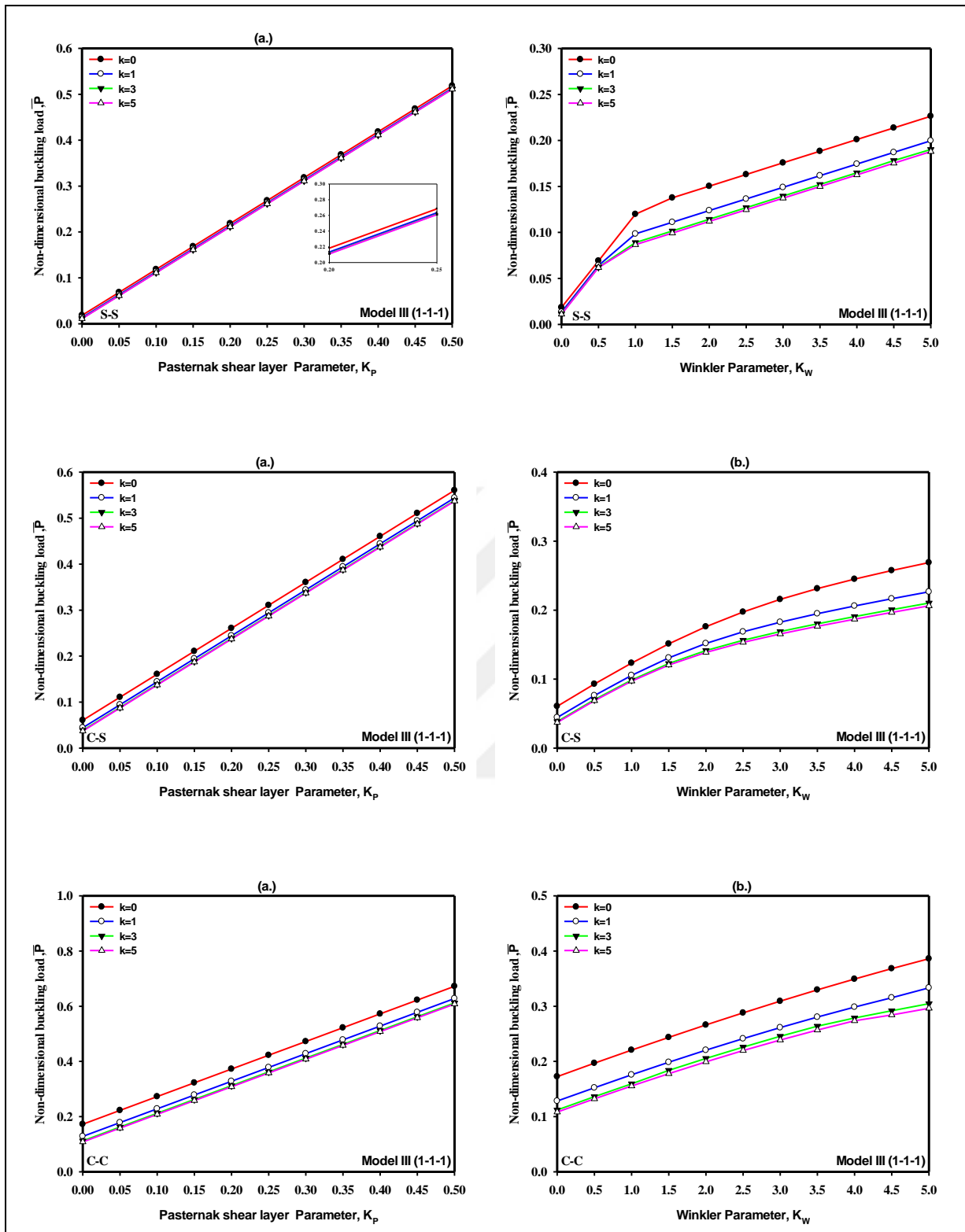


Figure 4.38 Effect of the Winkler and Pasternak shear parameter on the dimensionless buckling load, (\bar{P}) for $L/h = 10$ and $\alpha = 0.1$, $\beta = 0.2$ of SS sandwich microbeam for Model III (1-1-1) .(a) $K_w = 0$ (b) $K_p = 0$ with various boundary conditions.

The effect of temperature change (ΔT) on the dimensionless critical buckling load (\bar{P}) and fundamental frequency ($\bar{\omega}$) with different value of thermal effect ($\Delta T = 0, 20, 40, 80$) and various cross section shapes (symmetrical and un-symmetrical) of size dependent FG microbeams respectively, for certain ($K_w = K_p = 0$) power law index $k = 1$, $\beta = 0.2$, dimensionless nonlocal parameter $\alpha = 0.1$, and various boundary conditions can be observed in tables 4.23 and 4.24 respectively. .

Table 4.23 Dimensionless natural frequency ($\bar{\omega} = \omega L^2 / h \sqrt{\rho_m / E_m}$) of sandwich FG microbeams (PSDBT) with $k = 1$, $L/h = 10$, $\beta = 0.2$, $\alpha = 0.1$, and $K_w = K_p = 0$.

B.Cs	Model	ΔT	Symmetrical cross section				Un-symmetrical cross section		
			1-1-1	1-2-1	1-8-1	2-1-2	1-2-3	2-3-1	3-1-2
S-S Boundary Condition	Model II	0	4.2154	4.2274	4.2580	4.2090	4.5756	4.0804	4.0830
		20	4.0499	4.0593	4.0855	4.0457	4.4181	3.9086	3.9175
		40	3.8907	3.8980	3.9209	3.8884	4.2727	3.7410	3.7551
		80	3.5080	3.5080	3.5186	3.5120	3.9094	3.3418	3.3737
	Model III	0	4.4498	4.7401	5.4510	4.2589	4.5059	4.7573	4.2268
		20	4.2810	4.5816	5.3129	4.0825	4.3393	4.5994	4.0490
		40	4.1255	4.4388	5.1945	3.9172	4.1859	4.4572	3.8819
		80	3.7734	4.1156	4.9246	3.5428	3.8393	4.1354	3.5033
C-S Boundary Condition	Model II	0	9.3404	9.3653	9.4286	9.3273	10.1668	9.0225	9.0231
		20	9.2338	9.2569	9.3173	9.2221	10.0654	8.9118	8.9163
		40	9.1258	9.1472	9.2047	9.1155	9.9281	8.7996	8.8081
		80	8.9055	8.9232	8.9748	8.8984	9.7542	8.5703	8.5874
	Model III	0	9.9096	10.5460	12.0884	9.4869	10.0226	10.5812	9.4128
		20	9.8011	10.4440	11.9993	9.3736	9.9154	10.4796	9.2986
		40	9.6913	10.3409	11.9096	9.2588	9.8069	10.3769	9.1829
		80	9.4675	10.1314	11.7278	9.0245	9.5860	10.1681	8.9467
C-C Boundary Condition	Model II	0	18.0899	18.1321	18.2405	18.0676	19.7701	17.4205	17.4086
		20	18.0192	18.0603	18.1668	17.9978	19.7030	17.3470	17.3370
		40	17.9481	17.9881	18.0926	17.9277	19.6356	17.2731	17.2664
		80	17.8051	17.8427	17.9434	17.7867	19.5000	17.1242	17.1228
	Model III	0	19.3303	20.5432	23.4350	18.5125	19.5162	20.6030	18.3601
		20	19.2587	20.4758	23.3759	18.4377	19.4453	20.5358	18.2848
		40	19.1867	20.4081	23.6167	18.3626	19.3741	20.4684	18.2090
		80	19.0419	20.2720	23.1977	18.2113	19.2309	20.3327	18.0565

The dimensionless critical buckling load and natural frequency decrease with the increase of temperature change (ΔT) from 0 to 20, 40 and 80. The effective elasticity modulus of sandwich FG micro-beam decrease when the temperature change increase and make sandwich FG micro-beam more softening. This lead to lower dimensionless fundamental frequency and buckling load for all cross section shapes and various boundary conditions.

Table 4.24 Dimensionless critical buckling load ($\bar{P} = PL^2/E_m I$) of sandwich FG microbeams (PSDBT) with $k = 1$, $L/h = 10$, $\beta = 0.2$, $\alpha = 0.1$, and $K_w = K_p = 0$.

B.Cs		Model	ΔT	Symmetrical cross section				Un-symmetrical cross section		
				1-1-1	1-2-1	1-8-1	2-1-2	1-2-3	2-3-1	3-1-2
S-S Boundary Condition	Model II	0	16.1926	16.2828	16.5129	16.1447	16.8804	16.0404	16.0630	
		20	14.9456	15.0128	15.2015	14.9161	15.7379	14.7183	14.7869	
		40	13.7943	13.8442	14.0015	13.7788	14.7190	13.4833	13.5868	
		80	11.3961	11.4055	11.4902	11.4129	12.5576	10.9262	11.1105	
	Model III	0	13.7208	14.8464	17.7595	13.0158	14.1238	14.9688	12.9401	
		20	14.7745	15.8164	18.5785	14.1363	15.1774	15.9388	14.0772	
		40	13.7208	14.8464	17.7595	13.0158	14.1238	14.9688	12.9401	
		80	11.4786	12.7630	15.9621	10.6465	11.8817	12.8854	10.5390	
C-S Boundary Condition	Model II	0	53.4719	53.7515	54.4662	53.3237	55.9894	52.7923	52.8209	
		20	52.2280	52.4845	53.1575	52.0983	54.8509	51.4726	51.5474	
		40	50.9841	51.2175	51.8491	50.8728	53.7124	50.1529	50.2739	
		80	48.4963	48.6835	49.2320	48.4220	51.4355	47.5135	47.7269	
	Model III	0	53.1315	56.2668	64.6622	51.2272	54.3706	56.6477	51.0579	
		20	51.9468	55.1579	63.6898	49.9819	53.1859	55.5389	49.7974	
		40	50.7622	54.0491	62.7174	48.7366	52.0013	54.4300	48.5370	
		80	48.3929	51.8314	60.7726	46.2460	49.6320	52.2123	46.0160	
C-C Boundary Condition	Model II	0	152.859	153.575	155.417	152.481	161.168	150.131	150.018	
		20	151.615	152.308	154.108	151.255	160.030	148.812	148.744	
		40	150.371	151.041	152.800	150.030	158.891	147.492	147.471	
		80	147.884	148.507	150.183	147.579	156.614	144.853	144.924	
	Model III	0	153.775	162.480	185.225	148.348	156.896	163.463	147.752	
		20	152.591	161.371	184.253	147.103	155.711	162.354	146.492	
		40	151.4060	160.2620	183.2800	145.8580	154.5260	161.2450	145.2310	
		80	149.0370	158.0450	181.3360	143.3670	152.1570	159.0270	142.7100	

Figs.(4.39) and (4.40) present the effect of temperature change (ΔT) on the dimensionless buckling load and fundamental frequency as a function of the various aspect ratio (L/h) with a certain power law index ($k = 2$), $\alpha = 0.1$, $\beta = 0.2$, Model III with cross section shape (1-2-1) and various boundary conditions (i.e. S-S, C-S, C-C) for sandwich FG micro-beam. For given value of an aspect ratio (L/h), the dimensionless critical buckling load (\bar{P}) and fundamental frequency ($\bar{\omega}$) decrease with increase the temperature change (ΔT) due to with larger temperature change (ΔT) make sandwich FG microbeam with less stiffness. Therefore the sandwich FG micro-beam become flexible and it can also explicit that the temperature change is more significant for S-S boundary condition and insensitive to for C-C boundary condition. It can be noticed also when the aspect ratio is less than 15 the dimensionless buckling load and fundamental frequency decrease rapidly with increase the aspect ratio for all boundary conditions. Then (\bar{P}) and ($\bar{\omega}$) are insignificant to thermal effect when the aspect ratio less than 15 and more significant after that.

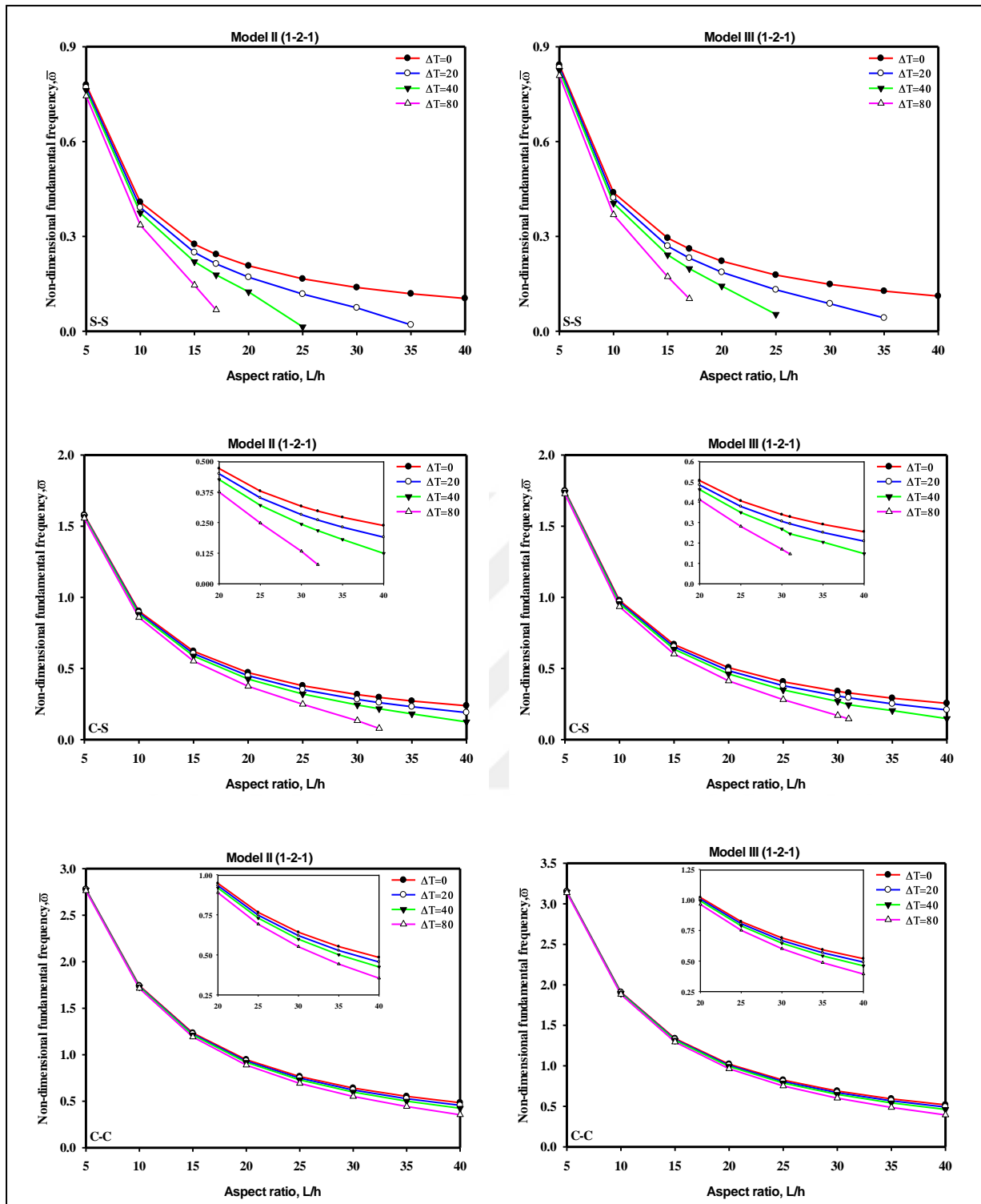


Figure 4.39 Thermal effect on the dimensionless fundamental frequency, $\bar{\omega} = \omega L \sqrt{\rho_m / E_m}$ with $k = 2$, $K_W = K_P = 0$, $\beta = 0.2$, $\alpha = 0.1$, and cross section shape (1-2-1) sandwich FG micro-beam.

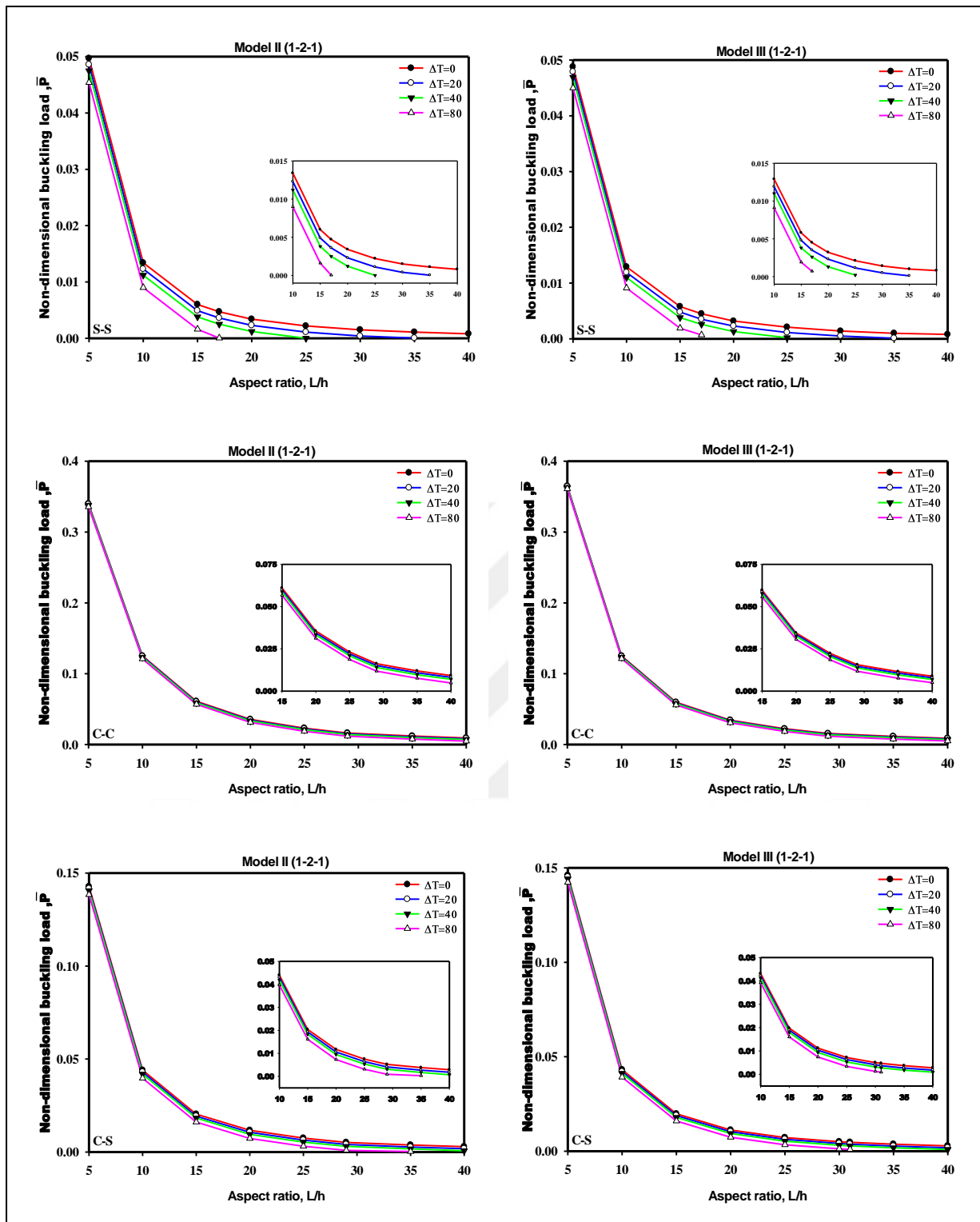


Figure 4.40 Thermal effect on the dimensionless critical buckling load ($\bar{P} = P/E_m bh$) with $k = 2$, $K_W = K_P = 0$, $\beta = 0.2$, $\alpha = 0.1$, and cross section shape (1-2-1) sandwich FG micro-beam.

Fig. (4.41) gives the influence of various boundary conditions on the dimensionless critical buckling load and fundamental frequency of size dependent sandwich FG microbeam Model III with cross section shape (1-1-1) for fixed $\beta = 0.2$, $\alpha = 0.1$, $L/h = 10$, without elastic foundation ($K_w = K_p = 0$) and $\Delta T = 0$. It is observed that the dimensionless buckling load and fundamental frequency of C-C boundary condition is much more C-S and S-S respectively. This is due to the fact that sandwich FG microbeam with C-C has more rigidity stiffness than those in C-S and S-S sandwich FG microbeam respectively.

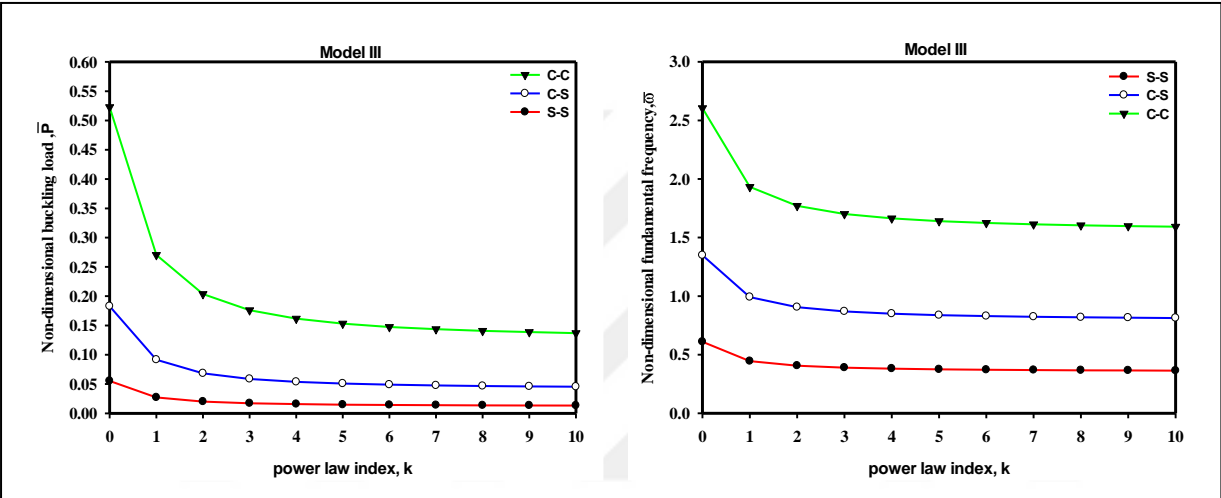


Figure 4.41 Variation of the dimensionless fundamental frequency ($\bar{\omega}$) and buckling load (\bar{P}) with the power-law exponent (k) for cross-section shape (1-1-1) sandwich FG microbeam, $L/h = 10$, $\beta = 0.2$, $\alpha = 0.1$, and for different boundary conditions.

CONCLUSIONS AND FUTURE WORK**5.1 Conclusions**

In this thesis, the static, free vibration, buckling analysis, and dynamic stability of size-dependent sandwich FG micro-beam subjected to the parametric excitation resting on elastic Winkler and Pasternak foundations with temperature change is illustrated. According to the different higher-order deformation micro-beam theories (HOBTs), Timoshenko beam theory (TBT) and Euler beam theory (EBT) in conjunction with the nonlocal strain gradient theory (NLSGT) with the Hamilton's principle, the governing equations and associated various boundary condition (i.e. simply-simply, clamped-clamped, and clamped-simply) can be obtained for sandwich FG micro-beam structure. The effective material properties of the functionally graded part of sandwich FG micro-beam are varied gradually through the thickness are calculated by using the Mori-Tanaka homogenization and the rule of mixture method. The dynamic stability, static bending, buckling and fundamental frequency can be determined with various boundary conditions (i.e. simply-simply, clamped-clamped, and clamped-simply) by using GDQM. The sandwich functionally graded micro-beams is considered with three different models and various cross section shapes. The influence of the dimensionless nonlocal parameter (α), the non-dimensional material length scale parameter (β), aspect ratio (L/h), power law index (k), static load factor (η_s), temperature change (ΔT), and various cross section shapes on the dynamic stability, static, free and buckling analysis of the sandwich micro-beam are discussed.

Beside that following conclusions are derived

1. The dimensionless buckling load and fundamental frequency increase of the sandwich functionally graded micro-beams structure with the increase of elastic foundation of both Winkler and Pasternak shear layer, moreover, the dimensionless transverse deflection

decrease with increase of the elastic foundations. It can be also observed that Pasternak shear layer has the greater effect than Winkler elastic foundation.

2. The dimensionless buckling load and fundamental frequency decrease when the material property gradient index (k) increase for all the boundary conditions of size-dependent sandwich FG micro-beams and conversely for dimensionless transverse deflection.

3. When the decrease in the gradient index (k), the instability region moves to higher excitation frequency and these regions become more wider.

4. When dimensionless Winkler and Pasternak shear parameters increase leads to higher excitation frequencies ($\bar{\Omega}$), and the width of the instability region is increased for all types of sandwich FG micro-beam at given dynamic load factor and the excitation frequency on dimensionless Pasternak shear parameter is larger than that on the dimensionless Winkler parameter with all kinds of sandwich FG micro-beam.

5. At lower value power law index (k), the dimensionless transverse deflection for Model III is lower than those with Model II and the dimensionless buckling load and the fundamental frequency is greater for Model III than these of Model II.

6. The size-dependent sandwich FG micro-beam with different cross-section shapes will be the effect on the dimensionless transverse deflection, the critical buckling forces and fundamental frequency as the relative volumes of phase materials are changing.

7. The dimensionless transverse deflection with the higher-order beam theories (HOBTs) is lower than those of Timoshenko theory (FSDBT) and greater than those of Euler theory (EBBT). On the other hand for dimensionless buckling loads and fundamental frequency the behavior is conversely. The results for TBT and HOBTs are slight differences and when the slenderness ratio decreases (L/h) these results are close to each other.

8. Dimensionless nonlocal parameter and material length scale parameter can be used in combination for refined calibration of experimental results as stiffness is proportional to the (β) whereas it is inversely proportional to the (α).

9. When the dimensionless nonlocal parameter is lower than the dimensionless material length scale parameter, the sandwich FG micro-beams have a stiffness-hardening effect.

Moreover, when the (β) is smaller than the (α) , the sandwich FG micro-beams have a stiffness-softening effect.

10. The dimensionless buckling load and fundamental frequency increase and dimensionless transverse deflections decrease with the increase of (β) or the decrease of (α) .

11. When the $(\beta = l_m/L)$ increase, the higher dimensionless excitation frequencies and also the width of the instability regions will be wider. Moreover, for dimensionless nonlocal parameter $(\alpha = ea/L)$ the behavior is conversely.

12. For clamped-clamped boundary condition (stiffer configurations) tend to have higher excitation frequencies and wider instability regions when compared to simple-simple boundary condition (flexible configurations).

13. For larger values of aspect ratio, the influence of temperature change $(\Delta T = 0)$ on the dimensionless fundamental frequencies and critical buckling forces of sandwich FG microbeam is more significant. On the other hand, with small values of aspect ratio (L/h) , the temperature change ΔT on (\bar{P}) and $(\bar{\omega})$ is slight.

14. The dimensionless transverse deflection (\bar{w}) increase with increasing the temperature change (ΔT) , while the dimensionless critical buckling forces (\bar{P}) and natural frequencies $(\bar{\omega})$ decrease with increase (ΔT) .

15. The instability regions shifts to lower (higher) excitation frequencies with the increase (decrease) in the temperature change and the instability region no change in the width with the increase in temperature change (ΔT) a certain dynamic load factor for size dependent sandwich FG micro-beam with all boundary conditions.

5.2 Future Work

The current illustration presents some of the very essential sides of the static, free, buckling analysis and dynamic stability of the sandwich FG micro-beam. Otherwise, some aspects of the sandwich FG micro-beams with dynamic stability, static, buckling and free vibration are not studied in the present thesis. Therefore the research topics of the sandwich FG micro-beams which deserve further investigation in future are presented at some point

- The nonlinear static, buckling analysis, dynamic stability and vibration analysis of size dependent sandwich FG micro-beams.
- Static, free, buckling analysis and dynamic stability of Bi-directional sandwich FG micro-beams structure.
- Experimental analysis of dynamic stability, static, buckling analysis and free vibration of sandwich FG micro-beam can be study in a future to compare the experimental results in conjunction with theoretical results.
- The present thesis can be extended to study static, buckling, free vibration and the dynamic stability of other structural elements such as sandwich FG micro-plates and micro-shells.



REFERENCES

-
- [1] Nguyen, T.K., Nguyen, T.T.P. and Vo, T.P., (2015). "Vibration and buckling analysis of functionally graded sandwich beams by a new higher-order shear deformation theory." *Composites Part- B*, 76: 273-285.
- [2] Nguyen, T.K., Vo, T.P., Nguyen, B.D. and Lee, J., (2016). "An analytical solution for buckling and vibration analysis of functionally graded sandwich beams using a quasi-3D shear deformation theory." *Composite Structures*, 156: 238–252.
- [3] Vo, T.P., Thai, H.T., Nguyen, T.K., Inam, F. and Lee, J., (2015). "Static behaviour of functionally graded sandwich beams using a quasi-3D theory." *Composites Part-B*, 68: 59-74.
- [4] Vo, T.P., Thai, H.T., Nguyen, T.K., Maheri, A. and Lee, J., (2014). "Finite element model for vibration and buckling of functionally graded sandwich beams based on a refined shear deformation theory." *Engineering Structures*, 64: 12–22.
- [5] Yang, Y., Lam, C.C., Kou, K.P. and Iu, V.P., (2014). "Free vibration analysis of the functionally graded sandwich beams by a meshfree boundary-domain integral equation method." *Composite Structures*, 117: 32–39.
- [6] Tossapanon, P. and Wattanasakulpong, N., (2016). "Stability and free vibration of functionally graded sandwich beams resting on two-parameter elastic foundation." *Composite Structures*, 142: 215–225.
- [7] Şimşek, M. and Al Shujairi, M., (2017). "Static, free and forced vibration of functionally graded (FG) sandwich beam excited by two successive moving harmonic loads." *Composites Part-B*, 108: 18-34.
- [8] Luan, T., Thuc, V., Adelaja, O. and Jaehong, L., (2016). "Fundamental frequency analysis of functionally graded sandwich beams based on the state space approach." *Composite Structures*, 156: 263–275.
- [9] Thuc, V., Huu-Tai, T., Trung-Kien, N., Fawad, I. and Jaehong, L., (2015). "A quasi-3D theory for vibration and buckling of functionally graded sandwich beams." *Composite Structures*, 119: 1–12.
- [10] Huu-Tai, T., Thuc, V., Trung-Kien, N. and Jaehong, L., (2015). "Size-dependent behavior of functionally graded sandwich microbeams based on the modified couple stress theory." *Composite Structures*, 123: 337–349.
- [11] Reddy, J.N., (2007). "Nonlocal theories for bending, buckling and vibration of beams." *International Journal of Engineering Science*, 45: 288–307.

- [12] Adali, S., (2008). "Variational principles for multi-walled carbon nanotubes undergoing buckling based on nonlocal elasticity theory." *Physics Letters A* ,372: 5701–5705.
- [13] Murmu, T. and Pradhan, S.C., (2009). "Buckling analysis of a single-walled carbon nanotube embedded in an elastic medium based on nonlocal elasticity and Timoshenko beam theory and using DQM." *Physica E*, 41: 1232–1239.
- [14] Pradhan, S.C. and Reddy, J.N., (2011). "Buckling analysis of single walled carbon nanotube on Winkler foundation using nonlocal elasticity theory and DTM." *Computational Materials Science*, 50: 1052–1056.
- [15] Ansari, R., Sahmani, S. and Rouhi, H., (2011). "Axial buckling analysis of single-walled carbon nanotubes in thermal environments via the Rayleigh–Ritz technique." *Computational Materials Science*, 50: 3050–3055.
- [16] Şimşek, M. and Yurtcu, H.H., (2013). "Analytical solutions for bending and buckling of functionally graded nanobeams based on the nonlocal Timoshenko beam theory." *Composite Structures*, 97: 378–386.
- [17] Aydogdu, M., (2009). "A general nonlocal beam theory: Its application to nanobeam bending, buckling and vibration." *Physica E*, 41: 1651–1655.
- [18] Murmu, T. and Pradhan, S.C., (2009). "Thermo-mechanical vibration of a single-walled carbon nanotube embedded in an elastic medium based on nonlocal elasticity theory." *Computational Materials Science*, 46: 854–859.
- [19] Şimşek, M., (2010). "Vibration analysis of a single-walled carbon nanotube under action of a moving harmonic load based on nonlocal elasticity theory." *Physica E* 43: 182–191.
- [20] Şimşek, M., (2011). "Nonlocal effects in the forced vibration of an elastically connected double-carbon nanotube system under a moving nanoparticle." *Computational Materials Science*, 50: 2112–2123.
- [21] Eltaher, M., Emam, S. and Mahmoud, F., (2012). "Free vibration analysis of functionally graded size-dependent nanobeams." *Applied Mathematics and Computation*, 218: 7406–7420.
- [22] Thai, H., (2012). "A nonlocal beam theory for bending, buckling, and vibration of nanobeams." *International Journal of Engineering Science*, 52: 56–64.
- [23] Şimşek, M., (2012). "Nonlocal effects in the free longitudinal vibration of axially functionally graded tapered nanorods." *Computational Materials Science*, 61: 257–265.
- [24] Rahmani, O. and Pedram, O., (2014). "Analysis and modeling the size effect on vibration of functionally graded nanobeams based on nonlocal Timoshenko beam theory." *International Journal of Engineering Science*, 77: 55–70.
- [25] Ebrahimi, F. and Erfan, S., (2015). "Thermal buckling and free vibration analysis of size dependent Timoshenko FG nanobeams in thermal environments." *Composite Structures*, 128: 363–380.
- [26] Ebrahimi, F. and Erfan, S., (2015). "Size-dependent free flexural vibrational behavior of functionally graded nanobeams using semi-analytical differential transform method." *Composites Part B*, 79: 156-169.

- [27] Ebrahimi, F. and Erfan S., (2015). "Thermo-mechanical vibration analysis of nonlocal temperature dependent FG nanobeams with various boundary conditions." *Composites Part B*, 78: 272-290.
- [28] Mohammad, N., Amin, H. and Abbas, R., (2016). "Buckling analysis of arbitrary two-directional functionally graded Euler–Bernoulli nano-beams based on nonlocal elasticity theory." *International Journal of Engineering Science*, 103: 1–10.
- [29] Ansari, R., Faraji, O.M., Gholami, R. and Sadeghi, F., (2016). "Thermo-electro-mechanical vibration of postbuckled piezoelectric Timoshenko nanobeams based on the nonlocal elasticity theory." *Composites Part B*, 89: 316-327.
- [30] Shengli, K., Shenjie, Z., Zhifeng, N. and Kai, W., (2009). "Static and dynamic analysis of micro beams based on strain gradient elasticity theory." *International Journal of Engineering Science*, 47: 487–498.
- [31] Akgöz, B. and Civalek, Ö., (2013). "A size-dependent shear deformation beam model based on the strain gradient elasticity theory." *International Journal of Engineering Science* 70: 1–14.
- [32] Binglei, W., Junfeng, Z. and Shenjie, Z., (2010). "A micro scale Timoshenko beam model based on strain gradient elasticity theory." *European Journal of Mechanics A/Solids*, 29: 591–599.
- [33] Akgöz B. and Civalek Ö., (2011). "Analysis of micro-sized beams for various boundary conditions based on the strain gradient elasticity theory." *Archive of Applied Mechanics*, 82:423–443.
- [34] Bo, Z., Yuming, H., Dabiao, L., Lei, S. and Jian,L., (2015). "Free vibration analysis of four-unknown shear deformable functionally graded cylindrical microshells based on the strain gradient elasticity theory." *Composite Structures*, 119: 578–597.
- [35] Wu, J., Li, X. and Cao, W., (2013). "Flexural waves in multi-walled carbon nanotubes using gradient elasticity beam theory." *Computational Materials Science* 67: 188–195.
- [36] Thai, S., Thai, H., Vo, T. and Patel, V., (2017). "Size-dependant behaviour of functionally graded microplates based on the modified strain gradient elasticity theory and isogeometric analysis." *Computers and Structures* 190: 219–241.
- [37] Akgöz, B. and Civalek, O., (2011). "Strain gradient elasticity and modified couple stress models for buckling analysis of axially loaded micro-scaled beams." *International Journal of Engineering Science* 49: 1268–1280.
- [38] Kahrobaiyan, M., Asghari, M. and Ahmadian, M., (2013). "Strain gradient beam element." *Finite Elements in Analysis and Design*, 68: 63–75.
- [39] Bo, Z., Yuming, H., Dabiao, L., Zhipeng, G. and Lei, S., (2014). "Non-classical Timoshenko beam element based on the strain gradient elasticity theory." *Finite Elements in Analysis and Design*, 79: 22–39.
- [40] Anqing, L., Shenjie, Z., Shasha, Z. and Binglei, W., (2014). "A size-dependent bilayered microbeam model based on strain gradient elasticity theory." *Composite Structures*, 108: 259–266.
- [41] Ansari, R., Gholami, R. and Sahmani, S., (2011). "Free vibration analysis of size-dependent functionally graded microbeams based on the strain gradient Timoshenko beam theory." *Composite Structures*, 94: 221–228.

- [42] Ansari, R., Gholami, R. and Sahmani, S., (2012). "Study of Small Scale Effects on the Nonlinear Vibration Response of Functionally Graded Timoshenko Microbeams Based on the Strain Gradient Theory." *Journal of Computational and Nonlinear Dynamics*, JULY, Vol. 7 / 031009-1.
- [43] Ansari, R., Gholami, R. and Sahmani, S., (2014). "Free Vibration of Size-Dependent Functionally Graded Microbeams Based on the Strain Gradient Reddy Beam Theory." *International Journal for Computational Methods in Engineering Science and Mechanics*, 15: 401–412.
- [44] Amin, S., Parviz, M. and Saeedreza, M., (2016). "Vibrational behavior of variable section functionally graded microbeams carrying microparticles in thermal environment." *Thin-Walled Structures*, 108: 122–137.
- [45] Hamid, Z. and Yaghoub, B., (2015). "Free vibration analysis of axially functionally graded nanobeam with radius varies along the length based on strain gradient theory." *Applied Mathematical Modelling*, 39: 5354–5369.
- [46] Bo, Z., Yuming, H., Dabiao, L., Lei, S. and Lei, S., (2015). "An efficient size-dependent plate theory for bending, buckling and free vibration analyses of functionally graded microplates resting on elastic foundation." *Applied Mathematical Modelling*, 39: 3814–3845.
- [47] Lim, C.W., Zhang, G. and Reddy, J.N., (2015). "A higher-order nonlocal elasticity and strain gradient theory and its applications in wave propagation." *Journal of the Mechanics and Physics of Solids*, 78: 298–313.
- [48] Lu, L., Xingming, G. and Jianzhong, Z., (2017). "Size-dependent vibration analysis of nanobeams based on the nonlocal strain gradient theory." *International Journal of Engineering Science*, 116: 12–24.
- [49] Li, L., Xiaobai, L. and Yujin, H., (2016). "Free vibration analysis of nonlocal strain gradient beams made of functionally graded material." *International Journal of Engineering Science*, 102: 77–92.
- [50] Li, L., Xiaobai, L., Yujin, H., Zhe, D. and Weiming, D., (2017). "Bending, buckling and vibration of axially functionally graded beams based on nonlocal strain gradient theory." *Composite Structures*, 165: 250–265.
- [51] Li, L., Yujin, H., Xiaobai, L. and Xiaobai L., (2016). "Longitudinal vibration of size-dependent rods via nonlocal strain gradient theory." *International Journal of Mechanical Sciences*, 115-116: 135–144.
- [52] Li, L. and Yujin, H., (2015). "Buckling analysis of size-dependent nonlinear beams based on a nonlocal strain gradient theory." *International Journal of Engineering Science*, 97: 84–94.
- [53] Li, L., Yujin, H. and Ling, L., (2015). "Flexural wave propagation in small-scaled functionally graded beams via a nonlocal strain gradient theory." *Composite Structures*, 133: 1079–1092.
- [54] Farzad, E. and Mohammad, R., (2017). "Hygrothermal effects on vibration characteristics of viscoelastic FG nanobeams based on nonlocal strain gradient theory." *Composite Structures*, 159: 433–444.
- [55] Şimşek, M., (2016). "Nonlinear free vibration of a functionally graded nanobeam using nonlocal strain gradient theory and a novel Hamiltonian approach." *International Journal of Engineering Science*, 105: 12–27.

- [56] Farzad, E. and Mohammad, B., (2016). "Wave propagation analysis of quasi-3D FG nanobeams in thermal environment based on nonlocal strain gradient theory." *Applied . Physics A*,122: 843.
- [57] Farzad, E. and Mohammad, B., (2017). "A nonlocal strain gradient refined beam model for buckling analysis of size-dependent shear-deformable curved FG nanobeams." *Composite Structures*, 159: 174–182.
- [58] Farzad, E. and Mohammad, B., (2016). "Size-dependent dynamic modeling of inhomogeneous curved nanobeams embedded in elastic medium based on nonlocal strain gradient theory, *Proceedings of the Institution of Mechanical Engineers.*" Part C: *Journal of Mechanical Engineering Science*,0: 1-13.
- [59] Li, L. and Yujin, H., (2016). "Nonlinear bending and free vibration analyses of nonlocal strain gradient beams made of functionally graded material." *International Journal of Engineering Science*, 107: 77–97.
- [60] Farzad, E. and Mohammad, B., (2017). "Vibration analysis of viscoelastic inhomogeneous nanobeams resting on a viscoelastic foundation based on nonlocal strain gradient theory incorporating surface and thermal effects, *Acta Mechanica*, 228: 1197–1210.
- [61] Liang L. and Wang Y., (2011). "Size effect on dynamic stability of functionally graded microbeams based on a modified couple stress theory." *Composite Structures*, 93: 342–350.
- [62] Saffari S., Hashemian M. and Toghraie D., (2017). "Dynamic stability of functionally graded nanobeam based on nonlocal Timoshenko theory considering surface effects." *Physica B*, 520: 97–105.
- [63] Helong, W., Jie, Y. and Sritawat, K., (2017). "Dynamic instability of functionally graded multilayer graphene nano composite beams in thermal environment." *Composite Structures*, 162: 244–254.
- [64] Sahmani, S., Ansari, R., Gholami, R. and Darvizeh, A., (2013). "Dynamic stability analysis of functionally graded higher- order shear deformable micro shells based on the modified couple stress elasticity theory." *Composites Part B*, 51: 44-53.
- [65] Ansari, R., Gholami, R., Sahmani, S., Norouzzadeh, A. and Bazdid- ahdati, M., (2015). "Dynamic stability analysis of embedded multi- walled carbon nanotubes in thermal environment." *Acta Mechanica Solida Sinica*, Vol. 28, No. 6
- [66] Ansari, R., Gholami, R. and Sahmani, S., (2012). "On the dynamic stability analysis of embedded single- walled carbon nanotubes including thermal environment effects." *Scientia tranica F*, 19: (3), 919-925.
- [67] Raheb, G., Reza, A., Abolfazl, D. and Saeed, S., (2014). "Axial Buckling and Dynamic Stability of Functionally Graded Microshells Based on the Modified Couple Stress Theory." *International Journal of Structural Stability and Dynamics* Vol. 15, No. 4: 1450070 (24 pages).
- [68] Liao, L., Jie, Y. and Sritawat, K., (2013). "Dynamic Stability of Functionally Graded Carbon Nanotube-Reinforced Composite Beams." *Mechanics of Advanced Materials and Structures*,20: 28–37.
- [69] Bolotin, V.V., (1964) "The Dynamic Stability of Elastic Systems, Holden-Day." San Francisco,.

- [70] Mohanty, S., Dash, R. and Rout, T., (2015). "Vibration and Dynamic Stability of Pre-Twisted Thick Cantilever Beam Made of Functionally Graded Material." *International Journal of Structural Stability and Dynamics* Vol. 15, No. 4: 1450058 (18 pages).
- [71] Pradyumna, S. and Bandyopadhyay, J.N., (2010). "Dynamic Instability of Functionally Graded Shells Using Higher-Order Theory." *Journal of engineering mechanics*, © ASCE / may, 551–561.
- [72] Piovan, M.T. and Machado, S. P., (2011). "Thermoelastic dynamic stability of thin-walled beams with graded material properties." *Thin-Walled Structures*, 49: 437-447.
- [73] Reddy, J.N., (2011). "Microstructure-dependent couple stress theories of functionally graded beams." *Journal of the Mechanics and Physics of Solids*, 59: 2382–2399.
- [74] Reddy, J.N. (1984). "A simple higher-order theory for laminated composite plates." *ASMEJ Applied Mechanical*, 51: 745–52.
- [75] Touratier, M., (1991). "An efficient standard plate theory." *International Journal of Engineering Science*, 29: 901–16.
- [76] Soldatos, K.P., (1992). "A transverse shear deformation theory for homogeneous monoclinic plates." *Acta Mechanica*, 94: 195–220.
- [77] Karama, M., Afaq, K.S. and Mistou, S. (2003). "Mechanical behaviour of laminated composite beam by the new multi-layered laminated composite structures model with transverse shear stress continuity." *International Journal Solids Structure*, 40: 1525–1546.
- [78] Aydogdu, M., (2009). "A new shear deformation theory for laminated composite plates." *Composite Structure*, 89: 94–101.
- [79] Eringen, A.C. (1972). "Nonlocal polar elastic continua, *International Journal of Engineering Science*, 10: 1–16.
- [80] Aifantis, E.C. (1992). "On the role of gradients in the localization of deformation and fracture." *International Journal of Engineering Science*, 30: 1279–1299.
- [81] Mindlin, R.D. (1964). "Micro-structure in linear elasticity." *Archive for Rational Mechanics and Analysis*, 16: 51–78.
- [82] Lam, C., Yang, F., Chong, M., Wang, J. and Tong, P., (2003). "Experiments and theory in strain gradient elasticity." *Journal of Mechanics and Physics of Solids*, 51: 1477–1508.
- [83] Yang, F., Chong, M., Lam, C. and Tong, P., (2002). "Couple stress based strain gradient theory for elasticity." *International Journal of Solids and Structures*, 39: 2731–2743.
- [84] Aifantis, C., On the gradient approach–Relation to Eringen's nonlocal theory. *International Journal of Engineering Science*, 49 (2011) 1367–1377.
- [85] Wang, Y., Zhang, Y., Wang, M. and Tan, C., (2007). "Buckling of Carbon Nanotubes: A Literature Survey." *Journal of Nanoscience and Nanotechnology*, 7: 4221–4247.
- [86] Dresselhaus, S., Dresselhaus, G., Charlier, C. and Hernandez, E., (2004). "Electronic, thermal and mechanical properties of carbon nanotubes." *Philosophical Transactions of the Royal Society A*, 362: 2065–2098.

- [87] Hong, S. and Myung, S., (2007). "Nanotube Electronics: A flexible approach to mobility." *Nature Nanotechnology*, 2: 207–208.
- [88] Mindlin, R. D. and Tiersten, H. F., (1962). "Effects of couple-stresses in linear elasticity." *Archive for Rational Mechanics and Analysis*, 11: 415–488.
- [89] Mindlin, R.D., (1963). "Influence of couple-stresses on stress-concentrations." *Experimental Mechanics*, 3: 1–7.
- [90] Şimşek, M., 2016. "Axial vibration analysis of a nanorod embedded in elastic medium using nonlocal strain gradient theory." *Çukurova University Journal of the Faculty of Engineering and Architecture*.
- [91] Şimşek, M., Kocatürk, T. and Akbaş, Ş.D., (2013). "Static bending of a functionally graded micro scale Timoshenko beam based on the modified couple stress theory." *Composite Structures*, 95: 740–747.
- [92] Şimşek, M. and J. N. Reddy, (2013). "Bending and vibration of functionally graded microbeams using a new higher order beam theory and the modified couple stress theory." *International Journal of Engineering Science*, 64: 37–53.
- [93] Şimşek, M. and J. N. Reddy, (2013). "A unified higher order beam theory for buckling of a functionally graded microbeam embedded in elastic medium using modified couple stress theory." *Composite Structures*, 101: 47–58.
- [94] Rastgoo A., Shafie, H. and Allahverdzadeh, A., (2005). "Instability of curved beams made of functionally graded material under thermal loading." *International Journal of Mechanics and Materials in Design*, 2: 117–128.
- [95] Lim, C.W., Yang, Q. and Lü, C.F., (2009). "Two-dimensional elasticity solutions for temperature dependent in-plane vibration of FGM circular arches." *Composite Structure*, 90: 323–9.
- [96] Malekzadeh, P., Haghghi, M.G. and Atashi, M.M., (2010). "Out-of-plane free vibration of functionally graded circular curved beams in thermal environment." *Composite Structure*, 92: 541–52.
- [97] Meziane, M., Abdelaziz, H. and Tounsi, A., (2014). "An efficient and simple refined theory for buckling and free vibration of exponentially graded sandwich plates under various boundary conditions." *Journal of Sandwich Structures and Materials*, 16: 293–318.
- [98] Tounsi, A., Houari, M. and Benyoucef, S., (2013). "A refined trigonometric shear deformation theory for thermo elastic bending of functionally graded sandwich plates." *Aerospace Science and Technology*, 24: 209–20.
- [99] Ebrahimi, F. and Barati, M.R., (2016). "A nonlocal higher-order shear deformation beam theory for vibration analysis of size-dependent functionally graded nanobeams." *Arabian Journal for Science and Engineering*, 41: 1679–90.
- [100] Ahouel, M., Houari, M., Bedia, E. and Tounsi, A., (2016). "Size-dependent mechanical behavior of functionally graded trigonometric shear deformable nanobeams including neutral surface position concept." *Steel Composite Structure*, 20: 963–81.
- [101] Zhang, B., He, Y., Liu, D., Gan, Z., Shen, L., (2014). "Size-dependent functionally graded beam model based on an improved third-order shear deformation theory, *European Journal of Mechanics-A/Solids*, 47: 211–230.

- [102] Zhang, Y. and Wang, C. N., (2009). "Challamel, Bending, buckling, and vibration of micro/nano-beams by hybrid nonlocal beam model." *Journal of Engineering Mechanics*, 136: 562–574.
- [103] S. Ramezani, (2012). "A micro scale geometrically non linear Timoshenko beam model based on strain gradient elasticity theory." *International Journal of Non-Linear Mechanics*, 47: 863–873.
- [104] Reddy, J.N. and Pang, S.D., (2008). "Nonlocal continuum theories of beams for the analysis of carbon nano tubes." *Journal of Applied Physics*, 103: 023511.
- [105] Mohanty, S.C. and Dashand R.R., (2011) "Parametric Instability of a Functionally Graded Timoshenko beam on Winkler's Elastic Foundation." *Nuclear Engineering and Design*, 241: 2698-2715.
- [106] Zenkour, A. M. and Alghamdi, N. A., (2010). "Bending Analysis of Functionally Graded Sandwich Plates Under the Effect of Mechanical and Thermal Loads." *Mechanics of Advanced Materials and Structures*, 17: 419–432.
- [107] Wattanasakulpong, N., Prusty, B. G. and Kelly, D. W., (2011). "Thermal buckling and elastic vibration of third order shear deformable functionally graded beams." *International Journal of Mechanical Science*, 53: 734-743.
- [108] Sabuncu, M. and Evran, K., (2006). "Dynamic stability of a rotating pre-twisted asymmetric cross-section Timoshenko beam subjected to an axial periodic force." *International Journal of Mechanical Sciences*, 48: 579–590.
- [109] Sabuncu, M. and Evran, K., (2006). "The dynamic stability of rotating asymmetric cross-section Timoshenko beam subjected to lateral parametric excitation." *Finite Elements in Analysis and Design*, 42: 454-469.
- [110] Sabuncu, M. and Evran, K., (2005). "Dynamic stability of a rotating asymmetric cross-section Timoshenko beam subjected to an axial periodic force." *Finite Elements in Analysis and Design*, 41: 1011–1026.
- [111] Pradeep, V., Ganesan, N. and Bhaskar, K., (2007). "Vibration and thermal buckling of composite sandwich beams with viscoelastic core." *Composite Structures*, 81: 60-69.
- [112] Pradhan, S. C. and Murmu, T., (2009). "Thermo mechanical vibration of FGM sandwich beams under variable elastic foundations using differential quadrature method." *Journal of Sound and Vibration*, 321: 342-362.
- [113] Tsepoura, K. G., Papargyri- Beskou, S., Polyzos, D. and Beskos, D. E., (2002). "Static and dynamic analysis of a gradient-elastic bar in tension." *Archive of Applied Mechanics*, 72: 83–4 97.
- [114] Papargyri-Beskou, S., Tsepoura, K. G., Polyzos, D. and Beskos, D. E., (2003). "Bending and stability analysis of gradient elastic beams. *International Journal of Solids and Structures*." 40: 385–400.
- [115] Aydogdu, M., (2009). "A general nonlocal beam theory: Its application to nanobeam bending, buckling and vibration." *Physica E*, 41: 1651–1655.

VIRTUAL STRAIN AND KINETIC ENERGY

A.1 First order shear deformation beam theory (FSDBT)

The strain field of Timoshenko beam theory

$$\varepsilon_{xx} = \frac{\partial u}{\partial x} - z \frac{\partial \phi}{\partial x} \quad (A1a)$$

$$\varepsilon_{yy} = \varepsilon_{zz} = \varepsilon_{xy} = \varepsilon_{yz} = 0 \quad (A1b)$$

$$\gamma_{xz} = 2\varepsilon_{xz} = \frac{\partial w}{\partial x} - \phi \quad (A1c)$$

The first variation of the internal strain energy of first shear deformation beam theory can be taken as follows

$$\begin{aligned} \therefore \delta \int_0^t U_s dt &= \int_0^t \int_0^L \left[N^c \frac{\partial \delta u}{\partial x} - M^c \frac{\partial \delta \phi}{\partial x} + Q^c \left(\frac{\partial \delta w}{\partial x} - \delta \phi \right) \right] dx dt \\ &+ \int_0^t \int_0^L \left[N^{nc} \frac{\partial \delta u}{\partial x} - M^{nc} \frac{\partial \delta \phi}{\partial x} + Q^{nc} \left(\frac{\partial \delta w}{\partial x} - \delta \phi \right) \right] dt \end{aligned} \quad (A1d)$$

The classical and non-classical stress resultants in above can be defined as

$$\begin{aligned} N &= \int_A t_{xx} dA & N^{(1)} &= \int_A \sigma_{xx}^{(1)} dA & Q &= k_s \int_A t_{xz} dA & Q^{(1)} &= k_s \int_A \sigma_{xz}^{(1)} dA \\ M^{(1)} &= \int_A z \sigma_{xx}^{(1)} dA & M &= \int_A z t_{xx} dA \end{aligned} \quad (A1e)$$

The first variation of the kinetic energy can be written as the form

$$\delta \int_0^t U_K dt = \int_0^t \int_0^L \left[I_0 \left(\frac{\partial u}{\partial t} \frac{\partial \delta u}{\partial t} + \frac{\partial w}{\partial t} \frac{\partial \delta w}{\partial t} \right) - I_1 \left(\frac{\partial u}{\partial t} \frac{\partial \delta \phi}{\partial t} + \frac{\partial \phi}{\partial t} \frac{\partial \delta u}{\partial t} \right) + I_2 \frac{\partial \phi}{\partial t} \frac{\partial \delta \phi}{\partial t} \right] dx dt \quad (\text{A1f})$$

A.2 Euler- Bernoulli beam theory (EBBT)

The strain field of Euler- Bernoulli beam theory

$$\varepsilon_{xx} = \frac{\partial u}{\partial x} - z \frac{\partial^2 w}{\partial x^2} \quad (\text{A2a})$$

$$\gamma_{xz} = 0 \quad (\text{A2b})$$

The first variation of the internal strain energy of Euler- Bernoulli beam theory can be taken as follows

$$\delta \int_0^t U_S dt = \int_0^t \int_0^L \left[N^c \frac{\partial \delta u}{\partial x} - M^c \frac{\partial^2 \delta w}{\partial x^2} \right] dx dt + \int_0^t \left[N^{nc} \frac{\partial \delta u}{\partial x} - M^{nc} \frac{\partial^2 \delta w}{\partial x^2} \right]_0^L dt \quad (\text{A2c})$$

The classical and non-classical stress resultants in above can be defined as:

$$\begin{aligned} N &= \int_A t_{xx} dA & M &= \int_A z t_{xx} dA \\ N^{(1)} &= \int_A \sigma_{xx}^{(1)} dA & M^{(1)} &= \int_A z \sigma_{xx}^{(1)} dA \end{aligned} \quad (\text{A2d})$$

The first variation of the kinetic energy of Euler- Bernoulli beam theory can be written as the form

$$\delta \int_0^t U_K dt = \int_0^t \int_0^L \left[I_0 \left(\frac{\partial u}{\partial t} \frac{\partial \delta u}{\partial t} + \frac{\partial w}{\partial t} \frac{\partial \delta w}{\partial t} \right) - I_1 \left(\frac{\partial u}{\partial t} \frac{\partial^2 \delta w}{\partial x \partial t} + \frac{\partial^2 w}{\partial x \partial t} \frac{\partial \delta u}{\partial t} \right) + I_3 \frac{\partial^2 w}{\partial x \partial t} \frac{\partial^2 \delta w}{\partial x \partial t} \right] dx dt \quad (\text{A2e})$$

APPENDIX-B

FREE VIBRATION WITH ANALYTICAL SOLUTION

B.1 Euler- Bernoulli beam theory (EBBT)

$$\left(\begin{bmatrix} K_{11} & K_{12} \\ K_{21} & K_{22} \end{bmatrix} - \omega_n^2 (1 + ea^2 \beta^2) \begin{bmatrix} M_{11} & M_{12} \\ M_{21} & M_{22} \end{bmatrix} \right) \begin{Bmatrix} U_n \\ W_n \end{Bmatrix} = \begin{Bmatrix} 0 \\ 0 \end{Bmatrix} \quad (\text{B1a})$$

$$M_{11} = I_0, \quad M_{12} = M_{21} = -I_1 \beta, \quad M_{22} = -I_3 \beta^2$$

B.2 First shear deformation beam theory (FSDBT)

$$\left(\begin{bmatrix} K_{11} & K_{12} & K_{13} \\ K_{21} & K_{22} & K_{23} \\ K_{31} & K_{32} & K_{33} \end{bmatrix} - \omega_n^2 (1 + ea^2 \beta^2) \begin{bmatrix} M_{11} & M_{12} & M_{13} \\ M_{21} & M_{22} & M_{23} \\ M_{31} & M_{32} & M_{33} \end{bmatrix} \right) \begin{Bmatrix} U_n \\ W_n \\ G_n \end{Bmatrix} = \begin{Bmatrix} 0 \\ 0 \\ 0 \end{Bmatrix} \quad (\text{B2a})$$

$$M_{11} = I_0, \quad M_{12} = M_{21} = 0, \quad M_{13} = M_{31} = I_1$$

$$M_{23} = M_{32} = 0, \quad M_{22} = I_0, \quad M_{33} = -I_2$$

CURRICULUM VITAE

PERSONAL INFORMATION

Name Surname : Mohammed AL-SHUIAIRI
Date of birth and place : 23-02-1979, Iraq-Babel
Foreign Languages : Arabic, English
E-mail : moh_saihood@yahoo.com

EDUCATION

Degree	Department	University	Date of Graduation
Master	Applied Mechanics	University of Babylon	2006
Undergraduate	Mechanical Engineering	University of Babylon	2002
High School	Applied Science	Mahaweel Secondary School	1998

PUBLISHMENTS

Papers

- [1] M. Şimşek, M. Al-Shujairi, Static, free and forced vibration of functionally graded (FG) sandwich beam excited by two successive moving harmonic loads. *Composites Part-B*, 108 (2017) 18-34.
- [2] M. Al-Shujairi, Ç. Mollamahmutoğlu, Dynamic stability of sandwich functionally graded micro-beam based on the nonlocal strain gradient theory with thermal effect. *Composite Structures*, 201 (2018) 1018–1030.



